

Moderate-Resolution Data and Gradient Nearest Neighbor Imputation for Regional-National Risk Assessment

*Kenneth B. Pierce, Jr.; C. Kenneth Brewer;
and Janet L. Ohmann*

Kenneth B. Pierce, Jr., research ecologist, USDA Forest Service, Forestry Sciences Lab, Corvallis, OR 97331 (now Department of Fish and Wildlife, Olympia, WA); **C.**

Kenneth Brewer, IAAA Program Leader, USDA Forest Service, Remote Sensing Applications Center, Salt Lake City, UT 84119; and **Janet L. Ohmann**, research ecologist, USDA Forest Service, Forestry Sciences Lab, Corvallis, OR 97331.

Abstract

This study was designed to test the feasibility of combining a method designed to populate pixels with inventory plot data at the 30-m scale with a new national predictor data set. The new national predictor data set was developed by the USDA Forest Service Remote Sensing Applications Center (hereafter RSAC) at the 250-m scale. Gradient Nearest Neighbor (GNN) imputation was designed by the USDA Forest Service Pacific Northwest Research Station (hereafter PNW) to assign a plot identifier, and, therefore, a link to associated plot data, to each pixel within a target raster. Gradient Nearest Neighbor was implemented at 30-m resolution in three separate multimillion-hectare regions of the Western United States. Concurrently, RSAC developed a set of spatial predictor surfaces at 250-m resolution for use in producing nationally consistent data products. These data have been used for modeling forest types and forest biomass for the conterminous United States and Alaska. These predictor data have also been used for large regional applications.

In this study, we substituted the 250-m predictor data for the 30-m predictor data used thus far in GNN. Our objective was to quantify the difference in performance using the lower spatial resolution predictors. We remodeled the same three regions that were mapped at 30 m with the 250-m data set and compared the error structure of the two modeling efforts. For species presence/absence models in the two areas with large environmental gradients, the Sierra Nevada and northeastern Washington, the species models

performed substantially the same at the two resolutions.

For the region with reduced environmental heterogeneity and moderate environmental gradients, coastal Oregon, species models did not work well with either the 30-m or 250-m studies. Models geared towards mapping forest structure did not perform as well as the 30-m models and may be insufficient for risk-assessment use.

Keywords: Gradient Nearest Neighbor, imputation, regional analysis, species distributions, vegetation mapping.

Introduction

A great wealth of resources has been expended to inventory our Nation's forests, and an equally substantial amount of effort has gone into acquiring remotely sensed data. As such, these two data types make up the ends of a continuum of detail. Plot inventory data are extremely sparse geographically but have a high level of information content regarding the resources at the inventory plot locations. Conversely, remotely sensed data cover the entire globe but with comparatively limited information at any single location. The common approach to leverage these two forms of data has been to create thematic maps of vegetation-related classes as well as response surfaces for other target variables of interest. With regard to vegetation mapping, these thematic maps typically describe dominant vegetation and include physiognomic, floristic, or structural characteristics, or all. These thematic maps often include some additional land use classes or map land use as a separate theme. The variables available for analysis are limited to the classes included in the map, and once the analysis is complete there is no ability to develop new attributes without a new mapping effort. Recently, a more flexible approach, single neighbor imputation, has been utilized to provide sample tree lists and plot-calculated variables for all the unsampled pixels in raster maps. Although not replacing traditional mapping methods, imputed maps can greatly enhance analytical flexibility and provide information in a familiar context that is often supported by extensive simulation modeling capability. Imputed maps are not intended to suggest that each pixel is in fact occupied by the imputed plot data, but rather given

current information, what do we expect. However, developing and mapping 30-m products over broad spatial extents is a lengthy process. This project was conducted in order to evaluate the differences in using a new national spatial predictor database at a coarser resolution (250 m) instead of the 30-m data used in the previous study.

Existing Methods for Regional-National Vegetation Mapping and Risk Assessment

Traditional Methods—

In recent years, many regions within the USDA Forest Service have implemented midlevel classification and mapping programs to provide thematic maps of existing vegetation for a wide variety of analysis applications. These programs are becoming more similar as they implement the USDA Forest Service direction established by the *Existing Vegetation Classification and Mapping Technical Guide* (hereafter technical guide) (Brohman and Bryant 2005). The vegetation classifications and mapping methodologies of these programs follow the technical guide's midlevel direction (Brewer and others 2005), and most use satellite remote sensing approaches to provide synoptic coverage of the mapping areas (e.g., Mellin and others 2004). Some of these programs also utilize summary databases populated by the USDA Forest Service Forest Inventory and Analysis (hereafter FIA) data to develop quantitative map unit descriptions including estimates of common inventory variables. This approach provides thematic map products with statistically sound estimates of inventory variables. These estimates are explicitly connected to the vegetation pattern depicted in the thematic map products. The approach is designed to support midlevel and broad-level analysis applications, as well as some project-level cumulative effects analyses.

As suggested in the technical guide, these midlevel map products can be used as is or rescaled for a variety of base-level analysis applications including project support, risk analysis, and watershed analysis at the scale of 4th and 5th Hydrologic Units, (USDA FS 1995). Unfortunately, the geographic extent of these base-level analysis applications is normally too small to effectively use FIA data as the inventory data source. Given the extensive design of the FIA

program without spatial intensification, each plot represents approximately 6,000 acres. This leaves forests and ranger districts faced with the difficult choice of using the midlevel map product as is with an inadequate sample size of associated FIA data or reverting to the use of often biased and outdated stand-exam data that cannot provide defensible statistical estimates and have no explicit relationship to the midlevel map data used for forest plan revision and project cumulative effects analyses. Alternatives to this untenable choice include several expensive and logistically difficult inventory approaches including intensifying the base grid to provide an adequate sample size or implementing a new traditional two-stage sample of the map features depicting vegetation pattern.

Imputation Methods—

A primary information need of land managers is consistent and continuous current vegetation data on each and every parcel of land in an analysis area sufficient to address the principal issues and resource concerns. As discussed above, where these data do exist they are normally based on a sampling inference procedure rather than wall-to-wall inventory data. Many of the analyses needed to address multiple resource issues at the project level are essentially analyses of vegetation pattern and process relationships through time and space. Inventory data based on traditional two-stage sampling or quantitative map unit descriptions from a systematic random grid are not sufficient to address the spatial or the temporal dimensions or both of these analyses. These data are not spatially explicit enough to identify important vegetation pattern relationships and do not provide adequate thematic detail (i.e., plot-level tree list data) for simulating vegetation change through time.

The ability to simulate these vegetation pattern relationships through space and time, particularly with a variety of management and disturbance alternatives, is important for effective land and resource planning. Despite the capability of simulation models and decision-support tools, comprehensive landscape-level planning is still difficult to implement because the inventory data are rarely complete or current or both. For planning purposes, it would be convenient to be able to operate as if detailed inventory

information were available for all units in the planning area (Moeur and Stage 1995).

As an alternative to historically common statistical approaches (e.g., regression estimates or stratum averages) to populating unsampled units with data, imputation can be used. Imputation involves estimating values for variables of interest (Y variables) by supplying realistic measurements from one or more sampled units to unsampled units with similar characteristics in auxiliary (X) variable space (Hassani and others 2004, LeMay and Temesgen 2005, McRoberts and others 2002, Moeur and Stage 1995, Ohmann and Gregory 2002, Temesgen and Gadow 2004). These auxiliary (X) variables typically include biophysical characteristics such as slope, aspect, precipitation, etc., as well as data from remotely sensed imagery such as aerial photography or satellite imagery.

Imputation of inventory data from sampled areas to similar unsampled areas produces data sets that function like wall-to-wall data for planning purposes. There are many methods and variations of imputation, both univariate and multivariate; however, multivariate approaches that impute a single plot tend to produce more realistic data sets for simulation modeling because they retain the original covariance structure of actual sample units. LeMay and Temesgen (2005) provided a brief summary of common imputation approaches and a detailed comparison of variable-space nearest neighbor (NN) methods for estimating basal area and stems per hectare using aerial auxiliary variables. LeMay and Temesgen (2005) also summarized variable-space nearest neighbor methods and compared them to other estimation methods. These summaries were the most comprehensive available in current literature when this paper was written.

In recent years, two modeling approaches have been developed that could potentially address this critical need through the imputation of inventory data. The first of these approaches, Most Similar Neighbor (MSN), was developed by Moeur and Stage (1995) to impute attributes measured on some sample units (e.g., stand polygons) to sample units where they were not measured. The MSN was originally designed to use a traditional two-stage inventory of forest stands, as described by Stage and Alley (1972), imputing

stand data to unsampled stands. The second of these approaches, Gradient Nearest Neighbor (GNN) developed by Ohmann and Gregory (2002), follows the same general analytical logic, but is designed to use vegetation information from regional grids of field plots (similar to an intensified FIA grid) with remotely sensed imagery and other spatial data to produce a continuous raster surface by imputing data from sampled grid cells to unsampled grid cells.

Study Objectives

Our primary objective was to quantify the difference in GNN model performance using the lower spatial resolution predictors. We remodeled the same three regions that were mapped at 30 m with the 250-m data set and compared the error structure of the two modeling efforts. As explained below, two effects occur when 30-m data are replaced with 250-m data, and both involve averaging across multiple pixels.

One of the reasons for implementing this study is that development of spatial products and modeling at 30 m could take several years to complete a large portion of the Western United States. We anticipate much faster turnaround if 250-m modeling proves sufficient. The 250-m data products could potentially be available for large areas such as the Western United States in 1 to 2 years of production.

Methods

The Study Area

Three western regions covering temperate steppe, coastal forest, and Mediterranean ecosystems were mapped using GNN imputation for a Joint Fire Sciences Program study (Figure 1). The original study examined the feasibility of mapping wildland fuels and vegetation structure to provide data for fire and fuels management planning (Pierce and others 2009, Wimberly and others 2003). The 2.86-million-ha coastal forest site was located in the coast range of Oregon extending as far inland as the western edge of the Willamette Valley (Figure 1). The forests are primarily coniferous with hardwoods occupying riparian and disturbed areas. The 4.1-million-ha Mediterranean site was located in the central Sierra Nevada occupied by savannah,



Figure 1—The Joint Fire Sciences project covered three western sites in contrasting ecosystems.

chaparral, mixed conifer, and alpine woodlands vegetation types. The site stretches from the northern border of Sequoia National Park north through the Plumas National Forest. The 5-million-ha temperate steppe in northeastern Washington was bounded on the west by the Cascade crest and on the south by the Columbia and Spokane Rivers (Figure 1). The temperate steppe site is dominated by a combination of mixed coniferous forest and extensive shrub steppe.

Vegetation Data from Field Plots

Vegetation data from regional inventories were derived in each of the three regions from multiple sources including Forest Inventory and Analysis (FIA) plots, Current Vegetation Survey/Pacific Northwest Region (R6) plots (CVS), Pacific Southwest Region (R5), Bureau Land Management (BLM), research Ecology Plots in North Cascades National Park (NCNP) (provided by Dave L. Peterson) and Yosemite National Park (provided by Jan Van Wagtenonk). The FIA,

R5, and CVS plots were installed on systematic grids. The CVS/R6 and R5 plots covered the national forests whereas FIA installed plots on all ownerships. The FIA and CVS inventory plots used five subplot arrays within a 1-ha area. Small trees, snags, coarse woody debris line-intercept transects, and ground cover were sampled on each subplot.

Because vegetation data were derived from multiple inventories with different sampling protocols, all individual tree records were converted to per-hectare values. For plots with multiple vegetation or land cover conditions, only the forested portion was used with expansion factors adjusted accordingly. Plot-level summary variables were calculated for each plot.

Stand-summary variables included total basal area, basal area by species, trees per hectare, quadratic-mean diameter, snags per hectare, percentage of tree canopy cover, and down-wood volume. Different inventories collected down-wood data using different sampling schemes

Table 1—Comparison of spatial data between the 30-m and 250-m analyses

250-m resolution	30-m resolution (Pierce and others 2009)
Elevation, slope, and aspect	Elevation, slope, and aspect
DAYMET shortwave radiation	Potential Relative Radiation
Ecological region layers	NA
USGS mapping zones, Bailey's ecoregions, and unified ecoregions for Alaska	NA
STATSGO data layers (lower 48)	NA
Available water capacity, soil bulk density, soil permeability, soil PH, soil porosity, soil plasticity, depth to bedrock, rock volume, soil types, and soil texture	None
MODIS Vegetation indices such as EVI, NDVI	Landsat TM band ratios, 3/4, 4/5, 5/7
MODIS Vegetation continuous fields	NA
MODIS fire points developed from the MODIS active fire maps	NA
MODIS 8-day composites, multiple dates from the spring, summer, and fall	TM-5 and ETM-7 data
NA	Within footprint spectral variability
All MODIS 32-day composite imagery that is cloud-free between the years 2001–2003	NA
USGS NLCD layers, percentage tree cover, percent herbaceous cover, and percentage bare ground	NA
DAYMET temperature and precipitation, mins, maxs, aves, SD (all, yearly, monthly)	DAYMET temperature and precipitation, mins, maxs, aves (all)

and minimum sizes. As a result, we focused primarily on species basal area.

Moderate-Resolution Predictor Data

Beginning in 2003, RSAC, in cooperation with the FIA remote sensing band, developed a national predictors database to support FIA national mapping efforts (e.g., national forest type maps, and national biomass maps) (Blackard and others 2008, Ruefenacht and others 2008). The original database included about 60 layers consisting primarily of MODIS imagery. The national predictors database has been extensively used with additional data layers added each year. The current version has more than 700 layers, which includes DAYMET climate data, additional MODIS imagery, derived MODIS-based vegetation indices, STATSGO soil layers, topography, and several derived thematic products (Table 1). These data cover the entire conterminous United States as well as Alaska and Puerto Rico.

To prepare these data for Gradient Nearest Neighbor analysis, all layers were sampled with all plot locations. With 30-m data, 13-pixel footprints were used to sample the spatial data to account for plots occupying more area than a

single 30-m pixel. With 250-m data, only a single pixel was necessary to represent each plot because the plot area is less than the area of one 250-m pixel. All predictor images were split into separate bands, comprising over 700 individual predictor layers. For example, some STATSGO soil layers comprised 11 soil horizons. Those 11 horizons were split into separate predictor layers. Before statistical modeling, the 700 bands were reduced to those without a correlation of > 0.90 with any other remaining predictor. For each of the three study areas, this left about 100 to 150 predictor layers. These predictors were entered as the predictor matrix in a stepwise canonical correspondence analysis. In each case, 10 to 15 predictors were sufficient to explain the primary gradients in vegetation composition.

Satellite Imagery

For the 30-m study, Landsat Thematic Mapper imagery (TM) was mosaiced and histogram matched. For the 250-m study, several products derived from MODIS imagery were used (Table 1). These products have a spatial extent covering our entire study regions, so no image matching was necessary.

Biophysical Environment Data

For both studies, biophysical data were derived from digital elevation models, including slope, aspect, and elevation. Both studies used climate data derived from DAYMET, although the 250-m data set used many more calculated variables. These variables included year-to-year variability by month. The DAYMET data are provided at 1-km resolution, so both the 30-m and 250-m DAYMET data were interpolated or resampled to their respective resolutions.

The 250-m data set also included STATSGO data layers, such as available water-holding capacity, soil bulk density, soil permeability, and soil pH. No analog for these data existed in the 30-m data set.

The Gradient Nearest Neighbor (GNN) Method of Predictive Vegetation Mapping

Imputation is a process in which values are assigned to unmeasured locations from either measured values or a statistical summary of a few selected measured values such as a mean (Moeur and Stage 1995). Unlike regression-based predictions, the assigned value is not a product of predictor variables and coefficients. The predictor variables are used to rank sample plots as to their similarity to a target location (30-m or 250-m-square pixel). In Gradient Nearest Neighbor imputation (GNN) we used the loadings for the ordination axes and their eigenvalues from a Canonical Correspondence Analysis (CCA) to relate the target locations to the locations of sample plots. This is achieved by calculating a Euclidean distance in eight-axis ordination space between the target pixel and each plot using the ordination loadings to weigh the spatial variables and the eigenvalues to weigh each axis. The distance in gradient space between the target location and each plot is used to rank the sample plots for potential assignment at each target pixel in our study regions (Ohmann and Gregory 2002). Because we use a multivariate response, which is analogous to a community representation of a plot, the variables selected must be of similar type. Our primary modeling scenarios have been species modeling, which involves using the total basal area of each individual species, and structure modeling, which has used basal area in different size classes

of hardwoods and conifers, snag density, coarse woody debris volume, and canopy cover.

When GNN is run as a single neighbor imputation, the closest plot in gradient space is assigned to each pixel in the landscape. Once the assignment has been made, any attribute calculated for all plots can be mapped, maintaining the original covariance structure for any/all other attributes to be mapped. Additionally, the ranking of potential neighbors provides a sample neighborhood of similar plots from which natural variability and sample sufficiency can be evaluated (Pierce and others 2009).

Gradient Nearest Neighbor Results Summary from Previous Studies

In the 30-m study, coastal Oregon had favorable results for structure models but substandard results for species models. This pattern was reversed in both Washington and California, where species models worked well, but structure models did a poor job with attributes such as quadratic mean diameter and trees per hectare. The purpose of the original study was to map wildland fuels and vegetation structure. Wildland fuel components, such as coarse woody debris and snag density, were not mapped adequately in any of the three sites (However, canopy-related fuels variables were more satisfactory.) This was partially due to remote sensing not directly detecting wildland fuels, which, in general, are below the canopy. Another factor is that coarse woody debris data are collected on only a relatively short transect on FIA plots such that the resulting sample size is too small to characterize individual plots. The original design of the coarse woody debris sampling was to create estimates for a region.

We expect that species models will perform more favorably than structure models with 250-m data. In the previous study, remote sensing imagery was very important for mapping structure and has a much finer spatial grain than our climate data. Although we had climate data at 30 m, it was interpolated from 1-km-resolution DAYMET data, which are interpolated from weather stations plus higher resolution covariates (elevation, topography, etc.). Therefore, climate data would change gradually over the course of a kilometer whereas TM data can change abruptly from one

30-m pixel to the next. Therefore, our change in resolution loses much more information for predictions relying heavily on imagery than those relying on climate.

Model Evaluation and Accuracy Assessment

To evaluate the results of the 30-m study compared with the 250-m study results, we used two primary approaches. For continuous variables, we calculated 2nd nearest neighbor correlations (analogous to r-squares from cross-validation), (see Ohmann and Gregory 2002). For discrete variables, such as species presence/absence, we used standard confusion matrices. Producers accuracy, users accuracy, and Kappa statistics were calculated for each species and compared for the two studies (Wilkie and Finn 1996). The Kappa statistic accounts for the probability of randomly assigning a plot to its correct class. As such, the random probability of assigning a species with a frequency of 0.9 to any plot is very high; Kappa statistics tend to be low as the probability of improving upon randomness decreases. Producers accuracy is the proportion of sample plots with a species present in which the species is predicted to occur. Users accuracy is the proportion of plots with the predicted species occurrence that actually had the species in the inventory.

Any discrepancies derived from changing the scale of the analysis stems from two primary effects, which are both aspects of spatial averaging. First, with the 30-m product, the predicted value for a plot is the average of the 13 pixels imputed to the plot footprint. In this way, the predicted value is subject to averaging over those 13 imputations. With the 250-m imputation, only a single plot is imputed for the same ~1 ha space. Therefore, the 250-m results will be slightly more variable. The second effect involves the spatial averaging of the predictor data set. The predictor variables are the averages of the 13 pixels within the individual predictor layers. In addition, we calculate two texture indices for the remote sensing data, which provides an estimate of variability within the footprint. With the 250-m data, a single pixel covers an area considerably larger than a 1-ha plot (62 500 m² vs. 11 700 m²). Thus, the spectral values are averaged over a larger area, and we have no estimate of within-plot variability.

Results

Gradients in Species Composition

Daubenmire (1952) noted the axiomatic relationship between climate and vegetation. Our CCA modeling results are consistent with this observation and suggest that climatic variables, as well as topographic and edaphic variables indirectly related to temperature and moisture, strongly influence the patterns of species composition. The gradients described by the three CCA models were composed of the dominant patterns in temperature and precipitation. In Washington, elevation, precipitation frequency, and brightness in MODIS 8-day composites separated warmer drought-tolerant conifers from both high-elevation wet and dry forests. In California, species were separated by September growing degree days, September average air temperature, April cooling degree days, and water vapor pressure variability in July. In Oregon, the dominant environmental variables were August mean precipitation, June cooling degree days, soil permeability, and June standard deviation of water vapor pressure.

Species Mapping Performance of GNN

Species performance from confusion matrices are listed for all species occurring with a frequency of at least 5 percent in the plot data set (Tables 2 and 3). California had the highest average Kappa statistics at 0.53 for the 30-m study and 0.48 for the 250-m study (Table 2). Washington was second with 0.46 and 0.43 (Table 3), followed by Oregon with 0.32 and 0.25 (Table 4). Patterns for producers and users accuracy were similar across sites, as were the actual values. In each case, the 30-m study had higher producers accuracy than the 250-m study by about 22 percent, whereas for users accuracy, the 250-m study was actually about 3 percent higher with an average across sites of 55 percent.

Structure Mapping Performance of GNN

To date we have only developed structure models for the Washington and Oregon study sites. Second nearest neighbor correlations for structure variables were generally low in both sites. In Washington, total basal area had an r-square of 0.06 compared to 0.17 for the 30-m analysis, 0.04 for snags per hectare compared to 0.16, and 0.01 for quadratic

Table 2—California species presence/absence results, N = 1,835 plots for species of ≥ 5 percent frequency on plots

Species	Kappa		Producers		Users		Plots
	30 m	250 m	30 m	250 m	30 m	250 m	
<i>Abies concolor</i>	0.51	0.47	0.88	0.67	0.64	0.68	761
<i>Calocedrus decurrens</i>	0.51	0.52	0.86	0.69	0.61	0.67	643
<i>Pinus ponderosa</i>	0.56	0.52	0.88	0.70	0.63	0.66	632
<i>Quercus kelloggii</i>	0.56	0.48	0.86	0.61	0.59	0.61	510
<i>Pinus jeffreyi</i>	0.49	0.46	0.82	0.61	0.54	0.60	488
<i>Pinus lambertiana</i>	0.42	0.36	0.80	0.54	0.49	0.50	468
<i>Abies magnifica</i>	0.63	0.55	0.85	0.65	0.63	0.65	389
<i>Pseudotsuga menziesii</i>	0.59	0.52	0.86	0.61	0.58	0.62	370
<i>Pinus contorta</i>	0.60	0.42	0.84	0.59	0.58	0.48	340
<i>Quercus chrysolepis</i>	0.54	0.43	0.78	0.50	0.52	0.51	264
<i>Pinus monticola</i>	0.52	0.39	0.70	0.48	0.49	0.43	189
<i>Quercus wislizeni</i>	0.53	0.53	0.71	0.59	0.47	0.52	108
<i>Juniperus occidentalis</i>	0.40	0.42	0.64	0.50	0.34	0.42	102
<i>Quercus douglasii</i>	0.53	0.67	0.65	0.69	0.48	0.69	89
Average	0.53	0.48	0.79	0.60	0.54	0.57	

Table 3—Washington species presence/absence results, N = 763 plots for species of ≥ 5 percent frequency on plots

Species	Kappa		Producers		Users		Plots
	30 m	250 m	30 m	250 m	30 m	250 m	
<i>Pseudotsuga menziesii</i>	0.43	0.43	0.97	0.89	0.85	0.86	1,835
<i>Pinus ponderosa</i>	0.53	0.52	0.91	0.74	0.65	0.69	971
<i>Pinus contorta</i>	0.32	0.41	0.82	0.63	0.50	0.61	827
<i>Larix occidentalis</i>	0.54	0.51	0.89	0.70	0.61	0.67	809
<i>Abies lasiocarpa</i>	0.52	0.50	0.87	0.65	0.58	0.64	707
<i>Picea engelmannii</i>	0.41	0.35	0.81	0.54	0.49	0.52	643
<i>Abies grandis</i>	0.57	0.55	0.87	0.68	0.58	0.64	587
<i>Thuja plicata</i>	0.53	0.51	0.82	0.61	0.51	0.58	393
<i>Tsuga heterophylla</i>	0.49	0.44	0.78	0.53	0.45	0.48	277
<i>Pinus monticola</i>	0.35	0.27	0.68	0.37	0.33	0.33	240
<i>Abies amabilis</i>	0.67	0.62	0.86	0.66	0.60	0.66	219
<i>Tsuga mertensiana</i>	0.58	0.49	0.81	0.52	0.50	0.52	179
<i>Pinus albicaulis</i>	0.55	0.47	0.77	0.50	0.47	0.51	152
<i>Populus tremuloides</i>	0.15	0.16	0.40	0.23	0.16	0.20	146
<i>Betula papyrifera</i>	0.29	0.26	0.51	0.30	0.25	0.29	119
Average	0.46	0.43	0.78	0.57	0.50	0.55	

mean diameter compared to an almost equally random 0.05 for the 30-m analysis. In Oregon, where we had quite good results for structure with 30-m data, we mapped basal area with an r-square of 0.09 compared to 0.59 for the 30-m analysis, 0.03 for snags per hectare compared to 0.09, and 0.08 for quadratic mean diameter compared to 0.69.

Discussion

Accuracy of GNN Vegetation Maps

For the Washington and California study sites, species distributions were modeled equally well with the 250-m data and the 30-m data. Both the Kappa statistics and visual inspection of species maps indicated essentially the same

Table 4—Oregon species presence/absence results, N = 2,325 plots for species of ≥ 5 percent frequency on plots

Species	Kappa		Producers		Users		Plots
	30 m	250 m	30 m	250 m	30 m	250 m	
<i>Pseudotsuga menziesii</i>	0.22	0.19	0.97	0.95	0.91	0.91	684
<i>Alnus rubra</i>	0.32	0.18	0.89	0.70	0.67	0.66	440
<i>Tsuga heterophylla</i>	0.27	0.27	0.85	0.63	0.52	0.60	320
<i>Acer macrophyllum</i>	0.25	0.26	0.78	0.49	0.42	0.47	228
<i>Thuja plicata</i>	0.11	0.06	0.56	0.24	0.26	0.25	150
<i>Picea sitchensis</i>	0.52	0.42	0.83	0.50	0.50	0.53	128
<i>Abies grandis (concolor)</i>	0.39	0.29	0.63	0.34	0.34	0.33	52
<i>Quercus garryana</i>	0.47	0.33	0.62	0.32	0.43	0.38	40
Average	0.32	0.25	0.77	0.52	0.51	0.52	

pattern when moving from 30-m to 250-m data. Because the gradient models were largely composed of climate variables, there is actually little loss in predictor data information when using the 250-m data. This is because the climate data for both the 250-m and 30-m studies were interpolated from the same 1-km-resolution data. Species performance in Oregon was not as good, though it was also less accurate for the 30-m data. In both the 30-m and 250-m studies, we saw some definite differences between the results for Oregon and the results for Washington and California. Both California and Washington are precipitation limited, receive most of their precipitation during winter, and have large elevation gradients. The Coast Range in Oregon has much higher precipitation, milder temperatures, and lower overall topographic variation resulting in less orographic precipitation. Coastal Oregon has also had a long history of timber management and, therefore, has a large patchwork of even-aged stands.

Sources of Error in GNN—

The GNN and all nearest neighbor techniques, are particularly susceptible to errors introduced by natural variability at spectrally and environmentally similar sites. Whereas regression techniques model a trend and the departure from that trend, imputation retains the full range of variability within a data set. As such, for a certain location, a regression model with little predictive capability will predict the mean plus some small departure based on predictor variables and coefficients, whereas imputation will find the most environmentally similar site and select it. The

tendency for imputation to impute values similar to the actual target values is constrained by the strength of the relationship between available spatial predictor variables and the target response variables.

Other sources of error include (1) residual spatial error of predictor data sets and plot locations as well as plot registration, (2) temporal mismatches between inventory dates and imagery dates, and (3) the lack of adequate spatial data on disturbance and management history across large regions.

Advantages of GNN for Risk Assessment—

There are several advantages to GNN for risk assessment. The GNN technique retains the covariance structure for multiple attributes by imputing whole plots and provides mapped estimates of natural variability and sample sufficiency (Pierce and others 2009). Comparative risk assessment requires spatially explicit data with estimates of variability (Borchers 2005) in order to create probability surfaces for different management scenarios. For instance, what is the probability of the desired outcome given two different management choices, and are they statistically different? Without an estimation of uncertainty, this type of analysis can't be performed. By using a set of multiple potential neighbors, the variability in potential neighbors for a selected attribute can be mapped. In addition, by using the frequency distribution of all interplot distances in gradient space, thresholds for closeness in gradient space can be assigned and the number of candidate plots within a threshold calculated. This gives an indication as to whether

or not the inventory can provide adequate information for a certain pixel, and, as such, a map depicting the sampling support can be created.

Species Response Models in Multispecies Mapping—

One of the key areas of interest in natural resource risk assessment is the interactions among species. The location of invasive species and the presence of host species are two data surfaces of interest to managers. Mapping with single neighbor imputation ensures that the assemblages of tree species mapped are consistent with actual inventoried assemblages. This has both benefits and limitations. The benefit is robust assemblages of species as they currently exist. The limitation is that prediction for new interactions can not be inferred on the basis of these maps. Single-species models are probably best suited for predicting suitable habitat for an individual species, or rather the present distribution of habitat consistent with currently occupied habitat.

Risk Assessment Applications of GNN Predictions—

Single-neighbor imputation using GNN provides a very flexible wall-to-wall data set that includes any variable that can be derived from those measured on all inventory plots. This includes the ability to derive new variables or vegetation classifications after the initial modeling. A GNN imputation also provides a link to the full tree lists allowing for almost any kind of ecological modeling. The inclusion of multiple neighbors provides uncertainty data for Monte Carlo simulations or analyses seeking to show the uncertainty associated with different scenarios. As new risks or identification of new data needs arise, imputation maps are ready to adapt to new needs without the necessary production of a new model. However, at the 250-m scale, the variables that are correlated with broad climate patterns, specifically species distributions, will probably be characterized the best. Structure attributes, such as coarse woody debris and quadratic mean diameter, can be mapped, but the mapped variability will likely overwhelm the utility of such products.

Acknowledgments

We would like to thank Jerry Beatty and Terry Shaw for support and comments on this project. We also thank Matt Gregory and Bonnie Rufenacht for technical assistance in conducting these analyses.

Literature Cited

- Blackard, J.; Finco, M.; Helmer, E. [and others]. 2008.** Mapping U.S. forest biomass using nationwide forest inventory data and moderate-resolution information. *Remote Sensing of Environment*. 112: 1658-1677.
- Borchers, J.G. 2005.** Accepting uncertainty, assessing risk: decision quality in managing wildfire, forest resource values, and new technology. *Forest Ecology and Management*. 211: 36.
- Brewer, C.K.; Schwind, B.; Warbington, R. [and others]. 2005.** Existing vegetation mapping protocol. In: Brohman, R.; Bryant, L., eds. Existing vegetation classification and mapping technical guide. Gen. Tech. Rep. WO-67. Washington, DC: U.S. Department of Agriculture, Forest Service, Washington Office, Ecosystem Management Coordination Staff. 306 p.
- Brohman, R.; Bryant, L., eds. 2005.** Existing vegetation classification and mapping technical guide. Washington, DC: U.S. Department of Agriculture, Forest Service. [Not paged].
- Daubenmire, R. 1952.** Forest vegetation of northern Idaho and adjacent Washington, and its bearing on concepts of vegetation classification. *Ecological Monographs*. 22: 301-330.
- Hassani, B.T.; LeMay, V.; Marshall, P.L. [and others]. 2004.** Regeneration imputation models for complex stands of Southeastern British Columbia. *Forestry Chronicle*. 80: 271-278.
- LeMay, V.; Temesgen, H. 2005.** Comparison of nearest neighbor methods for estimating basal area and stems per hectare using aerial auxiliary variables. *Forest Science*. 51: 109-119.

- McRoberts, R.E.; Nelson, M.D.; Wendt, D.G. 2002.** Stratified estimation of forest area using satellite imagery, inventory data, and the k-Nearest Neighbors technique. *Remote Sensing of Environment*. 82: 457–468.
- Mellin, T.C.; Krausmann, W.; Robbie, W. 2004.** The USDA Forest Service Southwestern Region mid-scale existing vegetation mapping project. In: *Remote sensing for field users: Proceedings of the 10th Forest Service remote sensing conference*. American Society of Photogrammetry and Remote Sensing: 1–6.
- Moeur, M.; Stage, A.R. 1995.** Most similar neighbor: an improved sampling inference procedure for natural resource planning. *Forest Science*. 41: 337–359.
- Ohmann, J.L.; Gregory, M.J. 2002.** Predictive mapping of forest composition and structure with direct gradient analysis and nearest-neighbor imputation in coastal Oregon, U.S.A. *Canadian Journal of Forest Research- Revue Canadienne De Recherche Forestiere*. 32: 725–741.
- Pierce, K.B.; Ohmann, J.L.; Wimberly, M.C. [and others]. 2009.** Mapping wildland fuels and forest structure for land management: a comparison of nearest neighbor imputation and other methods. *Canadian Journal of Forest Research*. 39(10): 1901–1916.
- Ruefenacht, B.; Finco, M.V.; Nelson, M.D. [and others]. 2008.** Conterminous U.S. and Alaska forest type mapping using forest inventory and analysis data. *Photogrammetric Engineering and Remote Sensing*. 74: 1379–1388.
- Stage, A.R.; Alley, J.R. 1972.** An inventory design using stand examinations for planning and programming timber management. Ogden, UT: U.S. Department of Agriculture, Forest Service, Intermountain Forest & Range Experiment Station. 32 p.
- Temesgen, H.; Gadow, K.V. 2004.** Generalized height-diameter models: an application for major tree species in complex stands of interior British Columbia. *European Journal of Forest Research*. 123: 45–51.
- U.S. Department of Agriculture, Forest Service [USDA FS]. 1995.** Ecosystem analysis at the watershed scale: Federal guide for watershed analysis. Version 2.2. Portland, OR: USDA Forest Service, Regional Ecosystem Office. <http://www.reo.geo/lirary/reports/watershed.pdf>. [Date accessed: February 2010].
- Wilkie, D.S.; Finn, J.T. 1996.** Remote sensing imagery for natural resources monitoring: a guide for first-time users. New York: Columbia University Press. 295 p.
- Wimberly, M.C.; Ohmann, J.L.; Pierce, K. [and others]. 2003.** A multivariate approach to mapping forest vegetation and fuels using GIS databases, satellite imagery, and forest inventory plots. In: *Proceedings of the 2nd International Wildland Fire Ecology and Fire Management Congress*. Orlando, FL: American Meteorological Society: http://ams.confex.com/ams/FIRE2003/techprogram/paper_65758.htm.

This page is intentionally left blank

Integration of Population Genetic Structure and Plant Response to Climate Change: Sustaining Genetic Resources Through Evaluation of Projected Threats

Bryce A. Richardson, Marcus V. Warwell, Mee-Sook Kim, Ned B. Klopfenstein, and GERAL I. McDONALD

Bryce A. Richardson, research geneticist, Rocky Mountain Research Station, Provo, UT; **Marcus V. Warwell**, geneticist; and **Ned B. Klopfenstein** and **GERAL I. McDONALD**, research plant pathologists, USDA Forest Service, Rocky Mountain Research Station, Moscow, ID 83843; **Mee-Sook Kim**, assistant professor, Kookmin University, Seoul, Korea.

Abstract

To assess threats or predict responses to disturbances, or both, it is essential to recognize and characterize the population structures of forest species in relation to changing environments. Appropriate management of these genetic resources in the future will require (1) understanding the existing genetic diversity/variation and population structure of forest trees, (2) understanding climatic change and its potential impacts on forest species and populations, and (3) development and use of new tools to identify populations at risk and geographic areas that will provide suitable habitat in the future. Forest trees exist within distinct geographic populations created by climatic shifts, evolutionary processes, the availability of suitable habitats, and other environmental factors. These processes have occurred over millennia and continue to shape the biogeography and genetic structure of these species. Forest trees in Western North America are being defined on the basis of molecular markers and quantitative traits. For example, studies of whitebark pine (*Pinus albicaulis*) and western white pine (*P. monticola*) demonstrate the existence of several distinct populations that likely developed via the long-term processes described above. These studies and others have shown that distinct populations exist within western conifer species and further indicate that the biogeographies of forest species are quite dynamic over time and space. Here, we present a case study using genetic data from whitebark pine and western white pine coupled with landscape-based, plant-climate modeling. Suitable contemporary habitat is

accurately predicted for both species based on presence/absence of field observations. General circulation models were used to predict areas of suitable habitat for both species under the current climate and the projected climate around the year 2030. These models predict that these species will respond differently to projected climate change. Suitable habitat (i.e., climate space) for whitebark pine is predicted to decline dramatically by ca. 2030. Populations in the lower latitudes (below 45° N) and those persisting at the low elevation limits show the greatest threat to extinction from climate change. Predictions also indicate that suitable habitat for western white pine will be reduced in some southern latitudes, whereas the suitable habitat will be increased in the northern latitudes of its distribution. For whitebark and western white pine, both molecular markers and quantitative traits frequently reveal congruent genetic structure for species conservation. The combination of genetic studies with climate modeling can provide base-line tools that will enable managers to focus genetic conservation efforts on populations at highest risk while restoring areas that have the lowest risk for predicted climatic extirpation. The ability to define forest populations and predict landscape-level effects of climate change is critical for sustaining future forest health.

Keywords: Bioclimatic models, biogeography, genetic conservation, western white pine, whitebark pine.

Introduction

Climate change and associated glacial/interglacial cycles have had a profound impact on the biogeography of plant communities. Paleocological data from pollen sediment cores and packrat middens have been used to uncover many of the past plant-climate associations (e.g., Thompson and Anderson 2000, Thompson and others 1993, Whitlock 1993). These climatic oscillations have also affected intra-species genetic relationships that are recorded in changes in gene frequencies or adaptive traits, or both (Davis and Shaw 2001). In western North America, most forest trees have

broad, disjunct distributions that are associated with variable environmental conditions. The combination of disjunct intra-species distributions and environmental variables can contribute to barriers in gene flow and changes in adaptive or neutral gene frequencies, or both, caused by selection or genetic drift (Richardson and others 2005). Population genetics typically assess neutral genetic variation and provide estimates of genetic diversity and partitioning among a spatial hierarchy. Population genetic studies can estimate both contemporary and historical gene flow, and thereby aid in elucidating past intraspecies relationships and distributions. Such genetic data, coupled with paleoecological data, provide inferences to historical changes in plant biogeography and postglacial expansion/contraction (e.g., Godbout and others 2005, Jackson 2006, Magri and others 2006, Petit and others 2004, Richardson and others 2002, Thompson and Anderson 2000). Knowledge of the population genetic structure and adaptation is critical for successful forest health management and conservation/restoration efforts.

Five-needled pines are keystone species in numerous ecosystems in western North America. This paper focuses on two case studies: whitebark pine (*Pinus albicaulis* Engelm.) and western white pine (*P. monticola* Dougl. ex D. Don). Whitebark pine occupies subalpine habitats across the northern Rocky, Cascade, and Sierra Nevada Mountains and mountains of northern Nevada. Seed dispersal is dependent on a coevolved mutualism with Clark's nutcracker (*Nucifraga columbiana*) that deposits seeds in caches for later consumption (Tomback 2001). Flight distances with seeds vary but have been reported as far as 22 km (Richardson and others 2002, Vander Wall and Balda 1981). Whitebark pine has been recognized as critical for wildlife (Mattson and others 2001) and watershed stability (Arno and Hoff 1989).

Western white pine occupies a wider ecological niche than whitebark pine, occurring from sea level in Washington and British Columbia to a predominately subalpine distribution from Sierra Nevada northward to the Cascades. In the northern Rocky Mountains, this species occupies wet montane to subalpine habitats (Wellner 1962). It is valued as a timber species because of its rapid growth, straight

bole, and ability to regenerate as a seral species from wind-dispersed seeds. Since the early 1900s, the abundance of both five-needled pines has dropped precipitously, mainly from white pine blister rust caused by the fungus *Cronartium ribicola* (McDonald and Hoff 2001). Major efforts and resources have been directed toward restoration of five-needled pine ecosystems. Unfortunately, most restoration efforts have been operating on the assumption that the climate will remain stable. For successful management and restoration of five-needled pine ecosystems, future climate change must be considered and integrated into current efforts and plans for species management/conservation.

Research corroborated by diverse sciences provides strong evidence that the Earth is experiencing a warming process driven by increased greenhouse gas concentrations. Records indicate that mean global temperature increased 0.6 °C during the 20th century, and global temperature is expected to further increase 1.4 to 5.8 °C over the next 100 years (IPCC 2001). This predicted rate of climate change is unprecedented within the available historical records. Because of the extremely fast rate of predicted climate change, determining the responses of forest tree species and populations is one of the major challenges for future threat assessment (Jump and Peñuelas 2005). Recent studies have developed plant-climate models that are highly accurate in predicting a suitable contemporary climate envelope for several western North American species (Rehfeldt and others 2006). These models serve as means to project future climate scenarios using general circulation models (GCMs).

It is well known that historical climatic oscillations have dramatically shifted species distributions. However, these historical climate changes typically occurred at a relatively slow rate over the course of millennia. The predicted rate of climate change, due to the anthropogenic release of greenhouse gases, will greatly exceed historical rates (IPCC 2001). Studies based on several climate models have shown the predicted rate of climate warming could jeopardize plant taxa with limited seed dispersal distances or disjunct habitats (Malcolm and others 2002). In this analysis, we develop an approach to evaluate potential impacts of future climate change on genetic diversity and biogeography of whitebark pine and western white pine. Our objectives include:

1. Assess the existing genetic diversity and population structure of whitebark pine and western white pine.
2. Model each species climate space (i.e., suitable habitat) for contemporary and year 2030 climate.
3. Use the predicted biogeographical changes to prioritize genetic conservation efforts by identifying populations at risk and determining areas suitable for restoration.

Material and Methods

Population Genetic Analyses

Sampling of needle and bud tissue was conducted across the range of both whitebark pine and western white pine. For whitebark pine, 28 sites were sampled and were combined into 6 regions ($n = 21$ to 72, Richardson and others 2002). Western white pine was sampled from 15 sites ($n = \sim 30$) across the range (Kim and others unpublished). Plant tissue was used to extract genomic DNA using previously published protocols (Kim and others 2003, Richardson and others 2002).

For whitebark pine, two types of DNA markers were used: mitochondrial DNA (mtDNA) and chloroplast microsatellites (cpSSR) haplotypes. These markers are uniparentally inherited enabling separate estimates of gene flow via pollen by cpSSR and via seed dispersal by mtDNA. Protocols for DNA typing and analyses are described by Richardson and others (2002). For western white pine, an amplified fragment length polymorphism (AFLP) approach was used to provide high-resolution markers that are typically biparentally inherited (i.e., nuclear markers). Western white pine AFLP protocols and analyses are described in Kim and others (2003).

Plant-Climate Modeling

Whitebark pine and western white pine bioclimatic models used species presence/absence data for more than 118,000 point locations described geographically by latitude, longitude, and elevation (see “Acknowledgments”). Climate was estimated for each of these locations using a spline climate model (Rehfeldt 2006). This procedure yielded a

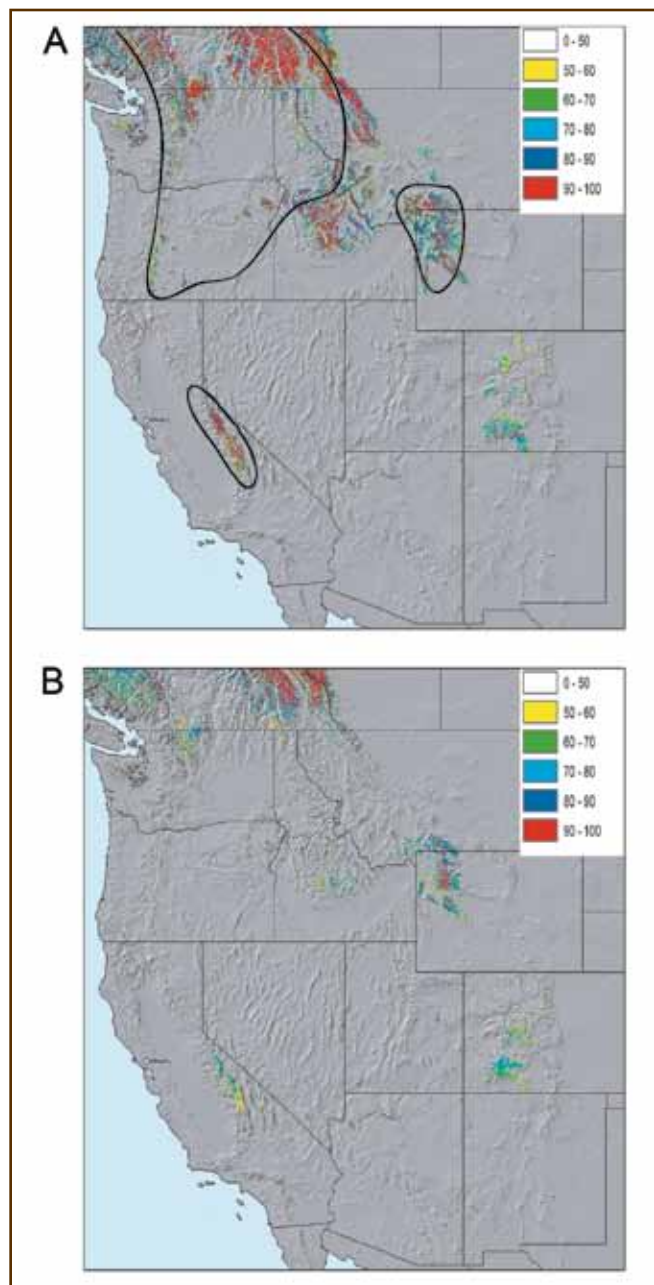


Figure 1—(A) The predicted contemporary distribution of whitebark pine (*Pinus albicaulis*) in the Western United States and southwestern Canada using a plant-climate model (Rehfeldt and others 2006). Pixel colors represent votes for whitebark pine occurrence; votes between 0 and 50 are not shown. The black drawn lines represent predicted metapopulations of whitebark pine based on chloroplast microsatellite molecular markers (Richardson and others 2002). (B) The predicted 2030 distribution of whitebark pine using the average of two general circulation models.

data set that described species presence or absence based on 33 climate variables representing simple interactions of

temperature or precipitation, or both, in relation to time, all of which have some relationship to plant responses. Random forests multiple classification tree analysis (Breiman 2001) was then used to identify climate variables important for predicting species presence and to build decision-tree-based bioclimatic models.

Arc map software (ESRI Inc.) was used to project the models predictions on a map. For this approach, the spline climate model was used to estimate climate in each 1-sq-km grid across the Western United States (more than 5.9 million pixels). Each pixel was then assessed using 100 independent decision trees. For each decision tree, a vote for or against species presence was cast. Pixels receiving vote tallies of 50 percent or greater were defined as having suitable climate space. These pixels are represented by the colored areas in Figures 1 and 2. These procedures are described in depth elsewhere (Rehfeldt and others 2006).

The response of a species contemporary suitable climate space under climate change was then assessed. The spline climate model was updated to the predicted climate of beginning in ca. 2030 using an average from the HadCM3GGa1 of the Hadley Centre (Gordon and others 2000) and CGCM2 of the Canadian Centre for Modeling and Analysis (Flato and Boer 2001) general circulation models. The procedure described in the previous paragraph was then repeated using the updated climate model to predict future climate for each pixel space.

Results

Whitebark Pine

Population Genetics—

Analysis of mtDNA reveals three haplotypes that are discretely partitioned among regions with two introgression zones. One introgression zone apparently occurs across a broad area in central Idaho, and another introgression zone occurs across a narrow area in the northern Cascades near Mount Rainier, Washington. The introgression of mtDNA haplotypes in the northern Cascades has been proposed to have resulted from the colonization of previously glaciated habitat during Holocene warming (Richardson and others 2002).

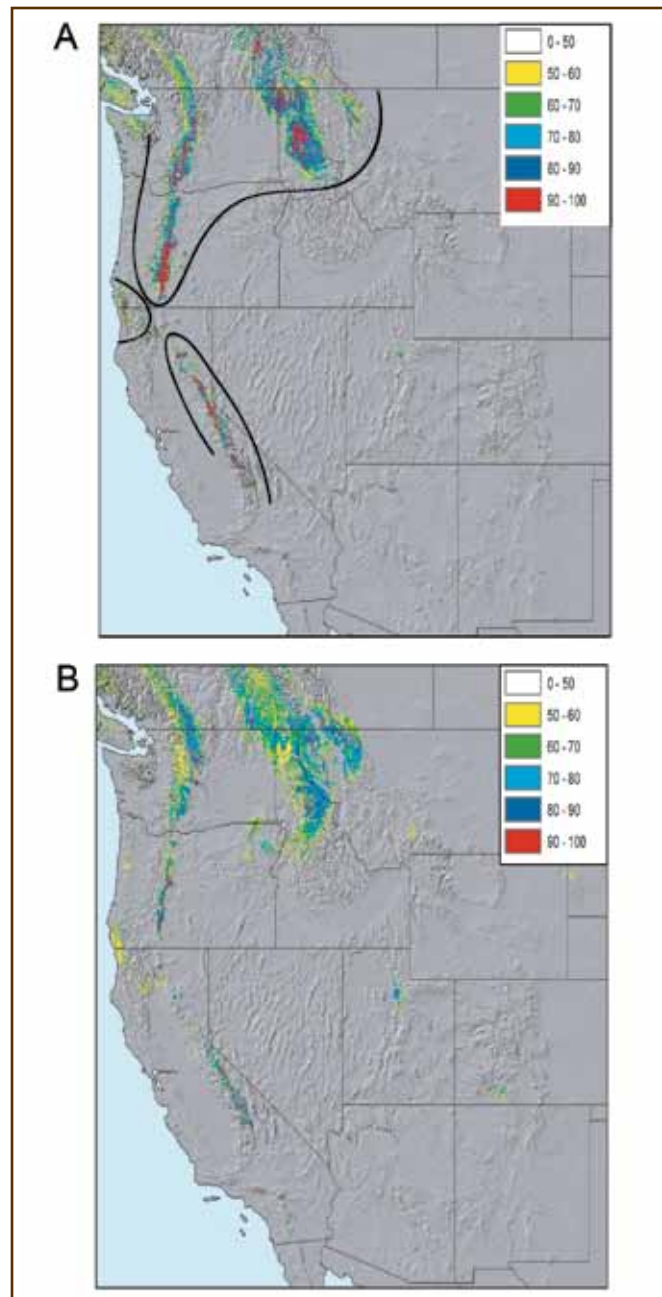


Figure 2—(A) The predicted contemporary distribution of western white pine (*Pinus moniticola*) in the Western United States and southwestern Canada using a plant-climate model (Rehfeldt and others 2006). Pixel colors represent votes for western white pine occurrence. The black drawn lines represent the predicted metapopulations of western white pine based on AFLP analyses. (B) The predicted 2030 distribution of western white pine using the average of two general circulation models.

Analysis of pollen gene flow using cpSSRs reveals broader population boundaries that include mtDNA

introgression zones. These data circumscribe three metapopulations: the Sierra Nevada Mountains, the Yellowstone region, and a large Pacific Northwest region that includes the northern Rocky Mountains and the Cascade (Figure 1A). Private alleles were typically found at low frequency within each region; however, one notable exception was the Sierra Nevada metapopulation that had a private allele at high frequency. Genetic diversity has been described as moderately high for cpSSR markers (Richardson and others 2002) to moderately low using allozyme analysis (reviewed in Bruederle and others 2001). Furthermore, genetic characterization of isolated populations in southern Oregon, northern California, and Nevada are still needed to assess genetic conservation efforts in these areas.

Plant-Climate Modeling—

The contemporary plant-climate model for whitebark pine fits its present distribution with remarkable precision. Comparisons between ground-truthed whitebark pine locations and predicted areas of suitable habitat showed an overall error rate of only 2.47 percent (Figure 1A). The mapped predictions for the occurrence of whitebark pine were more accurate than Little's (1971) published range maps (Warwell and others 2006). Based on two GCMs (Hadley and Canadian Centre for Climate Change), the projected climatic space for whitebark pine in ca. 2030 shows a dramatic change in comparison with the contemporary prediction. An estimated 70 percent of the current climate space for whitebark pine will be lost by 2030. Most of predicted loss occurs in the southern latitudes of the whitebark pine range, including the Oregon Cascades, Siskiyou, and northern Nevada mountain ranges, where current suitable habitats are limited to mountaintops in many locations (Figure 1B). The elevation of suitable climate space is also expected to rise 330 m, thereby leaving only the Sierra Nevada Mountains as a potential refuge with suitable climate space below 40° N latitude. In contrast, the model does predict suitable climate space will occur in central Colorado, which may represent a fundamental climate niche for whitebark pine. In the northern Rockies and Cascades, whitebark pine climate space is predicted to persist only among the highest elevations found in Yellowstone, south-central Idaho, Glacier National Park, and the northern Cascades. Areas north

of 50° N will also likely fit climatic space for whitebark pine, but these areas fell outside of the geographic window and are not included in the analyses.

Western White Pine

Population Genetics—

Analyses of AFLP loci discern three metapopulations in western white pine. These include a Pacific Northwest metapopulation that extends from the northern Rockies west to the Pacific and south along the Cascade Mountains to central Oregon. A distinct metapopulation exists in the Siskiyou Mountains of southern Oregon and northern California, and another metapopulation extends into the Sierra Nevada Mountains (Figure 2A). Like most other pines, western white pine contained moderate to high levels of heterozygosity in all three metapopulations (Kim and others unpublished).

Plant-Climate Modeling—

For western white pine, the contemporary climate space also fits with the current distribution with a small overall error of 3.85 percent. The projected current distribution of western white pine is shown in Figure 1A. The predicted 2030 climate space for western white pine provides a strong contrast with that of whitebark pine. Western white pine climate space is expected to increase 29 percent by 2030 (Figure 2B). Overall, suitable climate space for western white pine is expected to increase 157 m in elevation by 2030. This predicted expansion occurs in the northern latitudes, with notable expansion into northwestern Montana and northward into the Canadian Rocky Mountains. In the more southern latitudes of California and southern Oregon, populations are projected to persist at higher elevations. Predicted climate space is reduced in southern Oregon, thereby rendering the projected Sierra Nevada population more disjunct from the southern Cascades.

Discussion

Whitebark Pine

Past climate change has shaped the biogeography of whitebark pine and, hence, genetic relationships and potential adaptive traits. Since the last glacial maximum, whitebark

pine has apparently responded to the warming climate after the last glacial maximum by colonizing new habitat opened up by receding glaciers of the Canadian Rocky Mountains and the northern Cascades. Holocene expansion into the northern Cascade Mountains likely originated from source populations to the south and east of the north Cascades, based on the mtDNA at the contact zone (Richardson and others 2002). In contrast, a wider distribution of whitebark pine in more southern latitudes during the last glacial maximum was probably constricted to higher elevations by subsequent Holocene warming. This constriction in suitable habitat appears particularly dramatic in northern Nevada, where whitebark pine currently persists only on the highest mountaintops.

Population genetics of whitebark pine have identified distinct regional metapopulations occupying the Pacific Northwest (i.e., northern Rockies and Cascade Mountains), the greater Yellowstone region, and the Sierra Nevada. Other populations in the Great Basin and central Oregon have not been analyzed with mtDNA or cpSSR markers. However, allozyme analyses have shown distinct genetic structure among the Great Basin whitebark pine populations (Yandell 1992). Further studies to characterize genetic diversity and structure of whitebark pine in Washington and Oregon are in progress (Personal communication. C. Aubry. 2006. Area Geneticist, Olympia National Forest, 1835 Black Lake Blvd. Suite A, Olympia, WA 98512), and studies are assessing rangewide and regionwide adaptive traits in whitebark pine (Bower and Aitken 2006, Warwell and others unpublished). These studies and population genetic analyses are essential to determine appropriate genetic conservation efforts and proactive management that consider predicted climate change.

The contemporary climate space predicted using the plant-climate model is extremely precise for the distribution of whitebark pine. This precision has also been demonstrated with other western plant species (Rehfeldt and others 2006). The predicted suitable climate space for whitebark pine shows a dramatic reduction in the year 2030. At the highest risks are populations that currently only exist on mountaintops, where projected suitable climate space will be entirely lost from the region. Loss of local whitebark pine

populations is predicted to occur throughout the Oregon Cascades and mountaintops of northern Nevada, and further result in disjunct populations in the Sierra Nevada that will persist only at the highest elevations. These populations that face the highest risk of extirpation from predicted climate change and the white pine blister rust fungus should take priority for seed bank collections. Besides the Sierra Nevada, the plant-climate model predicts four major regions where climate space remains in the Western United States. These regions include the highest mountain ranges: the northern Cascades, Glacier National Park, south-central mountain ranges in Idaho, and the greater Yellowstone region. These regions that contain suitable climate space in 2030 predictions should be considered as priority regions for restoration efforts.

Western White Pine

Like whitebark pine, western white pine populations were also shaped by past climate change. This process created genetic structure with similarities to whitebark pine: a large Pacific Northwest metapopulation with partitions in southern Oregon and northern California (Kim and others unpublished). This population structure is also supported by an earlier study of isozyme markers (Steinhoff and others 1983). In addition, similar findings were reported in a study of adaptive traits for western white pine, showing a relationship between latitude and shoot elongation with a transition zone in southern Oregon (Rehfeldt and others 1984).

Again, the bioclimatic model predicted an excellent fit to the known distribution of western white pine. However, predicted 2030 climate space for western white pine shows a stark contrast to whitebark pine. The predicted increase in climate space is evident as an expansion in the northern Rocky Mountains that apparently relates to a slight increase in moisture. In the Sierra Nevada and Siskiyou Mountains, predicted climate space in 2030 does not show expansion. In these areas, moisture levels are predicted to increase more dramatically relative to the Pacific Northwest, and predicted climate becomes less suitable for western white pine, possibly owing to increased competition. Whereas losses of genetic diversity seem relatively small compared to whitebark pine, some areas of western white pine may

be at risk. Reductions in the abundance or extirpation of small isolated populations are conceivable for the Siskiyou Mountains and other areas of northern California where the western white pine populations exhibit a unique and diverse genetic background. Such populations should be considered as a priority for genetic conservation efforts.

Model Refinements and Uncertainties

Further refinements in the plant-climate model can be achieved by integrating knowledge from molecular and quantitative genetics. An important point is that this model currently utilizes ground-truthed locations for the entire distribution of each species for current and future predictions, ignoring genetic adaptation to local/regional climate. This model assumes that each climate-adapted population will be able to occupy its climate space in the future regardless of the geographic distance. For example, it is clear that the Sierra Nevada metapopulation of western white pine is genetically different and occupies a climate that is different from western white pine in the more northern latitudes. However, it is unclear where the populations occupying current climate space in Sierra Nevada may move in the future. Future plant-climate model improvements should be able to correlate climate variables and genetic data. Ongoing studies are focused on the delimiting population-based adaptive traits and refining molecular genetic data from western white pine populations to project suitable climates for these populations under current and future climate scenarios. Similar studies can be conducted with whitebark pine and other tree species, but this will require investing in efforts to conduct thorough, rangewide genetic studies.

Most uncertainty in the plant-climate model is associated with future climate scenarios and the GCMs. Precipitation is a major factor for predicting suitable climate space of plant species. For the Western United States and Canada, models display consistency for increased winter precipitation; however, summer precipitation predictions remain inconsistent (IPCC 2001). In addition, the time scale between loss of suitable climatic space and extirpation of local populations remains uncertain. Much of this uncertainty comes from site-specific biotic interactions. For example, two potential scenarios can be envisioned: (1) slow

attrition from succession where whitebark pine persists for decades or (2) stress from maladaptation leading to insect (e.g., bark beetle) outbreaks or disease (e.g., root rots) epidemics resulting in local extirpation within years. Projected scenarios are further complicated by mortality and loss of cone crops to white pine blister rust and insect attack. Continued studies are needed to address these uncertainties and improve predictions of climate-change impacts on distribution and population genetic structure of whitebark pine and western white pine.

Summary

Case studies were presented for whitebark pine and western white pine using plant-climate modeling of current and future climate predictions and genetic studies. These studies indicate dramatic differences in these two species' responses to climate change from the past and the future. These responses are largely dependent on the breadth of the ecological niches and life-history characteristics of each species. For whitebark pine, specialization for subalpine habitat is predicted to severely limit its distribution under future climate scenarios. Alternatively, coevolved relationships with Clark's nutcracker have enabled this species to colonize new habitat following Holocene warming. This characteristic may also aid its migration northward in the future, but successful migration to newly established suitable climate space is contingent upon the rate of climate change and the severity of impact from white pine blister rust and insect attack. Because western white pine has broader ecological range, it may be better suited to buffer effects of climate change. This ecological range is reflected in its predicted resilience under the future climate scenario. The creation of the plant-climate models and determining the impact from future climate scenarios for a particular species are dependent upon basic genetic research, both ecological and population genetics. Current research is focused on integration of genetic and climate data for these species. This approach represents a synthesis of multidisciplinary research to provide useful guidelines for forest management plans for genetic conservation and restoration that consider future climate change projections.

Acknowledgments

The authors thank Dr. Gerald Rehfeldt and Nick Crookston for their creative development of the plant-climate model used in this manuscript. Thanks to Drs. Carol Aubry and Dennis Ferguson for reviewing this manuscript. We also thank the following people and organizations for collections of whitebark pine and western white pine location data:

- Forest Inventory and Analysis (FIA)
- Andy Bower, Ph.D. Dissertation, University of British Columbia
- CalFlora Database (BLM: Eagle Lake Herbarium)
- CalFlora Database (Yosemite National Park Natural Resource Inventory)
- Donna Dekker (Lynn Wells and Ray Wiseman 1991 Report)
- John King and Mike Carlson, British Columbia Ministry of Forests
- Jodie Krakowski, Master's Thesis, University of British Columbia
- RMRS Field Data
- RMRS Northern Idaho Habitat Type Data
- Ulla Geralyn Yandell, Master's Thesis, University of Nevada, Reno
- USFS Whitebark Limber Pine Information System

Literature Cited

- Arno, S.F.; Hoff, R.J. 1989.** Silvics of whitebark pine (*Pinus albicaulis*). Gen. Tech. Rep. INT-253. Ogden, UT: U.S. Department of Agriculture, Forest Service, Intermountain Research Station. 11 p.
- Bower, A.D.; Aitken, S.N. 2006.** Geographic and seasonal variation in cold hardiness of whitebark pine. *Canadian Journal of Forest Research*. 36(7): 1842–1850.
- Breiman, L. 2001.** Random forests. *Mach Learn*. 45: 5–32.
- Bruederle, L.P.; Rogers, D.L.; Krutovskii, V.; Politov, D.V. 2001.** Population genetic and evolutionary implications. In: Tomback, D.F.; Arno, S.F.; Keane, R.E., eds. *Whitebark pine communities: ecology and restoration*. Washington, DC: Island Press: 137–153.
- Davis, M.B.; Shaw, R.G. 2001.** Range shifts and adaptive responses to quaternary climate change. *Science*. 292(5517): 673–679.
- Flato, G.M.; Boer, G.J. 2001.** Warming asymmetry in climate change simulations. *Geophysical Research Letters*. 28: 195–198.
- Godbout, J.; Jaramillo-Correa, P.; Beaulieu, J.; Bousquet, J. 2005.** A mitochondrial DNA minisatellite reveals the postglacial history of jack pine (*Pinus banksiana*), a broad-range North American conifer. *Molecular Ecology*. 14(11): 3497–3512.
- Gordon, C.; Cooper, C.; Senior, C.A. [and others]. 2000.** The simulation of SST, sea ice extents, and ocean heat transports in a version of the Hadley Centre coupled model without flux adjustments. *Climate Dynamics*. 16(2-3): 147–168.
- Intergovernmental Panel on Climate Change (IPCC). 2001.** The scientific basis: contributions of working group 1 to the second assessment report of IPCC. From <http://www.ipcc.ch/>. [Date accessed unknown].
- Jackson, S.T. 2006.** Forest genetics in space and time. *New Phytologist*. 171(1): 1–3.
- Jump, A.S.; Peñuelas, J. 2005.** Running to stand still: adaptation and the response of plants to rapid climate change. *Ecology Letters*. 8(9): 1010–1020.
- Kim, M.S.; Brunsfeld, S.J.; McDonald, G.I.; Klopfenstein, N.B. 2003.** Effect of white pine blister rust *Cronartium ribicola* and rust-resistance breeding on genetic variation in western white pine *Pinus monticola*. *Theoretical and Applied Genetics*. 106(6): 1004–1010.
- Little, E.L., Jr. 1971.** Atlas of United States trees. Misc. Pub. 1146. Washington, DC: U.S. Department of Agriculture, Forest Service. 320 p.
- Magri, D.; Vendramin, G.G.; Comps, B. [and others]. 2006.** A new scenario for the Quaternary history of European beech populations: palaeobotanical evidence and genetic consequences. *New Phytologist*. 171(1): 199–221.

- Malcolm, J.R.; Markham, A.; Neilson, R.P.; Garaci, M. 2002.** Estimated migration rates under scenarios of global climate change. *Journal of Biogeography*. 29(7): 835–849.
- Mattson, D.J.; Kendall, K.C.; Reinhart, D.P. 2001.** Whitebark pine, grizzly bears, and red squirrels. In: Tomback, D.F.; Arno, S.F.; Keane, R.E., eds. *Whitebark pine communities: ecology and restoration*. Washington, DC: Island Press: 121–136.
- McDonald, G.I.; Hoff, R.J. 2001.** Blister rust: an introduced plague. In: Tomback, D.F.; Arno, S.F.; Keane, R.E., eds. *Whitebark pine communities: ecology and restoration*. Washington, DC: Island Press: 193–220.
- Petit, R.J.; Bialozyt, R.; Garnier-Géré, P.; Hampe, A. 2004.** Ecology and genetics of tree invasions: from recent introductions to Quaternary migrations. *Forest Ecology and Management*. 197(1–3): 117–137.
- Rehfeldt, G. 2006.** A spline model of climate for the Western United States. Gen. Tech. Rep. RMRS-165. Fort Collins, CO: U.S. Department of Agriculture, Forest Service, Rocky Mountain Research Station. 21 p.
- Rehfeldt, G.E.; Crookston, N.L.; Warwell, M.V.; Evans, J.S. 2006.** Empirical analyses of plant-climate relationships for the Western United States. *International Journal of Plant Sciences*. 167: 1123–1150.
- Rehfeldt, G.E.; Hoff, R.J.; Steinhoff, R.J. 1984.** Geographic patterns of genetic variation in *Pinus monticola*. *Botanical Gazette*. 145: 229–239.
- Richardson, B.A.; Brunsfeld, S.J.; Klopfenstein, N.B. 2002.** DNA from bird-dispersed seed and wind-disseminated pollen provides insights into postglacial colonization and population genetic structure of whitebark pine (*Pinus albicaulis*). *Molecular Ecology*. 11(2): 215–227.
- Richardson, B.A.; Klopfenstein, N.B.; Peever, T.L. 2005.** Assessing forest-pathogen interactions at the population level. In: Lundquist, J.E.; Hamelin, R.C., eds. *Forest pathology: from genes to landscapes*. St. Paul, MN: APS Press: 21–30.
- Steinhoff, R.J.; Joyce, D.G.; Fins, L. 1983.** Isozyme variation in *Pinus monticola*. *Canadian Journal of Forest Research*. 13: 1122–1133.
- Thompson, R.S.; Anderson, K.H. 2000.** Biomes of Western North America at 18,000, 6000 and 0 C-14 yr BP reconstructed from pollen and packrat midden data. *Journal of Biogeography*. 27(3): 555–584.
- Thompson, R.S.; Whitlock, C.; Bartlein, P.J. [and others]. 1993.** Climatic changes in the Western United States since 18,000 year B.P. In: Wright, H.E.; Kutzbach, J.; Webb, T. [and others], eds. *Global climates since the last glacial maximum*. Minneapolis: University of Minnesota Press: 468–513.
- Tomback, D. 2001.** Clark's nutcracker: agents of regeneration. In: Tomback, D.F.; Arno, S.F.; Keane, R.E., eds. *Whitebark pine communities: ecology and restoration*. Washington, DC: Island Press: 89–104.
- Vander Wall, S.B.; Balda, R.P. 1981.** Ecology and evolution of food-storage behavior in conifer-seed-caching corvids. *Zeitschrift Fur Tier Psychologie*. 56: 217–242.
- Warwell, M.V.; Rehfeldt, G.E.; Crookston, N.L. 2006.** Modeling contemporary climate profiles of whitebark pine (*Pinus albicaulis*) and predicting responses to global warming. In: Goheen, E., ed. *Proceedings of the conference: Whitebark pine: a Pacific coast perspective*. R6-NR-FHP-2007-01. U.S. Department of Agriculture, Forest Service, Ashland, OR: 139–142. <http://www.fs.fed.us/r6/nr/fid/wbpine/papers/2007-wbp-climate-warwell.pdf>. [Date accessed unknown].
- Wellner, C.A. 1962.** Silvics of western white pine. Misc. Pub. 26. Ogden, UT: U.S. Department of Agriculture, Forest Service, Intermountain Forest and Range Experiment Station. 24 p.
- Whitlock, C. 1993.** Postglacial vegetation and climate of Grand Teton and Southern Yellowstone National Parks. *Ecological Monographs*. 63: 173–198.
- Yandell, U.G. 1992.** Allozyme analysis of whitebark pine. Reno, NV: University of Nevada. 59 p. M.S. thesis.

This page is intentionally left blank

Threats to Private Forest Lands in the U.S.A.: A Forests on the Edge Study

Susan M. Stein, Mark H. Hatfield, Ronald E. McRoberts, Dacia M. Meneguzzo, and Sara Comas

Susan M. Stein, Forests on the Edge Coordinator, USDA Forest Service, Cooperative Forestry Staff, State and Private Forestry, Washington, DC 20250; **Mark H. Hatfield**, forester, **Ronald E. McRoberts**, mathematical statistician, and **Dacia M. Meneguzzo**, forester, USDA Forest Service, Northern Research Station, St. Paul, MN 55108; and **Sara Comas**, wildlife specialist, USDA Forest Service, Cooperative Forestry Staff, State and Private Forestry, Washington, DC 20250.

Abstract

The Forests on the Edge project, sponsored by the USDA Forest Service, uses geographic information systems to construct and analyze maps depicting threats to the contributions of America's private forest lands. For this study, watersheds across the conterminous United States are evaluated with respect to the amount of their private forest land. Watersheds with at least 10 percent forest land, of which 50 percent is privately owned, are then ranked relative to the contributions of their private forest lands to water quality, timber supply, at-risk species habitat, and interior forest. In addition, threats from housing development, fire, air pollution, and insect pests and disease to private forest land contributions are assessed. Results indicate that private forest lands contributions and threats are concentrated in the Eastern and Southeastern United States but are also distributed throughout the north-central, central hardwoods, and Pacific Northwest regions.

Keywords: Ecological services, forest contributions, geographic information systems, fourth-level watershed, land use change, private forest, sustainable forest management.

Introduction

America's forest lands contribute in a myriad of ways to the economic, ecological, and social well-being of the

Nation. Increasingly, however, forest lands are threatened from a variety of sources including urbanization, low-density housing development, climate change, invasive flora and fauna, wildfire, pollution, fragmentation, and parcelization. The increasing emphasis on sustainable forest management and loss of open space requires quantitative and spatial assessments of the impacts of threats to forest lands and their contributions. The Forests on the Edge (FOTE) project, sponsored by the Cooperative Forestry Staff, State and Private Forestry, USDA Forest Service, conducts map-based assessments of threats to the private forest lands of the United States using spatial data layers and geographic information systems. The objectives of the study described here are threefold: (1) to construct nationally consistent data layers depicting the spatial location of private forest lands and their contributions; (2) to construct similar layers depicting threats to the contributions of private forest land from sources such as conversion to urban and exurban uses, wildfire, and pollution; and (3) to identify watersheds whose private forest lands simultaneously make the most important contributions and face the greatest threats.

The Montreal process criteria and indicators provide an appropriate context for framing and conducting these assessments (McRoberts and others 2004). For example, criterion 2, maintenance of the productive capacity of forest ecosystems, includes indicators related to forest area and timber production; criterion 3, maintenance of forest ecosystem health and vitality, includes indicators related to fire, wind, disease, and insects; and criterion 4, conservation and maintenance of soil and water resources, includes indicators related to the contributions of forests to water quality.

Data Layers

All data layers were obtained as or constructed to be nationally consistent and were summarized at the spatial scale of fourth-level watersheds (Steeves and Nebert 1994). Watersheds were selected as the analytical units because they highlight the important connections between private forests and ecological processes.

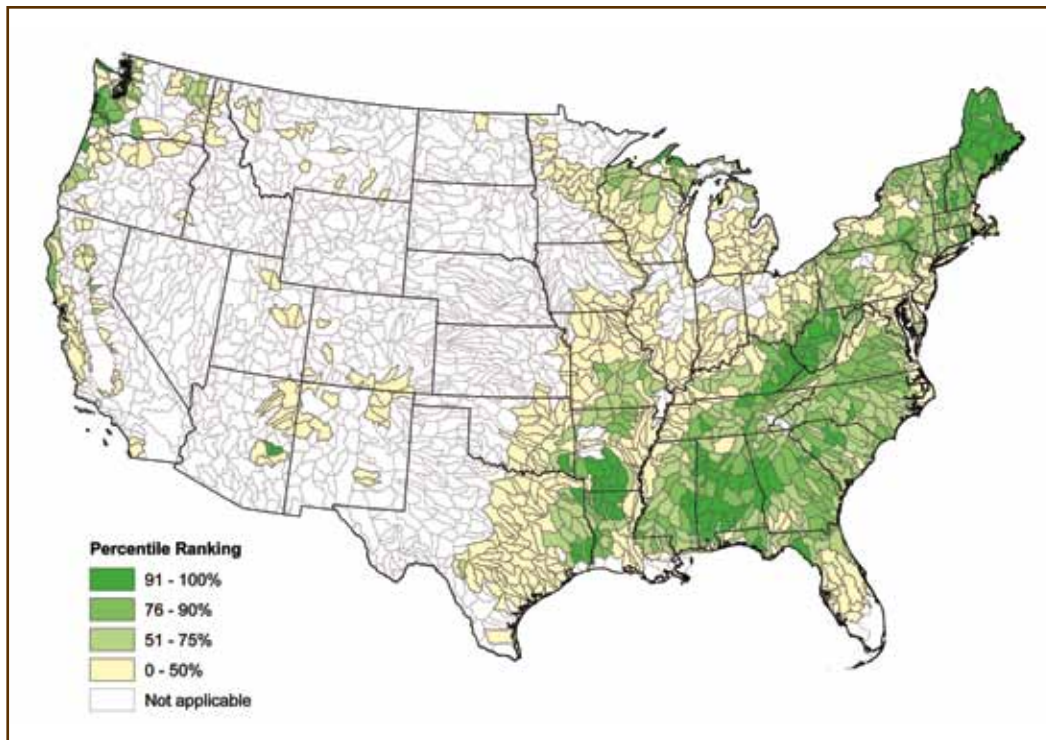


Figure 1—Percentile rankings of watersheds with respect to percentage of private forest land.

Private Forest Contributions

Area of Private Forest Land—

A 100-m-resolution forest ownership layer was constructed by aggregating the classes of the National Land Cover Dataset (NLCD) (Vogelmann and others 2001) into forest and nonforest classes and using the Protected Areas Database (PAD) (DellaSalla and others 2001) to distinguish ownership and protection categories. The emphasis for this study was private forest land, which includes tribal, forest industry, and nonindustrial ownerships. Stein and others 2005a, 2005b) provide detailed information on this layer. Only watersheds with at least 10 percent forest land, of which 50 percent is privately owned, qualified for subsequent analyses. Figure 1 depicts the percentile rankings of qualifying watersheds relative to the percentage of privately owned forest land; for example, a watershed in a 91 to 100-percentile category has a higher percentage of private forest land than at least 90 percent of the qualifying watersheds.

Water Quality—

Private forest lands provide nearly 60 percent of all water flow from U.S. forests and nearly 30 percent of the water

flow originating on land in the Lower 48 States (Personal communication. Thomas C. Brown. 2004. Hydrologist, Rocky Mountain Research Station, 2150 Centre Ave. Bldg. A, Suite 376, Fort Collins, CO 80526). Water flow from private forests is generally considered clean relative to water flow from other land uses and, therefore, makes a positive contribution to water quality. The water quality layer depicts the contribution of private forest land to the production of clean water and is based on three underlying assumptions: (1) water bodies near the heads of hydrologic networks are more sensitive to the loss of forest buffers than water bodies near the bases of the networks, (2) the presence or absence of upstream forest buffers influences water quality downstream in the networks, and (3) forest lands throughout watersheds, not just those in immediate proximity to water bodies, are important when considering the contributions of private forest land to water quality (FitzHugh 2001).

The water quality layer was constructed from two underlying layers, the forest ownership layer and the National Hydrography Dataset (NHD) (USGS 2000), which depicts water bodies in the 48 contiguous States. The

layer was constructed in four steps: (1) 30-m buffer was constructed around all water bodies, (2) the buffers were intersected with the private forest land class of the forest ownership layer to quantify the amount of private forest land in proximity to water bodies, (3) each buffer segment was assigned to one of four categories based on the relative position of the segment to the head of its hydrologic network, and (4) for each watershed, the percentage in each of the four categories was determined. Water quality index (WQI) was then calculated for each watershed as,

$$WQI = 0.6[A_1 + (A_1A_2)] + 0.4(0.48B_1 + 0.24B_2 + 0.16B_3 + 0.12B_4)$$

where A_1 = percentage of watershed in private forest land, A_2 = percentage of total forest land in watershed that is privately owned, B_1 = percentage of private forest land buffer in the first category (nearer head of hydrologic network headwater), B_2 = percentage of buffer in the second category, B_3 = percentage of buffer in third category, and B_4 = percentage of buffer in fourth category (farthest downstream from the head of hydrologic network). Variables A_1 and A_2 represent private forest coverage throughout the watershed, and variables B_1 through B_4 represent private forest coverage in the buffers. In WQI, A_1 and A_2 are collectively weighted 0.6, whereas variables B_1 through B_4 are collectively weighted 0.4 to reflect the third assumption above. Watershed boundaries for this and all other layers were determined using Steeves and Nebert (1994).

Timber Supply—

Private forest lands make a substantial contribution to America's timber resources, accounting for 92 percent of all timber harvested in the United States in 2001 (Smith and others 2004). The timber supply layer depicts the ranking of watersheds relative to an index of the importance of private timberland and is based on Forest Inventory and Analysis (FIA) plot data (<http://www.fia.fs.fed.us/tools-data/default.asp>). The private timberland importance index (TI) is based on three subindices of contributions of the timberland subset of private forest land. Timberland is defined by the FIA program as forest land that has not been withdrawn from production and that is capable of producing 20 cubic feet per year of industrial wood. For each watershed, the three subindices are calculated as follows: (1) growth index (GI)

is the average growing stock volume growth rate on private timberland in a watershed relative to the average across all private timberland, (2) volume index (VI) is the average net growing stock volume per acre on private timberland in a watershed relative to the average on all private timberland, and (3) area index (AI) is the ratio of private timberland area to total private land area in a watershed relative to the same ratio across all watersheds. TI was calculated for each watershed as, $TI = AI(GI + VI)$.

At-Risk Species—

Private forests provide the key to conservation for many species. In the Pacific Northwest, they provide significant habitat for the spotted owl (Holthausen and others 1995). NatureServe and its member Natural Heritage Programs and Conservation Data Centres, prepared a geographic data set depicting the number of at-risk species occurring on private forested lands within fourth-level watersheds in the Lower 48 States of the United States. At-risk species are defined as species with element occurrences (EO) that have been observed by an authoritative source within at least the last 50 years, and are either: (1) federally designated under the Endangered Species Act (Endangered, Threatened, Candidate, Proposed), or (2) designated as critically imperiled, imperiled, or vulnerable according to the NatureServe Conservation Status Ranking system (G1/T1- G3/T3) (<http://www.natureserve.org/explorer/ranking.htm>). An EO is an area of land or water, or both, in which a species or natural community is, or was, present.

NatureServe selected populations that only occur on private forested lands by conducting a geographic analysis comparing the location of at-risk populations with private forest locations (both protected and nonprotected). These species are labeled as forest-associated as opposed to forest-obligated because a separate analysis to refine this species list using knowledge of species habitat requirements and preferences was not conducted. Known data gaps include: (1) no at-risk species data available in Arizona, Massachusetts, and the District of Columbia, (2) no at-risk fish data available for Idaho, and (3) at-risk animal data in Washington are incomplete. Private forested lands were determined using the data layer described in the "Area of Private Forest Land" section.

Interior Forest and Habitat Contiguity—

Habitat contiguity is an index of the structural integrity of forests, an important conservation concern (Wear and others 2004). Habitat contiguity can be measured in terms of the amount of interior forest cover that is functionally distinct from forest edge. The interior forest layer was created using three steps. First, the forest cover layer described in the section “Area of Private Land” was used to identify forested pixels in each watershed. Second, forested pixels were labeled interior forest if 90 percent of the pixels in a surrounding 65-ha window were also forested. Third, the proportion of interior forest pixels in each watershed was determined, and all watersheds were assigned a percentile ranking based on this proportion. Note that a watershed could have very little forest land but a high proportion that satisfied the interior forest criteria.

Threats to Private Forest Lands**Development—**

The development layer depicts predicted threats to private forest lands resulting from conversion to urban or exurban uses. The layer is based on estimates of current population and housing density data obtained from the 2000 U.S. Census, and predictions of housing density increases. A spatially explicit model was used to predict the full urban-to-rural spectrum of housing densities (Theobald 2005). The model uses a supply-demand-allocation approach and is based on the assumption that future growth patterns will be similar to those in the past decade. Future patterns are forecast on a decadal basis in four steps:

1. The number of new housing units in the next decade is forced to meet the demands of the predicted populations.
2. A location-specific average population growth rate from the previous to current time step was computed for each of four density classes: urban, suburban, exurban, and rural.
3. The spatial distribution of predicted new housing units was adjusted with respect to accessibility to the nearest urban core area.
4. Predicted new housing density was added to the

current housing density under the assumption that housing densities do not decline over time.

For these analyses, predicted new housing was not permitted to occur on protected private land as indicated by PAD (DellaSalla and others 2001). The spatially explicit housing density predictions were combined with the forest ownership layer to identify watersheds with the greatest predicted conversion of private forest land to urban and exurban uses. Stein and others (2005b) provided detailed information on this layer.

Wildfire—

Although wildfire is one of the most compelling threats to forest land, particularly in the Western United States, predicting the threat of wildfire incidence is extremely complex and relies on a variety of regional models and regional variables. Further, even if the models could be readily implemented to construct a national layer, the geographic consistency of the layer would be questionable. Therefore, as a surrogate for wildfire risk, FOTE used the 1-km by 1-km-resolution current fire condition class (CFCC) data, which depict deviations of fire incidence from historical natural fire regimes and estimated efforts necessary to restore stands to historical regimes (Schmidt and others 2002). These data reflect the assignment of forest lands to one of three CFCC classes:

1. CFCC₁—forest lands with fire regimes that are within or near historical ranges and that can be maintained by treatments such as prescribed fire or fire use.
2. CFCC₂—forest lands with fire regimes that have been moderately altered from historical ranges and that may require moderate levels of prescribed fire, fire use, hand or mechanical treatment, or a combination to restore to historical fire regime.
3. CFCC₃—forest lands with fire regimes that have been substantially altered from historical ranges and that may need high levels of hand or mechanical treatment before fire is used to restore historical fire regimes.

The appeal of the CFCC classes is that they are objective, nationally consistent, and are assumed to correlate well

with the threat of wildfire incidence. Although these classes reflect the widely varying State-level commitments to wildfire mitigation efforts, they do not reflect ease of access to forest lands experiencing wildfire or the availability of resources to combat wildfires.

For each watershed, all private forest lands were assigned to one of the three CFCC classes, and a watershed-level index was calculated as,

$$CC = CC_1 + 2CC_2 + 4CC_3,$$

where CC_i is the area of private forest land in class $CFCC_i$. The wildfire layer used for this study depicts the percentile ranking of each watershed with respect to its CC index value.

Ozone

Ozone affects forest ecosystems by causing foliar lesions and rapid leaf aging, altering species compositions, and weakening pest resistance (Chappelka and others 1997, Miller and others 1996). It is the only gaseous air pollutant that has been measured at known phytotoxic levels at both remote and urbanized forest locations (US EPA 1996).

The ozone layer depicts private forest land threatened by ground-level ozone and was based on late summer observations by FIA field crews of ozone damage to bioindicator species known to be sensitive to ground-level ozone. Data for more than 2,500 FIA plots were available for the study. Each plot was assigned a biosite value based on a subjective assessment by trained observers of the quantity and severity of damages (Coulston and others 2003, Smith and others 2003). Inverse distance weighted interpolation was used to create a map of ozone damage. This map was then combined with the forest ownership layer to identify private forest land with elevated levels of ozone damage. For each watershed, the percentage of private forest land in moderate or high-damage categories was calculated.

Nitrate and Sulfate Deposition—

Acidic deposition, the transfer of strong acids and acid-forming substances from the atmosphere to the Earth, has become a critical stress affecting forested landscapes across the United States. Effects can include increased sulfate and nitrate levels in soils and waters, which, in

turn, can alter soil and water chemistry and affect trees and other living organisms that depend upon affected soils and waters (Driscoll and others 2001). The nitrate and sulfate layers were created from National Atmospheric Deposition Program data. The data were used to interpolate yearly wet sulfate and wet nitrate deposition maps using gradient plus inverse distance interpolation (Nalder and Wein 1998). This technique adjusts for elevational, longitudinal, and latitudinal gradients when present in the data based on local regression of the 20 nearest neighbors. The wet sulfate deposition maps (2000-2004) were then averaged to produce a map of average annual deposition 2000-2004 (kg/ha per year). The same was done for wet nitrate deposition. Cross-validation (Issaks and Srivastava 1989) was performed to estimate the bias and precision of the yearly map.

Insect Pests and Disease—

Forest insect pests and diseases can affect forest health, including the reduction of tree basal area. The Forest Health Monitoring Program of the USDA Forest Service formed a Risk Map Integration Team (RMIT) to coordinate the development of a nationally consistent database for mapping insect pest and disease risk. The RMIT developed a GIS-based multicriteria risk modeling framework based on Eastman's risk assessment process (Eastman and others 1997).

A five-step multicriteria process was used to construct a 1-km by 1-km-resolution map depicting risk (Krist and others 2006): (1) Identify a list of forest pests (risk agents) and their target host species; this is conducted at the regional level with certain models constrained to select geographic areas. (2) Identify, rank, and weight criteria (factors and constraints) that determine the susceptibility and vulnerability to each risk agent. (3) Standardize risk agent criteria values, and combine the resultant criteria maps in a final risk assessment using a series of weighted overlays. Users assign a level of potential to values within GIS layers that represent criteria. (4) Convert modeled values of potential risk of mortality for each pest to predicted basal area (BA) loss over a 15-year period. This is accomplished for each risk agent/forest host species pair included in the national risk assessment. (5) Compile the resultant values from step 4 and identify areas (1-km raster grid cells) on a national base

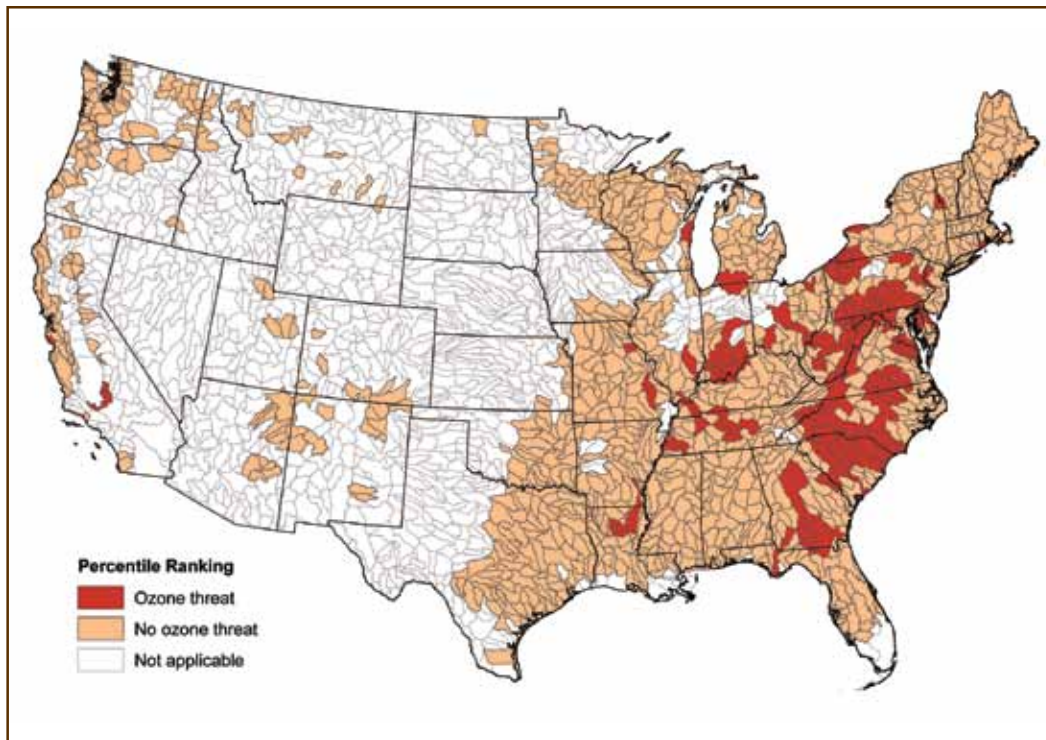


Figure 2—Percentile ranking of watersheds with respect to ozone threat.

map that are at risk of encountering a 25-percent or greater loss of total basal area in the next 15 years.

Methods

For each contribution and threat layer, the distribution of watershed index values was determined, and a percentile ranking was assigned to each watershed. Threats to particular contributions were evaluated in two steps. First, the averages of the contribution and threat percentile rankings were calculated on a watershed-by-watershed basis. Second, the distribution of the averages was determined and used to assign a new percentile ranking to each watershed. The results are depicted using percentile-based categories similar to those used for individual contributions and threats.

Results

The results are briefly discussed. Because of space limitations, only a few maps presenting data on individual layers of contributions or threats are displayed here. Instead, this paper focuses on some of the more interesting intersections of contributions and threats in the “Threats” section.

Contributions

Watersheds with the greatest percentages of private forest land are generally in New England, the Southeast, and the Pacific Northwest (Figure 1). The concentration in the East is not surprising because much of the forest land in the West is in public ownership. Watersheds whose private forests make the greatest contributions to water quality, timber supply, at-risk species habitat, and interior forest closely align with the watersheds with greatest amounts of private forest land.

Threats

Development threats to private forest land area are concentrated in southern New England and the Southeast, although some are also found in the Pacific Northwest; wildfire threats to private forest land (as indicated by the surrogate CC layer), are primarily in the Northeastern quadrant of the country. Data for these two layers are shown in conjunction with the “contributions” data in the next paragraphs. Threats to private forests from ozone are found scattered throughout the Eastern United States (Figure 2). Loss of basal area on

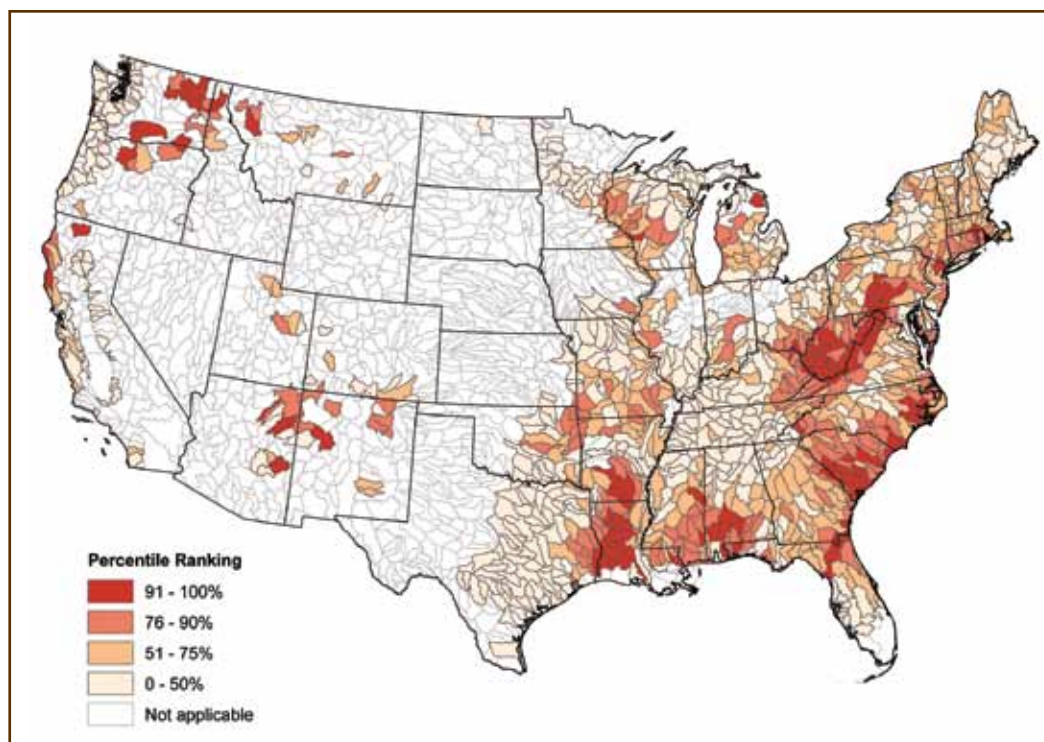


Figure 3—Percentile rankings of watersheds with respect to loss of basal area of private forests associated with insect pests and diseases.

private forest land from insect pests and diseases is most likely to occur in the East, but also in the lake States, the Southwest, California, and the Northwest (Figure 3).

Development threat to at-risk species associated with private forest is highest in the East, including Tennessee, North Carolina, and States immediately north and south of these States, as well as coastal California and the Pacific Northwest (Figure 4). Development threats to private interior forests are found throughout the Eastern United States and the Great Lakes area and are concentrated in the Southeast and Maine (Figure 5). Development threats to the contributions of private forest land to both water quality and timber supply are concentrated in southern New England and the Southeast (due to space limitations, these maps are not shown here).

Wildfire threats to both water quality and timber supply contributions are distributed throughout the East, the lake States, the central hardwoods region, and the Pacific Northwest (Figures 6 and 7).

Conclusions

Four primary conclusions may be drawn from this study:

1. The FOTE spatial approach to assessing threats to the contributions of private forest lands produces useful, visual information that is relatively easy to obtain. The only serious impediment is the difficulty in obtaining or constructing nationally consistent data layers that depict the contributions and threats of interest.
2. The watersheds making the greatest private forest contributions to water quality, timber supply, at-risk species, and interior forest are generally the watersheds with the greatest percentages of private forest land (i.e., those in the Eastern United States, particularly New England and the Southeast, and some watersheds in the Pacific Northwest). Two exceptions are noted. Some watersheds in western California and Florida do not have large amounts of private forest but do have large numbers of at-risk forest-associated species. In addition, some

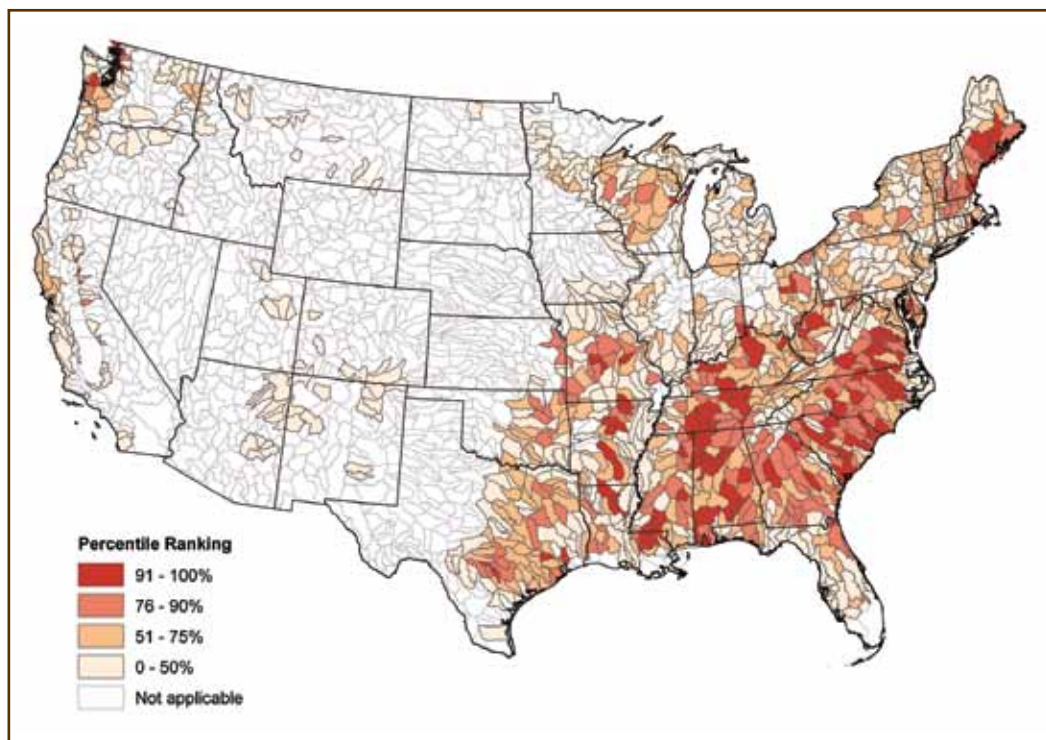


Figure 4—Percentile rankings of watersheds with respect to housing development threat to contribution of private forest land to at-risk species habitat.

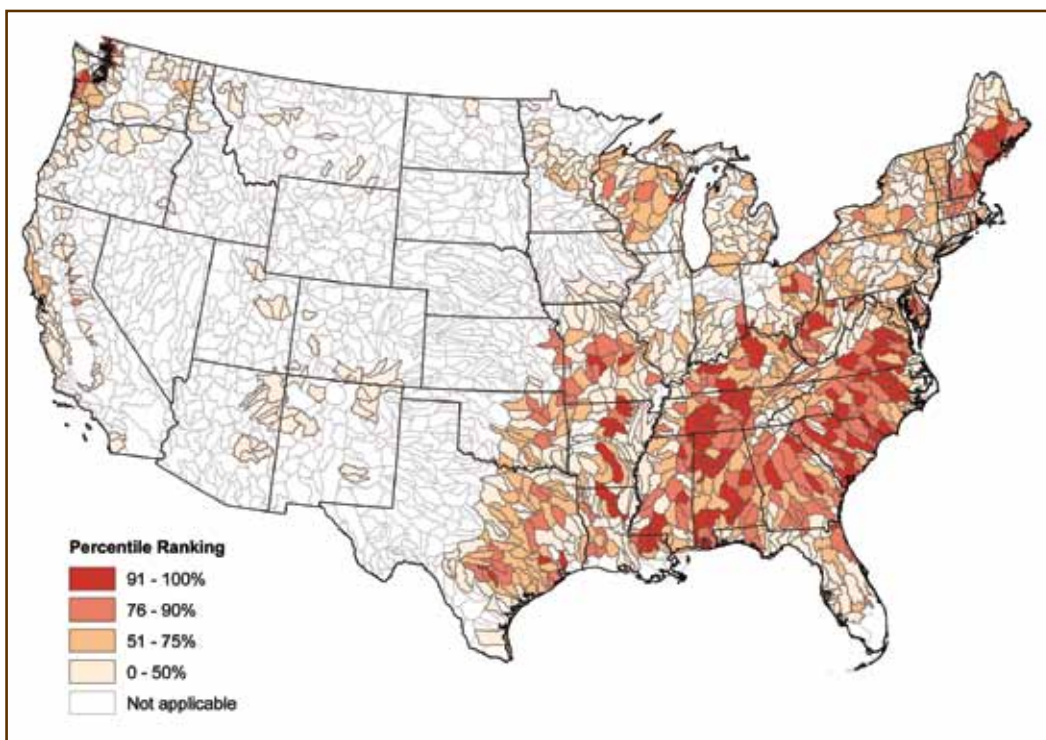


Figure 5—Percentile rankings of watersheds with respect to housing development threat to interior forest on private lands.

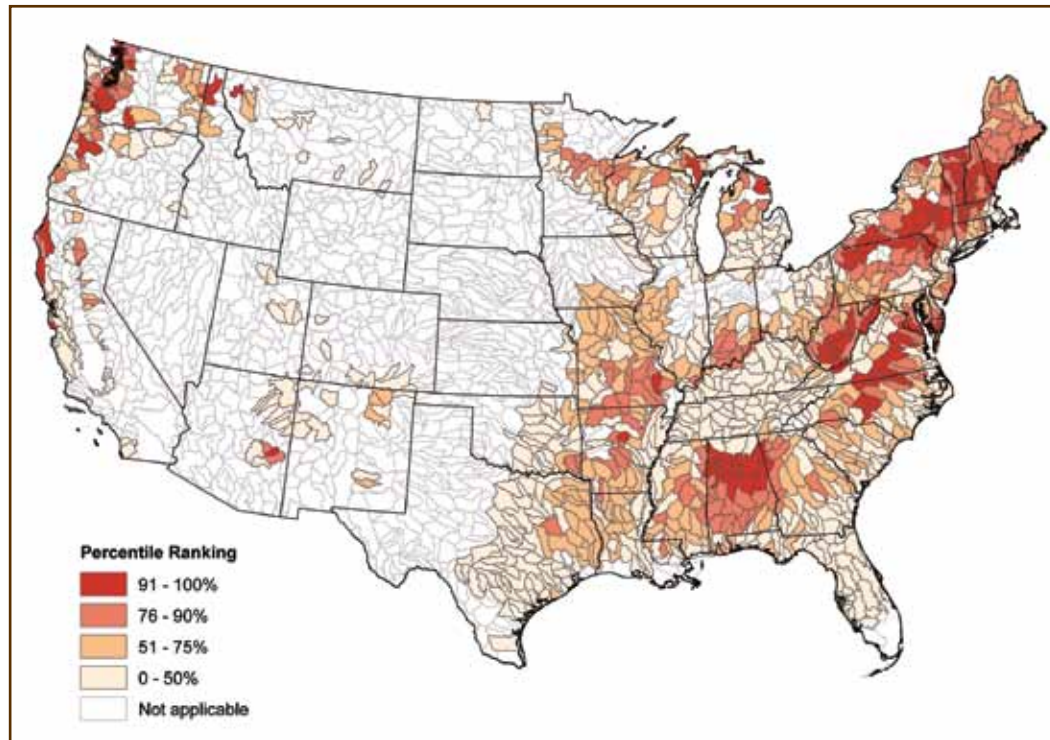


Figure 6—Percentile rankings of watersheds with respect to wildfire threat to contribution of private forest land to water quality.

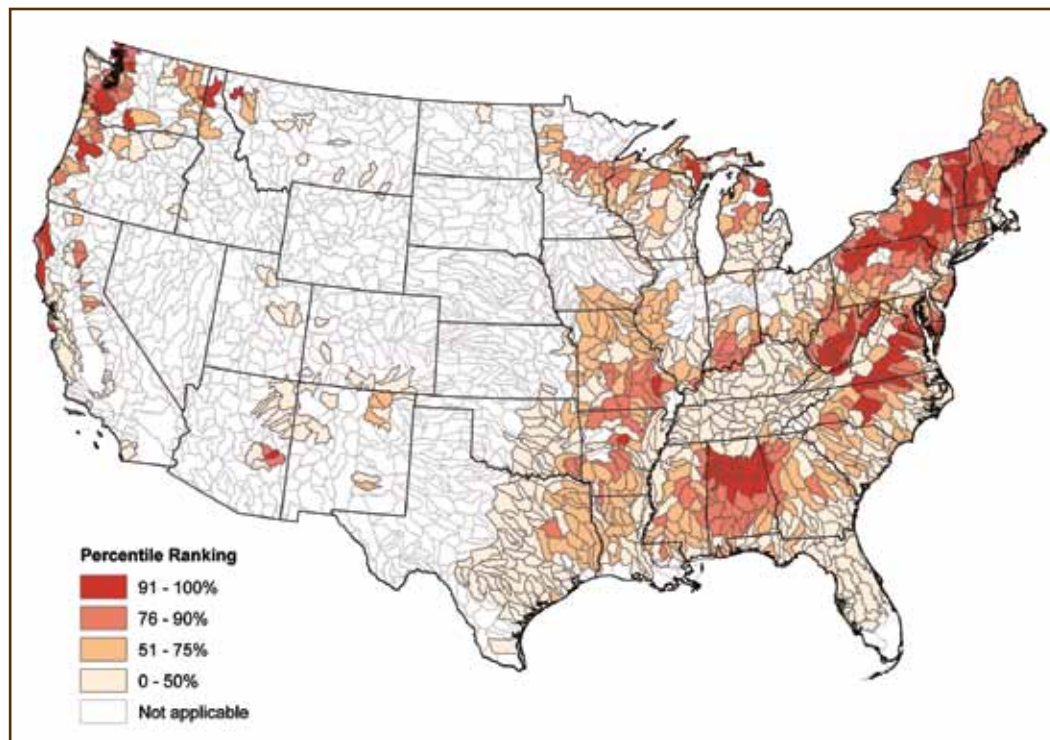


Figure 7—Percentile rankings of watersheds with respect to wildfire threat to contribution of private forest land to timber supply.

watersheds in eastern Texas, the Southwest, and Washington State also do not have large amounts of private forest but do have high proportions of private forest classified as interior forest.

3. Watersheds with the greatest development threat to the contributions to water quality, timber supply, at-risk species, and interior forest are also generally the watersheds with the greatest percentages of private forest land. The exceptions for at-risk species and interior forest noted in the previous paragraph apply here as well.
4. The CC surrogate for wildfire depicts the greatest threats to watersheds in the central part of the Eastern United States and the Pacific Northwest (although watersheds in the central part of the United States have relatively small percentages of private forest land). Percentile rankings of watersheds based on wildfire threat to private forest contribution to water quality and timber supply follow this pattern as well.

Future Forests on the Edge work will include assessment of additional contribution and risk intersections and the construction of an Internet-based system that permits users to select particular contribution and threat layers, options for combining them, and options for depicting the results. In addition, an assessment of national forests and grasslands most likely to experience increased pressures from housing development on adjacent lands is nearing completion. For more information on Forest on the Edge, go to our Web site at <http://www.fs.fed.us/openspace/fote>.

Acknowledgments

The authors acknowledge the contributions of the following individuals who constructed layers or provided assistance in data processing, coordination of contributions, and consultations: Xiaoping Zhou and John Mills of the Pacific Northwest Research Station, USDA Forest Service; Lisa Mahal, University of Nevada, Las Vegas; Greg Liknes, Northern Research Station, USDA Forest Service; John W. Coulston, Southern Research Station, USDA Forest Service; Frank Krist, Jr., Forest Health Technology Enterprise Team, USDA Forest Service; and Marcos Robles, NatureServe.

Literature Cited

- Chappelka, A.; Renfro, J.R.; Somers, G.L. 1997.** Evaluation of ozone injury on foliage of black cherry (*Prunus serotina*) and tall milkweed (*Asclepias exalta*) in Great Smokey Mountains National Park. *Environmental Pollution*. 95: 13–18.
- Coulston, J.W.; Smith, G.C.; Smith, W.D. 2003.** Regional assessment of ozone-sensitive tree species using bioindicator plants. *Environmental Monitoring and Assessment*. 83: 113–127.
- DellaSala, D.A.; Staus, N.L.; Strittholt, J.R. [and others]. 2001.** An updated protected areas database for the United States and Canada. *Natural Areas Journal*. 21: 124–135.
- Driscoll, C.T.; Lawrence, G.B.; Bulger, A.J. [and others]. 2001.** Acidic deposition in the Northeastern United States: sources and inputs, ecosystem effects, and management strategies. *Bioscience*. 51(3): 180–198.
- Eastman, J.R.; Emani, S.; Hulina, S. [and others]. 1997.** Applications of geographic information systems (GIS) technology in environmental risk assessment and management. Worcester, MA: Clark Labs/Clark University (In cooperation with UNEP). [Number of pages unknown].
- FitzHugh, T. 2001.** Watershed characteristics and aquatic ecological integrity: a literature review. The Nature Conservancy Freshwater Initiative. <http://conserveonline.org/docs/2001/06/watershed.pdf>. [Date accessed: September 17, 2007].
- Holthausen, R.S.; Raphael, M.G.; McKelvey, K.S. [and others]. 1995.** The contribution of Federal and non-Federal habitat to persistence of northern spotted owl on the Olympic Peninsula, Washington. Report of the reanalysis team. Gen. Tech. Rep. PNW-GTR-352. Portland, OR: U.S. Department of Agriculture, Forest Service, Pacific Northwest Research Station. 68 p.
- Issaks, E.H.; Srivastava, R.M. 1989.** An introduction to applied geostatistics. New York: Oxford University Press. 561 p.

- Krist, F.; Sapio, F.; Takcz, B. 2006.** [In review]. Mapping risk from forest insects and disease. U.S. Department of Agriculture, Forest Service. 39 p.
- McRoberts, R.E.; McWilliams, W.H.; Reams, G.A. [and others]. 2004.** Assessing sustainability using data from the Forest Inventory and Analysis program of the United States Forest Service. *Journal of Sustainable Forestry*. 18: 23–46.
- Miller, P.R.; Stolte, K.W.; Duriscoe, D.M.; Pronos, J. 1996.** Extent of ozone injury to trees in the Western United States. In: Evaluating ozone air pollution effects on pines in the Western United States. Gen. Tech. Rep. PSW-GTR-155. Berkeley, CA: U.S. Department of Agriculture, Forest Service, Pacific Southwest Research Station: 1–6.
- Nalder, I.A.; Wein, R.W. 1998.** Spatial interpolation of climatic normals: test of new methods in the Canadian boreal forest. *Agricultural and Forest Meteorology*. 92: 211–225.
- Schmidt, K.M.; Meankis, J.P.; Hardy, C.C. [and others]. 2002.** Development of coarse-scale spatial data for wildland fire and fuel management. Gen. Tech. Rep. RMRS-GTR-87. Fort Collins, CO: U.S. Department of Agriculture, Forest Service, Rocky Mountain Research Station. 41 p.
- Smith, G.C.; Coulston, J.W.; Jepsen, E.; Prichard, T. 2003.** A national ozone biomonitoring program: results from field surveys of ozone sensitive plants in northeastern forests (1994–2000). *Environmental Monitoring and Assessment*. 87: 271–291.
- Smith, W.B.; Miles, P.D.; Vissage, J.S.; Pugh, S.A. 2004.** Forest resources of the United States, 2002. Gen. Tech. Rep. NC-241. St. Paul, MN: U.S. Department of Agriculture, Forest Service, North Central Research Station. 137 p. http://www.ncrs.fs.fed.us/pubs/gtr/gtr_nc241.pdf. [Date accessed: February 28, 2005].
- Steeves, P.A.; Nebert, D.D. 1994.** Hydrological unit maps of the conterminous United States [Database]. U.S. Geological Survey, open-file data set “huc250,” ed. 1. Reston, VA: U.S. Geological Survey, <http://water.usgs.gov/GIS/metadata/usgswrd/XML/huc250k.xml>. [Date accessed: September 19, 2007].
- Stein, S.; McRoberts, R.E.; Nelson, M.D. [and others]. 2005a.** Forests on the Edge: a GIS-based approach to projecting housing development on private forests. In: Aguirre-Bravo, C. [and others], eds. *Monitoring science and technology symposium: Unifying knowledge for sustainability in the Western Hemisphere*. Proceedings RMRS-P-37CD. Fort Collins, CO: U.S. Department of Agriculture, Forest Service, Rocky Mountain Research Station. CD-ROM.
- Stein, S.; McRoberts, R.E.; Nelson, M.D. [and others]. 2005b.** Forests on the Edge: housing development on America’s private forests. Gen. Tech. Rep. PNW-GTR-636. Portland, OR: U.S. Department of Agriculture, Forest Service, Pacific Northwest Research Station. 15 p.
- Theobald, D.M. 2005.** Landscape patterns of exurban growth in the U.S.A. from 1980 to 2020. *Ecology and Society*. 10(1): 32.
- U.S. Environmental Protection Agency [US EPA]. 1996.** Air quality criteria for ozone and related photochemical oxidants. Vol. 1 and 2 of 3, Section 4.0, Environmental concentrations, patterns, and exposure estimates. EPA/600/P-93/004aF. Washington, DC: Office of Research and Development. [Page numbers unknown].
- U.S. Geological Survey [USGS]. 2000.** The national hydrology data set. <http://nhd.usgs.gov/>. [Date accessed: September 19, 2007].
- Vogelmann, J.E.; Howard, S.M.; Yang, L. [and others]. 2001.** Completion of the 1990s national land cover data set for the conterminous United States from Landsat thematic mapper data and ancillary data sources. *Photogrammetric Engineering and Remote Sensing*. 67: 650–662.

Wear, D.; Pye, J.; Riitters, K. 2004. Defining conservation priorities using fragmentation forecasts. *Ecology and Society*. 9(5):4. [Online] URL: <http://www.ecologyandsociety.org/vol19/iss5/art4>. [Date accessed Feburary 2010].

A Spatial Model for Predicting Effects of Climate Change on Swiss Needle Cast Disease Severity in Pacific Northwest Forests

Jeffrey K. Stone, Leonard B. Coop, and Daniel K. Manter

Jeffrey K. Stone and **Leonard B. Coop**, Department of Botany and Plant Pathology, Cordley Hall 2082, Oregon State University, Corvallis, OR 97331; **Daniel K. Manter**, USDA-ARS Soil Plant Nutrient Research Unit, Fort Collins, CO 80526.

Abstract

Swiss needle cast disease of Douglas-fir (*Pseudotsuga menziesii*) is caused by the ascomycete fungus *Phaeocryptopus gaeumannii*. Symptoms of the disease are foliage chlorosis and premature needle abscission due to occlusion of stomata by the ascocarps of the pathogen, resulting in impaired needle gas exchange. Severe defoliation and growth losses of 20 to 50 percent because of Swiss needle cast have been reported for about 150 000 ha of Douglas-fir plantations in western Oregon since 1996. Because the physiological effects of the disease (impaired CO₂ uptake and photosynthesis) are quantitatively related to the abundance of the pathogen (proportion of stomata occluded by ascocarps), pathogen abundance is directly related to disease and is a suitable response variable for assessing effects of climatic factors on disease. Climate factors most highly correlated with pathogen abundance are winter temperature and spring leaf wetness, and a model for prediction of disease severity based on these factors accounts for 77 percent and 78 percent of the variation in 1- and 2-year-old needles, respectively, for western Oregon sites. A trend of temperatures increasing by 0.2 to 0.4 °C during the winter months and spring precipitation increasing by 1.6 to 2.6 cm per decade since 1966 suggests that regional climate trends are influencing the current distribution and severity of Swiss needle cast disease. Forecasts of climate change in the Pacific Northwest region predict continued increases in temperatures during winter months of about 0.4 °C per decade through 2050, suggesting that the severity and distribution of Swiss needle cast is likely to increase in the coming decades as a result of climate change, with significant consequences for Pacific Northwest

forests. A climate-based disease prediction model is being developed as an online, interactive tool that can be used to guide further research, conduct extended model validations, perform climate change scenario analyses, and eventually to provide short- and long-term disease risk predictions and management cost/benefit analyses. The model will be useful for prediction of disease development trends under different climate change scenarios and temporal scales.

Keywords: Douglas-fir, foliage disease, forest pathology, *Phaeocryptopus gaeumannii*, *Pseudotsuga menziesii*.

History of the Problem

Swiss needle cast disease of Douglas-fir (*Pseudotsuga menziesii* (Mirb.) Franco) is caused by the ascomycete *Phaeocryptopus gaeumannii* (Rohde) Petrak. The disease, and the fungus that causes it, were first described from Douglas-fir plantations in Switzerland and Germany in 1925, and soon afterward reported from various locations in Europe, the British Isles, and Northeastern North America (Boyce 1940, Peace 1962). The causal agent, *P. gaeumannii*, was found to be abundant on foliage of diseased trees and was determined to be distinct from any previously described foliage fungi from coniferous hosts. Subsequent surveys of Douglas-fir in the Western United States found the pathogen was widespread throughout the Pacific Northwest region, where it had escaped notice because of its inconspicuous habit and negligible effect on its host. Boyce (1940) considered *P. gaeumannii* widespread but harmless on Douglas-fir in Western North America, and probably indigenous to the Pacific Northwest, where "...the fungus has been found at such widely separated localities in British Columbia, Washington, and Oregon that it must be considered generally distributed, although harmless, in the Douglas-fir region of the Pacific coast."

Douglas-fir is the only host of *P. gaeumannii*, which has accompanied cultivation of its host to various localities worldwide (Hood 1997, Temel and others 2003). Diseased trees have chlorotic foliage and may lose all but the current year's complement of needles (Figure 1). The earliest



Figure 1—Symptoms of Swiss needle cast, premature defoliation, loss of older needles.

confirmed records of *P. gaeumannii* in western North America are herbarium specimens collected by J.S. Boyce from Oregon and California in 1916 (Boyce 1940). The fungus occurs on both coastal (*Pseudotsuga menziesii* var. *menziesii*) and interior (*P. menziesii* var. *glauca* (Beissn.) Franco) forms of Douglas-fir throughout the natural range of the host (Boyce 1940, Hood 1982). The fungus has also been reported from *P. macrocarpa* (Vasey) Mayr in New Zealand (Gadgil 2005), although it has not been reported on this host in North America.

Although Swiss needle cast disease in Europe first brought attention to *Phaeocryptopus gaeumannii*, the fungus has long been considered a pathogen of negligible significance in western North American forests. Peace (1962) wrote of Swiss needle cast disease in Europe: “This is a classic case of a disease, of no importance in its native haunts, which has become damaging when transported to other areas.” With the growth of a commercial Douglas-fir Christmas tree industry in the Pacific Northwest in the 1970s, and the practice of shearing trees to promote a more compact growth form, Swiss needle cast first began to attract serious notice in its native region (Michaels and Chastagner 1984). Although episodic outbreaks of brief

duration in forest plantations in the Pacific Northwest were noted in the 1970s and 1980s (Russell 1981), Swiss needle cast was not considered a significant forest pathogen. The occurrence of Swiss needle cast disease primarily in forest plantations outside the native range of Douglas-fir, or on sheared Christmas tree plantations, has contributed to the perception of the disease as being primarily associated with inappropriate planting stock or stressed trees.

Current Extent and Impacts of Swiss Needle Cast in Pacific Northwest Forests

Since around 1990, unusually severe and persistent symptoms of Swiss needle cast have been observed in Douglas-fir forest plantations in western Oregon, particularly near the town of Tillamook (Hansen and others 2000). Annual aerial surveys conducted since 1996 by the Oregon Department of Forestry have documented the disease on about 150 000 ha of forest land in the Oregon Coast Range (Figure 2). Unlike Boyce’s (1940) characterization of the pathogen on native Douglas-fir as being inconspicuous and harmless, the fungus is abundant, trees frequently are defoliated of all but current-year needles, and attached foliage is often severely chlorotic (Figure 1). Growth reductions of 20 to 50 percent

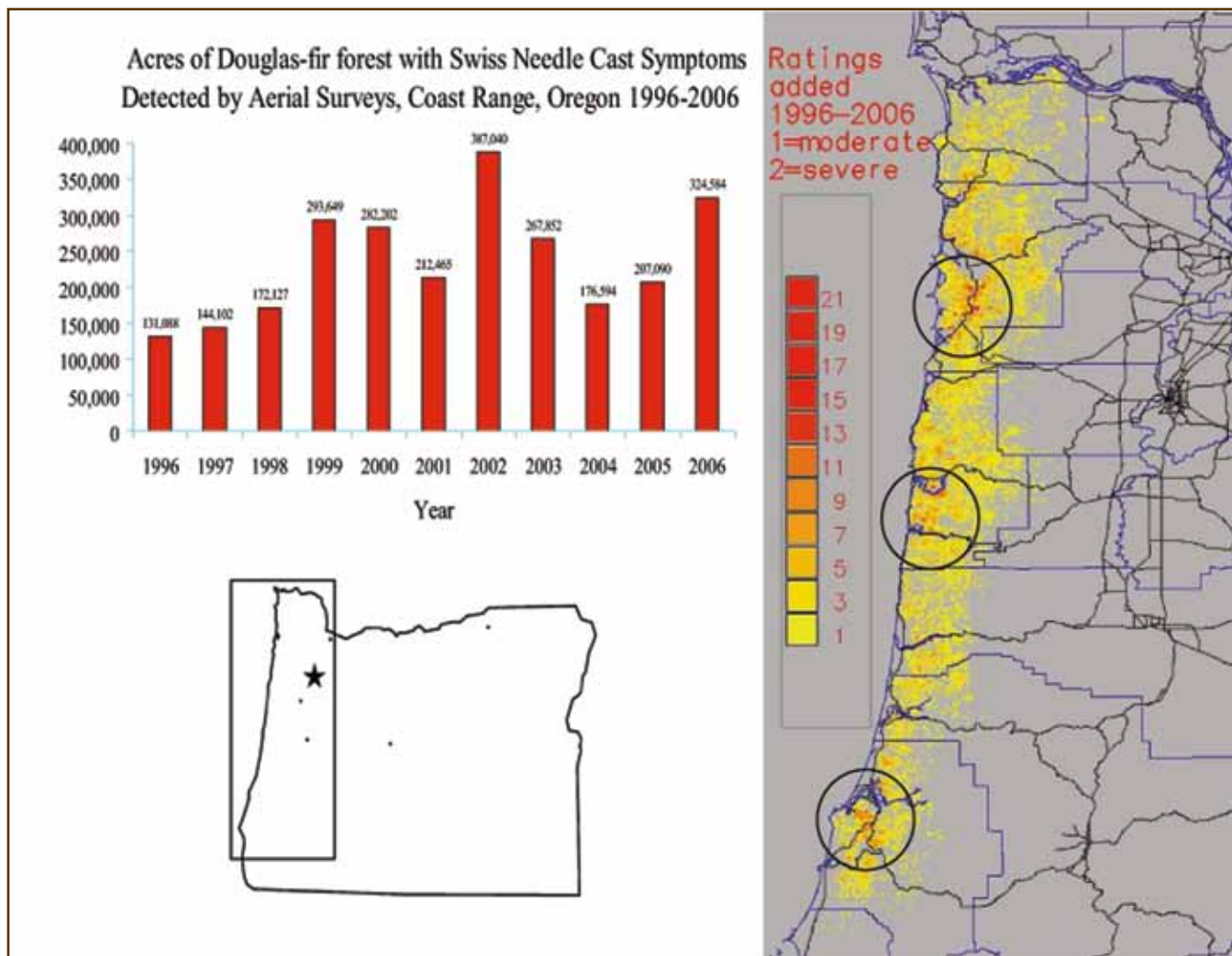


Figure 2—Annual variation in surveyed Swiss Needle Cast (SNC) area in western Oregon 1996–2006 (A) and combined disease severity survey scores for western Oregon (severity scores for all 11 years summed and superimposed on map B). Legend signifies 1 = disease moderate for single year to 22 = disease severe all 11 years of survey. Circled areas highlight regions where chronic SNC has been observed. Source data: Oregon Department of Forestry.

from Swiss needle cast have been measured in the affected area (Maguire and others 2002). The severity of the problem in Oregon has brought renewed interest in understanding the biology of the pathogen and epidemiology of Swiss needle cast disease. In particular, research has focused on understanding why an inconspicuous, insignificant native pathogen has become a significant forest health problem.

Aerial surveys for Swiss needle cast conducted by the Oregon Department of Forestry have classified patches of Swiss needle cast severity based on foliage discoloration, characterizing the discoloration as being severe or moderate. The affected area as determined by the aerial survey

lies along the entire length of the Oregon coast, extending inland about 40 km, with most symptoms occurring within 30 km of the coast. The crest of the Coast Range forms the approximate eastern edge of the affected area. The aerial survey covers about 1.2 million ha of coastal forest, with the symptomatic area comprising between 50 and 160 000 ha (Figure 2).

Disease severity (foliage retention, discoloration, crown sparseness, pathogen abundance) has also been monitored annually in permanent plots in the Oregon Coast Range (Hansen and others 2000) equipped with temperature and leaf wetness dataloggers. Foliage retention, and abundance

of *P. gaeumannii* ascocarps on 1- and 2-year-old needles have been monitored annually since 1996 in 9 to 12 Douglas-fir stands, initially aged 12 to 15 years. Study sites were selected to represent a range of elevations, distance from maritime influence, and disease severity. Within the area of severe disease, symptom severity is variable, but all Douglas-fir show some effects of the disease compared to healthy stands on the eastern slope of the Coast Range and in the Cascade Range. Normal needle retention in healthy coastal form Douglas-fir is about 4 years. Within the epidemic area, needle retention varies from about 1.5 to 2.6 years (Hansen and others 2000). Although symptom severity (e.g., foliage discoloration, needle retention) for all sites varies from year to year, relative disease severity (i.e., abundance of *P. gaeumannii* ascocarps on 1- and 2-year-old foliage) is fairly consistent. Disease tends to be more severe nearer the coast, at lower elevations, and on southern aspect slopes, gradually diminishing to the east (Hansen and others 2000, Manter and others 2003b, Rosso and Hansen 2003).

The Swiss needle cast epidemic area appears to correspond approximately to the Sitka spruce (*Picea sitchensis* (Bong.) Carr.) vegetation zone, a narrow strip of coastal forest characterized by elevations generally below 150 m, proximity to the ocean, a moderate climate, and a distinct forest type (Franklin and Dyrness 1973). Although Douglas-fir is considered the early seral dominant in the western hemlock vegetation zone, which borders the Sitka spruce zone to the east, its occurrence within the Sitka spruce zone is more sporadic. There Douglas-fir occurs mainly in mixtures with Sitka spruce and western hemlock (*Tsuga heterophylla* (Raf.) Sarg.), but normally not as pure stands as is typical of early postfire succession in the western hemlock zone (Franklin and Dyrness 1973).

The correspondence between the Sitka spruce zone and the main Swiss needle cast epidemic area suggests that environmental factors that influence the development of different plant associations in western Oregon may also influence the severity of Swiss needle cast. Irruption of the disease in the coastal zone may be owing changes in abundance of Douglas-fir in coastal forests owing to forest

management practices that favor the cultivation of Douglas-fir over other species (Hansen and others 2000). Swiss needle cast itself may be one such environmental determinant of the natural distribution of Douglas-fir in the western Coast Range, making it an inferior competitor where Swiss needle cast is severe (Hansen and Stone 2005).

But what factors affect the distribution and abundance of *P. gaeumannii*? It has long been suspected that local climate plays a key role in the pathogenicity of *P. gaeumannii*. Boyce (1940) suggested that seasonal patterns in local climate could differentially affect fungal growth and development, and this might explain the greater virulence of *P. gaeumannii* in Europe and the Eastern United States compared to the area where both *P. gaeumannii* and Douglas-fir are native. Within the Douglas-fir zone of the Pacific Northwest, there is also a relationship between disease severity and local climate. Hood (1982) found more *P. gaeumannii* in southern British Columbia and western Washington in coastal forests of Vancouver Island and the Olympic Peninsula, with lower levels in the rain shadow of eastern Vancouver Island and the interior, and attributed the difference mainly to precipitation patterns. More severe disease symptoms and greater fungal colonization are commonly observed on lower elevation sites near the coast, suggesting the possible involvement of maritime fog (Rosso and Hansen 2003).

Rosso and Hansen (2003) used a visual index of stand disease to investigate the relationship between several environmental variables and Swiss needle cast severity. The best model for predicting stand disease rating (a composite index of several factors) was a regression model that included July temperature, precipitation, and fog occurrence, which explained about 60 percent of the variation. Manter and others (2005) found a strong relationship between winter (Dec.–Feb.) mean daily temperature, spring (May–July) leaf wetness, and *P. gaeumannii* abundance.

Understanding the Disease

To better understand which environmental factors might be important regulators of *P. gaeumannii* abundance and how they affect the epidemiology of Swiss needle cast, it was essential to investigate the infection cycle of the pathogen

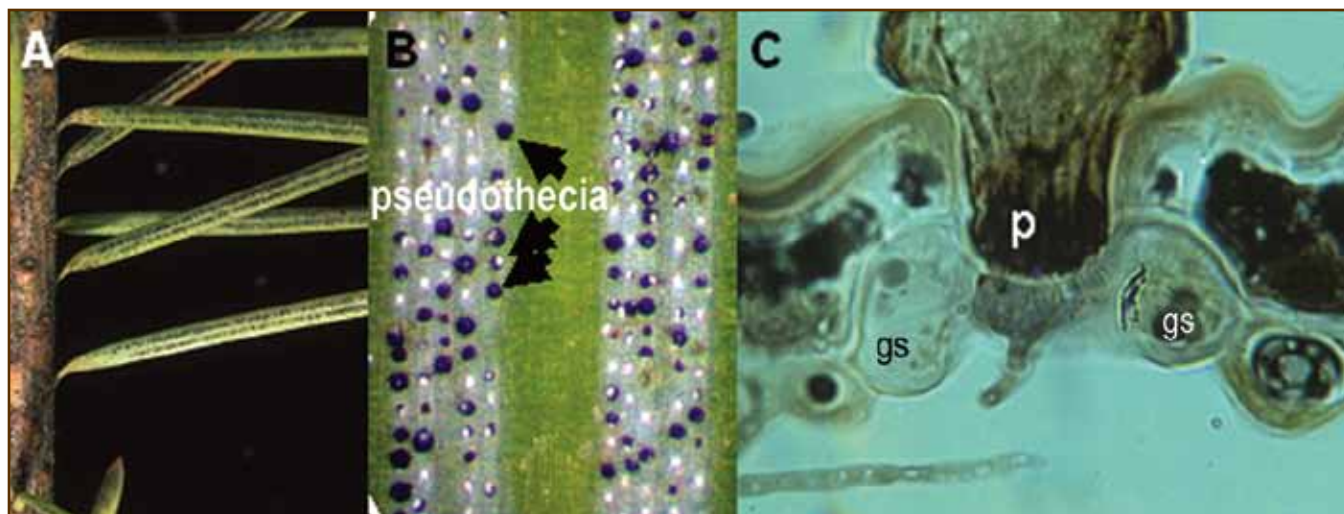


Figure 3—*Phaeocryptopus gaeumannii* on the underside of Douglas-fir needles with pseudothecia (fruiting bodies) emerging through stomata. A, B. Pseudothecia aligned along stomatal rows. C. Cross section through a stoma showing obstruction of the opening by the pseudothecium (p) between the guard cells (gc).

and its mechanism of pathogenicity. Ascospores of *P. gaeumannii* mature and are released during early May through late July, coinciding with bud break and shoot elongation of Douglas-fir. Ascospores are the only infective propagule; there is no conidial anamorph. Newly emerging foliage of Douglas-fir is most susceptible to infection. Infection of 1-year-old needles during the same period also occurs but is much less frequent. Germinating ascospores produce appressoria above stomata, and penetration pegs enter needles via stomata. Colonization within needles is exclusively intercellular; no intracellular hyphae or haustoria are produced. Internal colonization occurs gradually during the fall and winter. Ascocarp (pseudothecia) primordia begin to form in substomatal chambers at 4 to 9 months following infection. Concurrently with the formation of pseudothecial primordia, epiphytic hyphae emerge from the periphery of developing pseudothecia. These hyphae grow across the needle surface, form numerous anastomoses, and reenter the needle by producing appressoria above unoccupied stomata (Stone and others 2008). The importance of epiphytic hyphae in needle colonization and epidemiology of Swiss needle cast is not fully understood (Figure 3).

Internal colonization of needles continues as long as they remain attached, so numbers of ascocarps increase as needles age. Normally, fruiting bodies of the fungus are more abundant on needles aged 3 years or older and are

sparse or absent on younger foliage (Boyce 1940, Hood 1982). In recent years, however, trees having abundant fruiting bodies on current-year needles have been commonly observed in forest plantations along the Oregon coast, with older foliage being prematurely abscised due to the disease (Hansen and others 2000).

The ascocarp primordia completely occupy the substomatal space, thereby rendering the stoma nonfunctional. Occlusion of the stomata by pseudothecia of *P. gaeumannii* impedes gas exchange and regulation of transpiration, causing impaired photosynthetic activity and is considered the primary mechanism of pathogenicity (Manter and others 2000, 2003). Disruption of host cells by hyphal penetration has not been observed in infected needles examined in SEM and TEM preparations (Stone and others 2008), and attempts to find evidence of fungal phytotoxins to date have been inconclusive. Estimates of the effect of *P. gaeumannii* on CO₂ assimilation indicate that occlusion of 25 percent of stomata results in negative needle carbon budgets, i.e., respiration exceeds assimilation, on an annual basis (Figure 4) (Manter and others 2003a).

The abundance of pseudothecia is also highly correlated with needle abscission because of the effect on CO₂ assimilation. It has been suggested that foliage abscission occurs when needles switch from being carbon sources to carbon sinks (Cannell and Morgan 1990). The mechanism of

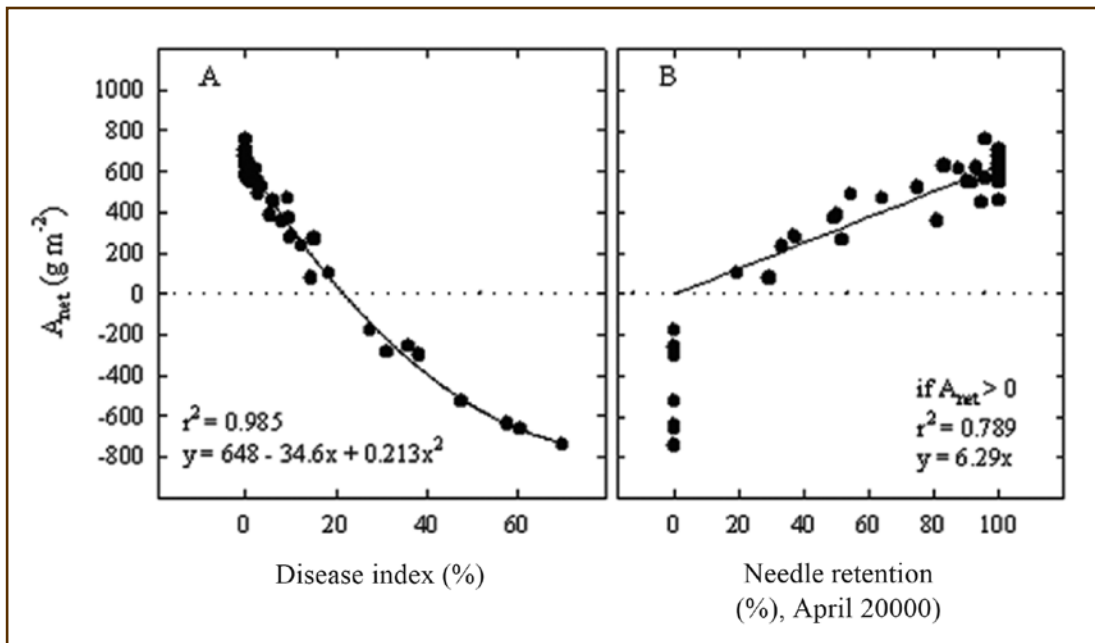


Figure 4—Relationship of net carbon dioxide uptake (A_{net}) per unit leaf area to [A] *Phaeocryptopus gaeumannii* pseudothecia abundance (disease index, percent) and [B] needle retention (percent). Taken from Manter and others (2003a).

pathogenicity of *P. gaeumannii*, therefore, can be accounted for by the physical blockage of the stomata and interference with photosynthetic gas exchange. The proportion of stomata occupied by pseudothecia on attached needles seldom exceeds 50 percent, suggesting that most needles are abscised before more than half the stomata are occluded by pseudothecia, regardless of needle age (Hansen and others 2000). Because the physiological effects of the disease (impaired CO₂ uptake and photosynthesis) are quantitatively related to the abundance of the pathogen (proportion of stomata occluded by ascomycetes), pathogen ascomycete abundance is a suitable response variable for assessing effects of climatic factors on disease.

Experimental Approaches to Understanding Climate-Disease Interactions

Because the most severe disease has been observed in sites within the low-elevation coastal fog zone (so called because of the frequency of summer maritime fog), the presence of free water on needle surfaces during the summer has been considered a possible factor affecting disease severity

(Hansen and others 2000, Rosso and Hansen 2003). Other investigators have noted a relationship between precipitation patterns and Swiss needle cast severity in the Pacific Northwest (Hood 1982, McDermott and Robinson 1989). Manter and others (2005) attempted to investigate the relative effects of individual climate factors on *P. gaeumannii* abundance experimentally. A factorial design was used to compare the effect of post-inoculation incubation conditions under two levels each of drip irrigation, shade, and intermittent mist on *P. gaeumannii* colonization. Seedling trees were exposed to inoculum in a diseased forest stand, then randomized and maintained under the different post-inoculation treatments. Abundance of *P. gaeumannii* ascomycetes on foliage was determined monthly. The different postinoculation conditions resulted in significant differences in *P. gaeumannii* development. Abundance of *P. gaeumannii* was negatively correlated with shade and mist—this unexpected outcome was interpreted as a result of indirect effects of shade and mist on temperature and not as a direct effect of shade or leaf wetness—and irrigation had no effect (Figure 5).

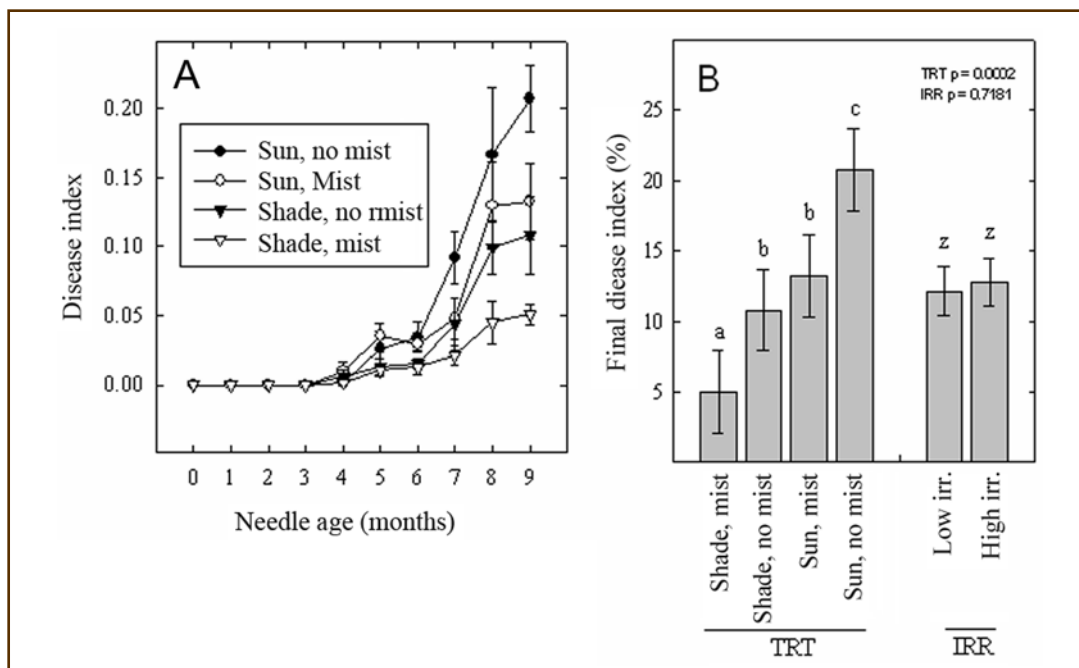


Figure 5—Final *Phaeocryptopus gaeumannii* disease index values for seedlings incubated under shade, mist, and irrigation treatments following inoculum exposure. Sun = 100 percent ambient, shade = 50 percent ambient, mist = three 2-hour overhead mist treatments per day, no mist = 0 overhead mist treatments per day, low irr. = 0.5 L day⁻¹ drip irrigation, and high irr. = 1.9 L day⁻¹ drip-irrigation. Bars are the arithmetic means and individual standard errors. Treatment effects were analyzed using a split-randomized complete block design, and bars with different letters are significant at $p < 0.05$. A. Monthly measurements of pseudothecia abundance by treatment. B. Final disease index by treatment. Taken from Manter and others (2005).

Modeling Swiss Needle Cast

The finding that small differences in temperature could affect rates of needle colonization and fungal development over the 11-month incubation period of *P. gaeumannii* prompted us to examine the effect of temperature in relation to infection data from field sites in western Oregon. Average daily temperature and cumulative leaf wetness hours were separated into 3-month groups, corresponding to major phases in the infection cycle, and subjected to stepwise regression against *P. gaeumannii* infection data to identify climate factors for use in a disease prediction model. Consistently strong correlations were found between winter (Dec.-Feb.) mean daily temperature and infection in both 1- and 2-year-old needles ($R^2 = 0.75$ to 0.92), and this was the only climate variable with R^2 values above 0.5. The best-fit climate model included winter mean daily temperature and cumulative spring leaf wetness hours, $R^2 = 0.78$ and 0.77 for 1- and 2-year-old needles, respectively. When this model was tested against infection data for different sites in

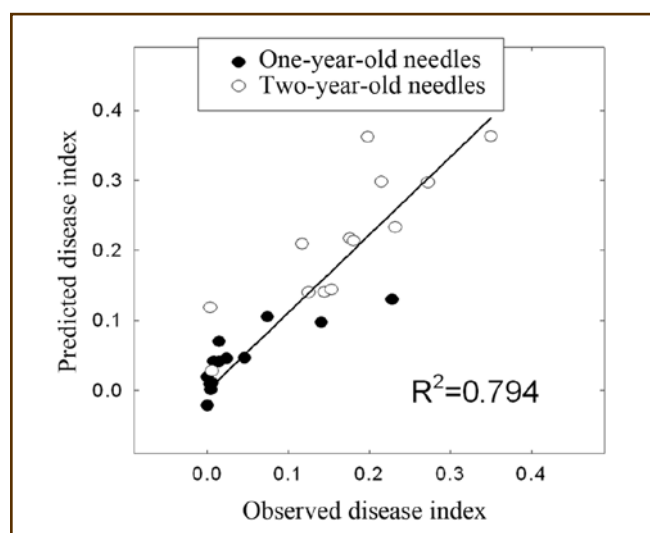


Figure 6—Best-fit model for predicting *Phaeocryptopus gaeumannii* abundance using only climate variables (winter temperature and spring leaf wetness), predicted vs. observed values. From Manter and others (2005).

different years, a significant 1:1 relationship was found ($R^2 = 0.79$, Figure 6).

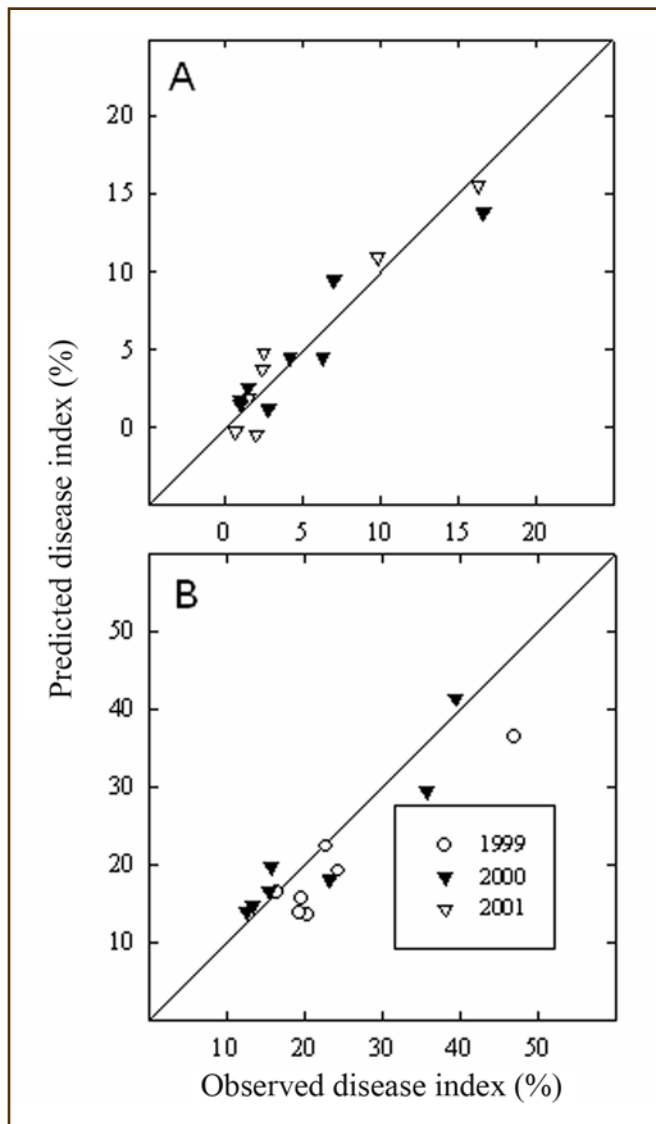


Figure 7—Plots of predicted vs. observed values for the best-fit model for predicting *Phaeocryptopus gaeumannii* abundance. Terms in the model were average daily winter temperature (Dec.-Feb.) and preceding year disease index for the corresponding needle cohort. From Manter and others (2005). Panel A, 1-year-old needles; panel B, 2-year-old needles.

A more general model was sought that could be used to predict geographic variation in Swiss needle cast severity with the aid of spatial climate models. However, because leaf wetness is not readily available in public meteorological databases or climate models, alternative models were tried. Winter temperature was the best single predictor of *P. gaeumannii* abundance, but its relationship with infection level varied by year. The abundance of *P. gaeumannii* and

severity of Swiss needle cast for a particular site in a given year are not independent of previous year disease severity for the site. Abundance of *P. gaeumannii* in 1-year-old needles is partly determined by the amount of inoculum present and the number of ascospores that initiate infection on a needle. Because ascospore infection of needles in their second year is negligible (Stone and others 2008, Hood and Kershaw 1975), abundance of *P. gaeumannii* on 2-year-old needles is partly determined by the degree of colonization in needles at the beginning of their second year. Therefore, two infection components, the amount of *P. gaeumannii* in 2-year-old and 1-year-old needles for the previous year, were added to the temperature model to predict infection in 1- and 2-year-old needles for the year of interest. Disease predictions generated by this model had a significant 1:1 relationship ($R^2 = 0.812$) when compared with observed values in the validation data set (Manter and others 2005), (Figure 7).

The temperature/infection model described above was then run over several iterations with temperature held constant over a range of values (2 to 10 °C). After five iterations, the infection level reaches a stable asymptote for any value of winter temperature. The maximum infection value is a function of winter temperature, regardless of initial infection level, and represents the point of equilibrium between colonization and inoculum production. A plot of the equilibrium infection level against temperature shows that between 3.77 and 8.90 °C, the range of average winter temperatures measured at coastal study sites, infection levels vary from zero to about 15 percent in 1-year-old needles and between 10 to about 40 percent in 2-year-old needles (Figure 8).

This model also was accurate for predicting disease levels for sites in the Western Coast Range ($R^2 = 0.85$) but was less accurate when infection data from sites from the east slope of the Coast Range and Willamette Valley were included ($R^2 = 0.70$). Observed infection levels for the inland sites were less than predicted by the equilibrium temperature model, and this is likely due to the comparative dryness of the inland sites. The model that included a term for spring leaf wetness was more accurate in predicting infection levels for the inland sites than the equilibrium

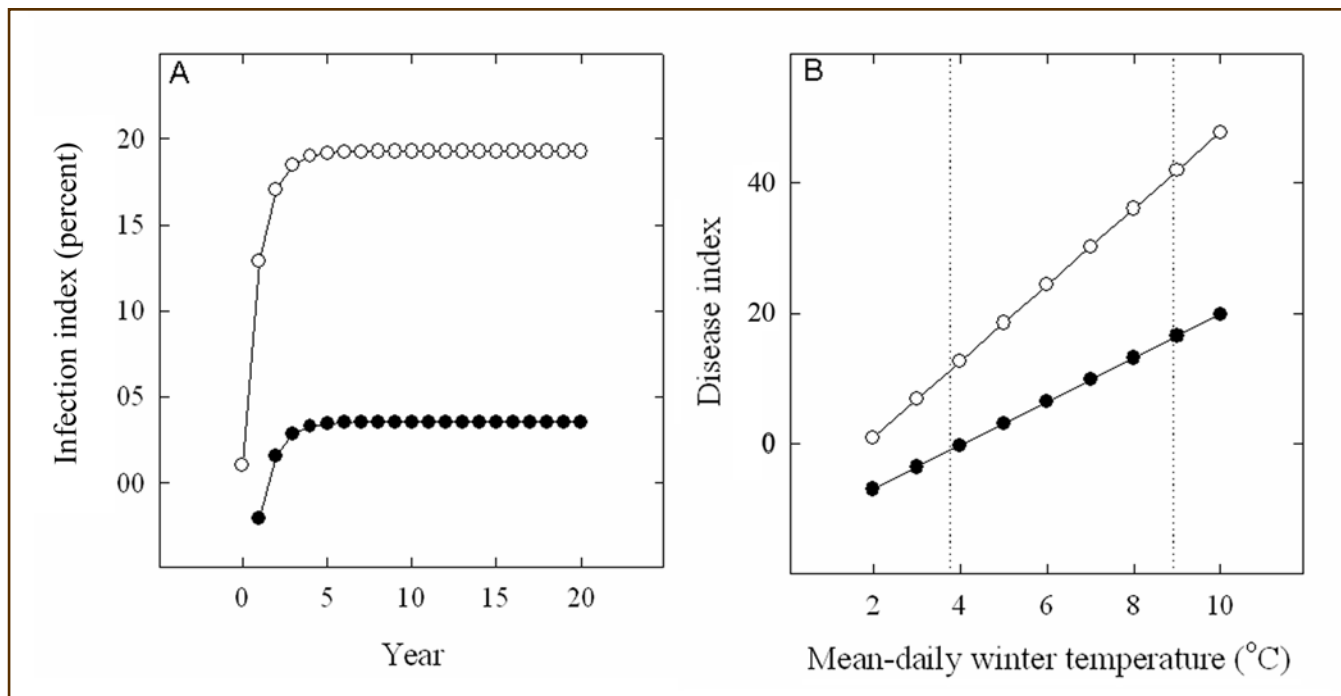


Figure 8—A. Simulation of *Phaeocryptopus gaeumannii* infection index over time as predicted by the combined winter temperature-infection model, with temperature held constant (5.13 °C) and initial infection index of 1 percent; B. Relationship between final equilibrium infection level and winter temperature for 1- (solid circles) and 2-year-old (open circles) needles.

temperature model, illustrating that the relative importance of different climate factors can vary spatially. The simple equilibrium temperature model appears suitable for predicting disease levels in the Western Coast Range, where spring surface moisture on foliage is probably rarely limiting, but additional parameters are necessary for disease prediction on more inland sites.

The equilibrium property of the model was then used to generate a disease prediction map for a portion of western Oregon based on the DAYMET climate model, a continuous surface at 1-km resolution base on 18-year (1980-1997) average temperatures (Figure 9). The model appears to correspond well with the distribution of disease symptoms as observed by aerial surveys and permanent monitoring plots. Research is in progress to compare disease distribution and severity predicted by different models with observed aerial survey data.

The sensitivity of *P. gaeumannii* to relatively small temperature differences helps to explain patterns of spatial variation in Swiss needle cast severity, and suggests that recent increases in Swiss needle cast severity

have been influenced by regional climate trends. Over the past century, average temperatures in the Pacific Northwest region have increased by about 0.8° C, with more warming occurring during winter months (Mote and others 2003). Average temperatures for the period January-March have increased by approximately 0.2 to 0.4 °C per decade since 1966 in coastal Oregon and Washington (USDC NOAA 2005). An increase in average winter temperature of 1 °C corresponds to an increase in infection index (proportion of stomata occluded) of 3 percent for 1-year-old needles and 6 percent for 2-year-old needles, based on the equilibrium temperature model. Spring precipitation has also increased on average by about 1.6 to 2.6 cm per decade since 1966 (USDC NOAA 2005). These climate trends suggest that over the past few decades, conditions have become more favorable for growth of *P. gaeumannii* and have contributed to increasing Swiss needle cast severity. Predictions for continued regional warming of about 0.4 °C per decade to 2050, together with increasing (+2 to 4 percent) spring precipitation (Mote and others 2003), suggest that conditions in the region will continue to be favorable for Swiss

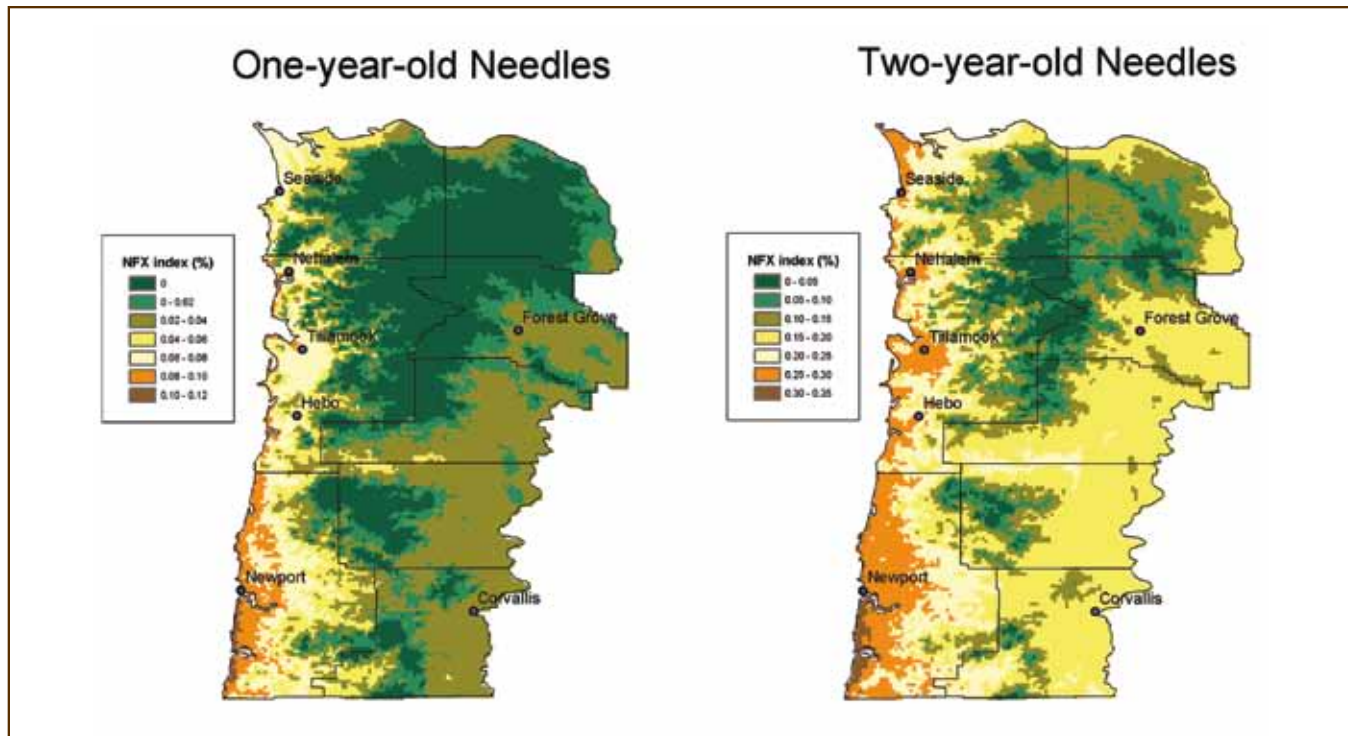


Figure 9—Disease prediction map for northwest Oregon as predicted by the equilibrium disease model. Infection indices were predicted from winter average daily temperatures from the DAYMET climate model. From Manter and others (2005).

needle cast development, and could result in expansion of the area affected by the disease beyond the Western Coast Range of Oregon. A goal of ongoing research is to develop an improved disease prediction model to investigate the interactions between climate and Swiss needle cast. An expanded disease prediction model will be designed to incorporate long-term climate trend forecasts to enable site-specific short- and long-term disease risk predictions, growth impact predictions, and incorporate climate change models to allow examination of disease development trends under different climate scenarios.

Conclusions

Improved understanding of the effects of climate factors on *P. gaumannii* abundance now helps to clarify the underlying causes for recently observed increases in Swiss needle cast in the Western Coast Range. Previous observations on the regional distribution of *P. gaumannii* in the Pacific Northwest have suggested a connection between *P. gaumannii* abundance and spring rainfall (Hood 1982). In

the Western Coast Range of Oregon, where spring precipitation is abundant, winter temperature has been found to be a highly reproducible predictor of the spatial variation in abundance of *P. gaumannii* and resulting Swiss needle cast severity, presumably because of its effect on fungal growth. Winter temperature alone is not a satisfactory predictor of *P. gaumannii* abundance regionwide or in areas where spring precipitation is not as abundant, such as the Willamette Valley, or Oregon Cascade Range, as shown by Manter and others (2005). The predictive disease model described here, therefore, is applicable for predicting spatial variation in *P. gaumannii* abundance and Swiss needle cast severity only for the western slope of the Oregon Coast Range. Within this area, there have been few historical reports of Swiss needle cast, and the disease has been considered an insignificant forest health issue. The natural distribution of Douglas-fir in the Western Coast Range has undoubtedly been influenced by *P. gaumannii* and Swiss needle cast, along with other disturbance agents. The effect of chronic, profuse *P. gaumannii* colonization of Douglas-fir foliage is to reduce growth rates of affected trees relative

to competing species, such as spruce and hemlock. Normally faster growing than western hemlock, Douglas-fir is an inferior competitor where Swiss needle cast disease pressure is high. In the coastal lowlands and interior valleys of the Western Coast Range, seasonal climatic conditions are the most favorable for *P. gaeumannii* growth and reproduction. In these areas, a distinct natural forest type has historically been dominated by western hemlock and Sitka spruce, with Douglas-fir occurring only sporadically. Douglas-fir gradually becomes more abundant in natural forests at higher elevations and further inland, as the Sitka spruce zone gradually merges into the western hemlock vegetation zone, where Douglas-fir is a successional dominant, and where climatic conditions are less favorable for *P. gaeumannii* growth. This leads to the conclusion that the Sitka spruce vegetation zone occurs as a consequence not only of favorable habitat for Sitka spruce and western hemlock, but also because of the inhibition of their main competitor, Douglas-fir, due to Swiss needle cast disease. This scenario also suggests that the severity of Swiss needle cast in the region may be the result of recent forest management in the Western Coast Range, where Douglas-fir has been strongly favored in forest plantations because of its greater economic value, increasing the abundance of the host species in the area most favorable for growth and reproduction of the pathogen. As noted above, however, recent climate trends also are likely to have contributed to current Swiss needle cast severity. Furthermore, forecasts of future climate trends for the Pacific Northwest suggest a probable expansion of the area affected by severe Swiss needle cast beyond the Western Coast Range as winter temperatures and spring precipitation continue to increase, resulting in greater disease pressure on Douglas-fir stands further inland.

Acknowledgments

This research was supported by the Office of Science, Biological and Environmental Research Program (BER), U.S. Department of Energy, through the Western Regional Center of the National Institute for Global Environmental Change (NIGEC) under Cooperative Agreement Nos.

DE-FC03-90ER61010 and DE-FCO2-03ER63613. Financial support does not constitute an endorsement by DOE of the views expressed in this article/report. Funding was also provided by the Swiss Needle Cast Cooperative of Oregon State University.

Literature Cited

- Boyce, J.S. 1940.** A needle-cast of Douglas-fir associated with *Adelopus gaeumannii*. *Phytopathology*. 30: 649–59.
- Cannell, M.G.R.; Morgan, J. 1990.** Theoretical study of variables affecting the export of assimilates from branches of *Picea*. *Tree Physiology*. 6: 257–266.
- Franklin, J.F.; Dyrness, C.T. 1973.** Natural vegetation of Oregon and Washington. Gen. Tech. Rep. PNW-8. Portland, OR: U.S. Department of Agriculture, Forest Service, Pacific Northwest Forest and Range Experiment Station. 417 p.
- Gadgil, P.D. 2005.** Fungi on trees and shrubs in New Zealand. Hong Kong: Fungal Diversity Press. 437 p.
- Hansen, E.M.; Stone, J.K. 2005.** Impacts of pathogens on plant communities. In: Dighton, J.; Oudemans, P.; White, J., eds. *The fungal community*. New York: Marcel Dekker: 461–474.
- Hansen, E.M.; Stone, J.K.; Capitano, B.R. [and others]. 2000.** Incidence and impact of Swiss needle cast in forest plantations of Douglas-fir in coastal Oregon. *Plant Disease*. 84: 773–778.
- Hood, I.A. 1982.** *Phaeocryptopus gaeumannii* on *Pseudotsuga menziesii* in southern British Columbia. *New Zealand Journal of Forestry Science*. 12: 415–424.
- Hood, I.A. 1997.** Swiss needle cast. In: Hansen E.M.; Lewis, K., eds. *Compendium of conifer diseases*. St. Paul, MN: APS Press: 55–56.
- Hood, I.A.; Kershaw, D.J. 1975.** Distribution and infection period of *Phaeocryptopus gaeumannii* in New Zealand. *New Zealand Journal of Forestry Science*. 5: 201–208.

- Maguire, D.A.; Kanaskie, A.; Johnson, R. [and others]. 2002.** Growth of young Douglas-fir plantations across a gradient of Swiss needle cast severity. *Western Journal of Applied Forestry*. 17: 86–95.
- Manter, D.K.; Bond, B.J.; Kavanagh, K.L. [and others]. 2000.** Pseudothecia of the Swiss needle cast fungus, *Phaeocryptopus gaeumannii*, physically block stomata of Douglas-fir, reducing CO₂ assimilation. *New Phytologist*. 148: 481–491.
- Manter, D.K.; Bond, B.J.; Kavanagh, K.L. [and others]. 2003a.** Modeling the impacts of the foliar pathogen, *Phaeocryptopus gaeumannii*, on Douglas-fir physiology: net canopy carbon assimilation, needle abscission, and growth. *Ecological Modeling*. 154: 211–226.
- Manter, D.K.; Reeser, P.W.; Stone, J.K. 2005.** A climate-based model for predicting geographic variation in Swiss needle cast severity in the Oregon Coast Range. *Phytopathology*. 95: 1256–1265.
- Manter, D.K.; Winton, L.M.; Filip, G.M.; Stone, J.K. 2003b.** Assessment of Swiss needle cast disease: temporal and spatial investigations of fungal colonization and symptom severity. *Journal of Phytopathology*. 151: 344–351.
- McDermott, J.M.; Robinson, R.A. 1989.** Provenance variation for disease resistance in *Pseudotsuga menziesii* to the Swiss needle cast pathogen, *Phaeocryptopus gaeumannii*. *Canadian Journal of Forest Research*. 19: 244–246.
- Michaels, E.; Chastagner, G.A. 1984.** Distribution, severity, and impact of Swiss needle cast in Douglas-fir Christmas trees in western Washington and Oregon. *Plant Disease*. 68: 939–942.
- Mote, P.W.; Parson, E.A.; Hamlet, A.F. [and others]. 2003.** Preparing for climatic change: the water, salmon, and forests of the Pacific Northwest. *Climatic Change*. 61: 45–88.
- Peace, T.R. 1962.** Diseases of trees and shrubs, with special reference to Britain. Oxford: Oxford University Press. 753 p.
- Rosso, P.; Hansen, E.M. 2003.** Predicting Swiss needle cast disease distribution and severity in young Douglas-fir plantations in coastal Oregon. *Phytopathology*. 93: 790–798.
- Russell, K. 1981. Swiss needle cast in Douglas-fir. Rep. 279.** Olympia: Washington Department of Natural Resources, Forest Land Management. [Number of pages unknown].
- Stone, J.K.; Capitano, B.; Kerrigan, J.L. 2008.** Mode of infection and colonization of Douglas-fir needles by *Phaeocryptopus gaeumannii*. *Mycologia*. 100(3): 431–444.
- Temel, F.; Stone, J.K.; Johnson, G.R. 2003.** First report of Swiss needle cast caused by *Phaeocryptopus gaeumannii* on Douglas-fir in Turkey. *Plant Disease*. 87: 1536.
- U.S. Department of Commerce, National Oceanic and Atmospheric Administration [USDC NOAA]. 2005.** U.S. temperature and precipitation trends. National Weather Service, Climate Prediction Center. U.S. <http://www.cpc.noaa.gov/trndtext.shtml>. [Date accessed unknown].

Analyzing Risks to Protected Areas Using the Human Modification Framework: A Colorado Case Study

David M. Theobald, Alisa Wade, Grant Wilcox, and Nate Peterson

David M. Theobald, research scientist, Natural Resource Ecology Lab, and associate professor, Department of Human Dimensions of Natural Resources, **Alisa Wade**, graduate student, Department of Forest, Range, and Watershed Stewardship, and **Grant Wilcox**, research scientist, Natural Resource Ecology Lab, Colorado State University, Fort Collins, CO 80523-1499; and **Nate Peterson**, GIS scientist, Institute of Sustainable Resources, Queensland University of Technology, Brisbane, Queensland 4001, Australia.

Abstract

A framework that organizes natural and protected areas is often used to help understand the potential risks to natural areas and aspects of their ecological and human dimensions. The spatial (or landscape) context of these dynamics is also a critical, but, rarely considered, factor. Common classification systems include the U.S. Geological (USGS) Gap Analysis Program (GAP) stewardship coding scheme, the International Union for the Conservation of Nature (IUCN) Protected Area Management Categories, and the American Planning Association (APA) Land-Based Classification Standards. The GAP and IUCN frameworks are coarse classifications (four to eight categories), whereas the APA focuses primarily on private land uses. To address these limitations, we develop here more refined implementation methods based on the human modification framework, which conceptually is rooted in characterizing the degree to which natural processes are free or controlled, and the degree to which landscape patterns are natural or artificial. To provide useful and tighter coupling of specific threats and spatial data surrogates, we refine the conceptual basis by identifying three primary types of human activities that cause modification of natural systems and patterns. These are land uses categorized as urban/built-up, recreation, and production/extraction. We detail specific metrics and common data used as surrogates that can provide a stronger basis for characterizing the degree of human modification.

We illustrate our methods by presenting analysis results for a Colorado case study.

Keywords: Human modification, protected areas, threat assessment, landscape pattern, land use.

Introduction

Overview of Conceptual Frameworks

A number of general wilderness frameworks have been established to provide a conceptual basis to understand protected areas. One of the earliest was provided by Brown and others (1978) who developed the Recreational Opportunity Spectrum (ROS), an approach that was based on characterizing resource, social, and managerial conditions for parks and recreation areas. The ROS has less well-developed guidance for characterizing threats and conservation on working and private lands. In Australia, Lesslie and Taylor (1985) developed the wilderness continuum concept that provided the basis for developing an inventory of high-quality wilderness areas. More recently, Cordell and others (2005) provided a concise review of the two most widely accepted attributes of wildlands: naturalness and wildness.

A number of efforts have built on these conceptual frameworks to provide detailed characterizations of wilderness through fine-grained mapping. Lesslie and others (1988) provided an early mapping technique based on overlaying distance classes from settlement and road infrastructure. Kliskey (1998) developed a method to better link perception of wilderness to the ROS in a spatially explicit mapping framework. Aplet and others (2000) developed a nationwide map of wilderness by distinguishing managed from natural landscapes and mapping a multidimensional index at 1-km resolution. Building on earlier work in Australia and the United States, Sanderson and others (2002) mapped the human footprint for the entire globe at 1-km resolution.

More recently, scientists have been moving from employing general indicators of wilderness (or degree of human modification) to recognizing specific indirect and direct threats (e.g., to wilderness ecosystems by Cole and Landres 1996) and the relative degree to which different

types of protected areas function to protect biodiversity. A common approach to categorizing or organizing different types of protections or threats has been to define categories based on whether land is managed for permanent biodiversity maintenance through some legal or institutional mechanism, or both. Both the World Conservation Union (IUCN) and the U.S. Geological Survey's (USGS) Gap Analysis Program (GAP) use this approach, though their protection categories differ somewhat (Davey 1998, Scott and others 1993). For example, the IUCN contains eight categories (IUCN 1994): I—scientific reserve/strict nature reserve; II—national park; III—natural monument/natural landmark; IV—managed nature reserve/wildlife sanctuary; V—protected landscapes; VI—resource reserve; VII—natural biotic area/anthropological reserve; and VIII—multiple-use management area/managed resource area.

The USGS GAP program found these too vague for their uses, and so they devised a stewardship classification with four status classes (Csuti and Crist 2000): (1) permanent protection from conversion of natural land cover, with natural disturbance events allowed; (2) permanent protection and some suppression of natural disturbance; (3) some extractive uses permitted; and (4) no protection from conversion of natural land cover.

The Land-Based Classification Standards (APA 2003) provide a multidimensional land use classification model based on five characteristics: activities (land use based on observable characteristics), functions (economic purpose), building types (structures), site development character (physical characteristics such as land cover types), and ownership constraints (private vs. public, or other legal devices to constrain use). They are richly developed for private land but are less directly applicable to public protected or conserved areas.

The IUCN categories have been revised substantially in the Conservation Measures Partnership, a collaborative effort mostly among nongovernmental organizations that includes The Nature Conservancy, World Wildlife Fund, and Conservation International, in addition to the IUCN. They recognize 11 classes of direct threats (IUCN-CMP 2006): residential and commercial development; agriculture and aquaculture; energy production and mining;

transportation and service corridors; biological resource use; human intrusions and disturbance (e.g., recreation, war, etc.); natural system modifications (e.g., fire suppression); invasive species and genes; pollution; geologic events; and climate change and severe weather.

Several alternative approaches have recently emerged. For example, the human footprint (Sanderson and others 2002) represents, in a general way, the total footprint of all the human population's influence as a continuum stretched across the land surface. Implicit in nearly all these approaches is that if an area is of high value, and it is unprotected, then it is vulnerable. However, incorporation of threat directly into these frameworks is underdeveloped, and these approaches have been critiqued because they neglect a means to assess the relative imminence of the threat or urgency of conservation action need—Are some gaps more important than others, and, if so, which ones (Margules and Pressey 2000, Theobald 2003)?

Objectives

We find four main limitations of these existing frameworks. First, they are often based on ad hoc categories or classes, with little or minimal attention to establishing explicit measures of threat. Second, they are based on discrete categories or classes, and so cannot resolve small differences. Also, because they are based on class (or nominal) data, they cannot be easily integrated at different spatial scales to examine landscape context. Third, the surrogate spatial variables that are used as a basis for classifying are generally too coarse grained to capture fine-grain patterns, ultimately limiting detailed characterization. Finally, and, especially, most approaches examine the in situ landscape content of a park or protected area (PPA) using levels of threat or protection. Typically, an individual PPA receives a single score, regardless of size or the types of adjacent land uses. For example, although national parks often have an intensely used, built-up portion (e.g., Yosemite Valley in Yosemite National Park) directly adjacent with designated wilderness, typical protocols and methods result in only a single value being applied to the entire PPA. In addition to content, we believe that the landscape context of a PPA is important as well. This aligns analytical methods with

Table 1—Example land uses along human modification gradient for each factor. Each row provides an example of a possible human use along the “wild” (0.0) to human-dominated (1.0) gradient for each of the three factors (columns)

Value	Convert (urban/built-up)	Extract (production/extraction)	Visit (recreation/work)
0.0	Wilderness	Wilderness	Municipal watershed (no access)
0.1	Wilderness with trails	Gathering	Private preserve (guided access)
0.2	Wilderness w/trails, bridges	Public grazing allotments	Wilderness area
0.3	Multiuse forest	-	Backcountry forest
0.4	Rural housing density	Timber selective cut	Multiuse forest
0.5	Campground	Hay meadow	Highuse trail/destination
0.6	Exurban housing density	Timber clearcut	Motorized recreation
0.7	Visitor center	Dryland crop	Cross-country ski resort
0.8	Suburban housing density	Oil/gas well	Downhill ski resort
0.9	Urban residential	Mine	Urban park
1.0	Commercial/industrial	Irrigated cropland	Sports stadium/complex

the growing concerns of land managers over these external threats. For example, two of the main threats to the National Forest System (loss of open space due to housing development and invasive species) are external (Bosworth 2004), and changes in surrounding land use are a leading threat to resources in United States national parks (GAO 1994).

We aim to address these limitations by building on the human modification framework (HMF) (Theobald 2004). The HMF is based on two dimensions: the degree to which natural processes are free or controlled, and the degree to which landscape patterns are natural or artificial. To provide useful and tighter coupling of specific threats and spatial data surrogates, we refine the conceptual framework by identifying three primary types of human activities that cause human modification of natural systems and patterns. These are land uses categorized as urban/built-up, recreation, and production/extraction. We detail specific metrics and common data used as surrogates that can be used to implement each of these factors to provide a stronger basis for characterizing the degree of human modification. Our overall goal in this paper is to develop a general yet simple method to characterize threats associated with human land use activities for managing landscapes and to provide metrics and more directly capture threats in a detailed, spatially explicit manner. Our objectives are to describe factors that can be used to refine the HMF, identify common surrogates of these factors that can be mapped at relatively fine grain, conduct a spatially explicit analysis of

the landscape context, and illustrate these methods using a case study example for the State of Colorado.

Methods

Human Modification Framework

Here we further refine the HMF to emphasize three primary factors that can be used to characterize land use based on what human activities occur at a given location. Principally, humans go to an area to produce or remove natural resources (production/extraction), visit but do not extract significant resources (recreation/tourism), or concentrate or intensify resources by reconfiguring and constructing buildings and other infrastructure (urban/built-up). Each of these three factors begins with a value of 0.0 denoting no human influence (i.e., a wild location), and 1.0 representing an area that is strongly influenced (developed) by human activities. We seek to fully characterize the spatial heterogeneity of threats by characterizing land uses at a relatively fine grain ($<1 \text{ km}^2$ cells or minimum mapping unit), rather than attributing an average or overall value across a broader spatial extent (e.g., a GAP stewardship value for an entire national park). We then can overlay our threat maps with a map of protected areas to assess gaps and opportunities.

For each factor, we explicitly place values for different levels of threat along a 0 to 1.0 axis (Table 1). Although these values are either assigned arbitrarily, based on expert opinion, mapped through surrogate variables, or quantified

Table 2—Possible surrogate spatial data for urban/built-up factor

Data	Source	Scale (extent/grain)	Notes
Housing density	Census Bureau; SERGoM v2 (Theobald 2005)	Nationwide/block Nationwide/1 ha	Better indicator of landscape change than population density
Population density	Census Bureau	Nationwide/block	Commonly used
Road density	Census TIGER; GDT; NavTec	Nationwide/1:100K	Need to identify the radius or size of the moving window in computing density. Major road types are often distinguished and weighted when computing road density. Need to extend to characterize road use (i.e., traffic volume) as well. Poor representation of rural, forest, park areas
Structures (houses, buildings, bridges)	Parcel-level National forest/park unit	County by county	Critical data for fine-grained analysis, but very limited availability etc.
Trail density	National forest/PPA	PPA/1:24K, GPS	Need to specify radius of moving window when computing density (~ 500 m) Can major differences in trail types, such as modes of use, use level be distinguished? Standardized, consistent data on trails are not available
Campground density	USFS	PPA/1:24K	Location of campgrounds, number of units/sites, and type of use
Dam density	National Inventory of Dams 1: 1,000,000	Nationwide/	For major dams (> 4 m in height); spatial precision issues; incomplete attributes such as year built, storage volume, etc.
Land cover	National Land Cover Data set (NLCD)	Nationwide/900 m ²	Urban/built-up classes (21, 22, 23)—update with NLCD 2001 when available

Each row provides an example of a possible spatial datum that is commonly used as a surrogate for this factor.

PPA = park or protected area.

using some combination of these, it is critical that we make our assumptions quantitatively explicit, at the very least to communicate how threats may affect a location and their relative importance to other threats. Also note that this approach is agnostic to land ownership—that is, land use activities for each of these factors can occur on both private and public lands (though some types may be more dominated than others). For example, although built-up is often associated with urban areas, some localized areas within protected areas (e.g., a national park visitor center) can be

highly built-up as well. Table 2 proceeds a short, preliminary listing of surrogate maps that are commonly used to estimate these activities for the three factors—yet much work needs to be done to fill these critical data gaps. Again, we emphasize that often these values are arbitrary, but providing explicit values is a useful and important exercise.

Urban/Built-Up—

This factor characterizes the intensity to which humans occupy a given location. Human activities often concentrate

or intensify resources by reconfiguring resources or constructing buildings and other infrastructure such as roads, dams, bridges, etc. Table 2 provides a list of useful data layers that can be used to measure the degree of the urban/built-up factor. Common surrogate spatial variables include population density and housing density. We prefer housing density because it more directly characterizes landscape and ecological changes on the ground, whereas population density is attributed typically only for primary residences. Data on residential land cover (e.g., from National Land Cover Data (NLCD)) are often used to represent built-up areas, though additional data from the Census Bureau (or parcel level) are needed to characterize lower density development beyond the urban fringe. Commercial, industrial, and transportation land uses also are associated with high levels of human modification (e.g., high levels of impervious surface), population density (less direct), etc. Data on transportation infrastructure, such as road density (e.g., Theobald 2003), are also strong measures of land uses associated with built-up areas. We believe that housing density and road density provide complementary information—high density of roads can occur not only in urban areas but also in remote rural areas (e.g., forest logging roads). Recently, researchers are beginning to distinguish major road types (e.g., interstate vs. secondary roads) when computing road density, though more work to characterize road use rather than the existence of roads is needed. Improved data sets are needed to better identify the location and intensity of structures in rural areas, particularly bridges, culverts, roadway fences, utility corridors (e.g., power lines, pipelines, etc.).

Production/Extraction—

This factor characterizes the intensity of human activities associated with the amount and intensity of extracting or removing resources. Agricultural production, especially cropland, but, also, grazing and mining and timber activities are common forms of this activity type (Table 3). It is common to use land cover data to map production land uses that have caused land cover conversion, such as agricultural croplands and orchards. The intense changes in pattern and the high degree of modification of ecological processes mean that this is a critical component to map. A variety of

also additional activities also contribute to human modification for which data are less commonly available. This would include spatially explicit information about grazing (intensity and animal density) through permits on public lands and stocking rates on private lands. Extraction of natural resources in the form of quarries and mines that cause significant land surface modification can be readily identified. However, activities with extensive but more diffuse disturbance (e.g., oil and gas wells or selective harvesting/thinning of forest products) are more difficult to identify and generate metrics from typical satellite imagery, though increasingly specialized databases (e.g., well locations) are being developed.

Recreation and Tourism—

This factor characterizes the intensity of human activities associated with use or visitation of an area. This is best represented by recreation and tourism activities, but can also include work-related activities. It includes the amount and type (mode) of recreational use (i.e., pedestrian only, passive, motorized, etc.). There are a large number of important data gaps here—particularly whether areas are publicly accessible, motorized vs. nonmotorized use, visitor use levels, etc. (Table 4).

Spatially explicit data on this aspect of human modification are particularly underdeveloped. Although general visitor use levels may be available for whole parks or national forests, more detailed data to map the visitation levels (and the timing) are particularly poor. Use has been estimated based on trail density (Schumacher and others 2000), though this suffers from the same limitation as road density methods—namely the assumption that areas close to trail heads receive the same amount of use as those more distant. Methods to estimate visitor use via spatial models of accessibility are increasingly common (Geertman and van Eck 1995).

Assessing Landscape Context—

To characterize risks within the landscape, we assign each factor a value along a 0 to 1.0 axis based on explicit criteria (Table 5). We use a fuzzy average approach to combine our individual surrogate layers (in GIS) into a composite value layer for each factor. This is calculated simply as

Table 3—Possible surrogate spatial data for production/extraction factor

Data	Source	Scale (extent/grain)	Notes
Grazing	U.S. Forest service; BLM; private	National/1:100K	Characterize by animal unit months, permit locations—but these data are mostly unavailable in electronic, spatial format
Oil & gas well density	Colorado Oil & Gas Conservation Commission	Statewide/1:100K	Point locations of wells, need to define “footprint”
Cropland, grazing	USGS National Land Cover Data set	National/0.09 ha	Cropland (NLCD classes 81-85) Grazing estimated from grassland, shrubland, and forested land
Mining (gravel, hard-rock, etc.)	Colorado Division of Minerals and Geology	Statewide/1:100k	-
Groundwater wells	State water engineer	Statewide/1:100K	Poor availability of data on recharge rate, spatial location often tied to center of Public Land Survey Section

Each row provides an example of a possible spatial datum that is commonly used as a surrogate for this factor.

Table 4—Possible surrogate spatial data for recreation/visitation factor

Data	Source	Scale (extent/grain)	Notes
Parks and protected areas	World Protected Areas Database Protected Areas Database; COMaP	Nationwide/block Nationwide/1 ha	Inconsistent; poor data for State, local (city and county), private (reserves, conservation easements)
Visitor use levels	National Forest Service survey?	Nationwide/?	Very coarse (State/forest) data, need data to be tied to trailheads
Recreational facilities (golf courses, ski areas, etc.)	Census TIGER; GDT; NavTec	Nationwide/1:100K	Use levels (visitor days per year) would be useful
Accessibility from urban populations	Cost distance weighting	Nationwide/1:100K	-

Each row provides an example of a possible spatial datum that is commonly used as a surrogate for this factor.

the maximum value (at every cell) of any single input. These ratio values are then spatially averaged over different neighborhood sizes and shapes to establish a measure of landscape context. A challenging part of developing estimates along the three factors is to be explicit about the spatial characterization. That is, for example, when a value for wilderness is prescribed, does this apply to an entire wilderness area (as a political designation), or within some defined neighborhood (e.g., within a 1-km circular window)? The spatial grain needs to be considered before one

provides or computes estimates of any given factor. Here we summarize the spatial context using circular moving windows with radii of 1 and 5 km. These distance values are arbitrary, but attempt to capture the relatively local and midscale spatial context pattern. Again, our goal here is to provide an illustration of the broader method, and users will likely want to employ different values that reflect the species, process, or patterning that they are concerned about, which likely varies across ecoregions.

Table 5—Surrogate variables used for human modification framework factors for Colorado

Surrogate variable	Factor		
	Convert urban/built-up	Extract Production/extraction	Visit Recreation/work
Land cover (NLCD) ¹	Comm/ind (23) = 1.0 High dens. res. (22) = 0.9 Low dens. res. (21) = 0.8 Barren (33) = 0.6 Grass/parks (85) = 0.5	Orchards (61) = 0.6 Pasture (81) = 0.5 Row crops (82) = 1.0 Nonrow crops (83) = 0.7 Other ag (84) = 0.8 Quarries/mines (32) = 0.9	-
2000 housing density ²	Urban (13-15) = 0.9 Suburban (12) = 0.8 Exurban (7-11) = 0.6 Rural (4-6) = 0.4	-	-
Roadedness ³	Interstates (CFC A1x) = 1.0, 60-m buffer Highways (CFCC A2x) = 1.0, 30-m buffer Secondary (CFCC A3x) = 1.0, no buffer Local (CFCC 4x) = 0.5, no buffer 4WD (CFCC 5x) = 0.2, no buffer	-	-
Accessibility (only public lands) ⁴	-	-	<0.5 hrs = 1.0 0.5-1 hr = 0.8 1-2 hrs = 0.5 2-4 hrs = 0.3 4-8 hrs = 0.1 >8 hrs = 0.0
Oil & gas wells ⁵	-	W/in 60-m radius = 1.0, w/in 100 m = 0.7, w/in 200 m = 0.3, w/in 300 m = 0.1	-
Mining operations ⁶	-	Coal exploration and unknown = 0.3 m, underground = 0.5, heap leach = 0.8, in-situ = 0.8, surface and underground = 0.9	-
COMaP (NF management types)	-	-	Ski resorts = 0.8 Motorized = 0.6 Multiuse = 0.4 Backcountry = 0.3 Wilderness = 0.2

¹ USGS National Land Cover Dataset, 0.09-ha resolution, ~1992-94.

² U.S. Census Bureau 2000 <http://www.census.gov>, Theobald 2005 www.asri.com/data, 1-ha resolution.

³ Created from ESRI Streetmap 2006 data.

⁴ Created from travel time along major roads, weighted by population size to nearest urban area, for urban areas with population > 100k and ≤ 100k, data from ESRI Streetmap 2006.

⁵ Colorado Oil and Gas Conservation Commission, Well and facility shapefiles, downloaded 16 July 2006 from <http://www.oil-gas.state.co.us>.

⁶ Mining data converted points to circles with area equal to permitted area ($\sqrt{[\text{Permit_acr}] * 4048 / 3.1415}$).

Note: CFCC = census feature class code; 4WD = four-wheel drive.

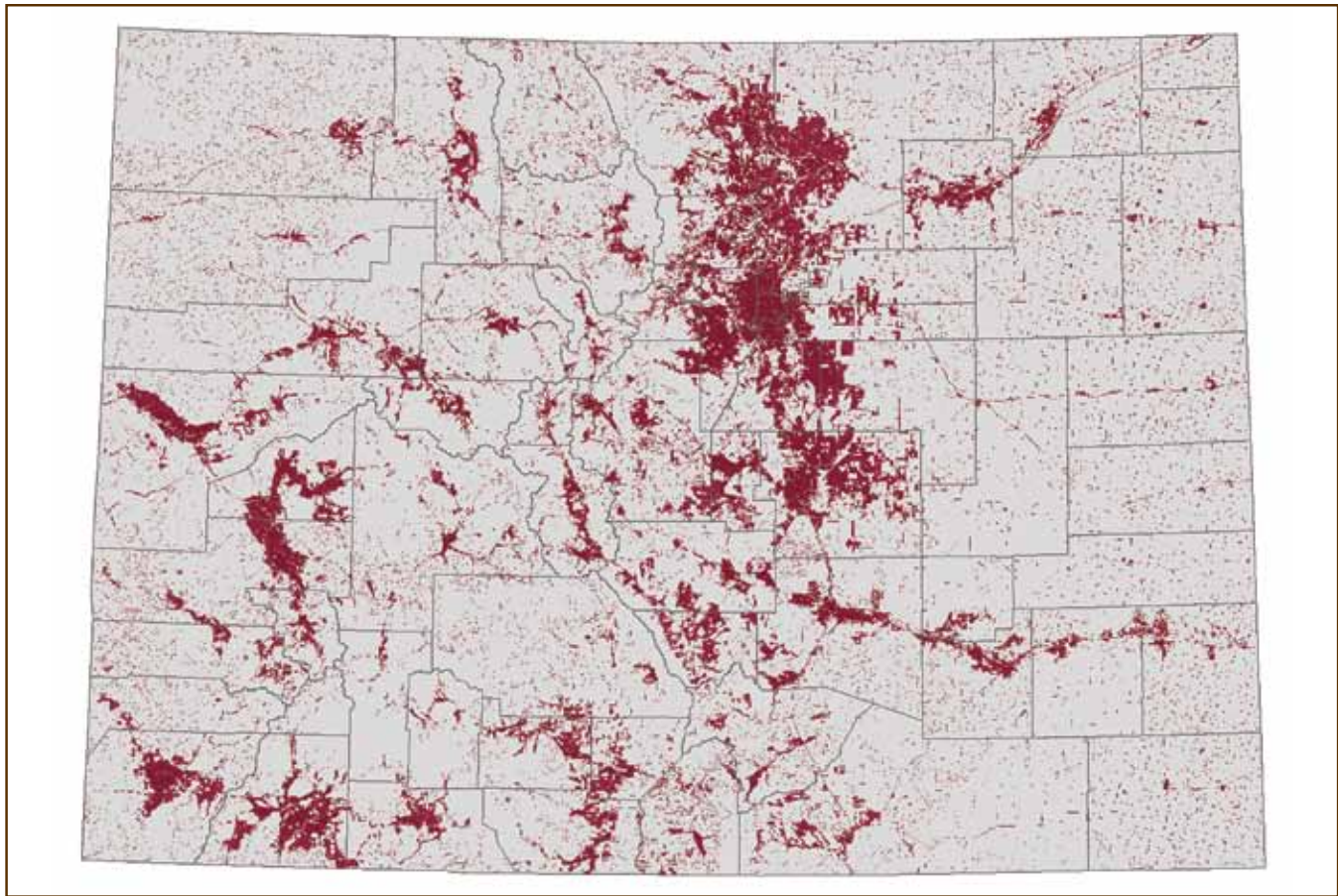


Figure 1—This composite map for urban/built-up areas in Colorado shows the degree to which locations have been converted, or built-up. This is a composite of commercial, industrial, and residential development (from National Land Cover Data Set); a “roadedness” layer that depicts the footprint of interstates, highways, and roads; and housing density (including exurban and rural densities) from SERGoM v2 (Theobald 2005). Darker shades show a higher level of built-up, grey shows absence, and grey lines show county boundaries. Note that the Front Range (Fort Collins, Denver, Colorado Springs) is clearly visible, as are many of the mountain valleys.

Results

The composite map of the degree to which an area is urban/built-up shows a relatively familiar pattern of urban areas, particularly the cities along the Colorado Front Range (Figure 1). Including information on slightly lower density of houses provides a fairly large expansion of locations that are developed beyond those locations identified in NLCD, particularly along mountain valleys.

The composite map of production and extraction-oriented land use provides a fairly different picture of Colorado (Figure 2). Extensive lands have been converted to cropland agriculture in the eastern plains and San Luis Valley. Another factor included is the extensive distribution of

oil and gas wells, particularly in the northern Front Range area and western slope.

Perhaps the most unique contribution of this map is to portray the distribution of the extent and types of recreational uses found in Colorado (Figure 3). Compared with the typical map of public land ownership, portraying national forests, grasslands, and parks as being largely the same, this map clearly differentiates the heavy influence that accessibility to large populations (like the Front Range) can have. Accessibility here is computed as the one-way travel time (along roads) from urban areas. Also differentiated are the types of land management activities on public lands, distinguishing the heavily-recreated resort areas such as Aspen, Vail, and Breckenridge. This map also reflects

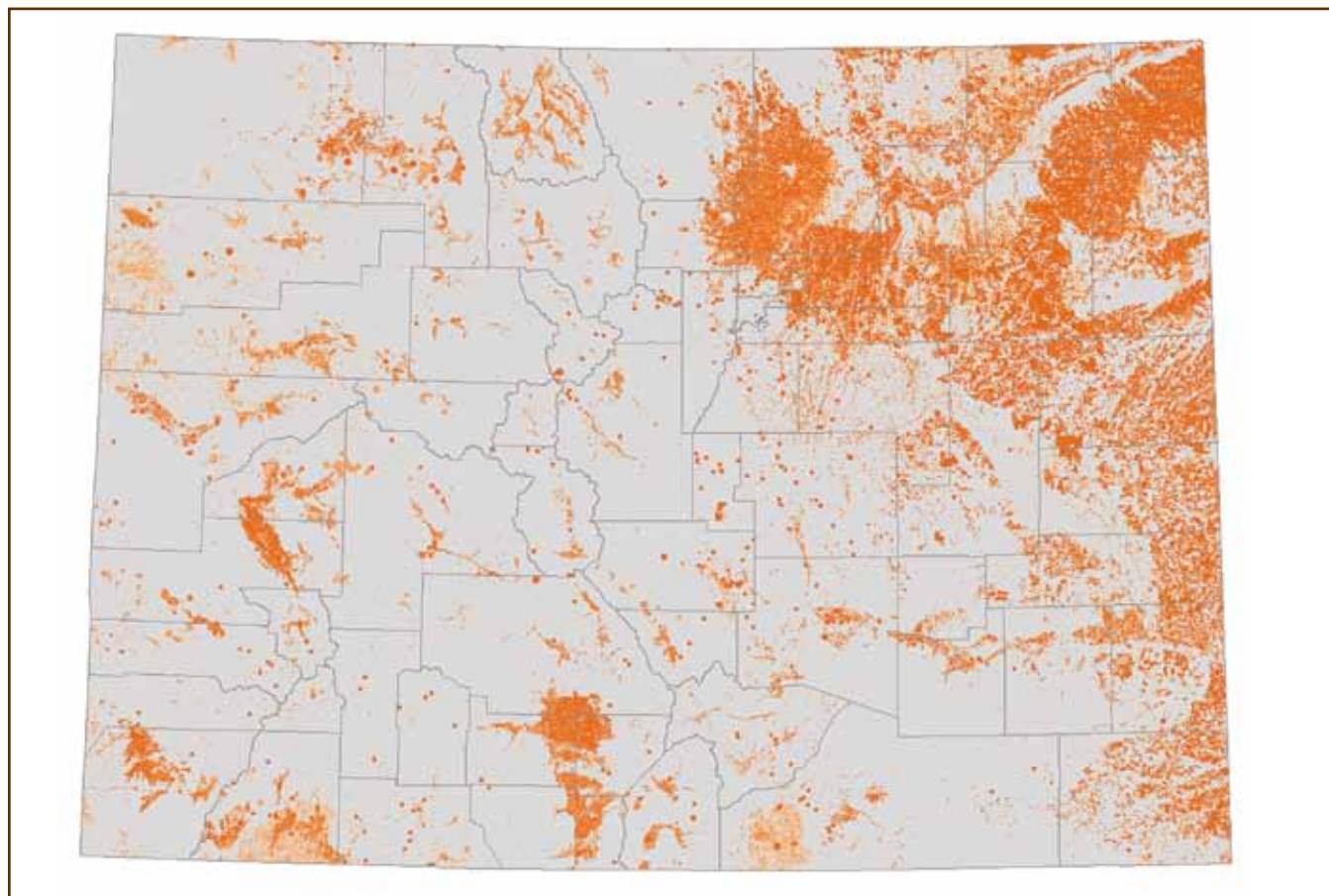


Figure 2—This map of Colorado shows the degree to which locations have some production or extraction-oriented land use. This is a composite of agricultural lands (from National Land Cover Data Set); mining activities; and oil and gas wells. Darker shades of orange show a higher level of activity, grey shows absence, and grey lines show county boundaries. Note that the productive agricultural lands of Weld and Adams County are clearly visible, as are the northeastern plains counties, whereas the San Luis Valley is visible in the south-central part of Colorado.

locations that are dominated by motorized vs. non-motorized recreation (future improvements should incorporate specific travel management plans).

The degree of human modification values vary across the State, with fine-grained differences particularly noticeable in riparian zones (Figure 4). The average HMF value is 0.392 (SD = 0.231). The range and distribution of HMF values can also be summarized by various ecological system types, such as lower montane, mixed, and upper montane zone (Table 6). Our results show that the midmontane zone has the largest average HMF score (0.428), indicating the highest degree of human activities that may modify or affect ecological systems in this zone. The upper montane zone (0.329) is the lowest of the conifer-dominated zones

(lower montane = 0.405), but aspen forests have the overall lowest degree of human modification (0.313). In addition to summarizing by counties, different analytical units such as watersheds, ecoregions, ecosystems, etc., can be supported. It is important to note that although one can summarize values over fairly large areas, as we have done by major ecological system type, the fine-grained data will allow differentiation of more localized areas that are particularly impacted or have particularly low HMF values.

Commonly, population density is used as a surrogate indicator of the degree of impact on ecological systems. Although we found a loose relationship between population density and HMF score (Figure 5), there is a fair amount of variation as well, showing the additional information that

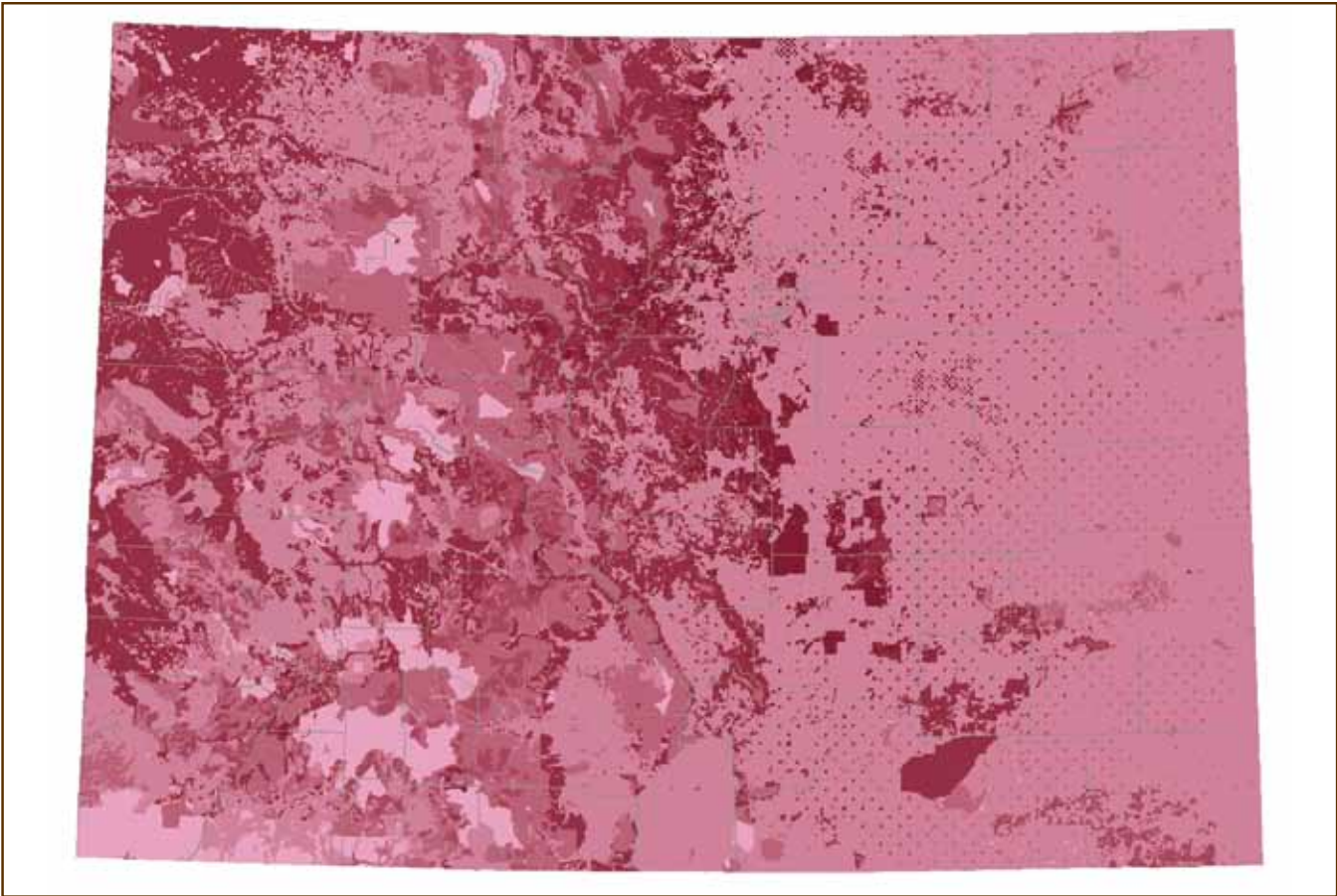


Figure 3—This composite map of Colorado for recreation/visitation shows the degree to which locations are likely to have recreation or tourism-oriented land use. This is a composite of an accessibility map that depicts the one-way travel time (along roads) from urban areas, and the type of public recreation and visitation targeted for different land management categories (especially for national parks and forests—data from the Colorado Ownership Management & Protection project). Darker shades of maroon show a higher level of activity and grey lines show county boundaries. Note that the public lands directly adjacent (mostly west of) the Front Range are highly affected, as are downhill ski resorts, and motorized recreation areas.

Table 6—Summary statistics for forested ecosystems in Colorado

Ecological systems ^a	Mean HMF (SD)
Upper montane (spruce-fir; 24, 26, 28)	0.329 (0.159)
Midmontane (Douglas-fir, lodgepole pine; 29, 30, 32)	0.428 (0.192)
Lower montane (ponderosa pine, pinyon-juniper; 34, 35, 36)	0.405 (0.203)
Aspen (22, 38)	0.313 (0.135)

^a Data from the Southwest ReGap program.

The mean and standard deviation (SD) of the final human modification (HMF) score for upper, mid, and lower montane, and aspen forests.

Table 7—Summary statistics of human modification framework (HMF) scores as summarized by GAP status level in Colorado

GAP status ^a	Mean HMF (SD)	Minimum and maximum HMF
1	0.244 (0.149)	0.1, 0.893
2	0.295 (0.166)	0.098, 1.0
3	0.421 (0.133)	0.1, 1.0
4	0.397 (0.192)	0.1, 1.0

^a Data from the Southwest ReGap program.

The mean, standard deviation (SD), minimum, and maximum of the final human modification score summarized for GAP status levels.

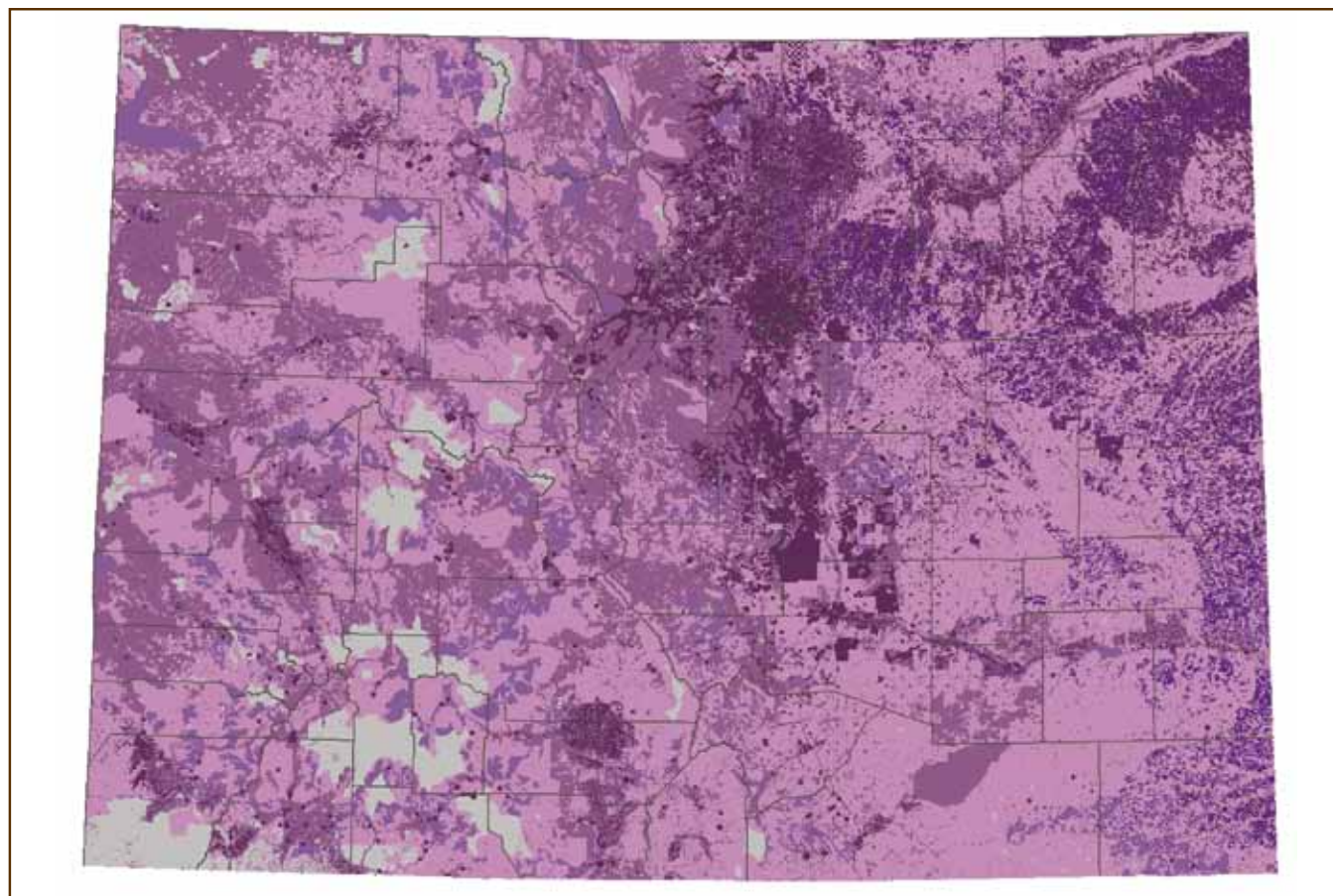


Figure 4—This map of Colorado shows the final map of degree of human modification (darker shade depicts higher degree of modification). This is a composite map of the urban/built-up, production/extraction, and recreation factor maps.

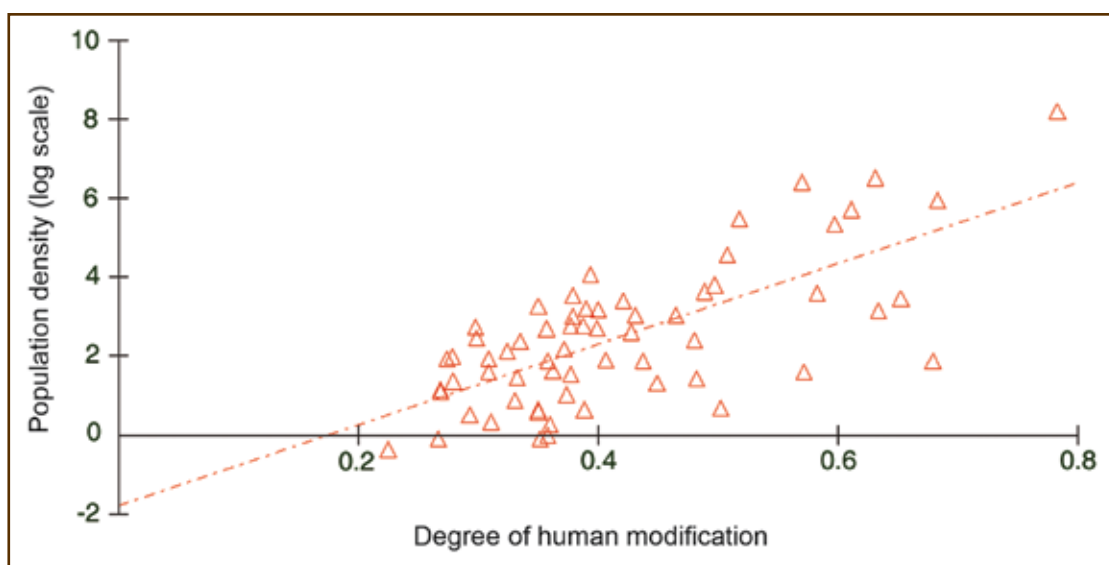


Figure 5—Population and degree of modification are compared in this graph of the county population for 2000 against the mean degree of human modification score. Although some counties fall along the linear relationship line, supporting the notion that larger populations lead to larger effects, there is a fair amount of variation as well.

this approach provides. By the same token, HMF provides a finer degree of detail than housing density—although housing density had a strong relationship.

We also compared HMF to GAP stewardship categories from the Southwest Regional GAP study (Table 7). We found that status 1 lands had lower average HMF values than status 2 (0.244 vs. 0.295), which were less than status 3 and 4. Interestingly, we found that status 4 had a lower mean HMF value than level 3 (0.397 vs. 0.421). Also, all status levels had very large maximum values (0.89 for level 1 and 1.0 for 2, 3, and 4).

Conclusion

In summary, we offer the human modification framework as an explicit approach to better quantify the spatial patterning and degree to which locations have been altered by human activities. We found that in our case study area, HMF showed markedly different results, particularly in the spatial patterns and distribution of disturbed areas, as compared to GAP status levels. An important, nonintuitive result is that we found that level 4 had less evidence of alteration than did level 3. This can occur because the HMF relies on surrogate variables that characterize current land use activities that have been shown to have effects on biodiversity. In contrast, GAP status levels characterize the legal protection from land use conversion (or management plans)—not the current condition *per se*. It is important to note that the HMF, as employed in this paper, shows existing (or at least currently known) modifications to the landscape, whereas the GAP and IUCN approach estimate long-term protection (in perpetuity). Although we did not document these trends here, the HMF methods could be easily applied to future growth or potential land use scenarios to examine the differences between their effects. The fine-grained approach and spatial context analysis in particular would be sensitive to differences in patterns of potential future land uses.

We believe that current approaches to estimating the degree of human modification can be improved in three ways. First, as understanding and elicitation of threats to protected areas matures, we believe that approaches will

need to move from using general surrogates to factors that are more closely linked to the threats, ideally in a mechanistic way. In addition, we believe that finer-grained data are increasingly required to address concerns about fragmentation and other pattern issues. Finally, the spatial (or perhaps landscape) context is critical to incorporate. Further work is needed to develop methods for generating landscape context that more directly reflect ecological processes. For example, neighborhoods for freshwater should use a series of flow-connected watersheds. Similarly, the flow or movement of processes through other transport vectors such as air, soil transport, animal movement, seed dispersal, etc., should be explicitly represented as well.

There are a number of data gaps that need to be filled. Some of these gaps could be filled by collecting data from field offices, standardizing the data and entering them into an electronic database (with spatial coordinates recorded). For example, grazing permit data have been collected for many decades, but much of it remains in an unstandardized, unmapped, and nonelectronic format. The location of timber harvests (year, harvest method) data are available, but not in a consistent, easy-to-use format. Another type of data gap would simply require acquisition and compilation of existing spatial databases (e.g., highway structures such as fencing, culverts, bridges, etc., or hiking trails that would include structures, tread type, width, use, etc.). Spatial data about water infrastructure, in addition to large dams, would be useful as well for structures such as ditches, levees, rip-rap, and channelized segments.

Acknowledgments

This research was supported in part by a grant from the USDA National Research Initiative (Award No. 2003-35401-13801, NRI, CSREES, USDA).

Literature Cited

APA (American Planning Association). 2003. Land-based classification standards. [online] URL: <http://www.planning.org/lbcs/>. (December 7, 2006).

- Aplet, G.; Thomson, J.; Wilbert, M. 2000.** Indicators of wildness: using attributes of the land to assess the context of wilderness. In: Cole, D.N.; McCool, S.F., eds. *Proceedings: Wilderness science in a time of change.* RMRS-P-15-VOL-5. Fort Collins, CO: U.S. Department of Agriculture, Forest Service, Rocky Mountain Research Station: [Not paged].
- Bosworth, D. 2004.** Four threats to the Nation's forests and grasslands. Speech at the Idaho Environmental Forum, Boise, ID, 16 January. [online] URL: <http://www.fs.fed.us/news/2004/speeches/01/idaho-four-threats.shtml>. [Date accessed: December 7, 2006].
- Brown, P.J.; Driver, B.L.; McConnell, C. 1978.** The opportunity spectrum concept and behavioral information in outdoor recreation resource supply inventories: background and application. In: Lunde, G.H. and others, eds. *Proceedings: Integrated inventories of renewable natural resources.* Gen. Tech. Rep. RM-55. USDA Forest Service, Rocky Mountain Research Station, Fort Collins, CO: 73–84.
- Cole, D.N.; Landres, P.B. 1996.** Threats to wilderness ecosystems: impacts and research needs. *Ecological Applications*. 6(1): 168–184.
- Cordell, H.K.; Bergstrom, J.C.; Bowker, J.M., eds. 2005.** The multiple values of wilderness. State College, PA: Venture Publishing. [Not paged].
- Csuti, B.; Crist, P. 2000.** Mapping and categorizing land stewardship. Version 2.1.0. A handbook for conducting gap analysis. Moscow, ID: University of Idaho. [Not paged].
- Davey, A.G., ed. 1998.** National system planning for protected areas. Gland, Switzerland: World Conservation Union. [Not paged].
- GAO (U.S. General Accounting Office). 1994.** Activities outside park borders have caused damage to resources and will likely cause more. [Place of publication unknown]: U.S. Government Printing Office, GAO/RCED-94-59. [Not paged].
- Geertman, S.C.M.; van Eck, J.R.R. 1995.** GIS and models of accessibility potential: an application in planning. *International Journal of Geographical Information Systems*. 9(1): 67–80.
- IUCN (International Union for the Conservation of Nature). 1994.** Guidelines for protected area management categories. Gland, Switzerland: IUCN. 261 p.
- IUCN-CMP 2006.** Unified Classification of Conservation Actions, Version 1.0. [online] Conservation Measures Partnership URL: http://conservationmeasures.org/CMP/IUCN/Site_Page.cfm. [Date accessed: December 7, 2006].
- Kliskey, A.D. 1998.** Linking the wilderness perception mapping concept to the recreation opportunity spectrum. *Environmental Management*. 22(1): 79–88.
- Lesslie, R.G.; Mackey, B.G.; Preece, K.M. 1988.** A computer-based method of wilderness evaluation. *Environmental Conservation*. 15(3): 225–232.
- Lesslie, R.G.; Taylor, S.G. 1985.** The wilderness continuum concept and its implications for wilderness preservation policy. *Biological Conservation*. 32: 309–333.
- Margules, C.R.; Pressey, R.L. 2000.** Systematic conservation planning. *Nature*. 405: 243–253.
- Sanderson, E.W.; Jaiteh, M.; Levy, M.A. [and others]. 2002.** The human footprint and the last of the wild. *BioScience*. 52(10): 891–904.
- Schumacher, J.V.; Redmond, R.L.; Hart, M.M.; Jensen, M.E. 2000.** Mapping patterns of human use and potential resource conflicts on public lands. *Environmental Monitoring and Assessment*. 64: 127–137.
- Scott, J.M.; Davis, F.; Csuti, B. [and others]. 1993.** Gap analysis: a geographic approach to protection of biological diversity. *Wildlife Monographs*. 123: 1–41.

- Theobald, D.M. 2003.** Targeting conservation action through assessment of protection and exurban threats. *Conservation Biology*. 17(6): 1624–1637.
- Theobald, D.M. 2004.** Placing exurban land use change in a human modification framework. *Frontiers in Ecology and Environment*. 2(3): 139–144.
- Theobald, D.M. 2005.** Landscape patterns of exurban growth in the U.S.A. from 1980 to 2020. *Ecology and Society*. 10(1): 32. [online] URL: <http://www.ecologyandsociety.org/vol10/iss1/art32/>. [Date accessed: December 7, 2006].

Modeling Species' Realized Climatic Niche Space and Predicting Their Response to Global Warming for Several Western Forest Species With Small Geographic Distributions

Marcus V. Warwell, Gerald E. Rehfeldt,
and Nicholas L. Crookston

Marcus V. Warwell, geneticist, **Gerald E. Rehfeldt**, plant geneticist (emeritus), and **Nicholas L. Crookston**, operations research analyst, USDA Forest Service, Rocky Mountain Research Station, Forestry Sciences Laboratory, Moscow, ID 83843.

Abstract

The Random Forests multiple regression tree was used to develop an empirically based bioclimatic model of the presence-absence of species occupying small geographic distributions in western North America. The species assessed were subalpine larch (*Larix lyallii*), smooth Arizona cypress (*Cupressus arizonica* ssp. *glabra*), Paiute cypress (syn. Piute cypress) (*Cupressus arizonica* ssp. *nevadensis*), and Macfarlane's four-o'clock (*Mirabilis macfarlanei*). Independent variables included 33 simple expressions of temperature and precipitation and their interactions. These climate variables were derived from a spline climate model for the Western United States that provides point estimates (latitude, longitude, and altitude). Analyses used presence-absence data largely from the Forest Inventory and Analysis, USDA Forest Service database. Overall errors of classification ranged from 1.39 percent for Macfarlane's four-o'clock to 3.55 percent for smooth Arizona cypress. The mapped predictions of species occurrence using the estimated realized climatic niche space were more accurate than published range maps. The Hadley and Canadian general circulation models (scenario IS92a for 1 percent increase GGa/year) were then used to illustrate the potential response of the species' contemporary realized climatic niche space to climate change. Predictions were mapped at a 1-km² resolution. Concurrence between species' geographic distribution and their contemporary realized climatic niche rapidly disassociates through the century. These models demonstrate the heightened risk for species occupying small geographic ranges of displacement into climatic

disequilibrium from rapid climate change and provide tools to assist decisionmakers in mitigating the threat.

Keywords: Bioclimatic models, climatic distributions, climatic niche, global warming, Random Forests multiple-regression tree, response to climate change, narrow endemic.

Introduction

Climate is a principle factor that controls where species occur in nature (Woodward 1987). As the climate changes so then does the distribution of species. Long-lived plant species have adapted repeatedly to past climate change (see Ackerly 2003). When climate change exceeds species' tolerance limits, continued survival is dependent on the species ability to genetically adapt or migrate, or both, to suitable climate. These processes have contributed successfully to the persistence of long-lived plant species in response to past climate change (Davis and Shaw 2001). Their effectiveness under future climate change may be exacerbated by the increased rate of change predicted to occur over the present century. Projections for change in global climate rival historical periods of climate change at an accelerated rate (Houghton and others 2001). The accelerated rate of change threatens to displace current plant species distributions into climatic disequilibrium resulting in an increased potential for extinction of all or portions of species' ranges (Thomas and others 2001).

The objective for these analyses was to develop bioclimatic models that predict the occurrence of species with small natural distributions in the Western United States and project where suitable climates for the natural occurrence of these species may occur in the future in response to global warming. Three species were selected for the purposes of this analysis. The first was subalpine larch (*Larix lyallii* Parl.), a high-elevation, deciduous conifer inhabiting the Pacific Northwest. The second included two subspecies of Arizona cypress (*Cupressus arizonica* Greene), the smooth Arizona cypress (*C. arizonica* var. *glabra* (Sudw.) Little), which is endemic to central Arizona, and the Paiute cypress

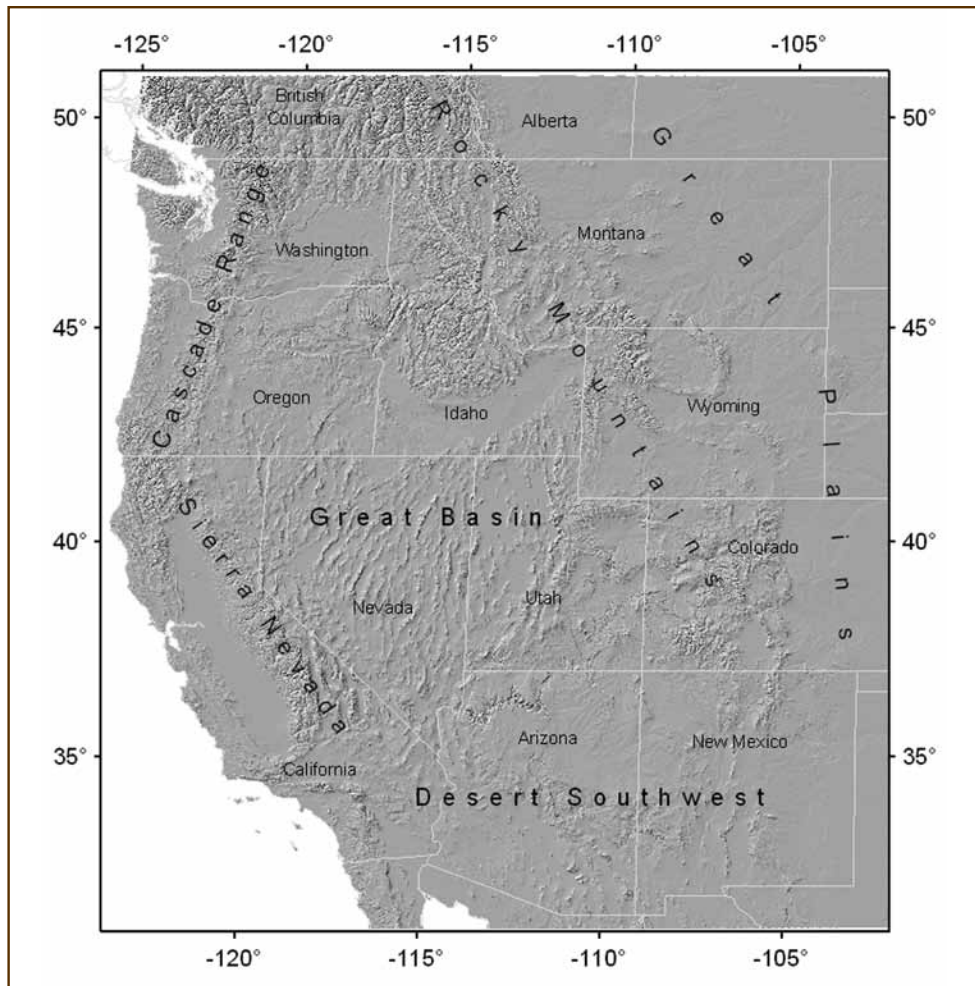


Figure 1—This shows the Western United States and southwestern Canada (from Rehfeldt and others 2006).

(syn. Piute cypress) (*C. arizonica* ssp. *nevadensis* Abrams E. Murray), which is endemic to the southern tip of the Sierra Nevada. The third was Macfarlane's four-o'clock (*Mirabilis macfarlanei* Constance & Rollins), a long-lived, deep-rooted perennial species that inhabits mid-to low-level canyon grasslands near the Oregon-Idaho northern border and is listed as endangered by the Bureau of Land Management (BLM) (USFWS 1996).

Methods

Study Area

The area of study consisted of the region supported by the climate surfaces of Rehfeldt (2006). This area encompasses

the Western United States and southwestern Canada, latitudes 31° to 51° N and longitudes 102° to 125° W (Figure 1).

Climate Estimates

Spline climate model (Rehfeldt 2006) was used to estimate climate at point locations (latitude, longitude, and altitude). The model is based on monthly minimum, maximum, and average temperatures and precipitation normalized for the period of 1961-90. This data was obtained from more than 3,000 weather stations dispersed throughout the conterminous Western United States and southwestern Canada. Hutchinson's (1991, 2000) thin plate splines were used to develop geographic surfaces for monthly data. The result produced 48 surfaces representing minimum, maximum, and average temperature and precipitation for each month

Table 1—Climate variables and their acronyms used as independent variables in regression analyses (from Rehfeldt and others 2006)

Acronym	Definition
MAT	Mean annual temperature
MTCM	Average temperature in the coldest month
MMIN	Minimum temperature in the coldest month
MTWM	Mean temperature in the warmest month
MMAX	Maximum temperature in the warmest month
MAP	Mean annual precipitation
GSP	Growing season precipitation, April through September
TDIFF	Summer-winter temperature differential, MTWM-MTCM
DD5	Degree-days > 5 °C
DD0	Degree-days < 0 °C
GSDD5	Accumulated growing-season degree days > 5 °C, April through September
MINDD0	Minimum degree-days < 0 °C
SDAY	Julian date of the last freezing date of spring
FDAY	Julian date of the first freezing date of autumn
FFP	Length of the frost-free period
D100	Julian date the sum of degree-days > 5 °C reaches 100
AMI	Annual moisture index, DD5/MAP
SMI	Summer moisture index, GSDD5/GSP
PRATIO	Ratio of summer precipitation to total precipitation, GSP/MAP
Interactions: MAP x DD5, MAP x MTCM, GSP x MTCM, GSP x DD5, DD5 x MTCM, MAP x TDIFF, GSP x TDIFF, MTCM/MAP, MTCM/GSP, AMI x MTCM, SMI x MTCM, TDIFF/MAP, TDIFF/GSP, PRATIO x MTCM, PRATIO x DD5	

of the year. For our analyses, these surfaces were used to estimate 33 climate variables that represent a range in climate variables from simple sums to complex interactions of temperature and precipitation (Table 1).

An updated version of the spline climate model was used to predict the effects of global warming for decades beginning in 2030, 2060, and 2090. The model used a regional summary of the IS92a scenario (1 percent per year increase in greenhouse gases after 1990) of the International Panel on Climate Change (Houghton and others 2001) from General Circulation Models (GCMs) produced by the Hadley Centre (HadCM3GGa1) (Gordon and others 2000) and

the Canadian Centre for Climate Modeling and Analysis (CGCM2_ghga) (Flato and Boer 2001). These two models are generally well respected, and averages of their predictions should provide an illustration of the potential effects of global warming.

Vegetation Data

Species were selected for this analysis based on their small geographic range and the availability of point location data to the authors. Species presence data were acquired from Barnes (1996) for Macfarlane's four-o'clock, Arno (1970), Khasa and others (2006), and Forest Inventory and Analysis, USDA Forest Service (FIA) database for subalpine larch, and unpublished field data from Forest Service RMRS, Moscow Forestry Sciences Laboratory, for smooth Arizona cypress and Paiute cypress (see Rehfeldt 1997). The FIA plot data were used to identify locations where the species did not occur. Their database was developed from a systematic sampling of woody vegetation permanent plots on forested and nonforested lands (Alerich and others 2004, Bechtold and Patterson 2005) within the United States. In accordance with FIA proprietary restrictions, plot locations are not available for publication. However, we were given access to their database to generate climate estimates for each plot directly from uncompromised field data. The resulting data sets include a tabulation of the presence-absence of species at approximately 117,000 locations.

Statistical Procedures

The Random Forests classification and regression tree package (Breiman 2001, Liaw and Wiener 2002, R Development Core Team 2004) was used to model species presence and absence. This tree-based method of regression uses a nonparametric approach and is resistant to overfitting, as multicollinearity and spatial correlation of residuals are not issues (Breiman 2001). Consequently, the algorithm was well suited for our analyses, which used variables among which intercorrelations could be pronounced.

An analysis data set was constructed for each species that initially included all predictor variables. Observations in this data set include all the observations with presence = yes weighted by a factor of 3. These observations made up

Table 2—Number of field plots in which each species was present, the number of locations contained within the 33-variable climatic envelope, the number of standard deviations for each climate variable in which the envelope was expanded, and the number of locations within the expanded envelope

Species	Number of plots			
	Present	Envelope	Standard deviations	Expanded envelope
Subalpine larch (<i>Larix lyallii</i>)	168	683	± 4.2	12,809
Smooth Arizona cypress (<i>Cupressus arizonica</i> ssp. <i>glabra</i>)	22	156	± 3.5	1,782
Paiute cypress (<i>Cupressus arizonica</i> ssp. <i>Nevadensis</i>)	49	537	± 11.6	3,811
Macfarlane's four-o'clock (<i>Mirabilis macfarlanei</i>)	27	107	± 3.0	1,910

40 percent of the total for a species (Table 2). The remaining observations (60 percent) of presence = no were selected by a stratified random sample of locations from two strata constructed using threshold values of the 33 predictor variables that define a climatic envelope for the species. The first stratum is the space formed by an expanded climatic envelope, where the expansion is defined by increasing the range for the threshold values of each climatic variable. The climate envelopes were expanded by factors large enough to produce about 20 times the number of locations sampled. The second stratum included locations outside the expanded envelope.

Regression analysis used 10 independent forests of 100 independent regression trees. Random Forests builds each tree using a separate boot-strap sample of the analysis data resulting in about 36 percent of the observations being used to compute classification error.

A set of regressions were run. The first regression used 33 climate predictors. Random Forest produces indices of variable importance (mean decrease in accuracy). The 12 least important variables were dropped after the first run. The regression procedure was then rerun nine more times with the remaining predictors, whereby the least important 1 to 3 predictors were dropped at each run until classification errors began to increase. The Random Forests run with the fewest variables selected prior to detecting an increase in classification error was considered the most parsimonious bioclimatic model for the species.

Mapping Procedure

Rehfeldt's climate surfaces (2006) and those updated to convey global warming were used to estimate the climate for nearly 5.9 million pixels (1 km² resolution) representing the terrestrial portion of the study area. The average altitude was made available from Globe (1999). The estimated climate and projected climates of each pixel were run down the 100 regression trees in the final set and the number of trees that predict the species is present and the number predicting absence were tabulated. A single-tree prediction is termed a vote. The votes were grouped into six categories: < 50, 50-60, 60-70, 70-80, 80-90, 90-100 percent. We consider any pixel in the first group as not having suitable climate for the species and define pixels in the other five categories as the species' realized climatic niche space. The fit of the mapped projections were assessed visually by comparing them with locations where the species were observed or Little's range maps (1971, 1976) that are available as digitized files (USGS 2005), or both.

Results

We found that reasonably parsimonious bioclimatic models are driven by either three or four climate variables (Table 3). Overall out-of-bag classification errors from fitting of the Random Forests algorithm ranged from 1.39 percent for Macfarlane's four-o'clock to 2.2 percent for subalpine larch. The models predicted species occurrence where species were known to occur with perfect accuracy (0 errors of omission); the error therefore is due to commission,

Table 3—Statistical output from bioclimatic models: classification errors from the confusion matrix, and the important predictors according to mean decrease in accuracy; variable acronyms are keyed to Table 1

Species	Classification errors (%)			Important variables
	Omission ^a	Commission ^b	Overall ^c	
Subalpine larch (<i>Larix lyallii</i>)	0	3.94	2.2	GSP × TDIFF, MAP × MTCM, MMIN
Smooth Arizona cypress (<i>Cupressus arizonica</i> ssp. <i>glabra</i>)	0	6.37	3.55	PRATIO, GSP × TDIFF, TDIFF
Paiute cypress (<i>Cupressus arizonica</i> ssp. <i>Nevadensis</i>)	0	3.09	1.73	MMIN, MAP × DD5, MTCM × GSP, PRATIO
Macfarlane's four-o'clock (<i>Mirabilis macfarlanei</i>)	0	2.55	1.39	MINDD0, MAP × TDIFF, TDIFF

^a Errors of omission (species presence = yes but model prediction presence = no).

^b Error of commission (species presence = no but model prediction = yes).

^c Combined overall error from omission and commission statistics.

predicting the presence of a species when, in fact, it was absent. The use of digital elevation model (DEM) and GIS to make predictions on a 1-km grid introduces additional error and uncertainty. The use of Little's range maps to validate the models' mapped projections also introduced the possibility of error. Range maps are known to contain errors (see Rehfeldt and others 2006) but perhaps more importantly, they only provide two-dimensional limits of the species distribution and do not indicate where species actually occur within the species boundaries. Even so, a visual comparison between these range maps and our predictions can be used for general validation of the models.

Subalpine Larch

A visual comparison of Little's range map shows that the projection of the bioclimatic model overestimates the distribution of subalpine larch in the western portion of southwestern British Columbia and portions of the central Rocky Mountains (Figure 2A). Error associated with Canadian projections may have been exacerbated by the lack of species presence-absence data for that region. Nonetheless, the model does an excellent job of predicting the United States distribution. Here the majority of the pixels receiving the greatest proportion of votes occur well within the range limits.

Mapped projections for the effect of global warming on distribution of subalpine larch's realized climatic niche space in decades 2030 (Figure 2B), 2060 (Figure 2C) and

2090 (Figure 2D) indicate a rapid decline in distribution (Table 4). For area studied, about 62 percent of the contemporary realized climatic niche space is projected to disappear by the end of decade 2030 (Table 4). Only about one-third of the remaining proportion is expected to occur in pixels suitable for the species today. By decade 2030, the mean elevation of the realized climatic niche space is projected to occur 100 m higher in altitude, and the minimum elevation is expected to rise almost 300 m by the end of the century. Also, by the end of the century, only 3 percent of the contemporary realized climatic niche space is expected to remain and should be relegated to a few high mountain peaks in south-central Idaho, southwestern Montana, the northern Cascade Range in Washington and to the Grand Teton Range in northwestern Wyoming. Note that suitable climate space in the Grand Teton Range is projected to first occur in decade 2030 and persist in decades 2060 and 2090.

Smooth Arizona Cypress and Paiute Cypress

The predicted contemporary realized climatic niche space for smooth Arizona cypress and Paiute cypress better described actual distributions than Little's range map (Figures 3A, 4A). Although a few populations were not mapped in the realized climatic niche, we suspect that this omission was due to either a mapping resolution that was too coarse or to field locations that were not accurate enough.

In response to global warming under the IS92a scenario, the realized climatic niche space of Arizona smooth

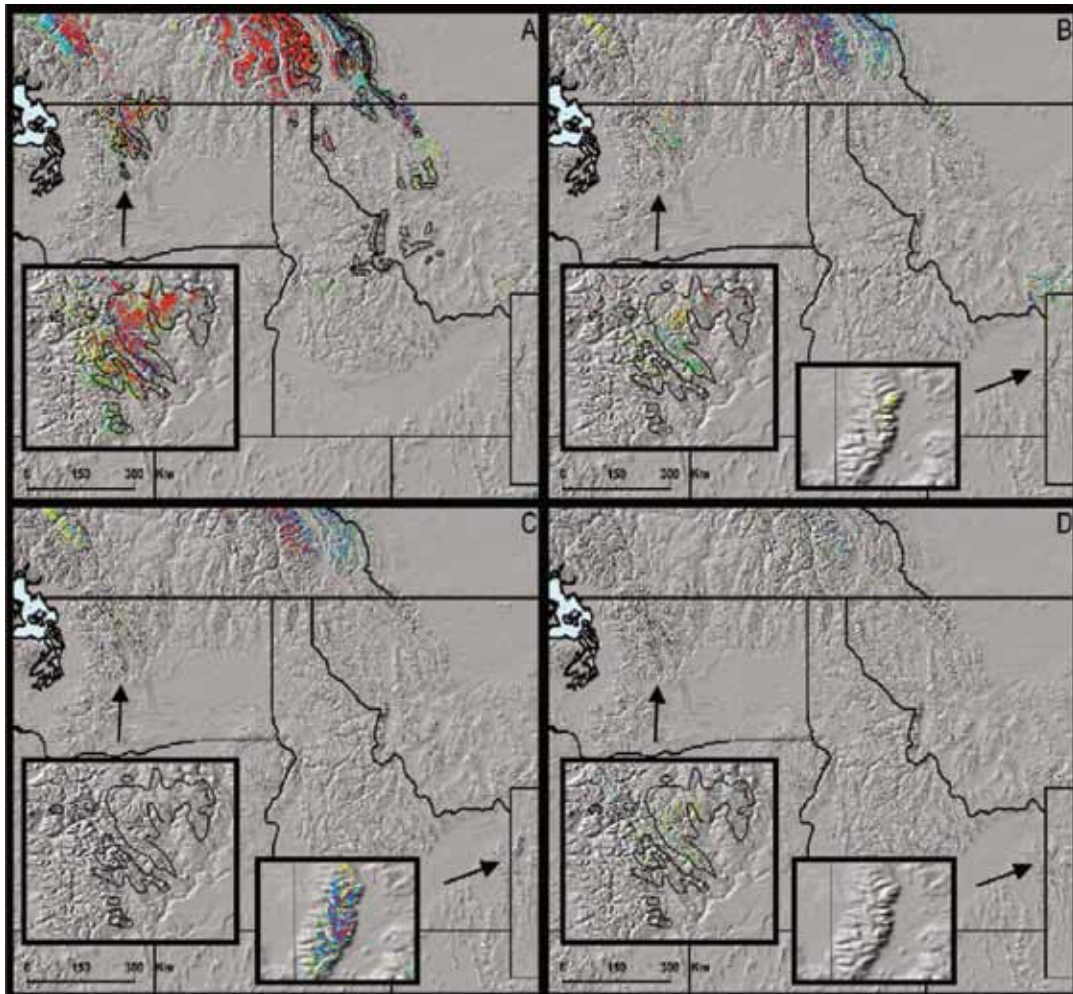


Figure 2—Modeled realized climatic niche for subalpine larch (*Larix lyallii*) and its predicted response to climate change for decades beginning in (B) 2030, (C) 2060, and (D) 2090. Areas in (A) outlined in black depict species boundaries defined by Little (1971). Colors code the proportions of votes received by a pixel in favor of being within the climate profile: no color 0%–50%; yellow 50%–60%; green 60%–70%; light blue 70%–80%; dark blue 80%–90%; and red 90%–100%.

cypress should shift about 200 to 350 km northwest of its contemporary location (Figures 3B, 3C, 3D). The area occupied should increase by about 1.5 and 2 times its contemporary size in decades 2030 and 2060, respectively (Table 4). In decade 2090, the area decreases to 1.2 times the contemporary size as the distribution shifts to northern Nevada and southwestern Colorado. In all three future decades, the contemporary realized climatic niche space is expected to be prominent in valleys where the Arizona, Nevada, and Utah borders meet. This includes the Virgin Mountains in Nevada, an area where naturalized populations of the subspecies have been observed (Charlet 1996).

Only 14 percent of the climate space is expected to remain in place in its contemporary location through the decade of 2030, and none is to remain in place for decades 2060 and 2090. By the end of the century, average elevation is projected to increase 611 m.

By decade 2030, the Paiute cypress realized climatic niche space will lie outside its contemporary distribution. The realized climatic niche space is projected to shift nearly 40 km to the east along the southeastern slopes of the Sierra Nevada (Figure 4B). Overall, the area of its distribution should shrink about 86 percent (Table 4). Altitudes, however, should increase by about 100 m. The realized

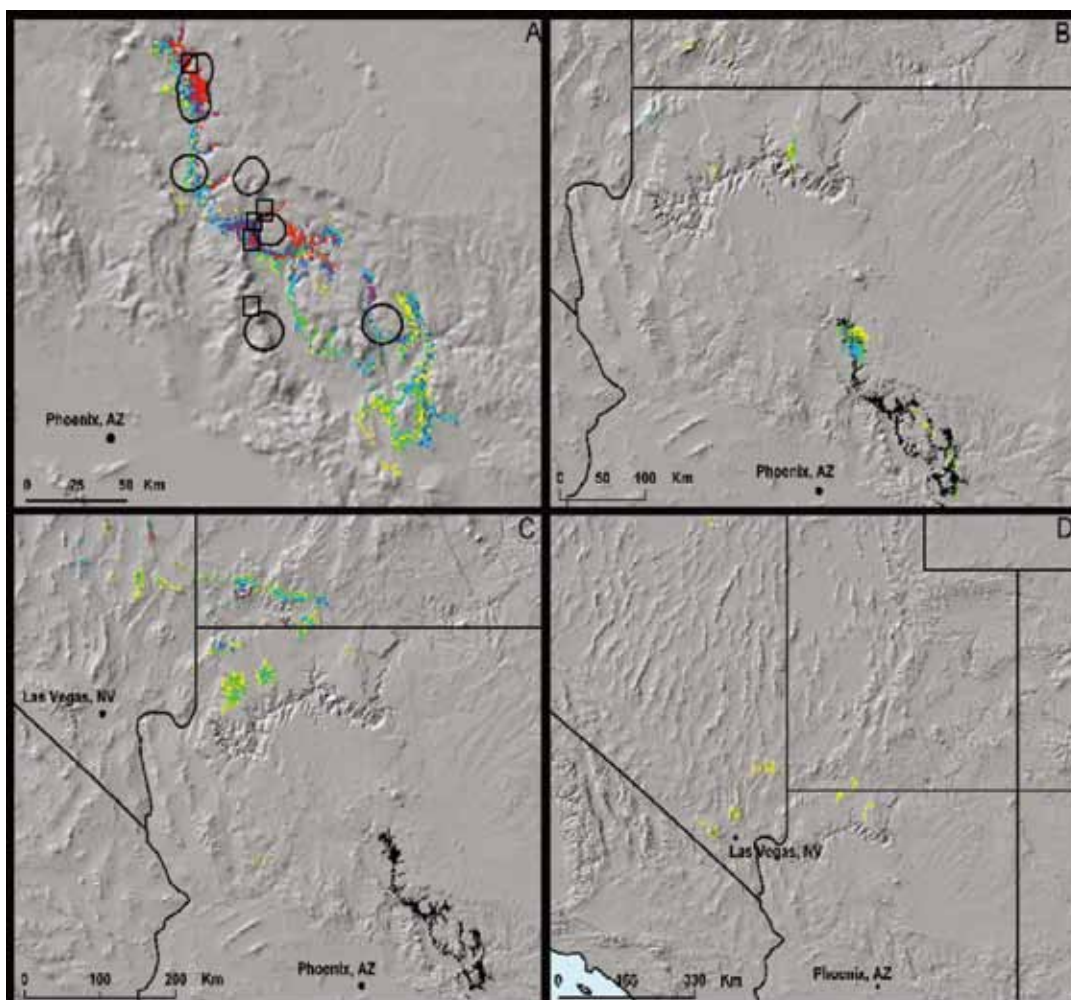


Figure 3—(A) Modeled realized climatic niche for smooth Arizona cypress (*Cupressus arizonica* ssp. *glabra*) and its predicted response to climate change for decades beginning in (B) 2030, (C) 2060, and (D) 2090. Areas in (A) outlined in black depict species boundaries defined by Little (1971) and squares indicate sites known to be inhabited. Colors code the proportions of votes received by a pixel in favor of being within the climate profile: no color 0%–50%; yellow 50%–60%; green 60%–70%; light blue 70%–80%; dark blue 80%–90%; and red 90%–100%.

Table 4—Projected change in area of species realized climatic niche space in response to climate change during three decades, and, in parenthesis, the percentage realized climatic niche space expected to match their contemporary distribution

Species	Year of projected change		
	2030	2060	2090
	Percent		
Subalpine larch (<i>Larix lyallii</i>)	-62 (26)	-76 (21)	-97 (3)
Smooth Arizona cypress (<i>Cupressus arizonica</i> ssp. <i>glabra</i>)	+158 (14)	+210 (0)	+115.7 (0)
Paiute cypress (<i>Cupressus arizonica</i> ssp. <i>nevadensis</i>)	-86 (0)	-91 (0)	-95 (0)
Macfarlane's four-o'clock (<i>Mirabilis macfarlanei</i>)	+807 (23)	+1912 (2)	+3343 (0)

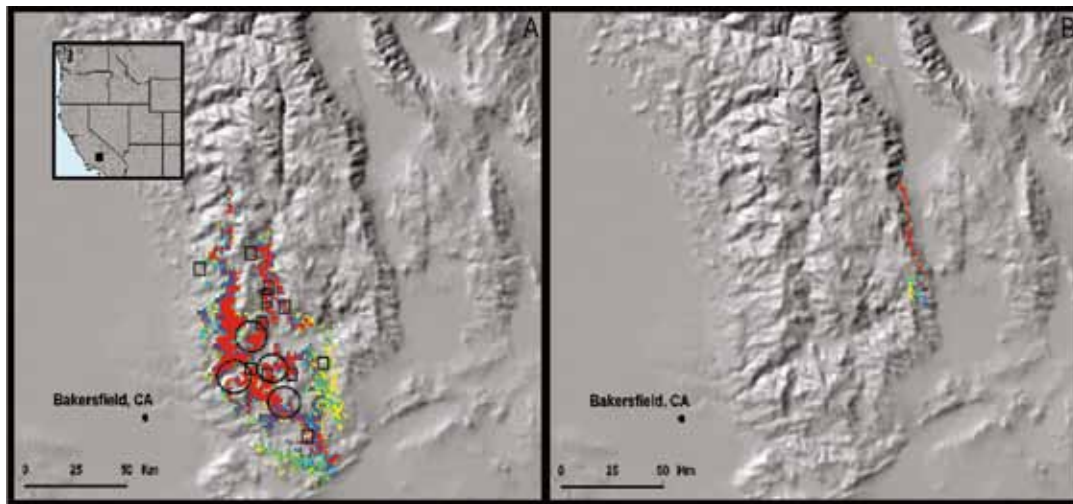


Figure 4—(A) Modeled realized climatic niche for Paiute cypress (*Cupressus arizonica* ssp. *nevadensis*) and its predicted response to climate change for the decade beginning in (B) 2030, in California. Areas in (A) outlined in black depict species boundaries defined by Little (1971) and squares indicate sites known to be inhabited. Colors code the proportions of votes received by a pixel in favor of being within the climate profile: no color 0%–50%; yellow 50%–60%; green 60%–70%; light blue 70%–80%; dark blue 80%–90%; and red 90%–100%.

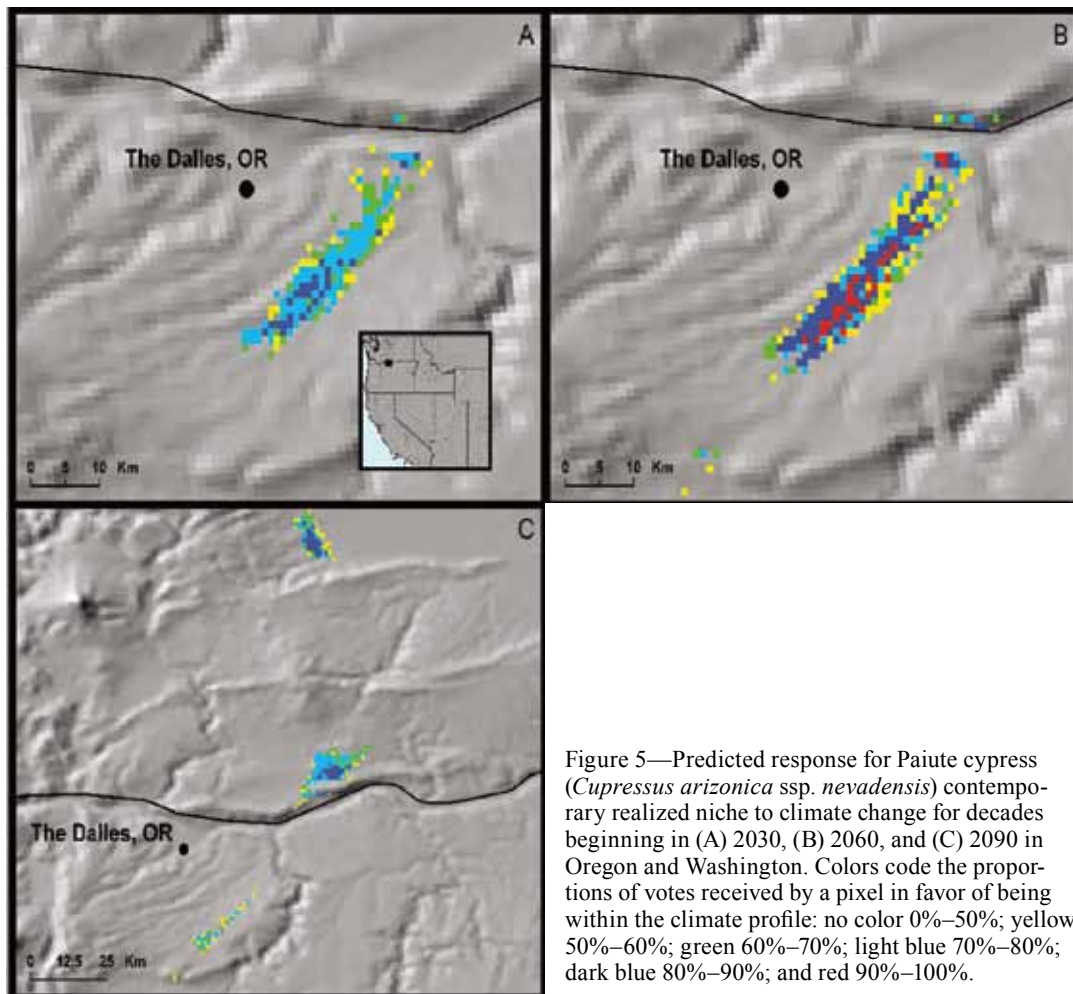


Figure 5—Predicted response for Paiute cypress (*Cupressus arizonica* ssp. *nevadensis*) contemporary realized niche to climate change for decades beginning in (A) 2030, (B) 2060, and (C) 2090 in Oregon and Washington. Colors code the proportions of votes received by a pixel in favor of being within the climate profile: no color 0%–50%; yellow 50%–60%; green 60%–70%; light blue 70%–80%; dark blue 80%–90%; and red 90%–100%.

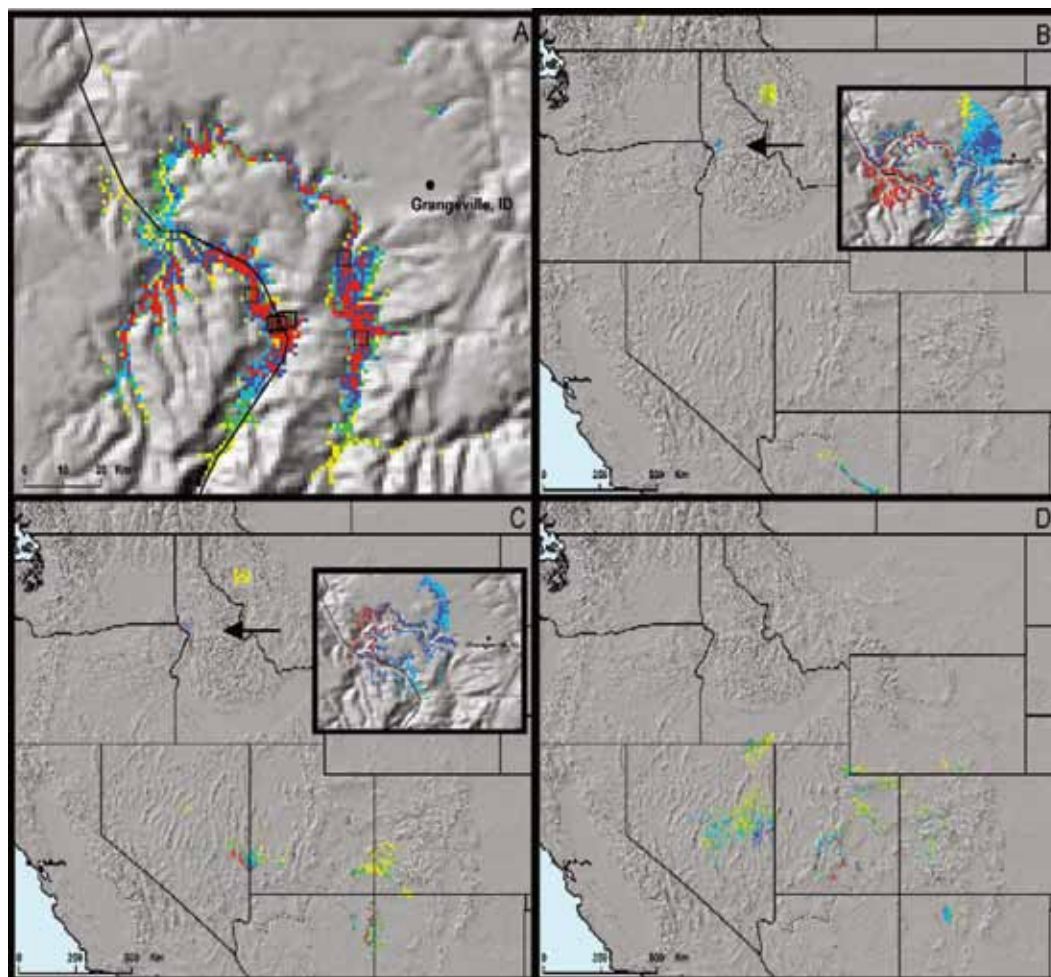


Figure 6—(A) Modeled realized climatic niche for Macfarlane's four-o'clock (*Mirabilis macfarlanei*) and its predicted response to climate change for decades beginning in (B) 2030, (C) 2060, and (D) 2090. Squares in (A) indicate sites known to be inhabited. Colors code the proportions of votes received by a pixel in favor of being within the climate profile: no color 0%–50%; yellow 50%–60%; green 60%–70%; light blue 70%–80%; dark blue 80%–90%; and red 90%–100%.

climatic niche space should also appear nearly 1100 km to the north near The Dalles, Oregon, by the decade of 2030 (Figure 5A) where it is projected to persist throughout the century (Figures 5B, 5C). In fact, by 2060, the realized climatic niche space of this subspecies occurs exclusively in Oregon and should occupy an area less than 90 percent of its contemporary distribution. The mean elevation for these new sites in Oregon and Washington are about 200 to 300 m lower in elevation than the contemporary distribution.

Macfarlane's Four-O'clock

Through most of the century, climate suitable to Macfarlane's four-o'clock should remain near its contemporary

location (Figures 6B, 6C). The realized climatic niche, however, is expected to climb the canyon's slopes along the Snake, Imnaha, and lower Salmon Rivers in decade 2030 (Figure 6B). In the decade of 2060, it should occur in these canyons at altitudes nearly 142 m higher than today (Figure 6C), but, by the end of the century, it should disappear in these particular canyons but reappear within the Snake River watershed in southern Idaho (Figure 6D). Elsewhere in the West, however, the profile of this species should expand rapidly and increase in altitude (Table 4, Figures 6B, 6C, 6D), increasing by a factor of 8, 19, and 34 times the contemporary realized climatic niche space in decades 2030, 2060, and 2090, respectively (Figure 6, Table 4).

Discussion

Our bioclimatic models predict the occurrence of species and attempt to identify suitable habitats. As shown, these models can also be updated with predicted future climates to project the redistribution of species' contemporary realized climatic niche. The validity of these projections are dependent on the accuracy of the bioclimatic models as well as how closely the predicted future climate using the IS92a scenario from the Canadian and Hadley GCMs matches the actual climate of the future.

The climate variables identified as important for predicting species occurrence differed among the species and subspecies analyzed. These differences suggest that they will respond uniquely to climate change. Despite these differences, it appears that their small geographic distributions predispose them to a shared threat of more rapid onset of climatic disequilibrium in comparison with species occupying large-scale distributions. Analyses of species occupying larger scale distributions tend to report greater areas of unaffected distribution and show less separation between existing distributions and the geographic occurrence of suitable climate (Bakkenes and others 2002, Iverson and Prasad 1998, Rehfeldt and others 2006). The extent of disequilibrium predicted by these studies may, however, be an underestimate owing to the potential for maladaptation to climate within species (Rehfeldt 2004, Rehfeldt and others 1999, Rice and Emery 2003).

As natural systems attempt to regain equilibrium with the novel distribution of climates, distributions will shift. Redistribution rates, however, will be influenced by genetic structure, autecology, life history, reproductive capabilities, and ecophysiology (see, for instance, Ackerly 2003). Consequently, all of these factors should be taken into consideration in interpreting projections from bioclimatic models. The physiology of subalpine larch, for instance, appears to be consistent with the climatic profile described by our models. Its realized niche seems dependent on a superior hardiness and resistance to winter desiccation (Burns and Honkala 1990). Subalpine larch, however, does not compete well with other evergreen species (Arno and Hammerly 1984). Hence, the continued warming trend will

likely eliminate subalpine larches from the Western United States through competitive exclusion. Common garden studies with smooth Arizona cypress and Paiute cypress by Rehfeldt (1997) revealed genetic variability equivalent to that conveyed by broadly distributed conifer species. This indicates populations within the species may only be adapted to a portion of its present or future realized climate space. In addition, both smooth Arizona cypress and Paiute cypress are fire dependent. Fire management practices may have had a substantial influence on limiting their distribution (Marshall 1963). Consequently, for these subspecies of *Cupressus arizonica*, our estimate of the realized climatic niche space may underestimate the breadth of climatically suitable area. Finally, Macfarlane's small distribution is attributed to reduced compatibility between its floral biology and pollinators (Barnes 1996). The rates that the range may expand would depend, therefore, on the presence of compatible pollinators.

Bioclimatic models represent tools that can be used to assist decisionmakers in managing threats associated with global warming. These models can be updated with predicted future climate to identify locations where suitable climate should occur. These predictions can be used by managers to assist the natural processes by transferring species to the future location of climate suitable for their survival. Ideally the application of bioclimate models for this purpose should use multiple general circulation models and climate change scenarios to reduce uncertainty associated with predicted future climate (see Rehfeldt and Jaquish 2010). To be sure, additional modeling is needed that integrates a general understanding of climate, climate change, and plant-climate relationships. Interpretation of results by resource managers also requires integration of additional layers of information such as land use (see Hannah 2006).

Literature Cited

Ackerly, D.D. 2003. Community assembly, niche space conservatism, and adaptive evolution in changing environments. 164 (Supplement): S165–S184.

- Alerich, C.A.; Klevgard, L.; Liff, C.; Miles, P.D. 2004.** The Forest Inventory and Analysis Database: database description and users guide. Ver. 1.7. http://ncrs2.fs.fed.us/4801/fiadb/fiadb_documentation/FIADB_v17_122104.pdf [Date accessed unknown].
- Arno, S.E.; Hammerly, R.P. 1984.** Timberline: mountain and arctic forest frontiers. Seattle: Mountaineers Books. 304 p.
- Arno, S.F. 1970.** Ecology of alpine larch (*Larix lyallii* Parl.) in the Pacific Northwest. Missoula, MT: University of Montana. 264 p. Ph.D. dissertation.
- Bakkenes, M.; Alkemade, J.R.M.; Ihle, F. [and others]. 2002.** Assessing effects of forecasted climate change on the diversity and distribution of European higher plants for 2050. *Global Change Biology*. 8: 390–407.
- Barnes, J.L. 1996.** Reproductive ecology, population genetics and clonal distribution of the narrow endemic: *Mirabilis macfarlanei* (Nyctaginaceae). Logan, UT: Utah State University. 106 p. M.S. thesis.
- Bechtold, W.; Patterson, P. 2005.** The enhanced forest inventory and analysis program: national sampling design and estimation procedures. Gen. Tech. Rep, SRS-80. Asheville, NC: U.S. Department of Agriculture, Forest Service, Southern Research Station. 85 p.
- Breiman, L. 2001.** Random Forests. *Machine Learning*. 45: 5–32.
- Burns, R.M.; Honkala, B.H. 1990.** Silvics of North America. Vol. 1. Conifers. Agric. Handb. 654. Washington, DC: U.S. Department of Agriculture. 877 p.
- Charlet, D.A. 1996.** Atlas of Nevada conifers: a phytogeographic reference. Reno: University of Nevada Press. 320 p.
- Crookston, N.L.; Rehfeldt, G.E.; Warwell, M.V. 2007.** Using FIA data to model plant-climate relationships. In: McRoberts, Ronald E.; Reams, Gregory A.; Van Deusen, Paul C.; McWilliams, William H., eds. Proceedings of the seventh annual forest inventory and analysis symposium. Gen. Tech. Rep. WO-77. Portland, ME: U.S. Department of Agriculture, Forest Service: 243–250.
- Davis, M.B.; Shaw, R.G. 2001.** Range shifts and adaptive responses to quaternary climate change. *Science*. 262: 673–679.
- Flato, G.M.; Boer, G.J. 2001.** Warming asymmetry in climate change simulations. *Geophysical Research Letters*. 28: 195–198.
- GLOBE TaskTeam. 1999.** The global land 1-kilometer base elevation (GLOBE) digital elevation model. Ver. 1.0. National Oceanic and Atmospheric Administration., National Geophysical Data Center. <http://www.ngdc.noaa.gov/seg/topo/globe.shtml>. [Date accessed unknown].
- Gordon, C.; Cooper, C.; Senior, C. [and others]. 2000.** The simulation of SST, sea-ice extents, and ocean heat transport in a version of the Hadley Centre coupled model without flux adjustments. *Climate Dynamics*. 16: 147–168.
- Hannah, L. 2006.** Regional biodiversity impact assessments for climate change: a guide for protected area managers. In: Hansen, L.J.; Biringer, J.L.; Hoffman, J.R., eds. A user's manual for building resistance and resilience to climate change in natural systems. Berlin, Germany: World Wildlife Fund Climate Change Program. [Not paged].
- Houghton, J.T.; Ding, Y.; Griggs, D.J. [and others]. 2001.** Climate change 2001: the scientific basis. (A contribution of Working Group 1 to the second assessment report of IPCC (Intergovernmental Panel on Climate Change). Cambridge, U.K.: Cambridge University Press. [Not paged].
- Hutchinson, M.F. 1991.** Continentwide data assimilation using thin plate smoothing splines. In: Jasper, J.D., ed. Data assimilation systems. BMRC Res. Rep. 27. Melbourne: Bureau of Meteorology: 104–113.
- Hutchinson, M.F. 2000.** ANUSPLIN Ver. 4.1. User's guide. Canberra: Australian National University, Centre for Resource and Environmental Studies. [Not paged].

- Iverson, L.R.; Prasad, A.M. 1998.** Predicting abundance of 80 tree species following climate change in the Eastern United States. *Ecological Monographs*. 68: 465–485.
- Khasa, D.P.; Jaramillo-Correa, J.P.; Jaquish, B.; Bousquet, J. 2006.** Contrasting microsatellite variation between subalpine and western larch, two closely related species with different distribution patterns. *Molecular Ecology*. 15(13): 3907–3918.
- Liaw, A.; Wiener, M. 2002.** Classification and regression by Random Forest. *R News*. 2(3): 18–22.
- Little, E.L., Jr. 1971.** Atlas of United States trees. Vol. 1. Conifers and important hardwoods. Misc. Publ. 1146. Washington, DC: U.S. Department of Agriculture. 9 p., 313 maps.
- Little, E.L., Jr. 1976.** Atlas of United States trees. Vol. 3. Minor western hardwoods. Misc. Publ. 1314. Washington, DC: U.S. Department of Agriculture. 13 p., 290 maps.
- Marshall, J.T., Jr. 1963.** Fire and birds in the mountains of southern Arizona. In: Komarek, E.V., Sr., chairman. Proceedings, 2nd annual Tall Timbers fire ecology conference. Tallahassee, FL: Tall Timbers Research Station: 135–141.
- R Development Core Team. 2004.** R: a language and environment for statistical computing. R Foundation for Statistical Computing. <http://www.et.bs.edu.es/soft/fullrefman.pdf> [Date accessed unknown].
- Rehfeldt, G.E. 1997.** Quantitative analyses of the genetic structure of closely related conifers with disparate distributions and demographics: the *Cupressus arizonica* (Cupressaceae) complex. *American Journal of Botany*. 84(2): 190–200.
- Rehfeldt, G.E. 2004.** Interspecific and intraspecific variation in *Picea engelmannii* and its congeneric cohorts: biosystematics, genecology, and climate change. Gen. Tech. Rep. RMRS-GTR-134. Fort Collins, CO: U.S. Department of Agriculture, Forest Service, Rocky Mountain Research Station. 18 p.
- Rehfeldt, G.E. 2006.** A spline model of climate for the Western United States. Gen. Tech. Rep. RMRS-GTR-165. Fort Collins, CO: U.S. Department of Agriculture, Forest Service, Rocky Mountain Research Station. 21 p.
- Rehfeldt, G.E.; Crookston, N.L.; Warwell, M.V.; Evans, J.S. 2006.** Empirical analyses of plant-climate relationships for the Western United States. *International Journal of Plant Sciences*. 167: 1123–1150.
- Rehfeldt, G.E.; Jaquish, B.C. 2010.** Ecological impacts and management strategies for western larch in the face of climate-change. *Mitigation and Adaptive Strategies for Global Change*. 15: 283–306.
- Rehfeldt, G.E.; Ying, C.C.; Spittlehouse, D.L.; Hamilton, D.A. 1999.** Genetic responses to climate in *Pinus contorta*: niche breadth, climate change, and reforestation. *Ecological Monographs*. 69: 375–407.
- Rice, K.J.; Emery, N.C. 2003.** Managing microevolution: restoration in the face of global change. *Frontiers in Ecology and the Environment*. 1: 469–478.
- Thomas, C.; Bodsworth, E.; Wilson, R. [and others]. 2001.** Ecological and evolutionary processes at expanding range margins. *Nature*. 411: 577–581.
- U.S. Fish and Wildlife Service [USFWS]. 1996.** Reclassification of *Mirabilis macfarlanei* (MacFarlane's four-o'clock) from endangered to threatened status. *Federal Register* 61: 10,693–10,697.
- U.S. Geological Service [USGS]. 2005.** Digital representations of tree species range maps from “Atlas of United States Trees” by Elbert L. Little, Jr. [Online]. Available: <http://esp.cr.usgs.gov/data/atlas/little/>. [Date accessed: May 27, 2008].
- Woodward, F.I. 1987.** Climate and plant distribution. New York: Cambridge University Press. 174 p.

AIR and WATER

Syntheses

This page is intentionally left blank

The Influence of Forest Management on Vulnerability of Forests to Severe Weather

Robert H. Beach, Erin O. Sills, Tzu-Ming Liu, and Subhrendu Pattanayak

Robert H. Beach, senior economics, Environmental, Technology, and Economics, Program, RTI International, Research Triangle Park, NC 27709-2194; **Erin O. Sills**, associate professor, Department of Forestry and Environmental Resources, North Carolina State University, Raleigh, NC 27695; **Tzu-Ming Liu**, assistant professor, Kainan University, Luchu, Taiwan; **Subhrendu Pattanayak**, associate professor, Duke University, Durham, NC.

Abstract

Excessive wind, ice, and snow regularly cause major disturbances to forests in many parts of the world, significantly impacting both ecological conditions and economic returns to forest landowners. These events cause immediate losses for landowners, and the broken and uprooted trees left in the wake of a storm increase the risk that wildfires, disease, and pest outbreaks will cause secondary damage to the surviving trees. Although weather severity (e.g., wind-speed and duration, or form and amount of precipitation) is clearly an important factor in the occurrence and severity of forest damage, site conditions, tree characteristics, and stand characteristics play a major role in determining resistance of a forest stand to wind, ice, and snow loading. However, the relationships between site, tree, and stand characteristics and weather damage are complex and vary spatially and temporally. In this article, we review and synthesize the literature on the risk of forest damages from severe weather—focusing on wind, ice, and snow—and the factors that influence vulnerability. Forest management decisions are found to play an important role in influencing risk associated with severe weather events. The risk of damages can be managed through strategies such as selection of planting site and species, stocking, and selection and timing of silvicultural treatments. Optimal management strategies under endogenous risk vary based on the probability of damage and management objectives.

Keywords: Damage mitigation, ice, natural disturbances, forest policy, risk management, wind.

Introduction

Natural disturbances play an important role in forest stand dynamics and ecology, with effects that are highly dependent on characteristics of the specific disturbance (Foster and Boose 1995). Severe weather events that bring high winds or heavy precipitation or both (e.g., hurricanes and ice, snow, and hailstorms), drought, flooding, lightning strikes, wildfires, and disease and pest outbreaks are a regular feature of forest landscapes. Although these disturbances may serve important ecological functions, they also significantly—and usually negatively—affect economic returns to forest landowners. Wind, ice, and snowstorms affect large areas of forest relatively frequently in some important timber production regions. These storms impact forest landowners by causing the loss of merchantable timber, increased risk of secondary damages to wildlife and from disease and pests in damaged stands, and depressed timber prices in the immediate aftermath of events that cause widespread damage. These risks have led to considerable interest in identifying factors that influence damage levels as well as ways to mitigate damages.

To optimally manage risk, it is necessary to identify and characterize the hazards faced, assess the risk associated with these hazards, identify options to mitigate risk, choose the optimal combination of options given the manager's objectives (e.g., producing amenities or maximizing profitability of timber production), and implement the strategy selected. In the case of forested landscape management, these tasks are complicated by long planning horizons, which lead to substantial uncertainty concerning future prices, production costs, forest policies and regulations, and objectives, in addition to uncertainty regarding severe weather impacts (Wilson and Baker 2001). Spatial and temporal heterogeneity combined with the infrequency of major storms impacting a given area (compared with a human lifespan) make it relatively difficult to learn from previous storms. Damage severity depends on the complex

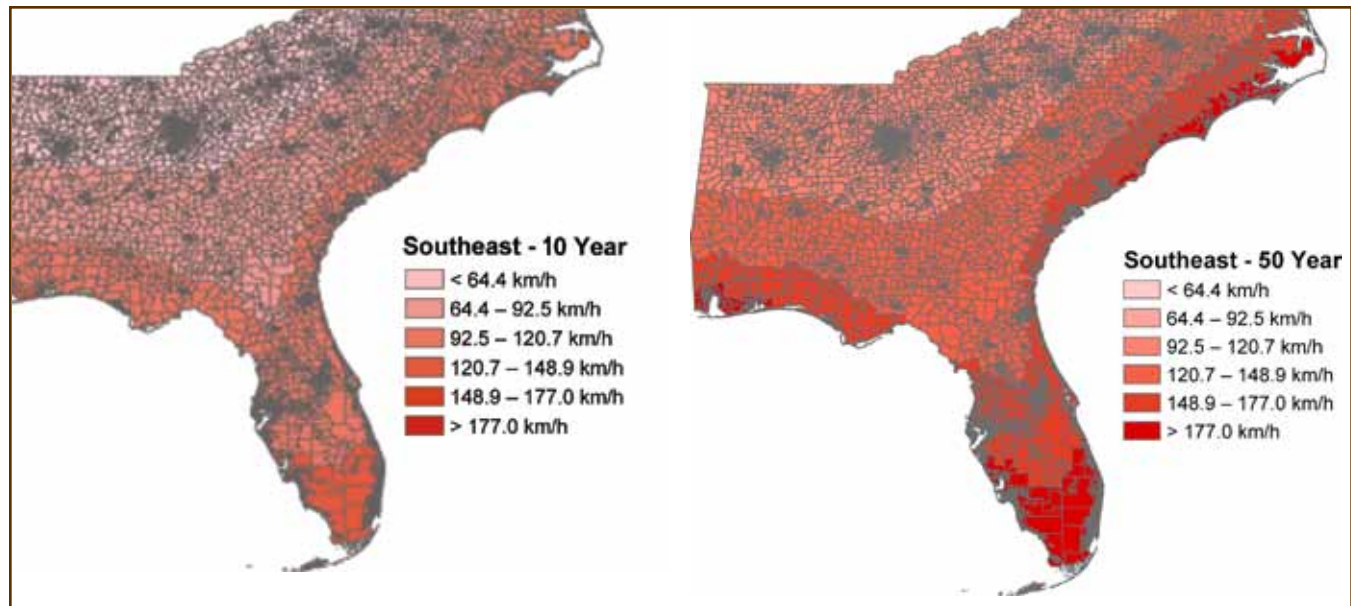


Figure 1—Simulated peak hurricane windspeed associated with hurricanes in the Southeast United States over 10- and 50-year periods using FEMA's HAZUS-MH model. In (a), which is for a 10-year period, only southern Florida and a few coastal census tracts in Alabama, South Carolina, and North Carolina are expected to experience hurricane-force winds (greater than 119 km per hour) within this time-frame. Over a 50-year period, however, the entire region is expected to have winds of at least tropical storm strength, with much higher winds in some coastal areas, as shown in (b). Source: FEMA HAZUS-MH model.

interaction of numerous tree, stand, and site characteristics. For instance, although windspeed is likely to be the most important determinant of timber losses, topography, soil conditions, planting density, species, stand age, the presence of gaps and edges, and other factors determine a stand's resistance to wind loading.

Many studies focus almost exclusively on biophysical properties of forest plots or individual trees to explain differences in damages without explicitly examining the role of landowners' forest management decisions in influencing those properties. However, forest management decisions can change susceptibility to wind damage through effects on tree and stand characteristics such as tree species, tree height, tree diameter, crown area, rooting depth and width, and stand density (Dunham and Cameron 2000, Kerzenmacher and Gardiner 1998, Peltola and others 1999, Peltola and others 2000). Stand age and forest structure may also contribute to vulnerability of forests to high winds (Everham and Brokaw 1996, Francis 2000, Mitchell 1995, Ruel 1995). Silvicultural treatments such as thinning and clearcutting adjacent stands are important as well (Foster 1988, Lohmander and Helles 1987, Mitchell 2000, Wilson

and Baker 2001). Similar factors have been related to the degree of ice damage to forests (Bragg and others 2003, Van Dyke 1999), though with different magnitudes and, in some cases, opposite direction of effect. Overlooking the impacts of management decisions on the vulnerability of a stand to weather damages may lead to inefficient decisionmaking by policymakers and private landowners.

In this article, we review and synthesize the literature on the risk of forest damages from severe wind, snow, and ice, the factors influencing the extent of damages in the event of severe weather, alternatives for mitigating weather damages, and policy implications. This type of information can inform forest management decisions and increase the efficiency of policy for managing public forest land as well as public policy that encourages timber stand management and compensates landowners for weather damages.

Severe Weather and Forest Impacts

This section describes characteristics of severe weather storms and selected major events that have taken place in recent years as well as resulting impacts on forests. These impacts include a variety of damages to trees because of

excessive loadings by high winds, ice storms, and snow accumulation. In addition to immediate uprooting and stem breakage, heightened tree mortality can continue over time as a result of substantial crown loss. Even trees that recover may have suffered permanent internal damage that reduces wood quality. In addition, damaged stands are more prone to secondary damages from fire, disease, insects, and competing plants.

High Winds

Hurricane-strength winds can cause severe defoliation and directly damage and kill trees through uprooting, breakage and loss of minor and major branches, and stem breakage. Biodiversity is affected through an increase in gaps of broken and uprooted trees and reallocation of light, water, nutrients, and other resources (Nowacki and Kramer 1998). The amenity value of a forest can decrease because of the higher proportion of treefall gaps. Wind damage imposes costs on commercial forestry owing to reduction in timber yields, unscheduled and costly thinnings, and added uncertainty for forestry planning (Quine and others 1995). In addition, broken and uprooted trees left unharvested can lead to additional costs by increasing the probability of disease outbreaks, insect infestations, and wildfires in the remaining growing stock as well as increasing the costs of containment.

Between 1900 and 2005, an average of 1.6 hurricanes per year made landfall between Texas and Maine, with an average of 0.6 major hurricanes (category 3 or above on the Saffir-Simpson scale) annually. In 2004 and 2005 alone, seven major hurricanes had an impact on the United States (Blake and others 2006). Figure 1 shows peak windspeeds associated with hurricanes in the Southeastern United States that are expected in 10-year and 50-year periods based on estimates from the Federal Emergency Management Agency's HAZUS-MH model. Within a 50-year period, the entire Southeast is expected to have winds of at least tropical storm strength.

Hurricanes resulting in the greatest loss of timber from 1900 to 2000 were the Hurricane of 1938 (in New England) and Hurricanes Camille (1969), Frederic (1979),

Hugo (1989), Opal (1995), and Fran (1996) (Lutz 2005). For example, Hurricane Hugo swept through South Carolina on September 21, 1989, damaging more than one-third of the State's timberland. The damaged volume of timber was estimated to be 36.8 million m³ (Remion 1990). More recently, Hurricanes Katrina and Rita damaged more than 2 million ha of forest in the gulf coast States, leading to timber losses of almost \$6 billion for affected landowners (though an estimated one-third of these losses may be recovered through salvage efforts) (SAF 2005).

Other regions are also affected by high winds. On average, there are almost 1,000 tornadoes per year in the United States, mostly in the continental interior. Although many are relatively small and weak and cause little damage, a small proportion do considerable damage to forests (see Peterson 2000). Dale and others (2001) estimate that tornado damage in the United States averages \$154 million annually. Other windstorms also occasionally result in major damages, such as the July 4, 1999, windstorm that severely impacted approximately 193 000 ha of Minnesota forest (Mattson and Shriner 2001). The hurricane-force winds that affect the coastal Pacific Northwest have a return interval of about 20 years (Wilson 2004).

Ice and Snow Storms

Recurring ice and snow storms are a significant hazard to forests in temperate climates. Snow or ice causes damage when the weight of frozen precipitation exceeds the buckling load of the portion of the tree bearing the load, causing bending or breakage. Bending can result in permanent internal damage without external signs of damage. There are important interactions between winter precipitation and wind because windspeeds required to cause damage are lower for trees loaded with snow and ice, all else equal. Every winter, ice and snow storms affect portions of eastern North America and Europe to some degree, with occasional major events covering millions of hectares and causing millions of dollars in damages. The majority of research on ice and snow damage has been conducted in these regions. Below, we focus on ice storms, recognizing that heavy snow can produce similar damages, particularly in the case of unusually wet snow.

Ice storms require a layer of warm air, with temperatures above freezing, between layers of air that are below freezing. As frozen precipitation falls through the layer of warm air, it melts and reaches the cold lower layer as rain. As the water droplets fall through this cold surface layer, they become supercooled, which means that the water in the droplets is cooled to temperatures below 0 °C without freezing. When this supercooled liquid strikes a cold surface, the impact triggers an almost instant transformation to a smooth thin layer of ice. Although ice storms can result in significant accumulation and major damages when conditions for ice formation are favorable, ice accumulation depends critically on characteristics of the layers of air and the water droplets. Small temporal or spatial differences in air temperature and droplet size frequently result in freezing rain mixed with sleet, snow, or nonfreezing rain, which substantially complicates area-specific forecasting of ice formation and accumulation (Heidorn 2001).

Ice accumulation is one of the most frequent forest disturbances in temperate regions (Irland 2000). However, most ice storms produce minimal ice accumulation and do not result in substantial losses. Some locations in North America experience at least some ice accumulation every 1 to 2 years on average, though most areas have return intervals of 5 years or more (Bragg and others 2003). Ice storms are estimated to occur about every 5 years in Northern New England States (Smith and Musser 1998), while ice storms have been estimated to occur every 6 years in the natural range of loblolly pine (*Pinus taeda* L.) (Shultz 1997) and every 5 to 12 years inland from the Gulf of Mexico (Bragg and others 2003).

Storms resulting in major damages are estimated to have a return time of 20 to 100 years in Northern North America (Van Dyke 1999). Several recent ice storms have caused catastrophic damages over very large areas. For instance, a 1998 ice storm in southeastern Canada and the Northeastern United States damaged over 10 million forested hectares (Irland 1998, Miller-Weeks and others 1999). The Southern United States is less prone to major ice storms, but the region has experienced a number of major events such as the December 2000 ice storms in Arkansas



Steven Katovich, USDA Forest Service, Bugwood.org

Figure 2—Bending and windthrow due to a major windstorm. Illustrated in this picture is wind damage in quaking aspen (*Populus tremuloides*) in Chequamegon National Forest, northern Wisconsin, resulting from a windstorm in July 1999. The majority of damage is in the form of bending and windthrow rather than stem breakage.

that damaged an estimated 40 percent of the 7.4 million ha of forest in the State (Bragg and others 2003).

Tree Damage and Mortality

Wind can cause severe defoliation and can directly injure and kill trees through obvious damage such as uprooting (see Figure 2), breakage and loss of minor and major branches, and stem breakage (see Figure 3). Trees can be permanently damaged by the bending caused by wind, ice, and snow (see Figures 2 and 4), and compression injuries may be present even in seemingly undamaged trees. Severe bole injuries can lead to sap rot, slower growth, formation of compression wood, unusual growth rings, and intercellular voids between rings (Bragg and others 2003). Winds often carry saltwater inland, and foliage may die on trees that receive salt spray, although most affected trees will grow new leaves and recover (Gresham 2004).

The type of damage suffered tends to differ by tree size. Younger trees are more likely to bend with the wind without suffering serious damage, whereas older trees are more likely to uproot or break. Similarly, saplings and small-diameter trees can become seriously bent by ice accumulation, although these trees often recover. As diameter increases, the proportion of bending to breakage decreases. The majority of ice damage in larger trees is loss of branches and breakage of the main stem within the crown

Ronald F. Billings, Texas Forest Service, Bugwood.org



Figure 3—Stem breakage from a tornado. Widespread stem breakage is pictured in loblolly pine (*Pinus taeda*) from tornado winds in Texas. The damage appears very similar to that caused by major hurricanes.

(Van Dyke 1999). Understory trees may be damaged by windthrown trees or broken portions of trees. In addition, tree species differ in their ability to withstand high winds, ice, and snow. Key factors include shape and size of the crown, rooting depth, and wood strength.

Whether a tree recovers from damage depends significantly on crown loss. Hardwood trees are not usually killed by breakage, but those with greater than 75 percent crown loss are likely to die. Conifers broken below the live crown or that have lost a majority of the crown will generally not survive (Van Dyke 1999).

Increased Risk of Secondary Damages

The immediate loss of timber is not the only damage imposed by weather events. Uprooting of trees also causes significant soil turnover and increases risk of soil erosion (Lutz 1940, Lyford and MacLean 1966, Meyers and McSweeney 1995). In addition, the increased number of broken and uprooted trees raises the risk of wildfires as well as disease and pest outbreaks for the surviving trees, whereas newly created canopy gaps provide opportunities for plant invasions. The presence of damage and decay may also increase vulnerability to future wind, ice, and snow (Bragg and others 2003).

Fire hazard may be increased following major storms that result in increased dead tree biomass and low-growing



Figure 4—Tree bending from ice accumulation. The bending that can result from the weight of ice accumulation brought by a significant ice storm is shown in this picture. Although many of these trees will survive and may appear undamaged after they have straightened themselves, permanent internal damage may be present.

plants (Myers and Van Lear 1998). Federal and State forest resource departments frequently mention the heightened fire risk following major storm events as a key consideration for short-term forest recovery and management. In addition to increased fuel loading, access may be limited by downed trees, which further increases risk (Irland 2000). Myers and Van Lear (1998) examined the historical interaction between hurricanes and fires and concluded that these interactions had a major impact on the composition and structure of ecosystems in the Southern United States, although modern fire suppression efforts may have obscured this relationship in recent years.

Young trees can suffer bark damage following severe bending, which may increase susceptibility to disease. Any wounds permit disease fungi to infect damaged trees. Stain fungi may infect exposed wood within weeks, leading to wood quality degradation. Also, sap rot has been linked to sudden exposure of the stem to intense sunlight following canopy damage (Bragg and others 2003).

Broken and uprooted trees left unharvested also can lead to detrimental insect attacks on the remaining stand (Bakke 1989, Ravn 1985, Schroeder and Eidmann 1993). For example, severe outbreaks of spruce bark beetle (*Ips typographus*) occurred in Norway in 1971–1981, damaging trees equivalent to 5 million cubic meters of timber as

USDA Forest Service Archives, Bugwood.org

an indirect consequence of extensive wind damage (Bakke 1989). Cain and Shelton (1996) reported that an ice storm in southern Arkansas contributed to a southern pine beetle (*Dendroctonus frontalis*) outbreak. Hurricane Hugo caused large areas of loblolly pine (*Pinus taeda*) to be broken or uprooted, and these trees were susceptible to insect infestations (Yates and Miller 1996). Within months of Hurricane Katrina, virtually all of the downed material in De Soto National Forest in Mississippi had been infested by bark beetles and woodborers, and bark beetles (*Ips* engravers) had begun to infest and kill root-sprung trees (Meeker and others 2006).

Gaps resulting from tree fall and defoliation present opportunities for establishment of invasive plants (Burke and Grime 1996, D'Antonio 1993, Davis and others 2000, Hobbs 1989, Hobbs and Huenneke 1992, Réjmanek 1989), which may change forest structure and decrease populations of indigenous species. Increased light levels from large canopy gaps may also encourage the growth of invasive plant species, which could influence forest succession and alter ecosystem function. Snitzer and other (2005) found that mean cover percentage of invasive plants increased by 47.8 percent in high-light canopy gaps created by Hurricane Isabel and by only 4.2 percent in less-damaged forest. Invasive species such as cogongrass (*Imperata cylindrica* (L.) P. Beauv.) can also contribute to heightened wildfire risk (SAF 2005).

Economic Impacts

Because major severe weather events can cause the direct loss of great quantities of timber, large numbers of landowners can suffer revenue losses and the entire forest products sector can be affected. Revenues from salvage operations are generally lower than those from typical harvests because saleable volume is reduced, particularly in cases where there is extensive stem breakage, but also because fungal decay reduces wood quality. At the same time, costs of salvaging damaged stands are usually higher than costs of conventional harvesting. Manley and Wakelin (1989), who took into account the effects of increased costs and reduced revenues, calculated that the discounted net present value of an impacted forest decreases by as much

as 11 percent for a 1-percent annual level of damage. Forest landowners also may be affected by depressed timber market prices (at least in the short run) because of the large volume of salvaged timber on the market. Other things being equal, greater production risk unambiguously reduces optimal rotation length and decreases expected returns to forest land and land values, although the effects of price risk are ambiguous (Prestemon and Holmes 2000, Prestemon and others 2001). Prestemon and Holmes (this volume) provide more information on the economic impacts of hurricanes on landowners.

Factors That Influence Vulnerability

The severity of wind, ice, and snow damage depends on the interaction of numerous biological, topographic, stand, tree, and management factors. Before reviewing forest management activities to mitigate damage, we need to know what factors most strongly influence the severity of damage caused by wind, ice, and snow. Many empirical studies have indicated that the susceptibility of forests to damage depends on tree and stand characteristics such as species, height, diameter, crown area, rooting depth and width, stand density, and presence of forest gaps or edges (Dunham and Cameron 2000; Kerzenmacher and Gardiner 1998; Nykänen and others 1997; Peltola and others 1999, 2000; Quine 1995; Solantie 1994; Valinger and others 1993; Zeng and others 2004). However, the statistical significance and even the direction of the effect of individual variables differ across studies. The natural systems involved and the interactions among factors are complex, so these apparent inconsistencies may be a result of nonlinearities in response and the omission of individual variables in some studies.

Weather Severity

The intensity and duration of severe weather events are among the most important determinants of forest damage associated with severe weather. The greater the intensity and duration of loading placed on trees, the higher the likelihood this loading will exceed critical thresholds and cause damage. However, few empirical studies have explicitly incorporated spatially differentiated, quantitative, physical measures of severity or duration or both (e.g., peak

wind gusts or ice accumulation). Storm conditions can vary considerably within a relatively small region, so local storm severity must be gauged accurately if researchers are to properly evaluate the impact of local management activities on damages.

Greater windspeed and duration mean that more force is exerted on trees. Thus, the probability of uprooting, stem breakage, or other damages is expected to increase with windspeed and duration. However, forests in areas where strong winds are common may be less susceptible to catastrophic damage because they have developed higher wind resistance in response to greater normal loading. For related reasons, wind direction also influences damage. Storm winds that come from a direction other than the typical prevailing winds may cause greater damage (Ruel 1995). For winds of a given velocity, wind direction affects the loading placed on objects.

Similarly, the greater the accumulation of ice or snow on trees, the greater the likelihood that the trees will suffer structural failure. The National Weather Service declares an ice storm when there is at least 0.6 centimeters of ice accumulation, but minor glazing (0.6 to 1.3 centimeters) may cause little damage (Lemon 1961). Major events may result in accumulations as high as 10 to 20 centimeters (Bragg and others 2003). Depending on weather conditions, ice may remain on trees for some time before melting or being shed. As ice is retained on the trees for longer periods, damages increase (Schultz 1997).

Numerous mechanistic simulation models have been used to simulate the probability of structural failure in response to increased wind and ice, or snow loading or both (Blennow and Sallnäs 2004, Dunham and others 2000, Miller and others 2000, Peltola and others 1999, Talkkari and others 2000). These models generally predict critical windspeeds and ice or snow loading or both required for uprooting and breakage as a function of site, tree, and stand characteristics based on biomechanical properties. Several models incorporate both sources of risk to account for interactions between ice and snow loadings and wind risk (e.g., Miller and others 2000, Talkkari and others 2000).

A few empirical studies have included windspeed or ice and snow accumulation as explanatory variables in their

regression models. Ramsey and others (2001) incorporated windspeed and duration to explain the variation in hurricane damage among forest types along the Atchafalaya River basin of Louisiana. Using forest-type distribution from Landsat Thematic Mapper image data, hurricane-impact data from very high-resolution radiometer images, and windspeed and duration calculated from a wind field model, they found that the estimated impact for each forest type was strongly related to the duration and speed of extreme winds from Hurricane Andrew. Proulx and Greene (2001) found higher damage in northern hardwoods associated with greater ice accumulation, but Olthof and others (2004) did not find a direct relationship between ice storm precipitation and forest damage.

Site Conditions

Site conditions are commonly identified as influencing severe weather damage. These are physical properties of a location, such as topography and soil conditions, that cannot typically be directly modified in a particular stand through management actions.

Numerous studies have shown that local topography is a key determinant of risk of wind damage (e.g., Boose and others 2004, Foster and Boose 1992, Kulakowski and Veblen 2002, Quine 1995, Ruel 1995), but the relationship is complex, and specific topographic factors identified as important differ from study to study. Impacts may be increased when there is a barrier behind the stand (Talkkari and others 2000). Stands at higher elevations, on easterly slopes, and near ridges were more likely to suffer wind damage in Colorado (Kulakowski and Veblen 2002). The key issue for topography seems to be its influence on the probability of local windspeeds reaching critical speeds (Quine 1995). In many cases, the topography variables are serving as proxies of local wind intensity in the absence of direct measures of windspeed. Links between topography and ice and snow damages are less studied, but ice damages are increased at greater elevations (Olthof and others 2004, Rhoads and others 2002, Van Dyke 1999) as well as on steep slopes (Proulx and Greene 2001, Van Dyke 1999).

Findings about relationships between soil conditions and wind damage are relatively consistent (Wilson 2004).

Soil saturation is an important factor affecting the probability of windthrow. When hurricanes or other wind storms pass through an area following periods of heavy rainfall, blowdown is more likely (Ruel 1995). Deeper, well-drained soils lower the risk of wind damage. Beese (2001) found wet soil to be one of the largest contributing factors to wind damage. Similarly, damages from ice and snow are greater for wet soils (Van Dyke 1999). Other conditions that prevent establishment of deep roots, such as the presence of boulders, bedrock, or other barriers close to the surface, also increase the probability of uprooting (Rhoads 1999).

Tree Characteristics

A number of studies have focused on relationships between wind, ice, and snow damage and various tree characteristics. Tree characteristics of interest include species, health, age, size, height-to-diameter (H/D) ratio, crown shape, and canopy position.

Conifers tend to be more susceptible than hardwoods to hurricane damage (Foster 1988, Foster and Boose 1992, Jalkanen and Mattila 2000), though there are differences in susceptibility between taxa related to several species characteristics, including crown form, branching, rooting depth, center of gravity, and wood strength. Species susceptibility to hurricane-related damages also varies across types of damage, including breakage, uprooting, exposure to saltwater, and secondary insect and disease damage (Barry and others 1998). In addition, trees planted outside their natural range may be more susceptible to damage.

Differences in susceptibility to ice storms are related to species characteristics such as crown form, crown size, branch thickness, branch angle, root depth, and wood strength. Trees that have an excurrent form (apical dominance) are better able to shed ice and snow than those with decurrent form, and the vase-shaped form of many elms and oaks makes these trees especially vulnerable to ice and snow accumulation (Van Dyke 1999). Trees with branches that are pliable may better withstand ice and snow accumulation because they can shed ice or transfer the force to other parts of the tree, the ground, or neighboring trees. However, wood that is cold, “green,” or less dense has lower

resistance to breakage than warm seasoned wood of the same species (Bragg and others 2003).

Root and stem rots, cankers, insect infestation, or any form of prior injury increases the probability of wind damage (Wilson and Baker 2001) and ice damage (Van Dyke 1999) (with the possible exception of defoliating insects or other agents that reduce crown surface area). Trees are likely to break at the point of decay when exposed to excessive loading by wind, ice, and snow. For instance, trees with advanced beech bark disease experienced more ice damage (Rhoads and others 2002). Vine coverage may also increase susceptibility to glaze damage by increasing the surface area available for ice accumulation (Bragg and others 2003). Boose and others (2001) examined hurricanes affecting New England since European settlement in 1620 and found that forest damage from an event was strongly dependent on natural disturbance history. High proportions of compression wood, which can form in response to tree bending in past weather events, may increase storm damage (Dunham and Cameron 2000).

Stand age and tree size may also contribute to forest vulnerability to high winds. Although age and size are generally correlated, different studies alternately focus on age, height, diameter, or H/D ratio. Many studies indicate that susceptibility to wind damage increases with increasing stand age during the initial decades of forest development (Everham and Brokaw 1996, Francis 2000, Jalkanen and Mattila 2000). Foster (1988) found that conifers' susceptibility to wind damage increases rapidly after age 15, but hardwood damage increases more gradually with age. Foster and Boose (1992) found wind damage increased approximately linearly with stand height. Ametis and Burkhart (1996), on the other hand, argued that older, larger trees are stronger and have greater resistance to damage.

Francis (2000) and Greenberg and McNab (1998) also reported increasing uprooting with increasing tree height. Francis (2000) showed that tree height strongly influenced wind damage in San Juan during Hurricane Georges. Other authors suggested that height relative to the height of surrounding trees is the factor that most strongly determines susceptibility to wind damage (Asner and Goldstein 1997, Francis and Gillespie 1993, Hedden and

others 1995). Jalkanen and Mattila (2000) and Francis and Gillespie (1993) both showed that the susceptibility of a stand to wind damage was increased by larger mean diameter. Achim and others (2005) found that stem mass was the factor most highly correlated with wind damage. Francis and Gillespie (1993) related gust speed to tree damage in Hurricane Hugo, and their results indicate that the probability of a tree suffering some form of damage increases with increasing tree diameter.

Findings were mixed for ice damage. Bragg and others (2004) found the lowest levels of damage from ice in the oldest plantations. They found that the smallest trees were much more likely to bend severely in response to ice loading, that intermediate-sized trees had both bending and stem breakage, and that the largest trees had little of either but had more crown damage and branch loss. Rhoads and others (2002) found heavy ice damage in intermediate-sized trees that were 24 to 28 years old but little ice damage in younger stands in the affected forest. Proulx and Greene (2001) found that very small trees (3.2 to 9.5 cm in diameter) were more likely to suffer damage, that small and intermediate trees (<17.8 cm in diameter) were more likely to bend or snap, and that large trees were more likely to lose branches. Van Dyke (1999) indicated that older trees may be more susceptible to injury from ice because they have larger crowns, greater likelihood of internal decay, and decreased branch flexibility.

A number of studies have examined H/D ratios rather than either height or diameter individually and have typically found that larger H/D ratios tend to increase the risk of damage from high-wind events (Wilson and Baker 2001), snow (Kato and Nakatani 2000), and ice accumulation (Van Dyke 1999). However, Valinger and Fridman (1997) found that the ratio of the H/D ratio to the upper diameter (measured at 3 or 5 meters) was the best predictor of the probability of snow and wind damage, and that for a given upper diameter, the probability of damage was higher for a site with trees of low H/D.

In addition to looking just at tree height, diameter, or H/D ratio, some studies examine the influence of crown shape and canopy position. Mechanistic models of critical

wind, ice, and snow loading generally include crown size and shape because greater crown surface area increases the drag coefficient and potential for loading from accumulation (Peltola and others 1999, Talkkari and others 2000). Empirical observations and models have generally supported this assumption. Foliated trees and trees with large crowns have more surface area for ice and snow accumulation and for wind to act on, increasing vulnerability to damage; however, damage is lowered by greater crown symmetry (Bragg and others 2003, Kato and Nakatani 2000, Van Dyke 1999). Beese (2001) found greater wind damages in trees with larger crowns in montane coastal forests in British Columbia. Hardwoods are less susceptible than conifers to damage from ice or snow storms that occur during the winter months, when the hardwoods do not have foliage. Mitchell (1995) and Ruel (1995) reported that wind damage depends on canopy density and tree position in the canopy. Van Dyke (1999) indicated that dominant trees are more likely to suffer ice damage.

Stand Characteristics

Disturbances that open the canopy may increase the severity of damage from subsequent windstorms (Everham and Brokaw 1996). Stand density, thinning regime, and the presence of edges and gaps each have been found to influence forest damage from severe weather. However, the effects of density on forest damage depend on the interplay of a complex set of factors. Higher densities may lead to greater H/D ratios and trees that are less wind resistant. However, higher stand density may increase the probability of stem bending but decrease the probability of stem breakage because neighboring trees provide support for bending stems (Bragg and others 2004). Wind may move through low-density stands more freely, so that energy is dissipated and wind loadings are lowered. In addition, trees in the interior areas of low-density stands may normally receive higher winds and develop greater wind resistance than those in high-density stands. However, ice damage may be expected to increase at lower stand densities because trees in lower density stands develop larger crowns, and these tend to accumulate more ice and snow (Gardiner and Quine 2000).

It is also possible that bending or breakage of trees results in damage to other trees. When windthrow or breakage occurs in lower density stands, there is less chance that neighboring trees will be damaged (Baker and others 2002). Beese (2001) found that striking of trees by other trees was one of the most common categories of wind damage in their study region.

Recent thinning can increase vulnerability to wind, ice, and snow. Thinning removes structural support of proximate trees, and recently exposed pines tend to have relatively weak stems and ice-accumulating surfaces more concentrated in the crown (Bragg and others 2003). Burner and Ares (2004) found that thinning increases susceptibility to ice damage. Jalkanen and Mattila (2000) suggested that thinning will increase wind damage but decrease snow damage. Peltola and others (1999) simulated critical snow loading for both uprooting and stem breakage for managed and unmanaged stands of Scots pine (*Pinus sylvestris* L.) in southern Finland and concluded that critical snow loading for both uprooting and breakage is lower for unthinned stands than thinned stands.

Proximity to forest edge is highly related to wind (Wilson 2004) and ice storm damage (Olthof and others 2004). Zeng and others (2004) integrated a mechanistic wind damage model and an airflow model with a forest database containing information at the tree, stand, and regional levels and simulated damages for current forest edges and situations where new edges might be created through clearcutting. They found that clearcuttings increased windspeeds at forest edges and increased risk of damage for cases where vulnerable stands remained at the newly created edges. Others have found reduced damage at stand edges, however, especially when the edge has been established for a long time. This is likely due to trees on the edges facing greater wind loading on a normal basis and responding by increasing strength to resist wind loading (Foster 1988).

Management under Endogenous Risk

The probability of a severe weather event occurring is exogenous to the landowner; that is, landowners are unable to influence this probability through their own actions. However, although these events cannot be prevented, their

potential impact can be mitigated through forest management, so the extent of severe weather damages to a particular forest area is partially under the landowner's control. Recognizing this endogeneity of risk and understanding the factors that influence damage patterns are of key importance to efficient forest management. Although there is substantial variation in the empirical findings on the most important factors influencing weather damages, there are some common management recommendations. Landowners can incorporate expectations of severe weather damages into their decisions regarding site selection, species selection, silvicultural treatments, and planning for damage recovery to decrease expected impacts (Bragg and others 2003, Lohmander and Helles 1987, Olofsson and Blenow 2005, Persson 1975, Zeng and others 2004). Another strategy for the forest industry is to diversify spatially to manage risk across total forest holdings thereby avoiding the loss of a large share of their standing timber to a single weather event.

Moore and Quine (2000) presented one example of the ability of forest management to mitigate weather risk. They compared wind risk in Sitka spruce (*Picea sitchensis* (Bong.) Carr.) plantations in Great Britain with that in radiata pine (*Pinus radiata* D. Don) plantations in New Zealand using the FORESTGALES simulation model. They reported that the plantations in New Zealand were at greater risk of damage than those in Great Britain because of differences in management even though the New Zealand plantations were subjected to a less severe wind regime. In Great Britain, silvicultural practices have been adopted to reduce density, conduct more careful site preparation, and reduce thinning. This comparison demonstrates the influence of forest management on the risk of weather damage, but it also demonstrates that mitigation options adopted should reflect the level of risk faced. Managers of plantations in New Zealand have been able to focus on maximizing profit under a less constraining wind risk, and plantations in New Zealand are more profitable than those in Great Britain.

Of course, appropriate response depends on the degree of risk. In cases where the exogenous risk of damages is low, incorporation of weather risk into strategy may result in minimal or no change in optimal forest management.

In contrast, there may be no feasible strategy for reducing damages when the exogenous risk of damages is high other than simply limiting investments and therefore the expected cost of damages. In the intermediate case, where the exogenous risk of damages is significant but there are cost-effective strategies for mitigation, the incorporation of weather risk into decisionmaking may substantially alter optimal forest management practices (Gardiner and Quine 2000).

This implies that any evaluation comparing weather damages on managed and unmanaged sites will be inaccurate if it does not properly account for selection bias. Selection bias arises because the forest management strategies observed reflect decisions made by forest managers based in part on the perceived vulnerability of their stands to weather-related damages and the perceived effectiveness of potential silvicultural actions in those stands. Thus, the value of managing weather risk could be understated if these actions are selectively being undertaken in stands with high expected damages and the outcomes following a storm are compared with those in areas with low expected damages where managers chose to adopt fewer mitigation options. On the other hand, the effectiveness of damage reduction strategies may be overstated if little or no action to reduce impacts is being taken in certain stands because the expected damages in those locations are so large that there are few feasible mitigation options. Thus, careful and systematic program evaluation is needed to account for endogenous selection and to ensure that the effectiveness of damage mitigation options is being assessed after controlling for selection of mitigation options based on perceived baseline risk (Butry 2006).

Damage Mitigation Options

The primary categories of damage mitigation options are site and stand selection, selection and timing of silvicultural treatments, and stand recovery activities. Forest management is unlikely to significantly alter climate, topography, or soils in a given site. However, forest managers establishing a new stand can affect these conditions for forests they manage through site selection. In addition, owners with multiple sites can manage overall risk by selecting a portfolio of sites

that offers the desired risk-return profile. Typically, weather risk is not the overriding consideration in the selection of sites for forest investments, but taking the risk of forest damages into account when selecting a site may improve the ability to meet management objectives.

Similarly, among numerous other factors affecting choice of species (e.g., productivity, market forces, objectives of the forest manager), the differential weather risk associated with different species should be taken into account. Some species are more vulnerable to weather damage than others based on crown configuration, rooting, wood strength, and many other factors. In addition, planting trees outside of their natural range may increase their vulnerability to damage (Bragg and others 2003). Selecting a tree species that is less productive or has a lower market price but also provides a reduced risk of severe weather damage may result in a higher expected present value of the stand if the baseline risk of severe weather and the species-to-species difference in expected damages in the event of severe weather are sufficiently large.

The effects of management decisions about stocking, thinning, and pruning on storm damage risk have been identified as key issues in a number of studies. A number of trade-offs are associated with these activities, partly because short-term and long-term effects on risk may differ substantially. For instance, low-density stocking, thinning, or pruning may increase the risk of damage in the short term, but expected damages are reduced farther into the future as trees respond by growing stronger and more resistant to damages. Limited tree-size variation increases susceptibility to developing high H/D ratios in the dominant trees (Wilson 1998). There is typically less variation in tree size in plantations than in naturally regenerated stands, and this may lead to greater H/D ratios of dominant trees, reducing the stability of these trees. To keep H/D ratios down, it is necessary to conduct thinning operations before competition that leads to increased H/D (Wilson and Baker 2001). Similarly, Wilson and Oliver (2000) found that plantation H/D ratios can be lowered by reducing planting density or early thinning to encourage development of strong stems and crowns; later thinning did not appear to be as effective. Also, if the rotation length is reduced

sufficiently, the reduction of time at risk of damage may more than offset the increase in expected damages if an event does occur. One of the best defenses against weather damages may be to grow the trees out of vulnerable intermediate sizes as quickly as possible through the application of silvicultural practices such as reduced density and proper thinning and pruning to increase site productivity.

The standard Faustmann equation maximizes discounted net revenue from an infinite series of rotations, accounting for the costs of maintaining land in forest production. The optimal rotation under certainty occurs where the increase in stand value from one additional period of growth is equal to the costs of delaying current and future harvests by one period. Incorporating an exogenous positive probability of damages into the equation unambiguously yields a reduction in optimal rotation length (Martell 1980, Reed 1984, Reed and Errico 1985, Routledge 1980). Under some conditions, increased production risk may also lead to the use of lower intensity production methods such as naturally regenerated stands (Haight and others 1986). Accounting for endogeneity of expected forest damages alters optimal management strategies by explicitly recognizing effects of management decisions on the expected present value of the stand through accounting for changes in expected damages.

Stocking influences, in several ways, damages that result from weather events. Less densely stocked stands may be more vulnerable in the short term because they will have less support from their neighbors. However, less dense stocking increases the growth of individual trees and reduces the time trees require to reach marketable size. In addition, low stand density will result in trees that are more resistant to loading because they are larger and subject to greater loading on a normal basis. One caveat is that low stand density commonly results in trees with larger, less tapered crowns that will tend to accumulate more ice and snow, although their increased strength may offset this effect.

Thinning may result in stronger trees that are more able to withstand wind, ice, and snow (Kato and Nakatani 2000) a few years after thinning but increase the likelihood of damage in the interim. Coates (1997) found that partial

cutting doubled the percentage of trees with wind damage in the 2 years after thinning, from 1.1 percent to 2.2 percent but concluded that this increase in damage was too small to warrant changes in management (this increased damage may also be offset by increased tree growth rates that reduce the time spent at risk). Similarly, pruning can increase wind damage if a storm passes through the area soon after the treatment but can reduce damage in the future after trees have strengthened. Pruning was found to result in an increased resistance to snow damage in the short term, though, because the reduced surface area of the crown decreases accumulation. However, to the extent that heavy pruning reduces diameter growth more than height growth, resistance to snow loading may decline in the years after pruning because of increased H/D ratios (Kato and Nakatani 2000).

Thus, in areas that receive severe weather very frequently, managers may be less willing to conduct thinning or pruning because of the high probability that a storm will occur during the period when the stand is more vulnerable. In addition to removing support for remaining trees, thinning operations often cause minor damage to individual trees, and the damage sites can serve as entry points for insects and disease that then become established and infest the stand (Lohmander and Helles 1987). However, there is a reduced probability of trees damaging their neighbors following thinning because the spacing between trees is increased (Bragg and others 2003). In addition, identifying and removing trees most vulnerable to damage during thinning operations may be advantageous. Cameron and Dunham (1999) found that trees that were damaged by wind and snow had significantly more compression wood than did undamaged trees, and Dunham and Cameron (2000) therefore recommended preferentially removing trees likely to contain compression wood.

Because of the complexity of the interactions between various factors affecting expected forest damages, the relative costs and benefits of a particular action will vary spatially and temporally. Thus, optimal management strategies regarding planting density and whether, when, and how intensely thinning and pruning should be conducted need to be determined on a site-specific basis.

If a plan for stand recovery is formulated before a damaging event takes place, this can help mitigate the damage. Salvage efforts after ice storms should concentrate on minimizing economic losses from damage to timber. Timber subject to losing the greatest value to degradation in the short term should be salvaged first, although timber of all ages and sizes may require some remediation to lessen fire danger and insect outbreaks. Salvage of severely damaged pine is more time sensitive than salvage of severely damaged hardwoods because pine is more susceptible to infestation by bark beetles and wood borers, but downed hardwoods should also be salvaged as soon as possible to avoid degradation (Van Dyke 1999). Remedial actions following hurricanes, such as staking saplings upright, are not clearly effective and are feasible only on small areas. In one study, saplings left in a leaning position did not lose measurably more growth than those staked upright, and many righted themselves (Gresham 2004), although it is important to recognize that bent trees may have permanent internal damage. In some cases, severely bent trees will not fully recover and may die or grow at greatly reduced rates. Managers may wish to explore selective harvesting of damaged trees.

Optimal Thinning and Rotation Decisions

As an illustrative example of the implications of treating weather damage risk as endogenous, we examine optimal thinning and rotation decisions. The implications of production risk for optimal rotations have been examined in several previous studies, including Martell (1980), Routledge (1980), Reed (1984), and Reed and Errico (1985), all of which evaluated changes in optimal rotation length under the exogenous risk of forest fires. Each found that optimal rotation age unambiguously declined where production risk was assumed to exist. Thorsen and Helles (1998) modified these earlier models to treat risk as endogenous, focusing on the timing and intensity of thinning activities to influence the risk of damage. Thinning is one of the silvicultural practices that is most frequently mentioned in the literature as playing an important role in damage risk and as being readily applied.

Thinning offers the benefit of immediate income, and it promotes faster diameter growth of remaining trees, which increases net price received and reduces the risk of windthrow. Thinning also reduces the remaining volume that could potentially be damaged by storms. However, thinnings are costly because of fixed costs of thinning operations and increased risk of storm damage for several years after thinning. These dynamics are complex, but important to consider in determining optimal forest management strategies.

Thorsen and Helles (1998) examined an even-aged forest stand managed to maximize expected present value. They modeled the selection of an optimal thinning strategy and optimal rotation age (at which time the stand is clear-cut), taking into account the stand growth function, net timber price, and risk of severe weather damage. Stand density, age, site, tree, and stand characteristics, including time since thinning and thinning intensity, all affect the risk of damage. The damage risk functions describe how the stand's stability is impacted by current and past stand management decisions. The less the risk functions are affected by management decisions, the more resistant the stand is to disturbances such as thinning, and the less important it is to consider the implications of management decisions for weather damage risk. Thorsen and Helles (1998) used numerical optimization procedures to determine optimal management in the case of Norway spruce (*Picea abies* L. Karst.), which they identified as one of the species most often suffering from health or windthrow problems that necessitate salvage harvest of entire stands. Based on their assumptions regarding growth, risk dynamics, storm probability, and other variables, they found that optimal rotation age is reduced from 74 years under no risk to 69 years if storm risk is treated as exogenous, but 71 years when risk is assumed to be endogenous. In addition, the optimal number of thinnings increases from 10 to 11 between the case of no risk and exogenous risk. When risk is considered to be endogenous, the optimal number of thinnings increases to 18, but the intensity of each thinning is reduced. In addition, they found that incorporating endogeneity in determining optimal management increases expected present value of the stand.

The findings of this study are dependent on the growth, risk, and other dynamic relationships assumed. Optimal management will differ across stands depending on baseline damage risk, effects of thinning on growth rates and damage risk, prices and costs, and other variables (Straka and Baker 1991). In addition, this example assumes profit-maximizing behavior, which may be appropriate for forest industry but not for many nonindustrial private forest (NIPF) landowners or public forest managers. NIPF landowners and public forest managers are expected to consider the amenity value of standing forests, which would add an additional term measuring amenity value to the optimal control problem discussed above. This term would depend on site, tree, and stand characteristics. Nevertheless, treating severe weather risk as endogenous may enable both private and public managers to reduce damage risk while increasing the expected present value of their stands.

Policy Implications

To the extent that weather damage risk is endogenous, private and public forest managers may be able to improve ecological and economic returns by allowing for the effects of their decisions on risk. However, this does not tell us whether any particular strategy should be adopted in the case of any specific stand. Options to be adopted depend on managers' objectives and the cost of the option relative to the reduction in risk provided. Many key factors interact in a very complex manner to influence weather risk, making it vital to consider case-specific conditions in making decisions regarding mitigation of weather risk. It is important to consider joint risk of different types of weather events, which may reinforce or contradict each other.

Policy implications are expected to differ among forest industry, NIPF landowners, and public forest managers because these groups have different objectives. Forest industry managers are expected to be profit maximizing, whereas NIPF landowners likely have more varied objectives and value nontimber amenities of standing forests more highly. Damage mitigation options that would be optimal for forest industry may be less suitable for NIPF lands or vice versa, depending on the joint effects of the strategies on damage risk, expected present value, and stand amenity

values. Similarly, public land managers are expected to take various nontimber objectives into account. The presence of endogenous storm risk may be an opportunity for the public sector to provide incentives for private landowners to take actions to mitigate storm damage, especially where private inaction could result in secondary insect and disease infestations or other conditions that could have negative effects on neighboring properties.

Private Forest Management Decisions

For forest industry, management of weather risk should be selected to maximize expected profitability, assuming risk neutrality. Under risk neutrality, firms are interested in maximizing the expected value of profits without regard for variability, whereas risk-averse firms would be willing to accept lower expected returns in exchange for reduced variability of profits. Decisionmaking under risk aversion could be analyzed using similar methods but would have to account for risk tolerance. One strategy when operating under risk is to reduce rotation age. Accounting for damage risk reduces the optimal rotation age relative to that obtained by solution of the standard Faustmann equation under certainty (Gardiner and Quine 2000, Haight and others 1996). However, if risk is truly endogenous, then managers may be able to alter practices to mitigate risk and potentially even increase expected present value of a stand, as described in "Optimal Thinning and Rotation Decisions." Selective removal of specific high-risk trees when thinning, as well as adjustment of thinning timing and intensity could reduce risk of storm damage. However, it must be possible to identify and remove these trees cost effectively. Heavily damaged or dead trees are obvious candidates for removal, but it may be worth selectively removing those trees with features that increase their risk, such as large, asymmetric crowns, and trees that have been heavily bent.

Numerous other management strategies, including site selection, species selection, and planting density, could be modified to mitigate risk and should be adopted if they offer expected benefits exceeding their costs. Each of these strategies and combinations could be examined through empirical simulations using a model similar to that described in "Optional Thinning and Rotation Decisions."

To optimally incorporate these strategies into forest management practices, it is necessary to understand the implications of each for the dynamic risk of storm damage in the event of a storm at different points in time, forest growth rates, and stand value.

For NIPF landowners, behavior may be more complex because the perceived impacts on aesthetics, wildlife, and other nontimber amenities provided by standing forests are a more important part of their management objectives. These landowners are likely to have substantially different optimal management policies as a result, probably tending toward fewer thinnings and increased rotation age relative to land managed by the forest industry, although this may vary depending on the primary objectives of particular NIPF landowners.

Public Policy and Forest Stand Management—

Management of public lands to mitigate weather risk also is likely to differ from the profit-maximizing forest industry case. Wilson and Baker (2001) argued that managing stands to allow greater future flexibility may be more important in the case of public lands than in that of private lands because objectives of public land management are more likely to change over time with shifting political pressures. It is important to develop stands that are capable of producing multiple outputs, from timber to older forest habitat, when future objectives are uncertain. Like NIPF landowners, public land managers are likely to consider aesthetics, wildlife, recreation, and other nontimber products in determining optimal forest management strategies.

In addition, the presence of endogenous forest risk and the extensive losses that could result from a major event could lead public agencies to become involved in providing incentives for improved private forest management, especially to avoid secondary impacts such as insect and disease infestations that may negatively affect neighbors. Private landowners will not fully account for the damages that may result on neighbors' lands and may underinvest in storm damage mitigation relative to the socially optimal level. This negative externality may be an argument for government intervention to correct this market failure through subsidies of mitigation practices, by establishing penalties

for not following recommended practices, or by establishing regulations requiring specific practices. However, it is important to construct such programs with care to ensure that they result in net increases in forest investment and improvements in forest health and do not simply offset private investment that would occur in the absence of the policy.

In Switzerland, short-term damage resulting from storm Lothar was similar across cantons (states) even though different cantons employed significantly different forest protection measures (Bisang and Zimmerman 2006). More expensive measures adopted in some cantons were not much more effective in preserving forests and preventing forest damages than much less expensive options. In addition, forest owners' salvage decisions appeared to be independent of the financial incentives provided by cantons. Forest owners spent more of their private resources in cantons that provided minimal financial support, and their marketing of salvaged timber was less successful in these cantons than in those that provided greater public resources. Thus, the varying strategies for public involvement in providing financial incentives for forest management had important distributional effects for forest owners and government spending but not for forest health (Bisang and Zimmerman 2006).

Conclusions

Our review characterizes primary influences on damage risk as site, tree, or stand characteristics, each of which is influenced by forest management decisions. Findings about key factors differ from study to study, and this indicates both the complexity of storm damage and the substantial variation in data and methods used to conduct analyses. A few studies simultaneously incorporate many of the factors identified in the literature as having an important influence on damages; most focus on only a few variables and do not necessarily report statistical significance. Thus, it is unclear just how broadly applicable the findings of many studies are. This review reveals a need for additional empirical research to better quantify the effects of various factors influencing the risk of forest damages, particularly in the case of complex stands that are unlikely to be

captured adequately through standard mechanistic models. Future studies should place greater emphasis on empirical analyses that examine the effects of variables believed to affect damages and their interactions simultaneously. Another important issue is the need for more systematic program evaluation that accounts for endogenous selection of damage mitigation options to better identify the effects of management actions while controlling for differences in underlying conditions.

Our review indicates that some general management practices are likely to affect risk and that forest managers must consider the influence of their management decisions on the extent of weather damages. Site and species selection, as well as choice and timing of silvicultural treatments, affect expected damages. In the event of damage, the effectiveness of management plans for storm recovery is another key determinant of economic impacts and secondary damages, although management planning for storm recovery is not a focus of this chapter. Thus, optimal stand management where damage risk is treated as endogenous is likely to differ from management where risk is treated as completely exogenous. Treating risk as endogenous results in more frequent, less intense thinnings and a longer rotation age than when risk is treated as exogenous, though both cases have shorter optimal rotation ages than when there is assumed to be no weather risk (Thorsen and Helles 1998). This finding depends on a number of assumptions regarding the change in expected damages associated with thinning, however, and may differ across stands depending on their baseline risk of damage, effects of thinning on tree growth rates, timber price, thinning costs, and other variables. Developing better parameterizations of these relationships is an important area for additional research to better understand optimal decisionmaking under endogenous risk for a variety of climate and forest characteristics.

Management practices should be selected on the basis of the risk faced and management objectives. In the case of the forest industry, risk-neutral firms should undertake damage mitigation measures only if the increase in the expected present value of the stand exceeds the cost of the mitigation option. For NIPF landowners, management decisions under endogenous risk are generally expected to be more complex

because of objectives other than profit maximization. Thinning regime and rotation age have implications for nontimber amenities provided by forests. Therefore, to the extent that NIPF landowners have objectives that include the production of such amenities, management by NIPF landowners will differ from management where the goal is profit maximization. Incorporating the nontimber amenities provided by standing forest will probably tend to reduce the optimal number of thinnings and increase rotation age, although this may vary depending on the primary objectives of particular NIPF landowners (Foster and Orwig 2006). Similarly, the implications for public land management under endogenous risk are expected to differ from the profit-maximizing case based on the varied objectives of public agencies managing forest land.

Recognition of the endogenous nature of forest damages and the large potential losses could induce public agencies to provide incentives for private landowners to engage in improved management practices. This is particularly true when damages may lead to secondary impacts such as insect infestation or forest fires that could spread to neighbors' land. Landowners do not fully account for impacts on neighbors or invest at socially optimal levels in damage mitigation and stand recovery measures, and this provides a rationale for potential government intervention. However, it is important to construct such programs with care to ensure that they result in net increases in forest investment and improvements in forest health rather than simply offsetting private investment.

Literature Cited

- Achim, A.; Ruel, J.C.; Gardiner, B.A. [and others]. 2005.** Modelling the vulnerability of balsam fir forests to wind damage. *Forest Ecology and Management*. 204(1): 35–50.
- Ameteis, R.L.; Burkhardt, H.E. 1996.** Impact of heavy glaze in a loblolly pine spacing trial. *Southern Journal of Applied Forestry*. 20(3): 151–155.
- Asner, G.P.; Goldstein, G. 1997.** Correlating stem biomechanical properties of Hawaiian canopy trees with hurricane wind damage. *Biotropica*. 29: 145–150.

- Baker, W.L.; Flaherty, P.H.; Lindemann, J.D. [and others]. 2002.** Effect of vegetation on the impact of a severe blowdown in the southern Rocky Mountains, U.S.A. *Forest Ecology and Management*. 168(1–3): 63–75.
- Bakke, A. 1989.** The recent *Ips typographus* outbreak in Norway: experiences from a control program. *Holarctic Ecology*. 12: 515–519.
- Barry, P.J.; Doggett, C.; Anderson, R.L.; Swain, K.M. 1998.** How to evaluate and manage storm-damaged forest areas. South. Region Manage. Bull. R8-MB 63. Asheville, NC: U.S. Department of Agriculture, Forest Service. 11 p.
- Beese, W.J. 2001.** Windthrow monitoring of alternative silvicultural systems in montane coastal forests. In: Mitchell, S.J.; Rodney, J., comps. Windthrow assessment and management in British Columbia: Proceedings of the windthrow researchers' workshop. Richmond, BC: BC Forestry Continuing Studies Network. 229 p.
- Bisang, K.; Zimmerman, W. 2006.** Key concepts and methods of programme evaluation and conclusions from forestry practice in Switzerland. *Forest Policy and Economics*. 8(5): 502–511.
- Blake, E.S.; Jarrell, J.D.; Rappaport, E.N.; Landsea, C.W. 2006.** The deadliest, costliest, and most intense United States tropical cyclones from 1851 to 2005. Tech. Memorandum NWS TPC-4. Miami: NOAA. 51 p.
- Blennow, K.; Sallnäs, O. 2004.** WINDA—a system of models for assessing the probability of wind damage to forest stands within a landscape. *Ecological Modelling*. 175(1): 87–99.
- Boose, E.R.; Chamberlin, K.E.; Foster, D.R. 2001.** Landscape and regional impacts of hurricanes in New England. *Ecological Monographs*. 71: 27–48.
- Boose, E.R.; Serrano, M.I.; Foster, D.R. 2004.** Landscape and regional impacts of hurricanes in Puerto Rico. *Ecological Monographs*. 74: 335–352.
- Bragg, D.C.; Shelton, M.G.; Heitzman, E. 2004.** Relative impacts of ice storms on loblolly pine plantations in central Arkansas. In: Connor, K.F., ed. Proceedings of the 12th biennial southern silvicultural research conference. Gen. Tech. Rep. SRS-71. Asheville, NC: U.S. Department of Agriculture, Forest Service, Southern Research Station: 132–137.
- Bragg, D.C.; Shelton, M.G.; Zeide, B. 2003.** Impacts and management implications of ice storms on forests in the Southern United States. *Forest Ecology and Management*. 186(1): 99–123.
- Burke, M.J.; Grime, W.J.P. 1996.** An experimental study of plant community invasibility. *Ecology*. 77: 776–790.
- Burner, D.M.; Ares, A. 2004.** Ice damage in a chronosequence of agroforestry pine plantations in Arkansas, U.S.A. In: Connor, K.F., ed. Proceedings of the 12th biennial southern silvicultural research conference. Gen. Tech. Rep. SRS-71. Asheville, NC: U.S. Department of Agriculture, Forest Service, Southern Research Station: 158.
- Butry, D.T. 2006.** Fighting fire with fire: estimating returns to fire suppression and fuel management using propensity score and instrumental variable methods. Raleigh, NC: North Carolina State University. 118 p. Ph.D. dissertation.
- Cain, M.D.; Shelton, M.G. 1996.** The R.R. Reynolds Research Natural Area in southeastern Arkansas: a 56-year study in pine-hardwood sustainability. *Journal of Sustainable Forestry*. 3(4): 59–74.
- Cameron, A.D.; Dunham, R.A. 1999.** Strength properties of wind- and snow-damaged stems of *Picea sitchensis* and *Pinus sylvestris* in comparison with undamaged trees. *Canadian Journal of Forest Research*. 29(5): 595–599.
- Coates, K.D. 1997.** Windthrow damage 2 years after partial cutting at the Date Creek silvicultural systems study in the interior cedar-hemlock forests of northwestern British Columbia. *Canadian Journal of Forest Research*. 27(10): 1695–1710.

- Dale, V.H.; Joyce, L.A.; McNulty, S. [and others]. 2001.** Climate change and forest disturbances. *BioScience*. 51(9): 723–734.
- D’Antonio, C.M. 1993.** Mechanisms controlling invasion of coastal plant communities by the alien succulent *Carpobrotus edulis*. *Ecology*. 74(1): 83–95.
- Davis, M.A.; Grime, J.P.; Thompson, K. 2000.** Fluctuating resources in plant communities: a general theory of invasibility. *Journal of Ecology*. 88: 528–534.
- Dunham, R.; Gardiner, B.; Quine, C.; Suárez, J. 2000.** ForestGALES: a PC-based wind risk model for British forests. Users guide. Edinburgh: Forestry Commission. [Number of pages unknown].
- Dunham, R.A.; Cameron, A.D. 2000.** Crown, stem, and wood properties of wind-damaged and undamaged Sitka spruce. *Forest Ecology and Management*. 135(1–3): 73–81.
- Everham, E.M.; Brokaw, N.V.L. 1996.** Forest damage and recovery from catastrophic wind. *Botanical Review*. 62: 113–185.
- Foster, D.R. 1988.** Species and stand response to catastrophic wind in central New England, U.S.A. *The Journal of Ecology*. 76(1): 135–151.
- Foster, D.R.; Boose, E.R. 1992.** Patterns of forest damage resulting from catastrophic wind in central New England, USA. *The Journal of Ecology*. 80(1): 79–98.
- Foster, D.R.; Boose, E.R. 1995.** Hurricane disturbance regimes in temperate and tropical forest ecosystems. In: Coutts, M.P.; Grace, J., eds. *Wind and trees*. Cambridge, MA: Cambridge University Press: 305–339.
- Foster, D.R.; Orwig, D.A. 2006.** Preemptive and salvage harvesting of New England forests: when doing nothing is a viable alternative. *Conservation Biology*. 20(4): 959–970.
- Francis, J.K. 2000.** Comparison of hurricane damage to several species of urban trees in San Juan, Puerto Rico. *Journal of Arboriculture*. 26(4): 189–197.
- Francis, J.K.; Gillespie, A.J.R. 1993.** Relating gust speed to tree damage in Hurricane Hugo, 1989. *Journal of Arboriculture*. 19(6): 368–373.
- Gardiner, B.A.; Quine, C.P. 2000.** Management of forests to reduce the risk of abiotic damage—a review with particular reference to the effects of strong winds. *Forest Ecology and Management*. 135(1-3): 261–277.
- Greenberg, C.H.; McNab, W.H. 1998.** Forest disturbance in hurricane-related downbursts in the Appalachian Mountains of North Carolina. *Forest Ecology and Management*. 104(1-3): 179–191.
- Gresham, C.A. 2004.** Loblolly pine saplings affected by Hurricane Hugo retained growth. In: Connor, K.F., ed. *Proceedings of the 12th biennial southern silvicultural research conference*. Gen. Tech. Rep. SRS-71. Asheville, NC: U.S. Department of Agriculture, Forest Service, Southern Research Station: 196–198.
- Haight, R.G.; Smith, W.D.; Straka, T.J. 1996.** The economics of loblolly pine plantations under risk of hurricane damage. In: Haywood, J.L.; Harms, W.R., eds. *Hurricane Hugo: South Carolina forest land research and management related to the storm*. Gen. Tech. Rep. SRS-5. Asheville, NC: U.S. Department of Agriculture, Forest Service, Southern Research Station: 293–304.
- Hedden, R.L.; Fredericksen, T.S.; Williams, S.A. 1995.** Modeling the effect of crown shedding and streamlining on the survival of loblolly pine exposed to acute wind. *Canadian Journal of Forest Research*. 25: 704–712.
- Heidorn, K.C. 2001.** Ice storms: hazardous beauty. <http://www.islandnet.com/~see/weather/elements/icestorm.htm>. [Date accessed: June 22, 2006].
- Hobbs, R.J. 1989.** The nature and effects of disturbance relative to invasions. In: Drake, J.A.; Mooney, H.A.; di Castri, F. and others, eds. *Biological invasions: a global perspective*. Chichester, England: Wiley: 389–405.
- Hobbs, R.J.; Huenneke, L.F. 1992.** Disturbance, diversity, and invasion: implications for conservation. *Conservation Biology*. 6: 324–337.

- Irland, L.C. 1998.** Ice storm 1998 and the forests of the Northeast. *Journal of Forestry*. 96: 32–40.
- Irland, L.C. 2000.** Ice storms and forest impacts. *Science of the Total Environment*. 262: 231–242.
- Jalkanen, A.; Mattila, U. 2000.** Logistic regression models for wind and snow damage in northern Finland based on the National Forest Inventory data. *Forest Ecology and Management*. 135(1-3): 315–330.
- Kato, A.; Nakatani, K. 2000.** An approach for estimating resistance of Japanese cedar to snow accretion damage. *Forest Ecology and Management*. 135(1-3): 83–96.
- Kerzenmacher, T.; Gardiner, B. 1998.** A mathematical model to describe the dynamic response of a spruce tree to the wind. *Trees, Structure and Function*. 12(6): 385–394.
- Kulakowski, D.; Veblen, T.T. 2002.** Influences of fire history and topography on the pattern of a severe wind blowdown in a Colorado subalpine forest. *The Journal of Ecology*. 90(5): 806–819.
- Lemon, P.C. 1961.** Forest ecology of ice storms. *Bulletin of the Torrey Botanical Club*. 88: 21–29.
- Lohmander, P.; Helles, F. 1987.** Windthrow probability as a function of stand characteristics and shelter. *Scandinavian Journal of Forest Research*. 2: 227–238.
- Lutz, H.J. 1940.** Disturbance of forest soil resulting from the uprooting of trees. *Bull.* 45. New Haven, CT: Yale University School of Forestry. 53 p.
- Lutz, J. 2005.** Hurricanes and timberland investments. Poster presented at the Southern Forest Economics Workers conference, Baton Rouge, LA, April 18–20, 2005.
- Lyford, W.H.; MacLean, D.W. 1966.** Mound and pit microrelief in relation to soil disturbance and tree distribution in New Brunswick, Canada. *Harvard For. Pap.* 15. Petersham, MA: Harvard Forest. 18 p.
- Manley, B.R.; Wakelin, S.J. 1989.** Modelling the effect of wind at the estate level. In: Somerville, A.R.; Wakelin, S.J.; Whitehouse, L., eds. *Proceedings of workshop on wind damage in New Zealand exotic forests*. FRI Bull. 146. Rotorua, NZ: Ministry of Forestry: 66–72.
- Martell, D. 1980.** The optimal rotation of a flammable forest stand. *Canadian Journal of Forest Research*. 10: 30–34.
- Mattson, W.J.; Shriner, D.S., eds. 2001.** Northern Minnesota Independence Day storm: a research needs assessment. Gen. Tech. Rep. NC-216. St. Paul, MN: U.S. Department of Agriculture, Forest Service, North Central Station. 65 p.
- Meeker, J.R.; Haley, T.J.; Petty, S.D.; Windham, J.W. 2006.** Forest health evaluation of Hurricane Katrina tree damage: De Soto National Forest, Mississippi. Poster presented at the 2006 Forest Health Monitoring Working Group Meeting: Charleston, SC, January 31–February 2, 2006.
- Meyers, N.L.; McSweeney, K. 1995.** Influence of tree-throw on soil properties. *Soil Science Society of America Journal*. 59: 871–876.
- Miller, D.R.; Dunham, R.; Broadgate, M.L. [and others]. 2000.** A demonstrator of models for assessing wind, snow, and fire damage to forests using the WWW. *Forest Ecology and Management*. 135(1-3): 355–363.
- Miller-Weeks, M.; Eager, C.; Peterson, C.M. 1999.** The northeast ice storm 1998: a forest damage assessment. Concord, NH: North East State Foresters Association and U.S. Department of Agriculture, Forest Service, State and Private Forestry. 36 p.
- Mitchell, S.J. 1995.** The windthrow triangle: a relative windthrow hazard assessment procedure for forest managers. *Forestry Chronicle*. 71: 446–450.
- Mitchell, S.J. 2000.** Stem growth responses in Douglas-fir and Sitka spruce following thinning: implications for assessing wind-firmness. *Forest Ecology and Management*. 135(1-3): 105–114.

- Moore, J.; Quine, C.P. 2000.** A comparison of the relative risk of wind damage to planted forests in Border Forest Park, Great Britain, and the Central North Island, New Zealand. *Forest Ecology and Management*. 135(1–3): 345–353.
- Myers, R.K.; van Lear, D.H. 1998.** Hurricane-fire interactions in coastal forests of the South: a review and hypothesis. *Forest Ecology and Management*. 103(2–3): 265–276.
- Nowacki, G.J.; Kramer, M.G. 1998.** The effects of wind disturbance on temperate rain forest structure and dynamics of southeast Alaska. Gen. Tech. Rep. PNW-GTR-421. Portland, OR: U.S. Department of Agriculture, Forest Service, Pacific Northwest Station. 32 p.
- Nykänen, M.L.; Peltola, H.; Quine, C. [and others]. 1997.** Factors affecting snow damage of trees with particular reference to European conditions. *Silva Fennica*. 31: 193–213.
- Olofsson, E.; Blennow, K. 2005.** Decision support for identifying spruce forest stand edges with high probability of wind damage. *Forest Ecology and Management*. 207(1–2): 87–98.
- Olthof, I.; King, D.J.; Lautenschlager, R.A. 2004.** Mapping deciduous forest ice storm damage using Landsat and environmental data. *Remote Sensing of Environment*. 89: 484–496.
- Peltola, H.; Kellomäki, S.; Hassinen, A.; Granander, M. 2000.** Mechanical stability of Scots pine, Norway spruce, and birch: an analysis of tree-pulling experiments in Finland. *Forest Ecology and Management*. 135(1–3): 143–153.
- Peltola, H.; Kellomäki, S.; Väisänen, H.; Ikonen, V.P. 1999.** A mechanistic model for assessing the risk of wind and snow damage to single trees and stands of Scots pine, Norway spruce, and birch. *Canadian Journal of Forest Research*. 29(6): 647–661.
- Persson, P. 1975.** Windthrow in forests: its causes and the effect of forestry measures. Res. Note 36. Stockholm, Sweden: Department of Forest Yield Research, Royal College of Forestry. 294 p.
- Peterson, C.J. 2000.** Damage and recovery of tree species after two different tornadoes in the same old growth forest: a comparison of infrequent wind disturbances. *Forest Ecology and Management*. 135(1–3): 237–252.
- Prestemon, J.P.; Holmes, T.P. 2000.** Timber price dynamics following a natural catastrophe. *American Journal of Agricultural Economics*. 82(1): 145–160.
- Prestemon, J.P.; Holmes, T.P. 2009.** Economic impacts of hurricanes on forest owners. In: Pye, John M.; Rauscher, H. Michael; Sands, Yasmeen; Lee, Danny C.; and Beatty, Jerome S., tech. eds. *Advances in threat assessment and their application to forest and rangeland management*. Gen. Tech. Rep. PNW-GTR-802. Portland, OR: U.S. Department of Agriculture, Forest Service, Pacific Northwest and Southern Research Stations: 207–220. Vol. 1.
- Prestemon, J.P.; Pye, J.M.; Holmes, T.P. 2001.** Timber economics of natural catastrophes. In: Pelkki, M., ed. *Proceedings of the 2000 Southern Forest Economics Workshop*: Lexington, KY, [Publisher unknown] [Number of pages unknown].
- Proulx, R.J.; Greene, D.F. 2001.** The relationship between ice thickness and northern hardwood tree damage during ice storms. *Canadian Journal of Forest Research*. 31: 1758–1767.
- Quine, C.P. 1995.** Assessing the risk of wind damage to forests: practice and pitfalls. In: Coutts, M.P.; Grace, J., eds. *Wind and trees*. Cambridge, MA: Cambridge University Press: 379–403.
- Quine, C.P.; Coutts, M.P.; Gardiner, B.A.; Pyatt, D.G. 1995.** Forests and wind: management to minimize damage. *Forestry Commission Bulletin* 114. London: HMSO. 24 p.

- Ramsey, I.; Elijah, W.; Hodgson, M.E.; [and others].** 2001. Forest impact estimated with NOAA AVHRR and Landsat TM data related to an empirical hurricane wind-field distribution. *Remote Sensing of Environment*. 77(3): 279–292.
- Ravn, H.P. 1985.** Expansion of the population of *Ips typographus* (L.) (Coleoptera, Scolytidae) and their local dispersal following gale disaster in Denmark. *Zeitschrift für Angewandte Entomologie*. 99: 26–33.
- Reed, W.J. 1984.** The effects of the risk of fire on the optimal rotation of a forest. *Journal of Environmental Management*. 11: 180–190.
- Reed, W.J.; Errico, D. 1985.** Optimal harvest scheduling at the forest level in the presence of risk of fire. *Canadian Journal of Forest Research*. 15: 680–687.
- Réjmánek, M. 1989.** Invasibility of plant communities. In: Drake, J.A.; Mooney, H.A.; di Castri, F. and others, eds. *Biological invasions: a global perspective*. Chichester, England: Wiley: 369–388.
- Remion, M.C. 1990.** Assessment of Hurricane Hugo damage on State and private lands in South Carolina. In: Greer, J.D., ed. *Proceedings of the 3rd biennial remote sensing conference*. Tuscon, AZ: 41–47.
- Rhoads, A.G.; Hamburg, S.P.; Fahey, T.J. [and others].** 2002. Effects of an intense ice storm on the structure of a northern hardwood forest. *Canadian Journal of Forest Research*. 32(10): 1763–1775.
- Rhoads, R.W. 1999.** Ice storm damage in a small valley in southwestern Virginia. *Castanea*. 64: 243–251.
- Routledge, R.D. 1980.** The effect of potential catastrophic mortality and other unpredictable events on optimal forest rotation policy. *Forest Science*. 26: 389–399.
- Ruel, J.-C. 1995.** Understanding windthrow: silvicultural implications. *Forestry Chronicle*. 71: 434–445.
- Schroeder, F.; Eidmann, H.H. 1993.** Attacks of bark- and wood-boring Coleoptera on snow-broken conifers over a 2-year period. *Scandinavian Journal of Forest Research*. 8: 257–265.
- Schultz, R.P. 1997.** Loblolly pine: the ecology and culture of loblolly pine (*Pinus taeda* L.). *Agric. Handb.* 713. Washington, DC: U.S. Department of Agriculture, Forest Service. 493 p.
- Smith, W.H.; Musser, C.R. 1998.** Relation to disease and decay. In: Irland, L.C., coord. *Ice storm 1998 and the forests of the Northeast (special issue)*. *Journal of Forestry*. 96(9): 32–40.
- Snitzer, J.L.; Boucher, D.H.; Kyde, K.L. 2005.** Response of exotic invasive plant species to forest damage caused by Hurricane Isabel. In: Sellner, K.G., ed. *Hurricane Isabel in perspective*. CRC Pub. 05-160. Edgewater, MD: Chesapeake Research Consortium: 209–214.
- Society of American Foresters (SAF). 2005.** Prompt forest recovery is critical to restoring communities and way of life after Hurricanes Katrina and Rita. <http://www.safnet.org/policyandpress/psst/katrinaritadamage.pdf>. [Date accessed: June 23, 2006].
- Solantie, R. 1994.** Effect of weather and climatological background on snow damage of forests in Southern Finland in November 1991. *Silva Fennica*. 28(3): 203–211.
- Straka, T.J.; Baker, J.B. 1991.** A financial assessment of capital-extensive management alternatives for storm-damaged timber. *Southern Journal of Applied Forestry*. 15(4): 208–212.
- Talkkari, A.; Peltola, H.; Kellomäki, S.; Strandman, H. 2000.** Integration of component models from the tree, stand, and regional levels to assess the risk of wind damage at forest margins. *Forest Ecology and Management*. 135(1-3): 303–313.
- Thorsen, B.J.; Helles, F. 1998.** Optimal stand management with endogenous risk of sudden destruction. *Forest Ecology and Management*. 108: 287–299.
- Valinger, E.; Fridman, J. 1997.** Modelling probability of snow and wind damage in Scots pine stands using tree characteristics. *Forest Ecology and Management*. 97(3): 215–222.

- Valinger, E.; Lunquist, L.; Bondesson, L. 1993.** Assessing the risk of snow and wind damage from tree physical characteristics. *Forestry*. 66(3): 249–260.
- Van Dyke, O. 1999.** A literature review of ice storm impact on forests in eastern North America. SCSS Tech. Rep. 112. Pembroke, Ontario: Landmark Consulting. 33 p.
- Wilson, J.S. 1998.** Wind stability of naturally regenerated and planted Douglas-fir stands in coastal Washington, Oregon, and British Columbia. Seattle, WA: University of Washington. 160 p. Ph.D. dissertation.
- Wilson, J.S. 2004.** Vulnerability to wind damage in managed landscapes of the coastal Pacific Northwest. *Forest Ecology and Management*. 191(1–3): 341–351.
- Wilson, J.S.; Baker, P.J. 2001.** Flexibility in forest management: managing uncertainty in Douglas-fir forests of the Pacific Northwest. *Forest Ecology and Management*. 145(3): 219–227.
- Wilson, J.S.; Oliver, C.D. 2000.** Stability and density management in Douglas-fir plantations. *Canadian Journal of Forest Research*. 30(6): 910–920.
- Yates, H.O., III; Miller, T. 1996.** Post-Hurricane Hugo forest pest populations and damage. In: Haymond, J.L.; Hook, D.D.; Harms, W.R., eds. *Hurricane Hugo: South Carolina forest land research and management related to the storm*. Gen. Tech. Rep. SRS-5. Asheville, NC: U.S. Department of Agriculture, Forest Service, Southern Research Station: 380–384.
- Zeng, H.; Peltola, H.; Talkkari, A. [and others]. 2004.** Influence of clearcutting on the risk of wind damage at forest edges. *Forest Ecology and Management*. 203(1–3): 77–88.

Economic Impacts of Hurricanes on Forest Owners

Jeffrey P. Prestemon and Thomas P. Holmes

Jeffrey P. Prestemon and **Thomas P. Holmes**, research foresters, USDA Forest Service, Southern Research Station, Research Triangle Park, NC 27709.

Abstract

We present a conceptual model of the economic impacts of hurricanes on timber producers and consumers, offer a framework indicating how welfare impacts can be estimated using econometric estimates of timber price dynamics, and illustrate the advantages of using a welfare theoretic model, which includes (1) welfare estimates that are consistent with neo-classical economic theory, and (2) wealth transfers among various market participants that can be evaluated. Timber producers in the Southern United States are faced with the regular risk of damages from intense hurricanes. Individual events can kill several million cubic feet of standing timber, with attendant losses for forest owners. One result of using a welfare theoretic model that is not apparent using simpler models is that timber producers with undamaged timber suffer economic losses in the short term because of a price depression, and they may be compensated in the long term by an enhancement of market prices owing to the loss of standing inventory. Catastrophic storms induce losses to timber producers holding damaged timber owing to quality degrade, price depression, and the inability to salvage all of the damaged timber. To minimize decay-related losses, owners of damaged timber should salvage as quickly as possible and favor salvage of higher value trees. Owners of undamaged timber should delay harvesting until salvage wood is exhausted from the market. Evidence suggests that timberland investors under hurricane threat could benefit by diversifying their holdings geographically, favoring areas far enough from coastal counties to minimize catastrophic losses from such storms but close enough to benefit from market-level price enhancements resulting from regional inventory losses.

Keywords: Economic welfare, Hurricane Hugo, Hurricane Katrina, timber salvage, tropical cyclone.

Introduction

This paper provides a description of the hurricane process in the United States in the context of economic impacts on forest land owners, presents the welfare theoretic model used to quantify timber market impacts, describes and compares the impacts of a few large and recent hurricanes on timber markets in the South, and concludes with some recommendations for landowners based on the research. This section focuses on measurement of catastrophic storm impacts on landowners.

More than 150 hurricanes have struck the U.S. Atlantic and Gulf of Mexico coasts during the past century, and these storms have caused economic damages totaling billions of dollars (Blake and others 2007). Human loss of life and suffering, destruction of housing, and disruptions in economic activities are the most obvious impacts of catastrophic storms, and recent, large hurricanes are proof of their ability to economically and politically transform affected regions. States vulnerable to the most intense storms include Florida, Texas, North Carolina, and South Carolina, but all States in the South and some States in the mid-Atlantic region and the Northeastern United States are also vulnerable to hurricanes.

Less appreciated, perhaps, are the effects that catastrophic storms have on forests and the people who own them. The effects of hurricanes on landowners are a complex function of many factors, including storm severity (windspeeds), prior rainfall activity (whose effect in turn is modified partially by soils), the strength of the timber market, tree species affected, and timber decay rates. Overall effects on landowners from hurricanes depend on hurricane frequencies and intensities. Given these variables affecting damages, the long-term effect of hurricanes will depend on long-term trends in climate and the timber market.

Research has shown that individual storms can create forest damages into the billions of dollars, and those damages create widespread wealth redistributions. The timing, scale, and implications of these losses and benefits have been the subject of research by the authors of this paper and by others. We have learned that measuring the impacts

Table 1—Hurricane landfalls, 1851–2006, and timber growing-stock volumes and production, 2002

State	All categories (1-5)	Major hurricanes (3-5)	Standing growing-stock volume, 2002 <i>Million ft³</i>	Timber, production 2002 <i>Thousand ft³</i>
Florida	113	37	15,366	560,475
Texas	60	19	12,939	769,501
Louisiana	52	20	18,844	958,981
North Carolina	50	12	32,742	957,675
South Carolina	30	6	17,702	682,901
Alabama	26	6	27,847	1,298,533
Georgia	23	3	31,704	1,447,941
Mississippi	16	9	20,611	1,149,880
Virginia	10	1	26,487	654,829
New York	12	5	21,831	141,068
Connecticut	11	3	3,192	11,691
Massachusetts	11	3	5,732	26,437
Rhode Island	9	4	496	1,742
Maine	6	0	20,891	441,729
Maryland	2	0	5,092	40,507
Delaware	2	0	695	7,654
New Jersey	2	0	2,819	10,549
New Hampshire	2	0	9,015	140,282
Pennsylvania	1	0	24,903	215,912

Note: State-by-State information about the number and intensity ranges of hurricanes, where they made landfall (1851–2006), and the total current (nondamaged) amount of growing stock and timber production by State (for 2002) are given. Hurricane intensities are represented using Saffir-Simpson categories.

Sources: Blake and others (2007, p. 18); Smith and others (2004).

on landowners can be accomplished using standard economic concepts of supply and demand in combination with econometric analysis of timber price dynamics following a catastrophic event. This approach is consistent with welfare economic methods described by Just and others (1982) and as applied to forest impacts by Holmes (1991). These concepts have been used by the authors to measure the effects of Hurricane Hugo on prices, producers, and consumers (Prestemon and Holmes 2000, 2004). These techniques have also been used to quantify the timber market impacts of large-scale fires (e.g., Butry and others 2001, Prestemon and others 2006). The implications of these findings suggest that landowners can take steps before and after such events to reduce exposure to the risk process and to mitigate damages when subjected to it.

The Biophysical Risk Process of Atlantic Basin Hurricanes in the United States

This section provides a discussion of biophysical risk processes associated with timberland ownership in the Eastern and Southern States of the United States. Atlantic hurricane arrival rates are available from the National Oceanic and Atmospheric Administration, which are reported here to provide the scope of the issue for forest landowners. Table 1 and Figure 1 show the number of hurricanes, by Saffir-Simpson scale category, striking each State in the Atlantic Basin of the United States, 1851–2004. Table 1 can be used to infer the probability of a hurricane striking a specific State by dividing the number of years represented by the number of landfalls (although a spatially weighted probability listing would look different). This table shows that there is a coincidence of high hurricane frequency and high timber volumes. This coincidence is apparent when the

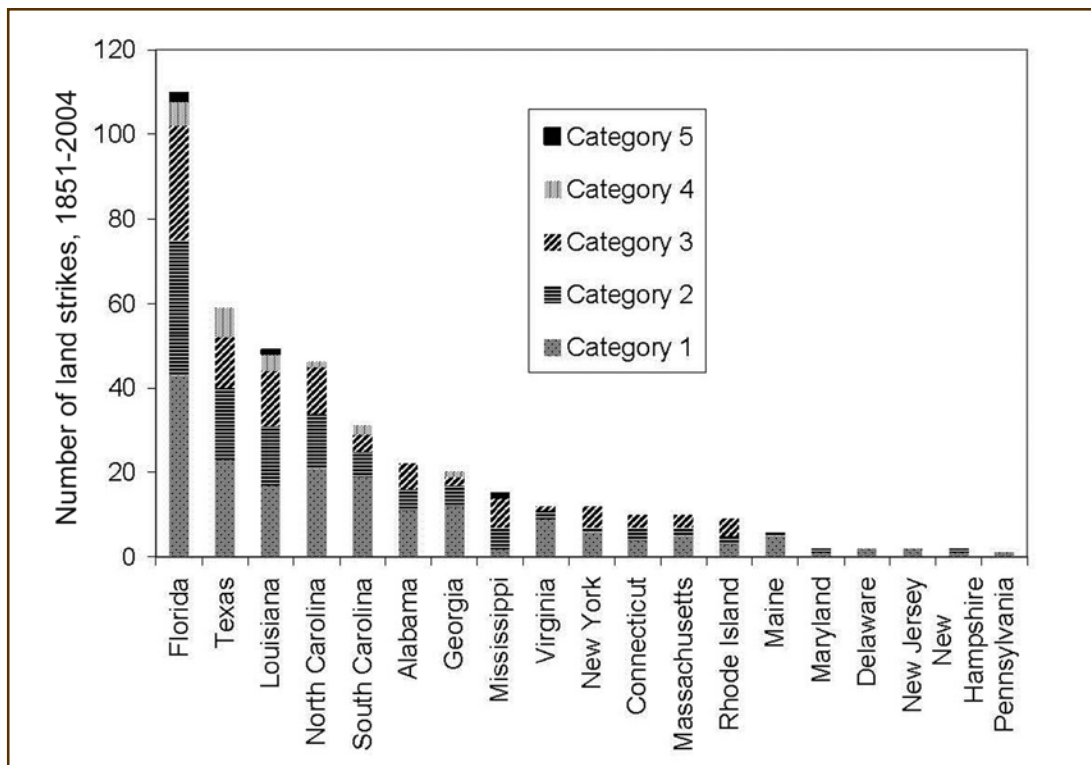


Figure 1—Atlantic hurricane strikes, 1851–2004, by State by Saffir-Simpson Category. Source: National Oceanic and Atmospheric Administration (2006).

States are ranked by hurricane landfall. The States with the greatest number of hurricanes are Florida, Texas, Louisiana, and, then, North and South Carolina. The strongest timber markets are found along the gulf coast, so the southern timber resource is particularly threatened by severe losses from large-scale wind events. In other words, timber owners in these high-frequency States are at particularly high risk of timber loss. See Stanturf and others (2007) for additional details about timber and hurricane frequencies and the United States Department of Commerce, National Hurricane Center (2007) for information on hurricane return intervals.

Data from the National Oceanic and Atmospheric Administration (2006) show that the number of hurricanes in the United States has recently demonstrated an upward trend. These data are consistent with Emanuel (2005) who indicated that hurricane intensities in many parts of the world appear to have risen over the past several decades. Both of these trends are consistent with some predictions of anticipated effects of climate change (e.g., Knutson and

Tuleya 2004) and with recent global ocean temperature rises (Barnett and others 2001). Whether or not the recent increase in hurricane activity is due to climate change (Gray 1984a, 1984b; Gray and others 1996) or primarily associated with multidecadal Atlantic Ocean sea surface temperature oscillations is still being debated. What is clear is that the Southern United States is facing a period in which substantial damage to timber resources from hurricanes can be anticipated, along with the associated consequences for forest landowners.

Timber Market Dynamics Following Hurricanes

This section provides information on (1) timber market shifts following natural disturbances, (2) resulting timber price movements through time, (3) welfare movements through time, and (4) salvage recovery values following natural disturbances. This will provide the reader with an overall picture of timber market behaviors and offer intuition about expected price movements and production

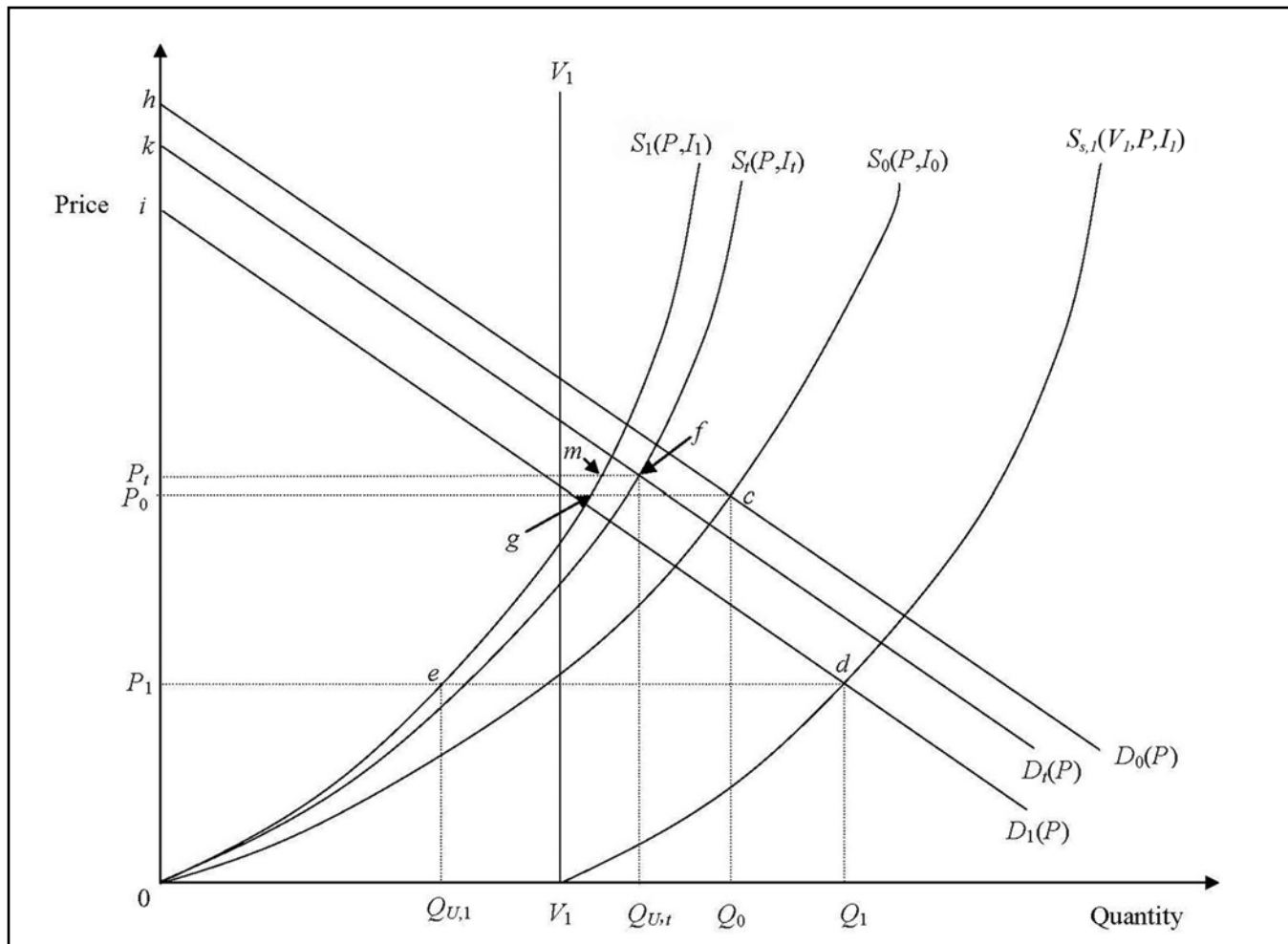


Figure 2—A representation of the timber market following a natural disaster such as a hurricane. The primary effect of hurricane damage to timber is to temporarily shift supply outward (from S_0 to $S_{s,1}$) during salvage and then shift back to S_1 due to salvage exhaustion and inventory loss. As inventory (I) regrows, supply shifts outward toward S_0 , and an intermediate position may be S_t . Demand, initially at D_0 , may shift backward to D_1 because of mill closures and higher market prices; intermediate demand level is at D_t during inventory regrowth. Price paths over time can be traced to these market shifts. Lower-case letters have been added at intersection points to facilitate detailed discussion in the text.

shifts in the aftermath of large-scale catastrophes affecting timber.

Graphical Overview of Market Shifts

Following a large hurricane (or any natural disaster), a timber market may undergo substantial changes in supply and demand. In Figure 2, supply of timber is represented as S_0 initially and is a function of price (P) and available inventory (I_0). Demand, also a function of price, is the curve sloping down from the left, and initial levels are represented by the curve D_0 . The initial (prestorm) price is designated as P_0 , and quantity is Q_0 . Following the storm, the timber

supply curve shifts inward to S_1 due to a reduction in available standing live inventory of undamaged timber (I_1). However, in the immediate aftermath of the storm, a pulse of timber salvage, V_1 , enters the market. This supply is zero when price is zero—i.e., it is a single point—but jumps to a large positive amount when price exceeds zero (Holmes 1991; Prestemon and Holmes 2000, 2004). In other words, the supply curve parallels the horizontal axis between 0 and the quantity V_1 . Any stand with fatally damaged timber with nonzero stumpage value is part of salvage supply. The combination of the inventory effect and the salvage effect is

to create a total market supply of $S_{s,1}$. Again, as in the case of the salvage supply, $S_{s,1}$ consists of a single point at (0,0) but jumps to V_1 when price slightly exceeds zero. During this salvage period, the equilibrium price is P_1 , lower than the prestorm price. When the pulse of salvaged timber is exhausted, the supply curve reverts to S_1 , with a higher price (P_1) than prior to the storm. As inventory grows over time, the supply curve gradually shifts back out to the original position of S_0 , achieving the original price and quantity at equilibrium. At that point, assuming no investment shifts owing to the storm, the effects of the hurricane disappear from the market.

In addition to impacts on timber supply, hurricanes might also impact timber demand. Many mills were closed because of either hurricane damage to mill facilities or anticipated long-term timber shortages following salvage operations after the passage of Hurricane Hugo. Syme and Saucier (1992) uncovered some evidence of short-term mill closures. In that case, demand might shift back (to D_1), as capital is reallocated to other, undamaged regions or out of the wood processing sector. The degree of backward shift in demand identified by Prestemon and Holmes (2004) was slight. Such a backward demand shift tended to dampen any price swings following Hugo. However, it could be that, with time, demand expands in response to timber inventory regrowth, allowing for prices that are not as low (e.g., P_1) as they would be if demand did not respond.

Timber Price Movements Through Time

Timber prices following a hurricane proceed through three phases: (1) price depression, (2) price enhancement, and (3) the gradual return of timber prices to prestorm levels, as implied by the discussion of the graphical representation of the hurricane's impact on a timber market. First, immediately following the storm, a price depression occurs, as was identified by Yin and Newman (1999) and Prestemon and Holmes (2000) following Hurricane Hugo. The finding of a price depression is consistent with what Holmes (1991) found in the case of southern pine beetle (*Dendroctonus frontalis* Zimmermann), and in all cases it is due to timber salvage activity, which drives down the market price owing to the supply expansion.

Prestemon and Holmes (2000) also found that there was a second stage involving a higher set of prices for timber products owing to the shortage of timber inventory following Hugo's destruction. This is the enhancement effect identified by them statistically, consistent with theory and with local markets where timber is expensive to move. Such an effect has been observed in other circumstances, as well (Berck and Bentley 1997, Olson and others 1988). In the third stage, timber returns to the prestorm level, when the inventory returns to normal levels.

Figure 3 illustrates timber price dynamics following a large-scale natural catastrophe. This figure shows a brief, negative price spike for timber because of salvage, a longer term price enhancement owing to inventory shortages, and then a gradual price reduction to precatastrophe levels as inventory regrows. Both a timber price index (where the precatastrophe timber is normalized at an index value of 100) and a timber inventory index (where the precatastrophe inventory volume is normalized at an index value of 1.00) are shown, indicating that 25 percent of timber inventory is killed. The figure is built upon assumptions of a constant demand elasticity with respect to timber price of -0.5 and constant supply elasticities with respect to price and inventory of 0.3 and 1.0, respectively. (These elasticities represent the percentage change in timber supplied to the market, given a 1-percent change in price or inventory volume, respectively). It also assumes that (1) 30 percent of timber killed is salvaged, (2) it takes 4 quarters (a quarter is 3 consecutive months) to exhaust the salvage, (3) the salvage quantity is highest immediately following the event and tapers off linearly following the event, and (4) the salvage quality discount factor is 5 (i.e., a unit of salvage timber has a quality discount of 80 percent).

Prestemon and Holmes (2000) conducted an intervention analysis of southern pine sawtimber and pulpwood stumpage (timber) prices, modeled after a similar analysis conducted by Holmes (1991). The approach was to model timber prices as autoregressive-integrated-moving average processes, including an intervention component that captured the effect of the hurricane on South Carolina timber prices. Comparison of the South Carolina price processes to price processes for the same product in other locations

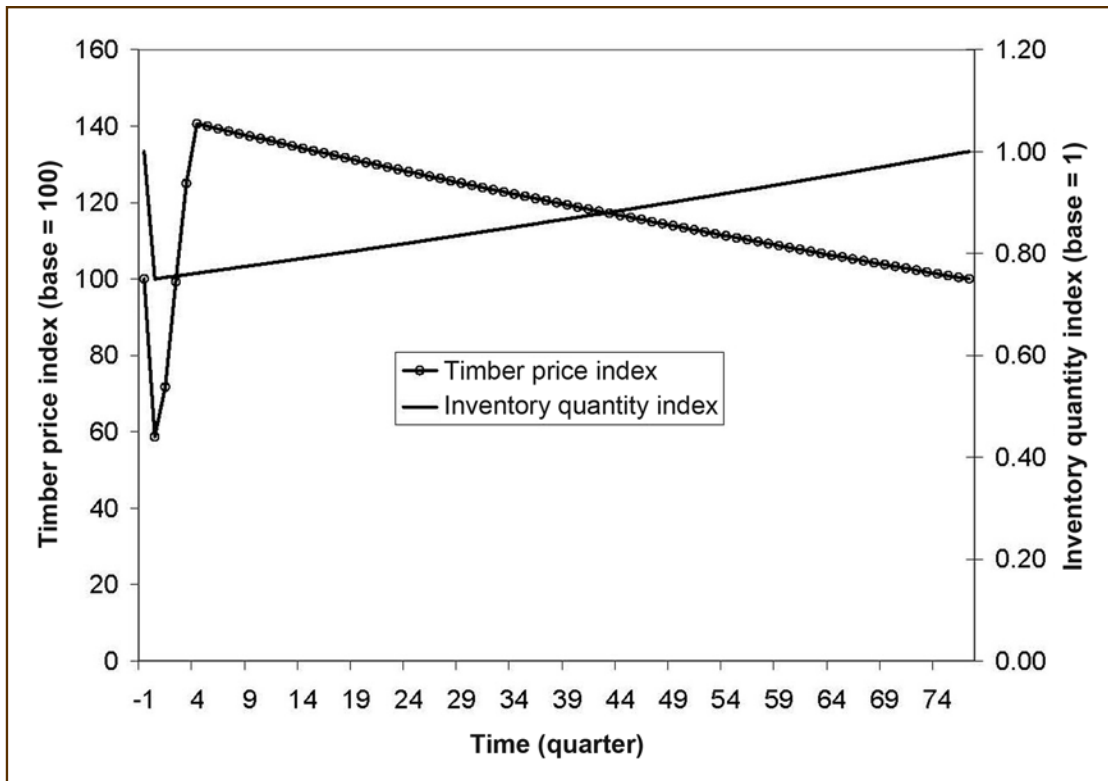


Figure 3—A hypothetical price path over time for timber following a large-scale natural catastrophe. In this figure, prices in the quarter immediately preceding the catastrophe (quarter -1) are at 100 and inventory is at 1.00. In the quarter of the catastrophe, inventory drops to about 0.75 and prices fall to 60 as salvage volume moves into the timber market. With salvage exhaustion, the inventory shortage effect is felt in timber prices, as they are temporarily elevated to as high as about 140. With time, prices recover to their original level as inventory returns to its initial volume.

in the South allowed identification of the full price effect of the storm, in both the short and long terms. As Holmes (1991) pointed out, statistical identification of the market price effects of such an event requires a sufficiently long series before and after the modeled event in order to identify derivative patterns in the prices owing to the event. Prestemon and Holmes (2000) found in their intervention analysis that salvage induced an average 30-percent decline in green (undamaged) pine pulpwood and pine sawtimber stumpage prices during the salvage period and that the inventory loss induced a persistent 10- to 30-percent enhancement (increase) in those prices after salvage was exhausted. This finding relied on tests that confirmed the nonstationarity of timber prices in South Carolina and identification of significant co-integration relations between South Carolina prices and those of other States. Nonstationarity of the State's timber prices has been also confirmed using longer

time series, inclusion and exclusion of time trends, alternative deflation methods, and alternative tests of stationarity by Prestemon and others (2004). Using a different approach that relied on an assumption of trend-stationary timber prices in South Carolina, Yin and Newman (1999) identified no long-run price enhancement in South Carolina.

Welfare Movements through Time

This section describes how timber damages, salvage, and price shifts result in effects on different segments of the timber market. Results from published research are used to illustrate these shifts. Prestemon and Holmes (2004) traced out the economic equity (welfare, or economic surplus) impacts of hurricanes and similar large-scale catastrophes in an analysis that is based on methods applied by Holmes (1991) and those of Just and others (1982). Thurman and Easley (1992) showed how, when an event occurs in a

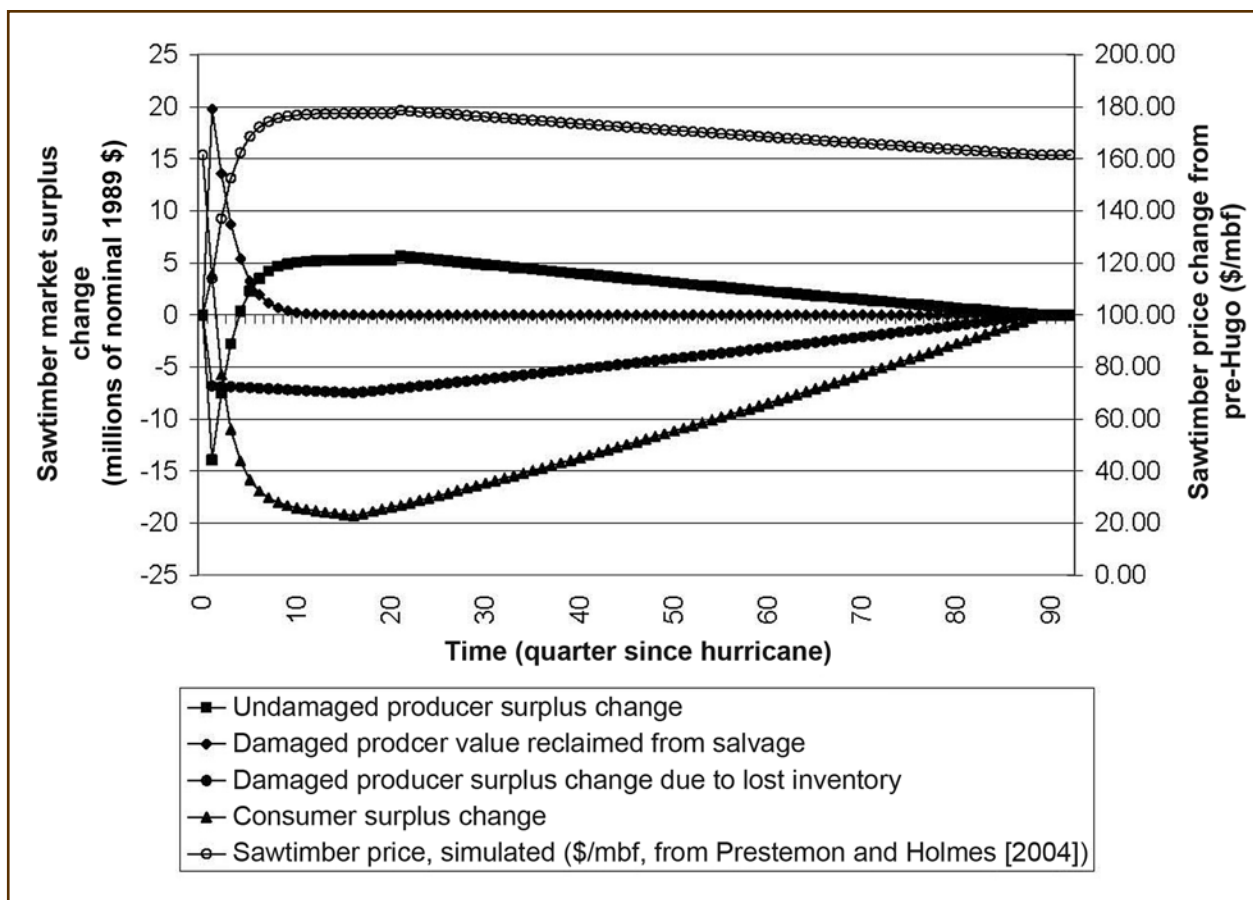


Figure 4—Identified price and welfare shifts in the Timber Mart-South (Norris Foundation, 2004–2006) Region 2 market, South Carolina, immediately before and after Hurricane Hugo, for southern pine sawtimber, by quarter. Figure based on the base case scenario data from Prestemon and Holmes (2004). [mbf = million board feet].

primary product market (such as timber), a welfare analysis of the economic impacts of the event on the primary market will capture the effects on all higher levels of processing deriving from that market. Given this, in our study, the full timber market economic impacts can be partitioned across owners of damaged timber, owners of undamaged timber, and timber consumers. This requires definition, however. Consumer surplus is defined, in Figure 2, as the area below the demand curve, above the equilibrium market price, and to the left of the equilibrium quantity supplied to the market. For example, before the hurricane, the consumer surplus is area P_0ch , while in the immediate aftermath of the storm, it was area P_1di . Producer surplus of undamaged producers is the area above and to the left of the supply curve and below price. Before the storm, producer surplus

was P_0c0 . In the immediate aftermath of the storm, producers of undamaged timber receive surplus represented by the area P_1e0 , but as timber salvage is exhausted, say in period t , this subset of producers actually gains, with their surplus valued as $0fmP_t$. The producer surplus gained by damaged producers upon salvage of their timber by the storm is equivalent to salvage volume (e.g., V_1) times the price received during the salvage period (P_1). This is the area represented by the rectangle P_1dQ_10 . In the immediate aftermath of the storm, then, these undamaged producers, because they cannot produce undamaged timber, also lose an area represented by a curved shape bounded by 0 , S_1 , S_0 , and demand curve, D_1 , the shape represented by the shape $0cgt$.

Figure 4 illustrates how changes in southern pine timber market economic surplus, salvage revenues, and timber

price varied over time following hurricane Hugo, as identified by Prestemon and Holmes (2004). In their simulations, inventory regrowth is projected, based on Forest Inventory and Analysis surveys in 1993 and 1999 in South Carolina. The rate of regrowth is a key determinant of the quantity and timing of post-hurricane welfare impacts. The figure shows that consumer welfare increased briefly following the hurricane because of lower prices and greater quantity consumed. Undamaged producers were briefly harmed from this salvage, but damaged producers captured some value for a few quarters. Consumers were harmed over the long term, undamaged producers gained over the long term, and damaged producers lost in the long term. In this figure, prices were determined to return to prestorm levels in the sawtimber market by 2012, about 90 quarters (23 years) after the storm. A similar price and welfare path was also traced out by Prestemon and Holmes (2004) for the southern pine pulpwood market there.

As shown, all of these losses and gains proceed into the future until the timber inventory returns to the prestorm inventory volume and timber production and price levels. The long-term discounted economic surplus lost and gained by the various market participants is tracked by tallying these changes for all periods into the future, discounting the values using an economic discount rate to the present. In a later section, we describe those changes for Hurricane Hugo in a table.

Salvage

This section describes how the value of salvage is calculated and some of the factors influencing the value recovered by salvaging timber. Readers interested in more detail about the economics of the salvage decision should review Haight and others (1996), whereas those interested in operational aspects of salvage should see Stanturf and others (2007). Our research and research conducted by others (e.g., Lowell and others 1992), indicate that the value of salvage depends on several factors: (1) the severity of initial damage (function of wind, prestorm rain); (2) the amount of timber decay, which is a function of tree species, the post-event ambient air temperature, the post-event ambient humidity, the dimensions of the materials, and time; (3) the aggregate

volume of salvage entering the timber market; and (4) market supply and demand sensitivities with respect to price and market supply sensitivity with respect to inventory. The species, temperature, humidity, log dimension, and time all govern the current value of the salvage discount factor, K . K is used to translate the salvage volume into a value-equivalent “green” timber volume for market valuation purposes (see Holmes 1991):

$$Q^S = Q^D K^{-1},$$

where Q^D is the raw quantity damaged or killed and Q^S is the value-equivalent of the timber in “green” timber volume. As K increases, the value-equivalent reduction in timber volume increases.

What the research implies is that hurricanes (which occur generally in warm, humid areas of the United States and cause a great amount of physical damage to the internal log structure from wind) produce values of K that are large. Prestemon and Holmes (2004) found that K likely averaged about 4.5 for southern pine sawtimber following Hugo and 6.6 for southern pine pulpwood. Events such as fires (e.g., Lowell and others 1992) and southern pine beetle outbreaks (e.g., de Steiguer and others 1987) produce smaller values for K (in the range of 1.1 to 1.5 in the months immediately following the event).

Forest and Timber Impacts of Recent Hurricanes

The need for landowners and policymakers to plan for effects of increased hurricane activity is discussed in this section, and comparative information about damage levels of recent vs. older hurricanes is provided. Recent hurricanes, including Ivan and Frances in 2004, and Katrina and Rita in 2005, provide evidence of the timber market impacts of these events, including their impacts on landowners. These can also be compared with the impacts of older hurricanes, such as Hugo in 1989 and Camille in 1969, to help us understand how changes in timber prices as well as volumes affected may be leading to rising economic impacts. Below, we focus on the kinds of losses experienced by owners of timber in terms of hardwood and softwood, pulpwood, and sawtimber-product categories.

Table 2—Timber damage volume and dollar impacts from six severe hurricanes affecting selected States in the United States Atlantic Basin

	Units	Camille, 1969 ¹	Hugo, 1989 ¹	Frances, 2004 ²	Ivan, 2004 ²	Katrina, 2005 ¹	Rita, 2005 ²
Softwood timber mortality							
South Carolina	million ft ³		1,008				
Florida	million ft ³			87	208		
Mississippi	million ft ³	216				619	
Louisiana	million ft ³					287	296
Alabama	million ft ³				603	126	
Texas	million ft ³						239
Hardwood timber mortality							
South Carolina	million ft ³		319				
Florida	million ft ³			58	94		
Mississippi	million ft ³	74				426	
Louisiana	million ft ³					193	177
Alabama	million ft ³				414	91	
Texas	million ft ³						293
Total timber mortality							
South Carolina	million ft ³		1,327				
Florida	million ft ³			145	302		
Mississippi	million ft ³	290				1,044	
Louisiana	million ft ³					480	473
Alabama	million ft ³				1,017	216	
Texas	million ft ³						532
Total, measured affected States, all species	million ft ³	290	1,327	145	1,319	1,740	1,005
Softwood portion of damaged volume	Percentage	74	76	60	61	54	53
Timber value damaged (price × quantity)							
Sawtimber value lost	Millions of 2005 dollars	177	494 ³	153	2,094	1,600	504
Pulpwood value lost	Millions of 2005 dollars	25	136 ³	9	83	113	32
All products	Millions of 2005 dollars	202	630 ³	162	2,177	1,713	536
Timber economic surplus							
Producer surplus lost, all owners and periods	Millions of 2005 dollars		121 ³				
Consumer surplus lost, all periods	Millions of 2005 dollars		1,402 ³				
All market groups	Millions of 2005 dollars		1,523 ³				

¹ Final USDA Forest Service Forest Inventory and Analysis estimates of volumes of timber mortality. Economic impacts in dollars based on these final estimates.

² Initial USDA Forest Service Forest Inventory and Analysis estimates of volumes of timber mortality. Economic impacts in dollars based on these initial estimates.

³ Dollar values shown for Hurricane Hugo are for softwood timber only.

Sources: Surplus values for Hurricane Hugo are from Prestemon and Holmes (2004); volumes for Camille are from Van Hooser and Hedlund (1969); pine values are from Mississippi Forestry and Agricultural Experiment Station (2006); baldcypress and hardwood values are from and Louisiana Department of Agriculture (1969); volumes for Frances, Ivan, Katrina, and Rita are from USDA Forest Service Forest Inventory and Analysis (2004a, 2004b, 2005a, 2005b), respectively; and values are from Norris Foundation (2005–2006).

The 2005 hurricane season was the worst, in terms of timber damages, in a generation—much bigger than the largest in the last two decades, Hurricane Hugo (Table 2) (USDA Forest Service, Forest Inventory and Analysis 2005a, 2005b). Hurricane Katrina damaged 1.74 billion cubic feet of timber, and about 41 percent of the volume was hardwood. Other estimates, not reported here, put long-term damages much higher than this. Hurricane Rita added to those damages, so when combined, these two storms damaged at least twice as much timber in the affected States of Alabama, Louisiana, Mississippi, and Texas as was damaged by Hugo in South Carolina in 1989 (although those South Carolina damages exclude damages in North Carolina, another affected State).

The market value of these timber inventory losses for Katrina and Rita was quantified in a special report provided to the Forest Service, expressed in terms of 2005 dollars to account for inflation. For this review, we also quantified the same values for Hurricane Frances (which affected Florida) and Hurricane Ivan (which affected both Florida and Alabama) in 2004. These economic effects are reported at the bottom of Table 2, principally in market-value terms. In Table 2, we also include the economic effects of two other large Hurricanes, Camille (1969) and Hugo (1989). At the bottom of Table 2, we include information for Hurricane Hugo, addressing both market value and economic surplus, as calculated by Prestemon and Holmes (2004). Market values can be termed timber value losses, whereas economic surpluses can be termed economic losses. We note that the welfare impacts for softwood calculated by Prestemon and Holmes (2004) depend on assumptions regarding market supply and demand parameters and timber regrowth rates, and they depend on the validity of the price paths identified by Prestemon and Holmes (2000). Prestemon and Holmes (2004) conducted Monte Carlo and sensitivity analyses on these damages, which report ranges of possible impacts. The welfare amounts shown in Table 2 for Hugo are average estimates.

Hurricane Frances is the smallest hurricane impact shown in the table, with 145 million cubic feet of damage. Camille damaged twice as much timber as Frances, but it still is small compared to the rest of the hurricanes shown

in the table. For example, Hurricane Ivan created timber damages that are comparable to those measured for Hugo. Rita created damages that totaled a billion cubic feet, about 75 percent the size of Hugo. The amount of softwood lost in these storms varied, mainly according to the amount of pre-existing softwood in the timber inventory. In the South, the amount generally exceeds 50 percent.

The values of timber damaged or killed in the storm are variable, as documented in Table 2. One surprising finding from this comparison is that Ivan's timber damages exceed the value of those found for Katrina. This is explained by the substantially higher timber prices in effect in Florida and Alabama prior to the hurricane, in comparison with the timber mainly damaged in Mississippi and Louisiana. It is also partially explained by the former hurricane's higher proportion of damage to softwood and sawtimber-sized trees. Still, when Rita's damages, which totaled over \$536 million, are added to those of Katrina, those two storms damaged volumes that are more than twice those of Hugo or Ivan.

Hugo's timber value lost in the southern pine market, measured as price times quantity, was \$630 million. The analysis by Prestemon and Holmes (2004) showed, however, that the market impacts in welfare terms were 2.4 times larger. This magnitude of difference between market value and welfare impact should be viewed with caution when attempting to translate between market-value losses to welfare losses for other storms or catastrophic events. Even for Hugo, this translation depended on many assumptions, especially regarding (1) timber salvage rates, market supply and demand sensitivities; (2) rates of timber inventory regrowth; (3) the reality of a long-term inventory-induced price enhancement; and (4) the scale of timber market demand and supply. Nonetheless, a rough calculation could be attempted that would suggest the economic surplus impacts of those other storms are much larger—maybe two to three times larger—than the timber value impacts shown. In short, recent hurricanes have created market losses totaling into the many billions of dollars. As Prestemon and Holmes (2004) and Holmes (1991) pointed out, these losses represent a net redistribution of wealth in the market,

in favor of undamaged producers and to the detriment of consumers and damaged producers.

There are obviously other potential outcomes of hurricanes on the broader economy as they relate to the timber market. Structure (e.g., housing) losses are quite high when large events such as Hurricane Katrina sweep through heavily populated areas. The National Oceanic and Atmospheric Administration (2006) indicated that hurricanes Katrina, Rita, and Wilma in 2005 combined to create nearly 2.8 million insurance claims, totaling \$40 billion in insured losses. Data provided by the American Red Cross, as cited by the National Association of Home Builders (2005), compiled preliminary estimates indicating that Hurricane Katrina damaged 275,000 homes in the Gulf States of Louisiana, Mississippi, and Alabama, 10 times the second-largest loss in homes, which was caused by Andrew in 1992 in south Florida. The National Association of Home Builders (2005) report stated that Katrina, coupled with Rita and Wilma (in Florida), would drive up prices for southern pine framing lumber, plywood, and other sheathing products. This price effect on forest products should filter back to the timberland, helping to support prices in the Southern United States during the reconstruction phase. The implication here is that landowners whose timber was unaffected by the storms should enjoy some price support, increasing the chances for a post-hurricane price enhancement, even if that enhancement does not emanate directly from lost timber inventory in the region.

Management Implications

We now discuss the future of hurricane activity in the United States and the implications of the existence of hurricane risk on land management strategies, with a focus on timber salvage. What we can glean from the previous discussion is that the impacts of hurricanes on landowners will be partitioned according to the location of the timberland. Hence, owners closer to the impact zone—typically, closer to the ocean—will face a higher likelihood of timber damages and long-term negative impacts. Those farther from the coast may face lower impacts and a greater chance that they could enjoy a long-term price enhancement owing to timber inventory losses and, potentially, output effects on

the construction market. Due at least partly to the species mixes and particular species vulnerabilities, it appears also that owners of softwood timber may face greater economic risks than owners of hardwood timber, but this is a hypothesis that remains to be tested in the literature. Hardwood damages frequently occur as degrade, rendering the stand lower in value in the long term and potentially vulnerable to a higher rate of mortality (Sheffield and Thompson 1992).

As we appear to be in a period (or riding a trend) of higher hurricane activity, we might expect that the frequency and magnitude of large-scale catastrophic hurricanes will increase or remain high for several years or decades. In response to damage, timberland owners would do well to prepare for such storms by assessing the value of the timber before the storm. Creditable casualty losses require that the current basis of affected timber be assessed. Following such storms, timberland owners whose timber is unaffected would benefit from withholding their mature timber from the timber market until after salvage material has been recovered from damaged forests and then consumed at area mills. As well, owners of damaged timber should endeavor to quickly arrange for the salvage of their timber, owing to the high likelihood of timber decay for killed timber. Here, some colloquial evidence suggests that hardwoods should receive lower priority, as they may remain alive and hence valuable for a longer period, compared to softwoods, which are more likely to die following a storm (Sheffield and Thompson 1992). Because of the rapid decay rate of killed timber, then, it is especially beneficial to quickly salvage such timber following the event, especially timber stocks with the least amount of damage, to justify salvage.

Government actions following catastrophic windstorms may have an effect on the value of salvaged timber. For example, timber salvage on publicly owned lands has a negative impact on private landowners but a positive impact on consumer welfare (Prestemon and others 2006). There are, however, government actions that can produce broader benefits. Governments can facilitate salvage activities by (1) rapidly clearing roads, (2) relaxing weight limits on roads to allow logging trucks to carry heavier loads, (3) permitting larger than normal log storage volumes at mills,

(4) subsidizing or providing tax breaks for mills to produce water storage facilities for logs, (5) aiding in post-hurricane damage assessment, and (6) assisting private landowners and nongovernmental organizations with salvage planning (Freeman 1996, Lupold 1996). However, we would caution that research is currently not available to help evaluate either the form or the scale of public interventions that would be economically or socially optimal.

Research Needs

We conclude our synthesis of the impacts of hurricanes on forest landowners with a discussion of the research needed to further advance our understanding of these impacts and to identify alternative strategies for coping with these storms. This assessment reveals a long list of potential research needs. A primary need in all timber market assessments of hurricanes is up-to-date and precise information on green timber supply, salvage supply, and demand function parameters. Our results for Hurricane Hugo depend critically on assumed market sensitivities, and conclusions about the ultimate economic (especially welfare) impacts of other events depend on similar assumptions that need to be evaluated. We would note that for published salvage studies (starting with Holmes 1991), assumptions were made about the perfect inelasticity of the salvage supply function. This function is unlikely to be perfectly inelastic (unresponsive to prices). Although sensitivity analysis is useful for establishing plausible bounds on potential economic impacts, up-to-date studies of southern pine supply and demand functions would reduce the need for making assumptions regarding market conditions. Additionally, new studies are needed to identify how hurricanes affect markets for products other than southern pine. A large component of total timber impact results from damages to hardwoods, yet hardwood markets are notoriously under-researched. Such studies could reveal not only the hardwood market economic impacts but also potentially identify new and innovative strategies that owners of hardwoods could apply before and after hurricanes and other catastrophic events.

Timber salvage is a means of recovering value following such storms, yet little is known about how various

factors affect the size of the timber salvage discount, particularly how it varies over time and among species. Such studies could provide valuable information regarding optimal salvage strategies following major hurricanes. Our economic calculations—and, hence, recommended salvage strategies—could be improved and changed with better information on this segment of the post-hurricane timber market.

Other analysts in these proceedings provide evaluations of the timber management consequences of holding timber assets that are subject to large-scale natural disturbances. However, research to date has not addressed whether long-term price enhancements emanating from a hurricane or other large natural disturbance can generate expected profits that are, in aggregate, greater than those expected in regions without such events. Timber losses occur in a subset of the timber market—consumers and damaged producers—but the gains could be significant for some landowners. Identifying the circumstances under which timberland owners gain, in aggregate, from these storms is an area worthy of further study.

Literature Cited

- Barnett, T.P.; Pierce, D.W.; Schnur, R. 2001.** Detection of anthropogenic climate change in the world's oceans. *Science*. 292: 270–274.
- Berck, P.; Bentley, W.R. 1997.** Hotelling's theory, enhancement, and the taking of the Redwood National Park. *American Journal of Agricultural Economics*. 79(2): 287–298.
- Blake, E.S.; Rappaport, E.N.; Jarrell, J.D.; Landsea, C.W. 2005.** The deadliest, costliest, and most intense United States tropical cyclones from 1851 to 2004 (and other frequently requested hurricane facts). National Oceanic and Atmospheric Administration Technical Memorandum NWS TPC-4. <http://www.nhc.noaa.gov/pdf/NWS-TPC-4.pdf>. [Date Accessed: July 13, 2006].

- Blake, E.S.; Rappaport, E.N.; Landsea, C.W. 2007.** The deadliest, costliest, and most intense United States tropical cyclones from 1851 to 2006 (and other frequently requested hurricane facts). [Updated 15 April 2007]. NOAA Technical Memorandum NWS TPC-5. 43 p. <http://www.nhc.noaa.gov/pdf/NWS-TPC-5.pdf>. [Date accessed May 17, 2007].
- Butry, D.T.; Mercer, D.E.; Prestemon, J.P. [and others]. 2001.** What is the price of catastrophic wildfire? *Journal of Forestry*. 99(11): 9–17.
- de Steiguer, J.E.; Hedden, R.L.; Pye, J.M. 1987.** Optimal level of expenditure to control the southern pine beetle. Res. Pap. SE-263. Asheville, NC: U.S. Department of Agriculture, Forest Service, Southeastern Forest Experiment Station. 30 p.
- Emanuel, K. 2005.** Increasing destructiveness of tropical cyclones over the past 30 years. *Nature*. 436: 686–688.
- Freeman, W.E. 1996.** Short-term planning and response to forest damage. In: Haymond, H.L.; Hook, D.D.; Harms, W.R., eds. Hurricane Hugo: South Carolina forest land research and management related to the storm. Gen. Tech. Rep. SRS-5. Asheville, NC: U.S. Department of Agriculture, Forest Service, Southern Research Station: 18–20.
- Gray, W.M. 1984a.** Atlantic seasonal hurricane frequency: Part 1. El Niño and 30 mb quasi-biennial oscillation influences. *Monthly Weather Review*. 112: 1649–1668.
- Gray, W.M. 1984b.** Atlantic seasonal hurricane frequency: Part 2. Forecasting its variability. *Monthly Weather Review*. 112: 1669–1683.
- Gray, W.M.; Sheaffer, J.D.; Landsea, C.W. 1996.** Climate trends associated with multi-decadal variability of intense Atlantic hurricane activity. In: Diaz, H.F.; Pulwarty, R.S., eds. Hurricanes, climatic change and socioeconomic impacts: a current perspective. Boulder, CO: Westview Press. 49 p. Chapter 2.
- Haight, R.G.; Smith, W.D.; Straka, T.J. 1996.** The economics of loblolly pine plantations under the risk of hurricane damage. In: Haymond, H.L.; Hook, D.D.; Harms, W.R., eds. Hurricane Hugo: South Carolina forest land research and management related to the storm. Gen. Tech. Rep. SRS-5. Asheville, NC: U.S. Department of Agriculture, Forest Service, Southern Research Station: 293–304.
- Holmes, T.P. 1991.** Price and welfare effects of catastrophic forest damage from southern pine beetle epidemics. *Forest Science*. 37(2): 500–516.
- Just, R.E.; Hueth, D.L.; Schmitz, A.S. 1982.** Applied welfare economics and public policy. Englewood Cliffs, NJ: Prentice-Hall, Inc. 491 p.
- Knutson, T.R.; Tuleya, R.E. 2004.** Impact of CO₂-induced warming on simulated hurricane intensity and precipitation: sensitivity to the choice of climate model and convective parameterization. *Journal of Climate*. 17: 3477–3495.
- Louisiana Department of Agriculture. 1969.** Louisiana timber products quarterly market report. 15(2): Available at <http://www.ldaf.state.la.us/multimedia/forestry/fpmud/quarterlyreports/originalreports/196924.pdf>.
- Lowell, E.C.; Willits, S.A.; Krahmer, R.A. 1992.** Deterioration of fire-killed and fire-damaged timber in the Western United States. Gen. Tech. Rep. PNW-GTR-292. Portland, OR: U.S. Department of Agriculture, Forest Service, Pacific Northwest Research Station. 27 p.
- Lupold, H.M. 1996.** Salvage of storm damaged timber. In: Haymond, H.L.; Hook, D.D.; Harms, W.R., eds. Hurricane Hugo: South Carolina forest land research and management related to the storm. Gen. Tech. Rep. SRS-5. Asheville, NC: U.S. Department of Agriculture, Forest Service, Southern Research Station: 21–27.
- Mississippi Forestry and Agricultural Experiment Station. 2006.** Forestry: timber price reporting for Mississippi: Mississippi timber price averages, 1957–1985. <http://msucare.com/forestry/prices/historic.pdf>. [Date accessed: August 14, 2006].

- National Association of Homebuilders. 2005.** Impact of Hurricane Katrina on building materials and prices. Press release. On file with: National Association of Homebuilders, 1201 15th St. NW, Washington, DC 20005.
- National Oceanic and Atmospheric Administration. 2006.** Economic statistics for NOAA, April 2006. 5th ed. Washington, DC: U.S. Department of Commerce. 70 p.
- Norris Foundation. 2004.** Timber Mart-South quarterly report. 2nd quarter, 2004. Athens, GA: University of Georgia. 16 p.
- Norris Foundation. 2005-2006.** Timber Mart-South quarterly price reports (various issues). Athens, GA: University of Georgia.
- Olson, K.W.; Moomaw, R.L.; Thompson, R.P. 1988.** Redwood National Park expansion: impact on old-growth redwood stumpage prices. *Land Economics*. 64(3): 269–275.
- Prestemon, J.P.; Holmes, T.P. 2000.** Timber price dynamics following a natural catastrophe. *American Journal of Agricultural Economics*. 82(1): 145–160.
- Prestemon, J.P.; Holmes, T.P. 2004.** Market dynamics and optimal timber salvage after a natural catastrophe. *Forest Science*. 50(4): 495–511.
- Prestemon, J.P.; Pye, J.M.; Holmes, T.P. 2004.** Temporal aggregation and testing for timber price behavior. *Natural Resource Modeling*. 17(2): 123–162.
- Prestemon, J.P.; Wear, D.N.; Holmes, T.P.; Stewart, F. 2006.** Wildfire, timber salvage, and the economics of expediency. *Forest Policy and Economics*. 8(3): 312–322.
- Sheffield, R.M.; Thompson, M.T. 1992.** Hurricane Hugo: effects on South Carolina's forest resources. Res. Pap. SE-284. Asheville, NC: U.S. Department of Agriculture Forest Service, Southeastern Forest Experiment Station. 51 p.
- Smith, W.B.; Miles, P.D.; Vissage, J.S.; Pugh, S.A. 2004.** Forest resources of the United States, 2002. Gen. Tech. Rep. NC-241. St. Paul, MN: U.S. Department of Agriculture, Forest Service, North Central Station. 137 p.
- Stanturf, J.A.; Goodrick, S.L.; Outcalt, K.W. 2007.** Disturbance and coastal forests: a strategic approach to forest management in hurricane impact zones. *Forest Ecology and Management*. 250: 119–135.
- Syme, J.H.; Saucier, J.R. 1992.** Impacts of Hugo timber damage on primary wood manufacturers in South Carolina. Gen. Tech. Rep. SE-80. Asheville, NC: U.S. Department of Agriculture, Forest Service, Southeastern Forest Experiment Station. 28 p.
- Thurman, W.N.; Easley, J.E., Jr. 1992.** Valuing changes in commercial fishery harvests: a general equilibrium derived demand analysis. *Journal of Environmental Economics and Management*. 22(3): 226–240.
- U.S. Department of Agriculture (USDA) Forest Service Forest Inventory and Analysis. 2004a.** Hurricane Frances preliminary timber damage estimate. [Excel spreadsheet]. On file with: Dennis Jacobs, Forest Inventory and Analysis, 4700 Old Kingston Pike, Knoxville, TN 37919.
- U.S. Department of Agriculture (USDA) Forest Service Forest Inventory and Analysis. 2004b.** Hurricane Ivan preliminary timber damage estimate. [Excel spreadsheet]. On file with: Dennis Jacobs, Forest Inventory and Analysis, 4700 Old Kingston Pike, Knoxville, TN 37919.
- U.S. Department of Agriculture (USDA) Forest Service Forest Inventory and Analysis. 2005a.** Hurricane Katrina preliminary timber damage estimate. [Excel spreadsheet]. On file with: Dennis Jacobs, Forest Inventory and Analysis, 4700 Old Kingston Pike, Knoxville, TN 37919.

U.S. Department of Agriculture (USDA) Forest Service

Forest Inventory and Analysis. 2005b. Hurricane Rita preliminary timber damage estimate. [Excel spreadsheet]. On file with: Dennis Jacobs, Forest Inventory and Analysis, 4700 Old Kingston Pike, Knoxville, TN 37919.

U.S. Department of Commerce, National Hurricane

Center. 2007. Return periods. <http://www.nhc.noaa.gov/HAW2/english/basics/return.shtml>.

Van Hooser, D.; Hedlund, A. 1969. Timber damaged by Hurricane Camille in Mississippi. Res. Note SO-96. New Orleans: U.S. Department of Agriculture, Forest Service, Southern Forest Experiment Station. 5 p.

Yin, R.; Newman, D.H. 1999. An intervention analysis of Hurricane Hugo's effect on South Carolina's stumpage prices. *Canadian Journal of Forest Research*. 29(6): 779–787.

This page is intentionally left blank

AIR and WATER

Case Studies

This page is intentionally left blank

Using Remotely Sensed Data and Elementary Analytical Techniques in Post-Katrina Mississippi to Examine Storm Damage Modeling

Curtis A. Collins, David L. Evans, Keith L. Belli, and Patrick A. Glass

Curtis A. Collins, research associate II, and **David L. Evans**, professor, Department of Forestry, Mississippi State University, Mississippi State, MS 39762; **Keith L. Belli**, Head, Department of Forestry, Wildlife and Fisheries, University of Tennessee, Knoxville, TN 37996; and **Patrick A. Glass**, Director of Operations, Mississippi Institute for Forest Inventory, Mississippi Forestry Commission, Jackson, MS 39201.

Abstract

Hurricane Katrina's passage through south Mississippi on August 29, 2005, which damaged or destroyed thousands of hectares of forest land, was followed by massive salvage, cleanup, and assessment efforts. An initial assessment by the Mississippi Forestry Commission estimated that over \$1 billion in raw wood material was downed by the storm, with county-level damage percentages ranging from 50 percent to 60 percent across Mississippi's three coastal counties. Remotely sensed data were used to provide a more complete picture of the damage inflicted by Katrina. Moderate (56- to 29-m) and high (1- to 0.3-m)-resolution data were acquired from spaceborne and airborne platforms in natural color and MultiSpectral (MS) formats. Transformed data such as Normalized Difference Vegetation Index (NDVI) and Normalized Difference Moisture Index (NDMI), along with damage estimates obtained by interpreting aerial photography, were also used as variables in a linear modeling process. This continuous damage prediction process demonstrated the effect of incorporating forest condition thematic information, prestorm moderate-resolution imagery with transforms, and poststorm moderate-resolution imagery with transforms. The resulting models, all of which used a large number of regressors, had overall fit values of $R^2_{\text{adj}} = 0.708$ and $\text{RMSE} = 0.130$ with all variable types used, $R^2_{\text{adj}} = 0.492$ and $\text{RMSE} = 0.172$ with all variables except the

forest condition data, and $R^2_{\text{adj}} = 0.599$ and $\text{RMSE} = 0.153$ with all variables except the poststorm imagery data.

Keywords: AWiFS, damage modeling, forest damage, hurricane damage, Katrina damage, timber damage.

Introduction

Overview

Hurricane Katrina made landfall in Mississippi near the outlet of the Pearl River on August 29, 2005, as a category 3 storm on the Saffir-Simpson scale (Knabb and others 2005). Loss of life and damage to property were catastrophic, as New Orleans was flooded, and many towns and cities along the Louisiana and Mississippi Gulf Coasts were destroyed or severely affected. Rural areas whose economy depends on agriculture and forest industry were devastated also. Accordingly, preliminary damage estimates obtained through aerial surveys of the affected region by the Mississippi Forestry Commission (MFC) exceeded \$1 billion in damaged wood and timber stumpage. These estimates underscore the need for more continuous damage estimates that can be developed when remotely sensed, storm, and pre-existing thematic data are employed in the modeling process.

Moderate-resolution remotely sensed data, from sources such as Landsat, have been used in modeling various forest parameters related to timber harvesting (Healey and others 2005), canopy closure (Butera, 1986, Cohen and others 2001, Larsson 1993), and other forest attributes (Cohen and others 2001, 2003). Cohen and others (2001) modeled percentage green canopy cover in a predominantly evergreen softwood region of the Pacific Northwest, similar to south Mississippi, with a coefficient of determination (R^2) of 0.74 and a root mean squared error (RMSE) of 12 percent. Similarly, Healey and others (2005) used a series of transformations on independent variables as well as a natural logarithm transformation on percentage cover, the dependent variable, in a series of simple linear regressions to determine adequate univariate models. The results of their work were promising with regard to using single Short

Wave InfraRed (SWIR) bands, as well as the Normalized Difference Vegetation Index (NDVI) and Normalized Difference Moisture Index (NDMI) transformations described in the methods section of this work.

Damage assessments of past catastrophic tropical storms in the Southeast United States were not able to use the large number of image sources and processing techniques that are presently available. The use of geographic information systems (GISs) and remote sensing techniques in these assessment activities were, for the most part, restricted to a minor role in the wake of Hurricane Hugo in South Carolina (Nix and others 1996) with an expanded role noted for Hurricane Andrew (Jacobs and Eggen-McIntosh 1993, Ramsey and others 1997, 2001). With these two storms and the studies mentioned, a progression of technology and techniques can be noted. In Nix and others (1996), remote Hugo forest damage assessments were made in a GIS through aerial photointerpretation and digitization. Jacobs and Eggen-McIntosh (1993) also used visual image interpretation to perform assessments of Hurricane Andrew-induced damage with the imagery taking the form of airborne digital video frames. The two works led by Ramsey (Ramsey and others 1997, 2001) show a final evolution to satellite acquired moderate (Landsat)- and coarse (Advanced Very High Resolution Radiometer or AVHRR)-resolution imagery, along with storm data, in identifying Andrew's damage in a largely hardwood area in south Louisiana.

Objectives

Because the MFC assessment was performed rapidly through aerial viewing using expert approximation, a more definitive and continuous damage assessment model was sought. In our work here, we studied the viability and possible methods needed to develop predictive storm damage assessment models. The acquisition and analysis of remotely sensed data acquired before and after hurricane Katrina, along with various storm data and pre-existing thematic data created for the Mississippi Institute for Forest Inventory (MIFI), were used to determine the feasibility of mapping storm impacts in a more accurate and continuous form.

Beyond characterization of Katrina-induced forest resource damage, we explored model development to predict the likely scope and severity of damage from future hurricanes. This procedure involved use of MIFI forest thematic data, storm data, prestorm imagery (which can be simulated to note the effects from different size and intensity storms), and poststorm imagery to determine their relative importance in producing predictive damage models. The implications here involve two aspects: (1) model performance without poststorm data so that predictive equations can be used to forecast future hurricane damage, and (2) level of predictive model improvement afforded by use of forest type and age thematic layers that accompany inventory protocol employed by MIFI.

Methodology

Remotely Sensed Data

Acquiring Remotely Sensed Data—

Moderate-Resolution Data

Indian Remote Sensing (IRS) Advanced Wide Field Sensor (AWiFS) data were acquired for use in pre- versus post-storm damage assessment as a moderate spatial resolution (56 m at nadir) data source. These data were selected for several reasons:

- Relatively high visibility, although minor cloud coverage was noted in both pre- and poststorm images.
- Compatibility of spatial resolution with Landsat Thematic Mapper (TM) data, which were used in the creation of thematic data also used in this study.
- Acquisition dates of June 19 (prestorm) and September 4 (poststorm), less than one week after Katrina's landfall in Mississippi.

Spectral attributes associated with the AWiFS sensor included four bands representing the following reflected energy wavelengths, respectively: green (520-590 nm), red (620-680 nm), near-infrared (NIR) (770-860 nm), and shortwave infrared (SWIR) (1550-1700 nm).

High-Resolution Data

We used prestorm digital imagery taken throughout the summer of 2004 (before Katrina's landfall) that was

acquired through the United States Department of Agriculture's (USDA) National Agriculture Inventory Program (NAIP) and made available via the internet by the Mississippi Automated Resource Information System (MARIS). These data were acquired in natural color, sampled at a spatial resolution of 1 m, and presented as mosaiced county-level images. Within 2 months of Katrina's landfall, a private contractor using a Leica ADS40 sensor provided post-Katrina digital imagery for the U.S. Army Corps of Engineers (USACE) over south Mississippi from 31° N to the Gulf Coast. These poststorm data were made available by the United States Geological Survey (USGS) via a disaster-support Web site. They were acquired in natural color with an approximate 0.3-m spatial resolution.

Preprocessing Remotely Sensed Data—

Using the existing thematic MIFI data as a georegistration base, the AWiFS data were georegistered in Leica's ERDAS Imagine 8.7 using first- or second-order polynomial models (ERDAS 2003) in order to achieve subpixel spatial root mean squared (RMS) values. The resulting products were thus projected into the Mississippi Transverse Mercator (MSTM) (MARIS 2005), as this was the native projection of the MIFI base data. This procedure, as recommended by Lillesand and Kiefer (2000) and Lu and others (2004) to analyze multitemporal imagery, ensured highly aligned overlapping pixel registration so that data extraction for later modeling purposes would use correctly sampled reflectance and thematic values. In contrast to AWiFS data, visual inspection of the spatial orientation of high-resolution data sets appeared to match the MIFI base data, so no georegistration was required.

Cloud cover and corresponding shade, although minimal, was present in the AWiFS data sets and required removal to reduce the possibility of sampling erroneous reflectance data. To achieve this removal, both pre- and poststorm rectified AWiFS imagery was clustered using the Iterative Self-Organizing Data Analysis Techniques (ISODATA) algorithm in Imagine (ERDAS 2003) with 250 clusters, 12 maximum iterations, and a convergence threshold of 0.95. The resulting two thematic layers were next interpreted, in a heads-up fashion, coded, and recoded in order to create two cloud and cloud shadow (code = 1)

versus noncloud (code = 0) masks. These masks were then used to remove all cloud-tainted spectral information from the rectified AWiFS images by recoding the eight image layers to zero (four per pre- and poststorm imagery) in these problem areas.

Transforming Remotely Sensed Data—

In exploring various simple band differences, general trends were noted to be unique but subtle for the green and red, NIR, and SWIR bands across the anticipated storm-damaged region. Visually, the red and green bands appeared highly correlated with each other. Because the red appeared more contrasting moving orthogonally from the anticipated center of damage just east of the eye's track (Boose and others 1994), it was chosen for further examination along with NIR and SWIR bands.

Previous studies confirmed the choice in directly using the red, NIR, and SWIR bands (Hame 1991), along with their use in two transformations. These transformations employed two band ratios proven to work in forest change detection: Normalized Difference Vegetation Index (NDVI) (Healey and others 2005; Jin and Sader 2005; Mukai and Hasegawa 2000; Ramsey and others 1997, 2001; Sader and others 2003) and Normalized Difference Moisture Index (NDMI) (Healey and others 2005, Jin and Sader 2005, Sader and others 2003). These indices not only use the visible and infrared bands of interest through proven functions, they also serve to reduce the dimensionality of the data to be analyzed. The formulae for NDVI and NDMI are:

$$NDVI = \frac{NIR\ band - Red\ band}{NIR\ band + Red\ band} \quad (1)$$

and

$$NDVI = \frac{NIR\ band - SWIR\ band}{NIR\ band + SWIR\ band} \quad (2)$$

Land Cover and Type Thematic Data

In Collins and others (2005), the creation of thematic data for use by MIFI in a statewide forest inventory, per the inventory's procedural pilot study (Parker and others 2005), was outlined and resulted in forest age and type thematic layers. The forest-age layer used an approximate 5-year temporal resolution back to the genesis of the Landsat

program in the early 1970s and covered the entire State. In other words, this data set attempted to identify the year of regeneration for areas harvested between 1972 and 2003 in 5-year increments. The data were created using Landsat Multi-Spectral Scanner (MSS) and TM data with the finished products' resolution taking on the finer TM resolution (29 m). The forest-type layer mapped the entire State into water, other nonforest, regenerating forest, softwood, mixed softwood-hardwood, and hardwood classes using 2002–03 TM imagery. Data were georegistered to USGS Digital Ortho Quarter Quadrangles (DOQQs) county-level mosaics, making this the base resolution and orientation for all subsequent analyses involved in this study.

Ancillary Storm Data

Four data set types were obtained from the Internet for use in this study as storm attribute layers. The first two types were acquired from the Atlantic Oceanographic and Meteorological Laboratory (AOML), a subunit of the National Oceanic and Atmospheric Administration's (NOAA's) Hurricane Research Division (HRD), in 14, 3-hour-interval gridded surface wind data sets depicting conditions from 21:00 CDT, August 28, 2005, to 12:00 CDT, August 30, 2005. The grid spacing of these data as the storm passed through south Mississippi was approximately 0.054 degrees in latitude and longitude resulting in a linear distance of approximately 5.25 km in easting and 6 km in northing near the city of Bay St. Louis, Mississippi. These data included sustained surface windspeed (mph) and direction (azimuth degrees), both of which are believed to be influential in structural (Powell and Houston 1996) and forest damage (Ramsey and others 2001) over time. The third data type also came from the AOML and was another gridded surface wind product demonstrating the maximum sustained windspeeds (mph) inflicted by Katrina as it moved through the entire State. The fourth and final storm attribute data obtained for this project included a storm surge extent vector layer acquired from Federal Emergency Management Agency's (FEMA's) Katrina recovery GIS Web site (http://www.fema.gov/hazard/flood/recoverydata/katrina/katrina_ms_gis.shtm).

Model Creation

Independent Variable Assignment—

Remotely Sensed Data

Using the two described band transforms, NDVI and NDMI, and the four original bands from both pre- and poststorm imagery, 18 remotely sensed variables were defined. These variables were created using bands one through four for both pre- and poststorm data sets as well as a delta variable whereby the six prestorm layers, comprising bands and transforms, were subtracted by their poststorm counterparts.

Land Cover and Type Thematic Data

The MIFI thematic data demonstrating statewide age and forest types were used as continuous variables and model strata, respectively. In this construct, age, which could at best be determined back to 1972, was used as a continuous variable with detected year of regeneration being reduced by 2, to account for nearly half the temporal resolution of the age-creation process, and then subtracted from 2005, the year of Katrina's landfall. If the year of regeneration was not found for a forested area, we assumed it was older than the timeframe afforded by the Landsat program, and it was coded with age 40 (2005 minus 1965). This represented a reduction of one temporal resolution interval of 5 minus the interval midpoint correction of 2 years for 1972, the last year of detection. Our assumption was that within the three forest types beyond this age, stand-stocking levels and size were probably more alike than not. As a discriminant, the types could or could not be used as classes for stratifying three different models for softwood, mixed, and hardwood areas.

Ancillary Storm Data

Among the four data set types downloaded for use in this study as storm attributes, one was removed from consideration, one was left alone, and two were compressed into a series of time- and location-dependent storm variables. The surge variable was removed owing to low sampling intensity because the data set indicated that 21 hardwood, 4 mixed, and 0 softwood plots were located within the area of mapped surge inundation. Unlike the 3-hour intervals of

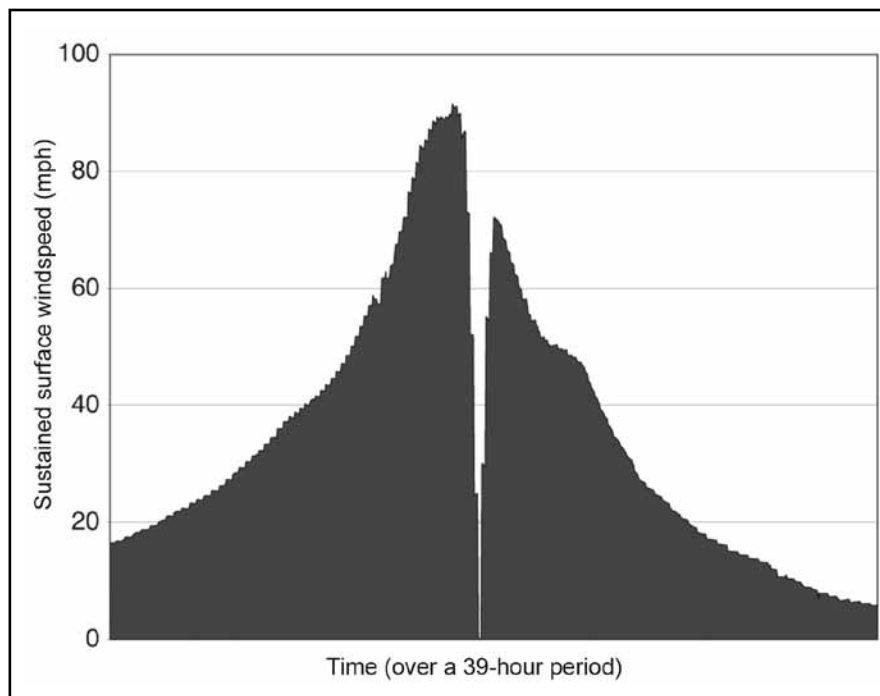


Figure 1—This is a plot-level graph of the resulting 3-minute-interval continuous wind-speeds over a 39-hour period from 21:00 CDT, August 28, 2005, to 12:00 CDT August 30, 2005, for a plot located along Katrina's eye track (note the drop to near zero in the graph's middle), illustrating the converted data used in determining wind duration and stability variables.

windspeed and direction data, the maximum sustained wind variable required no manipulation for use in the model, but it did require interpolation. Using Imagine 8.7, these gridded data were surfaced to the same resolution and orientation as the MIFI base data by using a linear rubber sheeting method (ERDAS 2003).

The first step in transforming the direction and speed attributes from the gridded 3-hour-interval surface wind field data into more usable variables was to create a Microsoft Excel spreadsheet. This helped interpolate the wind data at each plot into more continuous values with regard to speed; direction, as azimuth drastically steps between 360° and 0°; and time, which, in this case, was interpreted into 3-minute (0.05-hour) intervals. Azimuth values were converted to sine and cosine trigonometric function values, and the plot nearest a respective grid point at that point's designated time was allowed to assign its sine, cosine, and wind-speed values to that plot at that time. Time intervals located between fixed 3-hour periods were next assigned weighted x- and y-coordinate locations away from a weighted location

of the storm's eye. Weighting was defined so that proximity to the upper or lower 3-hour time bound for an interpolation time was used to create proportional weights, with the two weights summing to one, for calculating the location and variable weighted averages at an interpolation point. These weights were next used in weighted variable averaging by taking an interpolation time point's weighted location, with respect to storm eye, and calculating windspeed and directional values from the corresponding above and below bounding time points at the same relative weighted location. In Figure 1, a graph of the resulting 3-minute windspeeds for a plot located near Katrina's eye track, illustrates an example of this process's result.

The resulting 3-minute windspeed, sine, and cosine values were next used to create wind duration and stability variables per the anticipated applicability (Powell and Houston 1996, Ramsey and others 2001) of these variables in hurricane damage modeling. The duration variables were calculated over given windspeed thresholds in 10 mph intervals from 30 to 100 mph. For example, the variable for

wind duration at or above 40 mph at a specific plot would count the number of 3-minute time intervals attributed to that plot that were at or above 40 mph and multiply that count by 0.05 hours to get duration in hours. The stability values were also calculated over given windspeed thresholds in 10 mph intervals from 30 to 100 mph. They were done such that the sine and cosine values, isolated for interpolated time points that met the windspeed threshold criteria, were used to calculate two variances, one each for sine and cosine, and then combined into a pooled variance.

Dependent Variable Assignment—

To replace the lack of field data due to ongoing storm damage field sampling, we performed interpretations of high-resolution imagery, pre- and poststorm, with the expectation that aerial-viewed canopy damages were highly correlated with field-measured forest damage. The sample area included Mississippi's six southernmost counties, corresponding to that portion of south Mississippi from 31° N to the Gulf Coast. The USACE imagery was acquired and stratified into 54 interaction classes based on combined forest type, maximum sustained wind (max mph windspeed of >93.5, 93.5-76.5, and <76.5), and age (year constraints of >1993, 1993-88, 1987-83, 1982-78, 1977-70, and <1970). Then we randomly allocated 5 plots into each interaction class, yielding 270 total plots.

Crown closure interpretations and resulting pre- and poststorm differences began with the creation of GIS-generated 0.084-ha rectangular plots (29 by 29 m). Interpretation of these plots involved use of GIS-generated plot boundaries and regular dot grids to employ a systematic method for determining green canopy coverage. The grids were created in a 5 by 5 construct, allowing each dot to represent 4 percent of plot canopy, with outer rows and columns being spaced 2.9 m from their immediate plot bounds and inner rows being spaced 5.8 m in sequence from each other (Figure 2). Using this grid, interpretation was reduced from estimating plot-level green canopy percentages to counting the dots in each plot that fell on interpreted green canopy pixels. The purpose in creating this data set was to develop a bank of prestorm, poststorm, delta (i.e., pre- minus poststorm), or all, canopy data for use in model construction.

Resulting interpretation data were next edited to remove plots that fell within the cloud-classified areas in the AWiFS-derived cloud mask. This masking reduced the plot count from 270 to 252 with an additional 7 plots being removed in the photointerpretation phase owing to lack of forest canopy (this either indicated error in the MIFI forest type layer or canopy removal since acquisition of the 2003 imagery used to generate the MIFI product). The resulting 245 plots were situated across the mapped softwood, mixed, and hardwood forest types in counts of 82, 83, and 80, respectively.

Upon reviewing these edited prestorm, poststorm, and delta canopy measures, the intuitive dependent variable choice appeared to be the delta canopy variable (defined as pre- minus poststorm green canopy cover percentage). However, because these data were largely dependent on prestorm canopy data, this variable was added to the list of independent variables and incorporated into the list of prestorm variables. Also, we believe that prestorm canopy can be created for the study area with moderate to good success (Cohen and others 2001).

Model Definition and Fitting—

The model creation stage of this study was focused on creating multiple linear regression models using ordinary least squares. The sought-after final models were hoped to be parsimonious with optimistic fit values, which, in this case, were high adjusted coefficient of determination or R^2_{adj} values and low RMSE values, for the variable types of interest in the study's objectives. Initial attempts to use the 37 previously described variables (Table 1) in single linear terms produced unsatisfactory fit values. Immediate improvements, however, were noted with the introduction of interaction and quadratic terms (Rawlings and others 1998). The result of creating all these new variables from the above single variables increased the number of possible variables from 37 to 740.

With 740 possible variables available for use in this modeling exercise, a two-step process was organized to reduce the possible number of variables to 40 or fewer, which represented about half (or fewer) the number of plots in each forest type. The first reduction took place

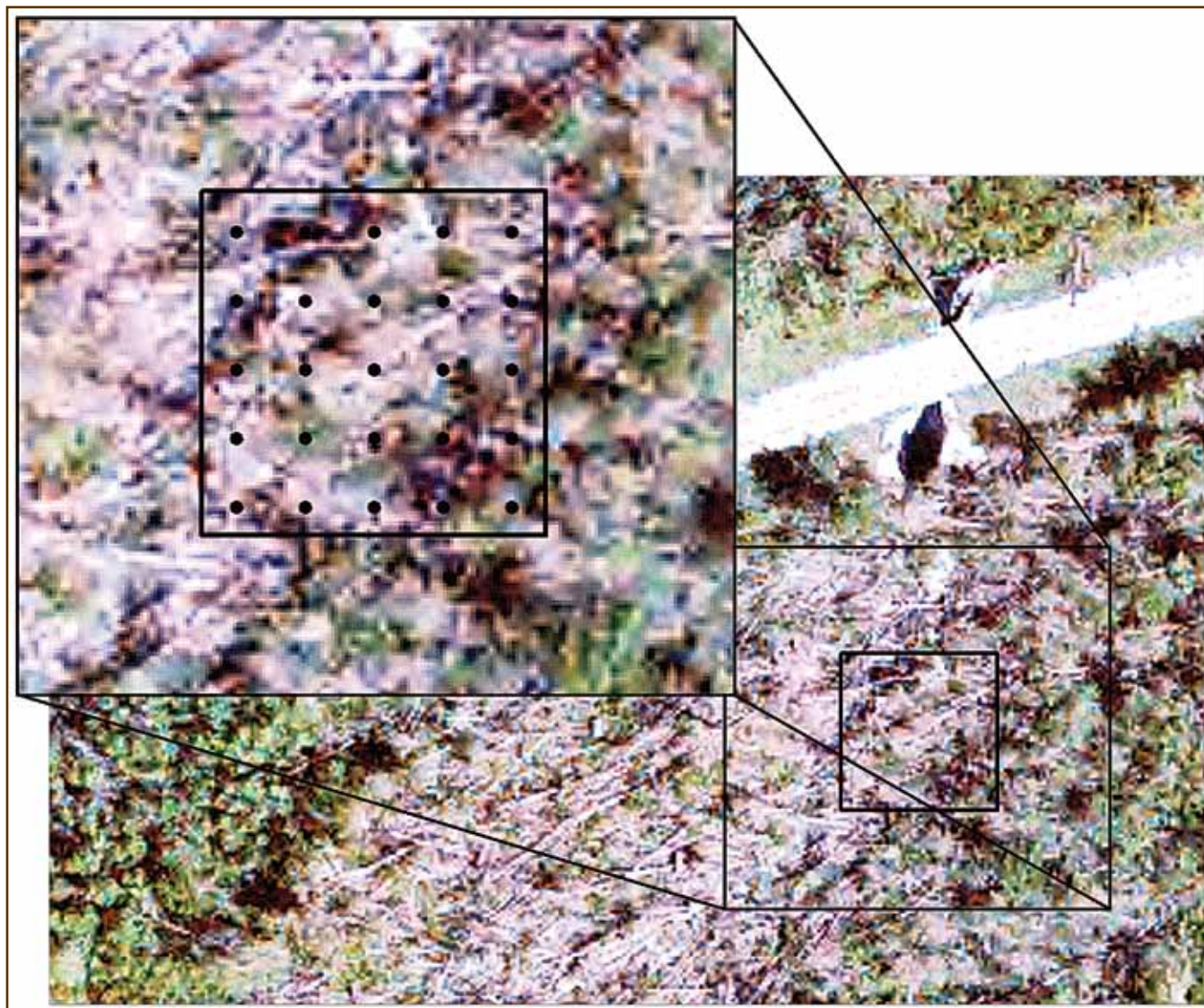


Figure 2—A plot-level view of a photointerpretation plot bound and grid. This image illustrates a highly storm-damaged plot from Pearl River County, Mississippi (note the southeast to northwest oriented downed stems). In the inset, the 5- by 5-point grid used in determining green canopy percentages along with the plot's boundary can be seen.

using stepwise regression methods in SAS's PROC REG procedure (SAS 1999). Using this method, eight model types were reduced using some or all available variables: an overall (regardless of forest type) pre- (including ancillary storm variables) and poststorm data model; an overall prestorm data model; three (for each forest type) prestorm, poststorm, and MIFI variable (forest age) models; and three prestorm and MIFI variable models. In order to regulate that the output stepwise models identify 40 or fewer independent variables for phase two reduction, the significance entry level (SLENTRY in SAS) was set at 0.5, whereas the

significance stay level (SLSTAY in SAS) was accordingly and incrementally adjusted up or down from an initial setting of 0.25 in 0.01 increments until 40 or fewer variables were isolated in the final step.

After isolating eight reduced but still cumbersome models, the leaps-and-bounds algorithm (Furnival and Wilson 1974) in PROC REG (SAS 1999) was employed to hone in on the eight best remaining variables from the field of 40 or fewer with respect to R^2_{adj} and RMSE. The use of R^2_{adj} was deemed advantageous at this point because this value tends to be more comparable than R^2 over models

Table 1—Individual (main effects) model variables and their types

Variable	MIFI	Pre-storm	Post-storm	Variable	MIFI	Pre-storm	Post-storm
Forest age	X			Delta AWiFS NDVI			X
Prestorm green canopy		X		Delta AWiFS NDMI			X
Max sustained wind		X		Wind duration > 30 mph		X	
Prestorm AWiFS band 1		X		Wind duration > 40 mph		X	
Prestorm AWiFS band 2		X		Wind duration > 50 mph		X	
Prestorm AWiFS band 3		X		Wind duration > 60 mph		X	
Prestorm AWiFS band 4		X		Wind duration > 70 mph		X	
Prestorm AWiFS NDVI		X		Wind duration > 80 mph		X	
Prestorm AWiFS NDMI		X		Wind duration > 90 mph		X	
Poststorm AWiFS band 1			X	Wind duration > 100 mph		X	
Poststorm AWiFS band 2			X	Wind stability > 30 mph		X	
Poststorm AWiFS band 3			X	Wind stability > 40 mph		X	
Poststorm AWiFS band 4			X	Wind stability > 50 mph		X	
Poststorm AWiFS NDVI			X	Wind stability > 60 mph		X	
Poststorm AWiFS NDMI			X	Wind stability > 70 mph		X	
Delta AWiFS band 1			X	Wind stability > 80 mph		X	
Delta AWiFS band 2			X	Wind stability > 90 mph		X	
Delta AWiFS band 3			X	Wind stability > 100 mph		X	
Delta AWiFS band 4			X				

Note: A listing of all 37 single variable or main effects used in the study's modeling exercise along with pertinent variable type classifications used in model comparisons. Even though MIFI forest type data were used, they were employed defining strata, not as a model variable.

involving different numbers of parameters (Rawlings and others 1998). This best-eight rule followed the rule of thumb to have 10 observations for each variable while being mindful that the hardwood strata had only 80 observations. To make a more theoretically sound set of model decisions, we also used Hocking's (1976) prediction criteria of using the smallest model, with regard to variable count, that had a Mallows's C_p (Rawlings and others 1998) value of less than or equal to 1 plus the particular model's variable count.

Results

In Table 2, the best eight variable models illustrate moderate fits with RMSE values below 0.15 in only one model and R^2_{adj} values above 0.55 in two models. Between the no MIFI variables pre- and poststorm models, there was a dramatic increase in R^2_{adj} from 0.176 in the prestorm model to 0.439 in the pre- and poststorm situation along

with a matching magnitude reduction in RMSE from 0.219 to 0.181, respectively. In order to compare these no MIFI models to MIFI models, which were created in multiples of three matching the three MIFI forest type designations, a set of pooled RMSE and R^2_{adj} values were created. This creation occurred by combining the three models' error sum of squares, in the case of RMSE values, and by combining the three error and total corrected mean sum of squares considering all three models' degrees of freedom, in the case of the R^2_{adj} values. Comparing these fit values for the eight variable models again demonstrated the drastic improvement in model fit. With the use of poststorm imagery, we observed R^2_{adj} values increasing from 0.381 to 0.506 and RMSE decreasing from 0.190 to 0.170. Additional gains were made in using the MIFI data in models by increasing prestorm no MIFI versus pooled R^2_{adj} values from 0.176 to 0.381 and reducing RMSE from 0.219 to

Table 2—Model fit results by variable types and variable selection criteria

Variables type(s) used	Forest type(s)	Best eight variable models		Hocking's criteria models			Other models of interest		
		R^2_{adj}	RMSE	No. of var.	R^2_{adj}	RMSE	No. of var.	R^2_{adj}	RMSE
Prestorm, post- storm ^a	All	0.4392	0.1805	23	0.4923	0.1717			
Prestorm, post- storm, MIFI	Softwood	0.6796	0.1168	24	0.7893	0.0947			
Prestorm, post- storm, MIFI	Mixed	0.5701	0.1800	25	0.8588	0.0860			
Prestorm, post- storm, MIFI	Hardwood	0.4897	0.2009	15	0.5881	0.1805			
Prestorm, post- storm, MIFI ^a	Pooled	0.5058	0.1694		0.7081	0.1302			
Prestorm ^a	All	0.1758	0.2188	21	0.2765	0.2050			
Prestorm, MIFI	Softwood	0.3366	0.1680	26	0.6405	0.1237			
Prestorm, MIFI	Mixed	0.4300	0.1727	37	0.7735	0.1088	25	0.7142	0.1223
Prestorm, MIFI	Hardwood	0.3647	0.2242	37	0.7542	0.1394	15	0.5258	0.1937
Prestorm, MIFI ^a	Pooled	0.3812	0.1896		0.7345	0.1242		0.5994	0.1525

Note: The modeling exercise results indicating variable types used and MIFI forest type usage along with fit values (adjusted R^2 or R^2_{adj} and RMSE) and number of variables used, when not fixed by the variable selection method.

^a All types or pooled model rows used in numerical data type comparisons.

0.190. Similarly, by incorporating MIFI thematic data, poststorm models were affected with an R^2_{adj} increase from 0.439 to 0.506 and an RMSE reduction from 0.181 to 0.170.

The models derived using Hocking's (1976) method (Table 2) illustrate the same general trend as the eight variable models. Again, improvements with the addition of MIFI and poststorm data were noted in overall (with no MIFI data) and pooled (with MIFI data) R^2_{adj} and RMSE values, except in cases where the application of Hocking's method yielded models with very large variable counts (2 instances used 37 variables). In an attempt to rectify this problem, the other models in Table 2 were created for models that still used a large number of variables. These further reduced models corresponded to the Hocking's identified MIFI, prestorm, and poststorm variable models in the number of employed variables for mixed and hardwood, MIFI, and prestorm models. Examination of these modified models indicates one difference from the eight variable comparisons. The pooled fit values for the prestorm and MIFI models (R^2_{adj} = 0.599 and RMSE = 0.153), in tandem

with the prestorm, poststorm, and MIFI models (R^2_{adj} = 0.708 and RMSE = 0.130), when compared to the pre- and poststorm model (R^2_{adj} = 0.492 and RMSE = 0.172) and prestorm model (R^2_{adj} = 0.277 and RMSE = 0.205) indicate an increased advantage from the eight variable models with regard to using MIFI data as opposed to poststorm image data.

Discussion

Model and Variable Characteristics

The prediction-minded evaluation of data/variable types reported in the previous section states the obvious—that more independent variables tend to improve model predictability of dependent variables. This situation says nothing about the direct applicability of all the work involved with this study and the possible creation of predicted damage values across or outside of the study area, or both, with the various models produced. What is of importance in this work, however, is where, with respect to the variables and variable types used, the gains in model fit occur, although

no statistical inference can be associated with these gains. We expect that similar models can yield predicted canopy changes with RMSE values at or near 0.13 (13 percent) for situations like the passage of a strong hurricane over a mostly undisturbed Southern forested area, such as south Mississippi before Katrina. These estimates can be improved from the forest industry perspective. Industry is often focused on the softwood resource in the South, which is where the best of the stratified models we developed demonstrated a RMSE 0.09 (9 percent). Model fit was comparable in mixed and softwood stands but was poor in hardwoods. This could be the result of a variety of issues from some unknown data bias that was unintentionally introduced into the modeling process or some natural occurrence unknown and unaccounted for in these analyses. These poor results could also illustrate the inherent difficulty and complexity in modeling conditions in hardwood areas.

Potential model flexibility to create comparable predictive models, regardless of the use of poststorm imagery, was a much sought-after finding in this study with mixed results. The reason for this exploration was to display the applicability of modeling anticipated storm damage prior to a weather event. This focus was best explored in comparing the other models (or adjusted) pooled fit values for the MIFI and prestorm variables models and Hocking method pooled MIFI, prestorm, and poststorm variables models where RMSE values were 0.153 versus 0.130, respectively. This comparison is somewhat indecisive as MIFI, prestorm, poststorm variables models outperformed the MIFI and prestorm variables models but only by a small amount (difference in RMSE of < 0.03). Similarly, in the corresponding eight variable models, there was a difference of 0.02 with respect to RMSE. This difference is of a smaller magnitude, however, than the lack of MIFI data comparisons of overall pre- and poststorm variables ($R^2_{\text{adj}} = 0.492$ and RMSE = 0.172) versus prestorm only variables ($R^2_{\text{adj}} = 0.277$ and RMSE = 0.205). In comparing the Hocking pre- and poststorm model (RMSE = 0.172) versus the adjusted pooled MIFI and prestorm model (RMSE = 0.153) and the corresponding eight variable models (RMSE = 0.181 versus

RMSE = 0.190), it does appear that use of the MIFI data in model development at least offsets, maybe even improves, model performance in using prestorm data with the absence of poststorm data.

Possible Model/Variable Improvements

Actual field damage values are being collected in MIFI's Southeast region, which includes Jefferson Davis, Covington, Jones, Wayne, Marion, Lamar, Forrest, Perry, Greene, Pearl River, Stone, George, Hancock, Harrison, and Jackson Counties. These data are the direct metric of interest in this series of work, as opposed to the photointerpreted canopy metric used here. Incorporation of these data is expected to improve development, although model fits may worsen, of any hurricane damage assessment model subsequently created owing to the dependent variable's added meaning. The data could also help address a noted problem of hardwood defoliation versus damage. Poststorm high-resolution imagery indicated that many hardwood areas, particularly in the Pearl River bottom, were defoliated with only minor damage to tree crowns and boles. Differences in this defoliation versus damage aspect of hardwood areas may also be more sensitive to individual hardwood species, which is one of the field metrics, as opposed to the whole hardwood type.

Along with the analysis of field data, future work will also incorporate statistically inferential results, such as variable significance, as opposed to the simple fit comparisons made in this work. These analyses will provide more meaningful results with potential adaptations for collinearity and validation of model assumptions. Model development for repeated application may also be achieved in order to create a more robust and possibly automated product.

Conclusions

Clutter and others (1983) defined risk in the statement: "the inability to estimate future cash flows with certainty is the basic cause of risk in an investment." At play in this analysis are other issues that effect the probability of acquiring an expected return. Examples include rotation lengths (with which MIFI type information may be of further use), intermediate weather conditions (i.e., droughts, floods, etc.), and market fluctuations. Whereas this study is not a risk

assessment in totality, it does place a foundation, albeit not a large one, for development in this direction.

The implications developed in this work with regard to variable creation and the data types utilized are promising for future meaningful region-level continuous damage assessment model creation. The thrust will continue to locate additional ancillary data that may serve to further supplant the advantages of poststorm imagery incorporation in the development of these models. Field data will soon replace the photointerpreted data so heavily relied upon here, and with it a new set of obstacles are expected. In all, however, it does appear possible to create a meaningful damage model that will aid in both economic recovery and assessment of risk associated with storms similar to Hurricane Katrina, possibly before said storms occur.

Acknowledgments

Prestorm aerial photography, which was acquired through the USDA's National Agriculture Inventory Program, was provided by MARIS. Poststorm aerial photography, which was acquired for the USACE as well as other remotely sensed data, were provided via an USGS disaster relief Web site. Storm attribute-related data sets were obtained from NOAA's HRD AOML (i.e., 3-hour-interval and overall max sustained surface wind data) and FEMA's Katrina recovery GIS Web site (i.e., storm surge extent). The primary author greatly appreciates the quantitative support provided by Dr. Thomas Matney.

Literature Cited

- Boose, E.R.; Foster, D.R.; Fluet, M. 1994.** Hurricane impacts to tropical and temperate forest landscapes. *Ecological Monographs*. 64(4): 369–400.
- Butera, M.K. 1986.** A correlation and regression analysis of percent canopy closure versus TMS spectral response for selected forest site in the San Juan National Forest, Colorado. *IEEE Transactions on Geoscience and Remote Sensing*. 24: 122–129.
- Clutter, J.L.; Fortson, J.C.; Pienaar, L.V. [and others]. 1983.** *Timber management: a quantitative approach*. Malabar, FL: Krieger Publishing. 333 p.
- Cohen, W.B.; Maiersperger, T.K.; Gower, S.T.; Turner, D.P. 2003.** An improved strategy for regression of biophysical variables and Landsat ETM+ data. *Remote Sensing of Environment*. 84: 561–571.
- Cohen, W.B.; Maiersperger, T.K.; Spies, T.A.; Oetter, D.R. 2001.** Modeling forest cover attributes as continuous variables in a regional context with Thematic Mapper data. *International Journal of Remote Sensing*. 22: 2279–2310.
- Collins, C.A.; Wilkinson, D.W.; Evans, D.L. 2005.** Multi-temporal analysis of Landsat data to determine forest age classes for the Mississippi statewide forest inventory: preliminary results. In: *Proceedings of 3rd international workshop on the analysis of multi-temporal remote sensing images*; Biloxi, MS. [CD-ROM]. [Place of publication unknown]: [Publisher unknown].
- Earth Resource Data Analysis System (ERDAS). 2003.** *ERDAS field guide*. 7th ed. Atlanta: Leica Geosystems GIS and Mapping. 672 p.
- Furnival, G.M.; Wilson, R.W. 1974.** Regression by leaps and bounds. *Technometrics*. 16: 499–511.
- Hame, T. 1991.** Spectral interpretation of changes in forest using satellite scanner images. *Acta Forestalia Fennica*. 222: 111.
- Healey, S.P.; Cohen, W.B.; Yang, Z.; Krankina, O.N. 2005.** Comparison of tasseled cap-based Landsat data structures for use in forest disturbance detection. *Remote Sensing Environment*. 97: 301–310.
- Hocking, R.R. 1976.** The analysis and selection of variables in linear regression. *Biometrics*. 32(1): 1–49.
- Jacobs, D.M.; Eggen-McIntosh, S. 1993.** Forest resource damage assessment of Hurricane Andrew in southern Louisiana using airborne videography. In: *Proceedings of the 14th biennial workshop on color aerial photography for resource monitoring*. Logan, UT: American Society for Photogrammetry and Remote Sensing: 115–124.

- Jin, S.; Sader, S.A. 2005.** Comparison of time series tasseled cap wetness and the normalized difference moisture index in detecting forest disturbances. *Remote Sensing of Environment*. 94: 364–372.
- Knabb, R.D.; Rhome, J.R.; Brown, D.P. 2005.** Tropical cyclone report: Hurricane Katrina, 23–30 August 2005. Miami: National Hurricane Center. http://www.nhc.noaa.gov/pdf/TCR-AL122005_Katrina.pdf. [Date accessed: May 30, 2006].
- Larsson, H. 1993.** Linear regressions for canopy cover estimation in *Acacia* woodlands using Landsat-TM, -MSS, and SPOT HRV XS data. *International Journal of Remote Sensing*. 14(11): 2129–2136.
- Lillesand, T.M.; Kiefer, R.W. 2000.** Remote sensing and image interpretation. 3rd ed. New York: John Wiley. 736 p.
- Lu, D.; Mausel, P.; Brondizio, E.; Moran, E. 2004.** Change detection techniques. *International Journal of Remote Sensing*. 25: 2365–2407.
- Mississippi Automated Resource Information System (MARIS). 2005.** Mississippi Transverse Mercator (MSTM) Projection. February 15, 2005. <http://www.maris.state.ms.us/htm/Other/MSTM.html>. [Date accessed: April 11, 2006].
- Mukai, Y.; Hasegawa, I. 2000.** Extraction of damaged areas of windfall trees by typhoons using Landsat TM data. *International Journal of Remote Sensing*. 21(4): 647–654.
- Nix, L.E.; Hook, D.D.; Williams, J.G.; Blaricom, D.V. 1996.** Assessment of hurricane damage to the Santee Experiment Forest and the Francis Marion National Forest with a geographic land research and management related to the storm. Gen. Tech. Rep. SRS-5. Asheville, NC: U.S. Department of Agriculture, Forest Service, Southern Research Station. 552 p.
- Parker, R.C.; Glass, P.A.; Londo, H.A. [and others]. 2005.** Mississippi's forest inventory pilot program: use of computer and spatial technologies in large area inventories. Forest and Wildlife Research Center Bull. FO 274. Mississippi State, MS: Mississippi State University. 43 p.
- Powell, M.D.; Houston, S.H. 1996.** Hurricane Andrew's landfall in south Florida. Part 2: surface wind fields and potential real-time applications. *Weather Forecast*. 11: 329–349.
- Ramsey, E.W.; Chappell, D.K.; Baldwin, D.G. 1997.** AVHRR imagery used to identify hurricane damage in a forested wetland of Louisiana. *Photogrammetric Engineering and Remote Sensing*. 63(3): 293–297.
- Ramsey, E.W.; Hodgson, M.E.; Sapkota, S.K.; Nelson, G.A. 2001.** Forest impact estimated with NOAA AVHRR and Landsat TM data related to an empirical hurricane wind-field distribution. *Remote Sensing of Environment*. 77: 279–292.
- Rawlings, J.O.; Pantula, S.G.; Dickey, D.A. 1998.** Applied regression analysis: a research tool. 2nd ed. New York: Springer. 657 p.
- Sader, S.A.; Bertrand, M.; Wilson, E.H. 2003.** Satellite change detection of forest harvest patterns on an industrial forest landscape. *Forest Science*. 49(3): 341–353.
- SAS. 1999.** SAS V8 online help. Cary, NC: SAS Institute Inc. [Date accessed: mid-2006].

Evaluating the Vulnerability of Maine Forests to Wind Damage

Thomas E. Perry and Jeremy S. Wilson

Thomas E. Perry, research professional and **Jeremy S. Wilson**, associate professor of forest management, University of Maine, Orono, ME 04469.

Abstract

Numerous factors, some of which cannot be controlled, are continually interacting with the forest resource, introducing risk to management, and making consistent predictable management outcomes uncertain. Included in these factors are threats or hazards such as windstorms and wildfire. Factors influencing the probability (risk) of windthrow or windsnap occurring can be grouped into four broad categories: regional climate, topographic exposure, soil properties, and stand characteristics. Of these categories, stand characteristics are most commonly and easily modified through forest management. To augment our understanding of the interaction between forest management and wind damage vulnerability in Maine, we developed a wind damage model that reflects site and stand characteristics. Model calibration used information from published literature and experiences of regional managers. The model was evaluated using spatially explicit wind damage records from a 40 800-ha managed forest area in northern Maine. A comparison of means analysis identified significant differences in vulnerability index values between categorical populations of stands that have either recorded blowdown or no recorded blowdown during the last 15 years.

Keywords: GIS, natural disturbance, vulnerability assessment, wind modeling, windthrow risk.

Introduction

“Windthrow is a complex process resulting from interactions between natural and anthropogenic factors” (Ruel 1995). Understanding the interactions between these factors and the inherent risk to stands from this disturbance has numerous benefits to natural resource managers. Windthrow is affected by several factors; climate, topography, physical and biological stand attributes, soil characteristics, and silviculture all play a role in the dynamics of wind disturbance (Ruel 1995).

Understanding windthrow risk throughout the landscape can provide insights into natural vegetation patterns and habitat types. Risk evaluation can also be used to help predict how current forests may change without harvesting and subsequent impacts to forest health. Risk evaluation can help managers (1) evaluate where to locate plantations, (2) decide which regeneration strategies are appropriate, (3) determine where thinning and other partial harvests are acceptable, and (4) determine what species composition or rotation length is desirable for individual sites. Predicting damage, or potential for damage, provides the opportunity for impacts to be considered during prescription development, allowing for revision of management objectives or incorporation of mitigative actions into management plans (Mitchell 1998).

Currently, little is known about the extent of both catastrophic and endemic wind damage in Maine. As a result, this project’s aim was to explore the nature of wind disturbance throughout the State’s large forest ownerships. To augment our understanding of the interaction between forest management and wind damage vulnerability, this project developed a generalized wind damage model that reflects topographic exposure (distance-limited Topex) (Ruel and others 1997), soil conditions (rooting depth), and stand characteristics (density, edge, height, species composition, and treatment history). Results from similar modeling projects in British Columbia suggest that these risk factors are consistent in varied locations, and this indicates that general models may be applicable to landscapes other than the ones for which they were developed (Lanquaye-Opoku and Mitchell 2005). This model was calibrated using information from published literature and experiences of regional managers. We then evaluated it using spatially explicit wind damage records from a 40 800-ha area of managed forest in northern Maine.

Methods

Windthrow risk in many parts of the world has been modeled and assessed. Empirical models are best suited for areas with complex, heterogeneous stand structure and composition (Lanquaye-Opoku and Mitchell 2005, Mitchell

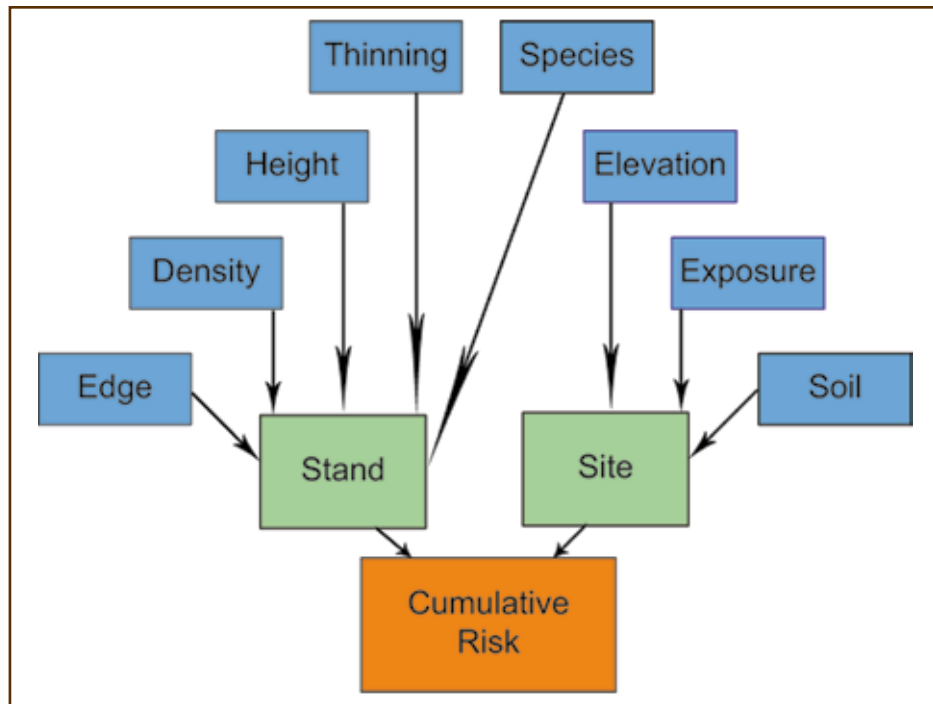


Figure 1—Flow chart of cumulative risk grid development shows the grouping and integration of individual variables into composite risk variables. Composite stand and site risk variables are then combined into a cumulative windthrow risk variable. All variables are indexed between 0 and 1 (high to low risk) and are combined additively.

and others 2001) like the forests of Maine. This empirical approach typically utilizes regression models relating wind damage to physical stand components. Generally, the models produce a probability value rating or index of damage potential based on the stand's suite of environmental conditions. Index modeling of spatial phenomena is enhanced with GIS, which allows for the integration of spatially explicit model parameters.

Logistic regression is commonly used for evaluating these models and isolating highly correlated component variables (Lanquaye-Opoku and Mitchell 2005, Mitchell and others 2001). Rather than using logistic regression, this project produced a generalized model, retaining variables that would not be statistically significant in a logistic regression analysis. This approach is unique because it attempts to create a model that may be applicable regionally and not be limited to the landscape where it was developed.

Eight environmental parameters (elevation, soil rooting depth, topographic exposure, stand species type, stand height, stand density, stand history, and exposed edges)

were used to generate a spatially explicit vulnerability index value. Mitchell (1995, 1998) advocated grouping the factors into three broad categories—exposure, soils, and stand characteristics—to form a windthrow triangle, a conceptual model of the relationships among these interacting factors. For this model, factors were broken down further into site and stand parameters and combined to generate the cumulative windthrow risk index (Figure 1). Data for model variables, including a spatially referenced database of windthrow history, was acquired from various sources and covered an area of private landholdings in the northern portion of the State.

Site: Exposure

Topographic exposure is a critical variable in assessing stand vulnerability. Several indices have been created to describe relative topographic exposure or topographic protection. Topex wind exposure index has been used for some time to assess windthrow risk in Great Britain (Miller 1985). The importance of topographic exposure in modeling windthrow

risk has been demonstrated in other areas with forest-based economies. According to Ruel and others (2002), this variable accounts for over 77 percent of the British wind hazard rating system's total score. Distance-limited Topex was chosen for this project because of its relatively easy calculation and strong correlation to wind tunnel simulation (Ruel and others 1997). Topographic exposure rasters were generated using a model developed and provided by The Windthrow Research Group, University of British Columbia, Vancouver, Canada. The scripts calculate an index of exposure that is the summation of the maximum and minimum angles to the skyline within a user-specified distance. The index can be calculated in the eight cardinal directions and weighted according to user preferences. Ten exposure grids were produced for this project, simulating unweighted exposure at two limiting distances (1000 m and 1500 m) and exposure in the eight cardinal directions (limiting distance of 1000 m).

Site: Soils

Forest soils are also a major component in understanding susceptibility of a forest stand to wind damage. Soil aeration, ease penetration by roots (rooting depth), and moisture-holding capacity all affect the pattern of root development. Generally, loose dry soils facilitate deeper rooting and spreading than do shallow clayey soils (Mergen 1954). Shallow soils, which limit rooting depth and saturate easily like those commonly found in the spruce flat forest type, are increasingly prone to windthrow when saturated. The mass of soil that roots adhere to for anchorage becomes so wet it no longer adheres to itself, and the tree loses a substantial portion of its basal mass, crucial for resistance to windthrow (Day 1950). To compound the problem on wet soils, the rocking of the root plate can pump mud out from under the tree, further reducing the tree's stability (Maccurach 1991).

Depth to groundwater was consistently cited by Maine forest-land managers as crucial to predicting the likelihood of blowdown in stands. The University of Maine's Cooperative Forestry Research Unit provided a continuous depth-to-water-table raster for this project. This variable was combined with coarse-scale soil depth data to create

a raster selecting the minimum depth of the two available data sources and indexed between 0 and 1.

Site: Elevation

Elevation was also incorporated into the site component of the model. Elevation values from a 30-m resolution digital elevation model (DEM) of the study were recalculated into an index between 0 and 1. Elevation had statistically significant correlation with wind damage in cut-block edge vulnerability modeling by Mitchell and others (2001). Studies by Worrall and Harrington (1988) in Crawford Notch, New Hampshire, found that gap size from chronic wind stress and windsnap or windthrow increased strongly with elevation from over 60 percent of the gap area at 764 m (2,521 feet) to almost 85 percent of the gap area at 1130 m (3,729 feet). Gap formation led to subsequent mortality from chronic wind stress and windthrow in gap edge trees. This trend was confirmed by Perkins and others (1992) on Camel's Hump in Vermont. These trends are driven by surface friction acting counter to the force of the wind. Windspeed will increase locally with elevation because surface friction will decrease (Bair 1992).

Stand: Composition and Characteristics

Variables describing stand composition and characteristics were extracted from the forest landowner GIS database, which contains stand-level information to a minimum size of 1 acre. Stand composition is recorded under a three-variable scheme (Table 1). The database also reports stand history from the present to the mid-1980s including stand damage by wind storms and previous harvest entries. The history records include the year of the event and the event type or silvicultural prescription. An iterative network of Microsoft Access™ queries was developed and used to isolate prior stand entry and wind damage events and to create vulnerability indices for individual stands based on stand type and the presence or absence of balsam fir, stand height, and stand density.

The species risk index assigns ranks for the four potential forest types ($H = 0.3$; $S = 0.7$; $HS = 0.45$; $SH = 0.55$). The forest type rank is combined additively with an adjustment factor for the presence of balsam fir (*Abies*

Table 1—Three-variable stand type scheme displays 64 unique stand type combinations possible

Species type code	Height code	Density code
H: > 75% hardwoods	1: seedlings	A: 100-75% crown closure
S: > 75% softwoods	2: saplings	B: 75-50% crown closure
HS: > 50% hardwoods	3: pole-size timber	C: 50-25% crown closure
SH: > 50% softwoods	4: sawlog timber	D: 25-0% crown closure

Each stand is assigned only one code per category; for example, SH2B, representing a softwood-dominated mixed-wood stand of saplings with crown closure between 75 and 50 percent. All stands in the GIS database are characterized by this three-variable code.

balsamea (L.) Mill.) in the overstory because high rates of root rot predispose fir to wind damage (Whitney 1989). The balsam fir adjustment considers the relative abundance of balsam fir in the overstory as the primary, secondary, or tertiary overstory species.

The stand height risk grid was built directly from the landowner database. The stand type height code was rasterized, creating a raster with five potential data values (0-nonforest; and 1 through 4 representing the height classes found in Table 1). The values were divided by 4, the maximum value, to create the desired index range between 0 and 1.

The density grid captures the overstory density of the stands in the study area. Access queries determined the height and density of the most dominant or two most dominant species in each stand, if more than one species were present. Queries assigned values corresponding to the original alphabetical density codes of the most dominant overstory species. Density of the primary overstory species was collected and modified if the secondary species was also in the same canopy strata.

Stand: Thinning

Stands are more vulnerable to windthrow following thinning for two reasons. First, the increase in spacing resulting from thinning creates more canopy roughness, which, in turn, increases turbulence of the wind at the canopy level. Increased turbulence and wind penetration result in reduced tree stability (Blackburn and others 1988, Maccurach 1991). Second, high initial stand density produces unfavorable height-to-diameter (H:D) ratios (Wilson and Oliver 2000). This is less of a problem if stand density remains high; however, thinning removes the support of neighboring

stems, dramatically increasing stand vulnerability. This period of vulnerability may last from a few years to over a decade.

Owing to the prominence of partial removal harvests in the State (McWilliams and others 2005), it was determined that a binary variable would best capture risk associated with stand entry from thinning and partial harvesting. A binary index raster of stand treatments was created from the records of stand entry in the landowner database. All prior entries that involved incomplete removal of the overstory and occurred in the decade preceding the most recent wind event (2001) were classified as thinned. Clearcuts and uncut stands were classified as unthinned. Thinned stands were assigned a value of 1, and unthinned stands a value of 0.

Stand: Edge

The edge raster variable represents the percentage of the stand classified as edge. For this project, edge is defined as a two height-class difference between stands. Production of this data layer was a multistep procedure. First a raster of stand height was produced. Topex scripts were run on this raster with a limiting distance of 30 m, or 1 pixel. This identified all height-class differences between stands across the landscape. Positive values indicated edges of shorter stands, and negative values indicated edges of taller stands. The original height grid was also analyzed with Arc9's zonal range statistics tool. Range statistics defined all edges classified by the height differences between the two adjacent stands. This raster was recoded to display only edges greater than two height-class differences. The Topex-generated edge raster and range statistics raster were combined to identify the edges of the taller stands (negative Topex scores) when the height difference between adjacent

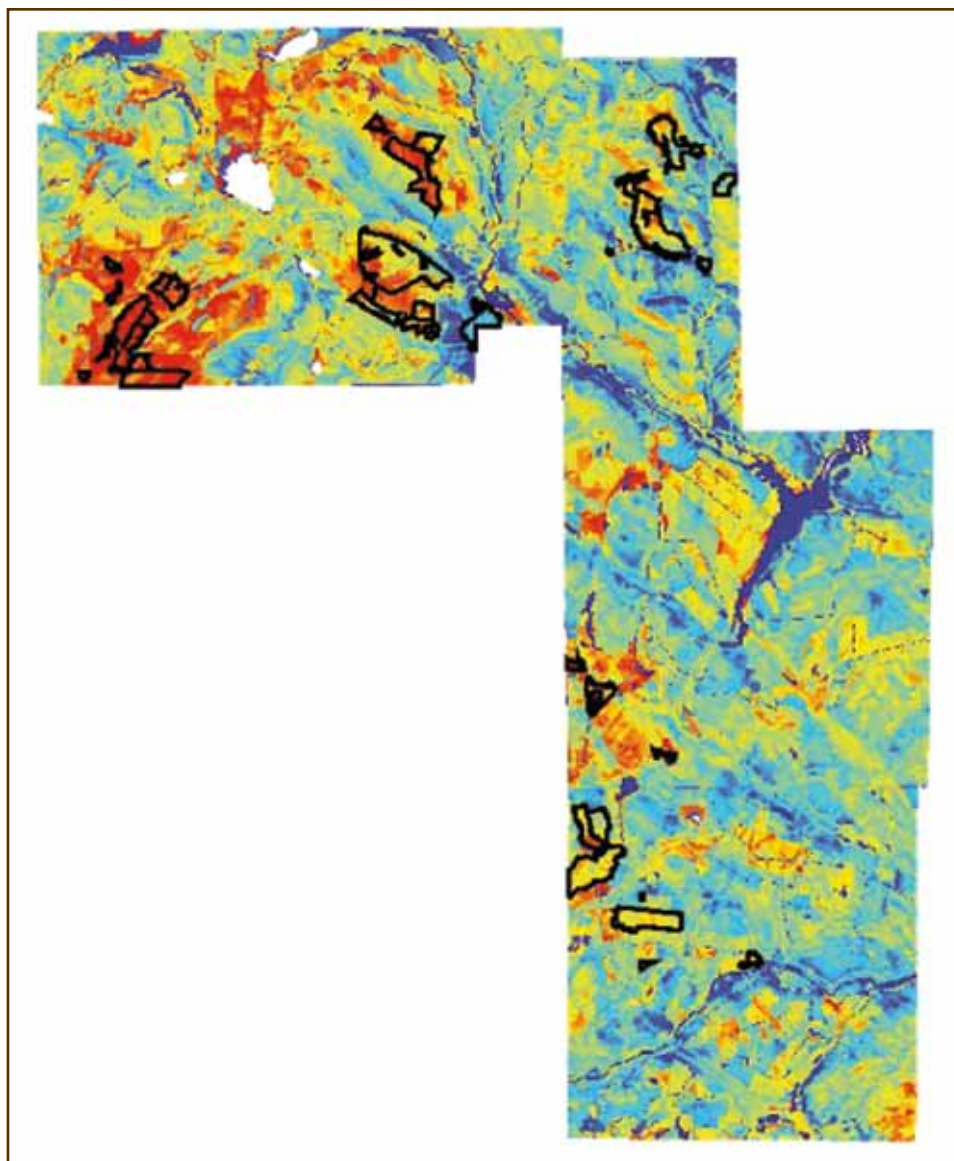


Figure 2—The cumulative wind damage risk grid represents the integration of the two composite model variables representing site and stand risk, generated from eight unique variables. Risk values are displayed along a color ramp from red to blue. Red represents the highest risk and blue the lowest. Actual areas of recorded wind damage are shown in black.

stands was greater than two height classes (range statistic greater than 2). Stands delineated in the GIS database were used as zones to calculate the percentage of edge within the individual stands, and the index was generated directly from these values.

Cumulative Risk

The cumulative risk grid is composed in two stages. In the first stage, the three individual site and five individual

stand components are combined additively to form separate composite site and composite stand grids. The second stage combines the composite site risk grid and composite stand risk grid additively to form a cumulative windthrow risk grid. Figure 2 displays the cumulative windthrow risk grid. Ten separate cumulative windthrow risk grids were produced, one for each unique exposure input grid (described in “Site: Exposure”). All grid combinations were performed

Table 2—Results for individual component variables

Variable	Minimum	Maximum	Direction	Consistent
Density	0.141	0.945	NS	—
Edge	0.001	0.969	Negative	No
Height	0.000	0.137	Positive	Yes
Species	0.060	0.960	NS	—
Thinning	0.000	0.000	Positive	Yes
Elevation	0.000	0.007	Positive	Yes
Soil depth	0.000	0.101	Negative	Yes
Expos_1000	0.050	0.929	Positive	No
Expos_1500	0.060	0.873	NS	—
Expos_north	0.002	0.805	Negative	No
Expos_ne	0.040	0.922	Negative	No
Expos_east	0.164	0.924	NS	—
Expos_se	0.247	0.926	NS	—
Expos_south	0.119	0.911	NS	—
Expos_sw	0.014	0.791	Positive	No
Expos_w	0.143	0.891	NS	—
Expos_nw	0.001	0.647	Negative	No

The table displays the minimum and maximum p-values obtained from the 10 samples in the comparison of means analysis. Exposure variables are listed by their corresponding directional weights. The column titled Direction indicates variable agreement with model assumptions, whereas NS indicates a nonsignificant response. The column titled Consistent indicates whether the variable's response was consistently statistically significant.

with the single output map algebra tool in Arc9's spatial analyst toolbox.

Model Evaluation

To avoid problems associated with spatial autocorrelation, the wind damage vulnerability model was analyzed with a comparison of means from a random sample of polygons within the study area. Hawth's analysis tools (Beyer 2006) were used to maintain a minimum distance between sampled points. To ensure consistent results, 10 separate random samples of polygons were drawn from the study area. These 10 samples are analyzed individually and the results pooled to measure consistency between the samples. Approximately 560 polygons are sampled in each iteration of random sampling, accounting for roughly 14 percent of the study area in each sample.

The analysis used either a two-sample t-test or a Mann-Whitney test to detect differences between the population means. Mann-Whitney was chosen as the default test because this nonparametric test is justified in all situations

where the t-test is applicable and in situations where the assumptions of the two-sample t-test are not met (Zar 1984).

The two-sample t-test was used for Mann-Whitney results indicating near statistical significance when variables met the assumptions of this test. Tests used an alpha of 0.05 to test the null hypothesis, which is that the two population means are equal: $H_0: \mu_1 = \mu_2$. Results from the analysis of the 10 samples were tested for consistency with a t-test. Significant results from the Mann-Whitney and two-sample t-tests were coded either 1, positive correlation with the model, or -1, negative correlation with the model. Non-significant results were coded as a 0.

The t-test procedure tested for statistically significant differences between the responses of the individual model variables across the 10 samples. A mean that was statistically not equal to 0 indicated consistent significance, reflecting either positive or negative correlation with the model. Tests used an alpha of 0.05 to test the null hypothesis that the means for the two populations are equal:

$H_0: \mu_1 = \mu_2$.

Table 3—Results for composite risk variables with minimum and maximum p-values obtained from the 10 samples in the comparison of means analysis

Variable	Minimum	Maximum	Direction	Consistent
STAND	0.000	0.000	Positive	Yes
SITE_1000	0.045	0.818	Positive	Yes
SITE_1500	0.046	0.793	Positive	Yes
SITE_north	0.214	0.968	NS	—
SITE_ne	0.101	0.968	NS	—
SITE_east	0.037	0.941	NS	—
SITE_se	0.002	0.348	Positive	Yes
SITE_south	0.127	0.190	NS	—
SITE_sw	0.002	0.343	NS	—
SITE_w	0.005	0.425	NS	—
SITE_nw	0.089	0.919	NS	—
CMLTV_1000	0.000	0.000	Positive	Yes
CMLTV_1500	0.000	0.000	Positive	Yes
CMLTV_north	0.000	0.000	Positive	Yes
CMLTV_ne	0.000	0.000	Positive	Yes
CMLTV_east	0.000	0.000	Positive	Yes
CMLTV_se	0.000	0.000	Positive	Yes
CMLTV_south	0.000	0.000	Positive	Yes
CMLTV_sw	0.000	0.000	Positive	Yes
CMLTV_w	0.000	0.000	Positive	Yes
CMLTV_nw	0.000	0.000	Positive	Yes

Site risk and cumulative risk variables are listed by their corresponding directional weights. The column titled Direction indicates variable agreement with model assumptions, whereas NS indicates a non-significant response. The column titled Consistent indicates whether the variable's response was consistently statistically significant.

Results and Discussion

Several model variables were found to have statistically significant differences between the two populations (blowdown and nonblowdown). However, not all statistically significant differences were in the direction expected. Positive differences indicate statistically significant population-to-population differences that are in the direction that is expected on the basis of preliminary model research. Negative differences indicate statistically significant population-to-population differences that are in a direction that is opposite the direction expected on the basis of preliminary model research.

The consistency analysis utilized a one-sample t-test. Variables that displayed the same relationship in all 10 iterations cannot be tested for consistency in this manner, but variables that displayed the same relationship in all 10

iterations are considered inherently consistent. The thinning, elevation, composite stand, and all 10 cumulative risk variables displayed a positive difference between the population means through all 10 iterations and are considered statistically consistent. Results are displayed in Tables 2 and 3.

For both tables, positive difference indicates that the mean risk value for the population of stands with recorded wind damage was higher than the mean risk value for the population of stands without recorded wind damage. Positive differences agree with the assumptions used during model construction. Negative difference indicates that the mean risk value for the population of stands with recorded wind damage was lower than the mean risk value for the population of stands without recorded wind damage. Negative differences do not agree with the assumptions used during model construction.

The density variable (Table 2) did not produce significant differences between the population means in any of the iterations. The assumption based on the wind vulnerability literature (Gardiner and others 1997, Lohmander and Helles 1987) was that the less dense stands would be more susceptible. This was thought to be the case in an area with a long management history of natural regeneration and frequent stand entry.

The edge variable (Table 2) had a negative difference between population means 30 percent of the time, not frequently enough to be considered statistically consistent. Most of the stands in the landscape being evaluated are in the two tallest height classes. This trend results in a landscape with very little edge in general. The edge that is present may be in areas at lower risk to wind or edge may not be a critical factor in this landscape.

The height variable (Table 2) had a positive difference between population means 90 percent of the time. This statistically consistent difference likely reflects the increased vulnerability to wind damage with increased tree size (Lohmander and Helles 1987, Peltola and others 1997, Smith and others 1997). The species variable (Table 2) did not have significant differences between the population means in any of the iterations. This was surprising considering managers all cited softwoods and, most notably, balsam fir, as being the most sensitive to wind disturbance. It may indicate homogeneity within the landscape or an insensitivity of the index to differences in composition.

The thinning variable (Table 2) had statistically significant positive differences between the population means 100 percent of the time. This agrees with conventional wisdom of the land managers—that windthrow is much more common in previously thinned stands. An evaluation of the landscape shows that 99.72 percent of the recorded blowdown occurred in thinned stands.

The composite stand grid, STAND, (Table 3) also had significant positive differences between the population means 100 percent of the time. This may be primarily driven by the combination of the height and thinning components that compose this composite variable. The thinning variable's binary property makes it a relatively powerful component of the composite grid.

Differences between population means for the topographic exposure variables (Table 2) were never statistically consistent. This trend was noticed by Mitchell and others (2001) when an analysis of their model revealed a level of contribution from topographic variables to the model lower than expected. Simple terrain variables may not adequately describe airflow phenomena induced by complex terrain (Mitchell and others 2001).

The elevation variable (Table 2) had a positive difference between population means in the model 100 percent of the time. This agrees with the assumption that susceptibility increases in higher areas of the landscape, where exposure and windspeed are greater (Bair 1992).

The soil variable (Table 2) had a negative difference between population means. This trend was statistically consistent, occurring 70 percent of the time. This is counter to the original assumption of the model that forests growing in areas with more restricted rooting depths would be more vulnerable to wind disturbance (Day 1950, Mergen 1954). An analysis of the correlation between soil depth and elevation in this landscape yields a mean Pearson correlation of 0.344 for the 10 iterations. This is substantially larger than the test statistic (0.088) for an alpha of 0.05 and a sample size greater than 100. This result indicates a statistically significant positive correlation between the two variables (Zar 1984); deeper soils are correlated with higher elevations in the landscape being evaluated.

Differences between population means for the composite site variables (Table 3) were either positive or non-significant. Differences between population means were statistically consistent for three exposure variants, both site grids with nondirectionally weighted exposure input variables (SITE_1500 and SITE_1000) and SITE_se, the site variant modeling topographic exposure to the southeast.

The positive difference between the population means of all site variables (with the exception of the north, northeast, and northwest exposure variants) suggests that topographic exposure is important, even though significant differences between the population means were not consistently detected for exposure as an individual variable.

Although the data within the GIS database are fairly coarse, the general spatial model we developed associates

moderate to high vulnerability ratings with reported wind damage in the landscape. All of the final risk assessment variables, CMLTV_direction (Table 3), have a positive difference between the population means. This validates the model's ability to differentiate between vulnerability of damaged stands and vulnerability of undamaged stands. The difference between the population means in the cumulative risk variables is highly significant with p-values of 0.000 recorded in all 10 iterations for all 10 exposure variants.

Conclusion

Wind damage to forests in Maine is a continual consideration for forest managers across the region. The importance of wind damage in the State is likely to increase as large areas of forest that were regenerated during the spruce budworm outbreak of the 1970s and 80s continue to mature. In addition, the vast majority of harvesting in the State utilizes partial harvesting techniques that increase stand susceptibility to windthrow. If these trends in stand height and area thinned continue, managers will need tools and techniques to help them manage the growing wind damage threat. Spatial risk index modeling with GIS provides an alternative view of the landscape, allowing for threat assessment and more informed decisionmaking. The wind vulnerability model developed for this project can be used as a tool to assist in forest planning and provide insight into historical trends in forest dynamics and habitat associations. This tool should be portable to other regions because it contains variables that are frequently identified as critical in predicting windthrow vulnerability. The stand-level variables are general enough to adapt to similar forest typing schemes used by other managers in the State.

There are multiple complexities associated with modeling vulnerability to wind damage in forests. Foremost among these is modeling the interaction of rare regional wind events, chaotic local wind behavior, changing soil conditions (saturation and freezing), and dynamic stand characteristics (growth and manipulation). One approach for managing the uncertainty surrounding wind damage is to develop relatively simple models of vulnerability based

on past observations of factors influencing damage. These more general models, like the one developed for this project, would not be expected to predict past wind damage as well as models developed directly from damage information collected after a particular storm or in a specific landscape. However, they may prove less biased towards particular sites, stand conditions, or individual wind events and, therefore, be more useful for guiding forest management across a large region or as stand conditions change through time.

Literature Cited

- Bair, F.E. 1992.** The weather almanac. 6th ed. Detroit, MI: Gale Research, Inc. 279 p.
- Beyer, H.L. 2006.** Hawth's analysis tools for ArcGIS, ver. 3.26 [software]. <http://www.spatialecology.com>.
- Blackburn, P.; Petty, J.A.; Miller, K.F. 1988.** An assessment of the static and dynamic factors involved in windthrow. *Forestry*. 61(1): 29–44.
- Day, W.R. 1950.** The soil conditions which determine windthrow in forests. *Forestry*. 23: 90–95
- Gardiner, B.A.; Stacey, G.R.; Belcher, R.E.; Wood, C.J. 1997.** Field and wind tunnel assessments of the implications of re-spacing and thinning for tree stability. *Forestry*. 70(2): 233–252.
- Langquaye-Opoku, N.; Mitchell, S.J. 2005.** Portability of stand-level empirical windthrow risk models. *Forest Ecology and Management*. 216: 134–148.
- Lohmander, P.; Helles, F. 1987.** Windthrow probability as a function of stand characteristics and shelter. *Scandinavian Journal of Forest Research*. 2: 227–238.
- Maccurach, R.S. 1991.** Spacing: an option for reducing storm damage. *Scottish Forestry*. 45: 285–297.
- McWilliams, W.H.; Butler, B.J.; Caldwell, L.E. [and others]. 2005.** The forests of Maine, 2003. *Resour. Bull. NE-164*. Newtown Square, PA: U.S. Department of Agriculture, Forest Service, Northeastern Research Station. 188 p.

- Mergen, Francois. 1954.** Mechanical aspects of windbreakage and windfirmness. *Journal of Forestry*. 52: 119–125.
- Miller, K.F. 1985.** Windthrow hazard classification. Forestry Commission Leaflet 85. London: Forestry Commission. [Not paged].
- Mitchell, S.J. 1995.** The windthrow triangle: a relative windthrow hazard assessment procedure for forest managers. *The Forestry Chronicle*. 71(4): 447–450.
- Mitchell, S.J. 1998.** A diagnostic framework for windthrow risk estimation. *The Forestry Chronicle*. 74(1): 100–105.
- Mitchell, S.J.; Hailemariam, T.; Kulis, Y. 2001.** Empirical modeling of cutblock edge windthrow risk on Vancouver Island, Canada, using stand level information. *Forest Ecology and Management*. 154: 117–130.
- Peltola, H.; Nykanen, M.; Kellomaki, S. 1997.** Model computations on the critical combinations of snow loading and windspeed for snow damage on Scots pine, Norway spruce, and Birch sp. at stand edge. *Forest Ecology and Management*. 95: 229–241.
- Perkins, T.D.; Klein, R.M.; Badger, G.J.; Easter, M.J. 1992.** Spruce-fir decline and gap dynamics on Camels Hump, Vermont. *Canadian Journal of Forest Research*. 22: 413–422.
- Ruel, Jean-Claude. 1995.** Understanding windthrow: silvicultural implications. *Forestry Chronicle*. 71(4): 434–444.
- Ruel, J.C.; Mitchell, S.J.; Dornier, M. 2002.** A GIS-based approach to map wind exposure for windthrow hazard rating. *Northern Journal of Applied Forestry*. 19(4): 183–187.
- Ruel, J.C.; Pin, D.; Spacek, L. [and others]. 1997.** The estimation of windthrow hazard rating: comparison between Strongblow, MC2, Topex and a wind tunnel study. *Forestry*. 70(3): 253–265.
- Smith, D.M.; Larson, B.C.; Kelty, M.J. [and others]. 1997.** *The practice of silviculture: applied forest ecology*. 9th ed. U.S.A.: John Wiley. 116 p.
- Whitney, R.D. 1989.** Root rot damage in naturally regenerated stands of spruce and balsam-fir in Ontario. *Canadian Journal of Forest Research*. 19: 295–308.
- Wilson, J.S.; Oliver, C.D. 2000.** Stability and density management in Douglas-fir plantations. *Canadian Journal of Forest Research*. 30: 910–920.
- Worrall, J.J.; Harrington, T.C. 1988.** Etiology of canopy gaps in spruce-fir forests at Crawford Notch, New Hampshire. *Canadian Journal of Forest Research*. 18: 1463–1469.
- Zar, J.H. 1984.** *Biostatistical analysis*. 2nd ed. Englewood Cliffs, NJ: Prentice-Hall. 130 p.

English Equivalents

When you know:	Multiply by:	To find:
Nanometers (nm)	3.94×10^{-8}	Inches (in)
Millimeters (mm)	0.0394	Inches
Centimeters (cm)	.394	Inches
Meters (m)	3.28	Feet (ft)
Cubic meters (m ³)	35.3	Cubic feet (ft ³)
Meter per second (m/s)	2.24	Miles per hour (mph)
Kilometers (km)	.621	Miles (mi)
Kilometers per hour (kph)	.621	Miles per hour
Hectares (ha)	2.47	Acres (ac)
Microliters (μL)	.0000338	Ounces (fluid)
Milliliters (mL)	.0338	Ounces (fluid)
Grams (g)	.0352	Ounces
Kilograms (kg)	2.205	Pounds
Kilograms per cubic meter (kg/m ³)	.0624	Pounds per cubic foot (lb/ft ³)
Kilograms per hectare (kg/ha)	.893	Pounds per acre (lb/ac)
Megagrams per hectare (Mg/ha)	.446	Tons per acre
Kiloequivalents per hectare (keq/ha)	.405	Kiloequivalents per acre
Trees per hectare	.405	Trees per acre
Micrograms per gram (μg/g)	1	Parts per million
Degrees Celcius (C)	$1.8C + 32$	Fahrenheit (F)

Pacific Northwest Research Station

Web site	http://www.fs.fed.us/pnw
Telephone	(503) 808-2592
Publication requests	(503) 808-2138
FAX	(503) 808-2130
E-mail	pnw_pnwpubs@fs.fed.us
Mailing address	Publications Distribution Pacific Northwest Research Station P.O. Box 3890 Portland, OR 97208-3890